Advanced Signal Processing and Control in Anaesthesia

by

Catarina Sofia da Costa Nunes, Lic.

Thesis submitted as a requirement for the degree of
Doctor of Philosophy
in the Department of Automatic Control and Systems Engineering,
The University of Sheffield
May 2002

Aos meus pais e a ti Carlos
Obrigada por tudo!

Acknowledgements

I would like to thank the Portuguese Foundation for Science and Technology for their financial support during the course of this research.

Fundação para a Ciência e Tecnologia
Ministério da Ciência e da Tecnologia
Portugal

I also wish to thank my supervisors Dr. Mahdi Mahfouf and Professor Derek Linkens, for their guidance throughout this research project. I thank them not only for their supervision of the scientific aspects but also for their support.

I sincerely thank Dr. J. E. Peacock of the Royal Hallamshire Hospital, Sheffield, for his help during the gathering of clinical data for this research, and also for his supporting words and advice. I also thank the patients that agreed to participate in this study.

Dr. M. Abbod has been most helpful with the kit for gathering of clinical data and his most useful advice. I also wish to thank Dr. Hoi Fei Kwok for her help in those stressing moments, and for her friendship.

I would like to thank Professor Pedro Lago and Dr. Teresa Mendonça of the University of Porto, Portugal, for their concern and support throughout my time in Sheffield.

I greatly appreciate the support of my friends Diana, Ruphina, Patricia and Sandra. I also thank my portuguese friends that even far away always knew the right words to put a smile back on my face. Thank you all for being there!

This thesis is dedicated to my parents, whom I deeply thank for their everlasting support and encouragement. Their understanding and love have been very important to me. I also thank my boyfriend Carlos for his everlasting patience and encouragement when these were most needed.

Publications

Nunes, C. S., Mahfouf, M., and Linkens, D. A. (2000). “A fuzzy relational classifier applied to depth of anaesthesia.” Proc. of the 7th UK Workshop on Fuzzy Systems, Whirlow Grange Conference Centre, Sheffield, UK, October 26-27, 2, 100-105.

Nunes, C. S., Mahfouf, M., and Linkens, D. A. (2001). “Fuzzy logic monitoring in anaesthesia.” Proc. of the Sixth Portuguese Conference on Biomedical Engineering, BioEng’2001, Faro, Portugal, June 11-12, 71-72.

Mahfouf, M., Nunes, C. S., and Linkens, D. A. (2001). “Closed loop control for depth of anaesthesia using a fuzzy PI structure.” Proc. of the International Conference on Neural Networks and Expert Systems in Medicine and Health Care, NNESMED 2001, Milos Island, Greece, June 20-22, 342-346.

Nunes, C. S., Mahfouf, M., and Linkens, D. A. (2001). “Fuzzy control of depth of anaesthesia.” Proc. of 2001 UK Workshop on Computational Intelligence, UKCI-01, Edinburgh-First Conference Centre, Edinburgh, UK, September 10-12, 99-104.

Nunes, C. S., Mahfouf, M., and Linkens, D. A. (2002). “Neuro-fuzzy modelling in anaesthesia.” Proc. of the Fifth Portuguese Conference on Automatic Control, CONTROLO’2002, Aveiro, Portugal, September 5-7 (Accepted).

Advanced Signal Processing and Control in Anaesthesia

Catarina Sofia da Costa Nunes

This thesis comprises three major stages: classification of depth of anaesthesia (DOA); modelling a typical patient's behaviour during a surgical procedure; and control of DOA with simultaneous administration of propofol and remifentanil. Clinical data gathered in the operating theatre was used in this project.

Multiresolution wavelet analysis was used to extract meaningful features from the auditory evoked potentials (AEP). These features were classified into different DOA levels using a fuzzy relational classifier (FRC). The FRC uses fuzzy clustering and fuzzy relational composition. The FRC had a good performance and was able to distinguish between the DOA levels.

A hybrid patient model was developed for the induction and maintenance phase of anaesthesia. An adaptive network-based fuzzy inference system was used to adapt Takagi-Sugeno-Kang (TSK) fuzzy models relating systolic arterial pressure (SAP), heart rate (HR), and the wavelet extracted AEP features with the effect concentrations of propofol and remifentanil. The effect of surgical stimuli on SAP and HR, and the analgesic properties of remifentanil were described by Mamdani fuzzy models, constructed with anaesthetist cooperation. The model proved to be adequate, reflecting the effect of drugs and surgical stimuli.

A multivariable fuzzy controller was developed for the simultaneous administration of propofol and remifentanil. The controller is based on linguistic rules that interact with three decision tables, one of which represents a fuzzy PI controller. The infusion rates of the two drugs are determined according to the DOA level and surgical stimulus. Remifentanil is titrated according to the required analgesia level and its synergistic interaction with propofol. The controller was able to adequately achieve and maintain the target DOA level, under different conditions.

Overall, it was possible to model the interaction between propofol and remifentanil, and to successfully use this model to develop a closed-loop system in anaesthesia.

Table of Contents

Chapter 1

Introduction

'Anaesthesia' and 'depth of anaesthesia' are two different entities that are frequently confused because they share a common word: anaesthesia. However, anaesthesia comprises muscle relaxation, analgesia and unconsciousness (i.e. depth of anaesthesia). In other words, depth of anaesthesia (DOA) is one of the components of anaesthesia. These concepts are still a matter of debate in the medical area, leading to the lack of a global standard definition.

Initially, a single drug was used and signs such as movement, lacrimation and sweating, helped to determine DOA. The introduction of balanced anaesthesia (the use of three drugs, i.e. a muscle relaxant, an analgesic and an anaesthetic) improved the safety and comfort of the patient facilitating the surgical procedure, but the clinical signs were obscured by the effects of the different drugs. The anaesthetist started to use the measurable cardiovascular parameters such as blood pressure and heart rate, to base his/her decision about DOA. However, these parameters are influenced by drugs such as β-blockers. In addition, different patients respond in different ways, increasing the variability of the clinical signs. Therefore, the search for an adequate DOA monitor turned to signals from within the central nervous system (CNS) (Stanski, 1994; Thornton and Jones, 1993).

The electroencephalogram (EEG) was one of the first signals studied. However, the EEG was found to respond differently to different anaesthetic agents (Iselin-Chaves *et al.*, 1998; Simanski *et al.*, 2001; Singh, 1999). An appropriate signal should show similar graded changes with anaesthetic concentrations for different agents, it should show appropriate changes with surgical stimulus, and indicate awareness and light anaesthesia. The auditory evoked potentials (AEP), which are the responses on the EEG to an auditory stimulus, have been the focus of many researches and have led to some very useful results in monitoring DOA (Backory, 1999; Elkfafi, 1995; Kenny, 2000; Kumar *et al.*, 2000; Nayak and Roy, 1998; Thornton and Sharpe, 1998; Thornton *et al.*, 1989a).

Unconsciousness (DOA) is very hard to define and to measure adequately, since no direct measurements exist. In addition, to distinguish between stages that could lead to implicit or explicit memory, with or without pain and the adequate stage of unconsciousness without memory or recall, is not a trivial task (Jones, 1994).

Methods need to be developed to extract relevant features from the AEP and to classify these features into different levels of DOA. This information could be used to construct a control system for DOA, considering the adequate infusion rate of the anaesthetic drug. In recent years, several researchers have developed different control structures for inhalational and intravenous agents, using the AEP and other monitoring techniques. Due to the complexity and importance of DOA, this is an area still open to improvement.

Balanced anaesthesia introduced the problem of drug interactions. The anaesthetic and analgesic drugs may have different types of interactions, increasing or decreasing the effects of each drug, potentiating the different side effects or even introducing new side effects (Berenbaum, 1989; Minto *et al.*, 2000). The anaesthetist needs to be aware of the interactions between drugs for the safety of patients. When considering drug interactions, several aspects need to be considered, such as the properties of the two drugs, the presence of surgical stimulus and the level of DOA. In addition, there are pharmacokinetic and pharmacodynamic interactions, the first relating to the distribution and clearance of the drugs in the body, the second concerned mainly with the effects of the drugs. The study and quantification of the effects inherent to the simultaneous administration of the two drugs is a new and challenging area of great importance.

Propofol is the most used intravenous anaesthetic agent for its hypnotic properties and almost lack of side effects compared to inhalational agents. In general, propofol is combined with one of the synthetic opioids so as to provide analgesia. However, the optimal propofol infusion rate and concentration are largely affected by the choice of opioid and, in some cases, by the duration of the infusion (Vuyk, 1999, 2000). Therefore, it is important to analyse the effects of opioids so as to decrease the amount of drug infused and the recovery time. One of the advantages of propofol and many of the opioids is that they can be infused automatically using infusion pumps and titrated according to patient's needs.

Target controlled infusion (TCI) systems are widely implemented in the operating theatre, determining the infusion rate of propofol based on a target plasma concentration which is set by the anaesthetist. This may insert a delay in the patient's response, since the drug effect is governed by the effect concentration and not the plasma concentration (Bovill,

2000; Morita *et al.*, 2000; Shafer and Varvel, 1991). In addition, the opioids are administered in bolus doses or constant continuous infusions by the anaesthetist.

The introduction of the new and ultra-short acting opioid remifentanil, improved the operating conditions, increased the ability to rapidly control the level of analgesia and reduced the recovery time (Camu and Royston, 1999). However, remifentanil has strong interactions with propofol, which could be used to an advantage in reducing the overall amount of drug infused.

Analgesia, i.e. pain relief, is difficult to establish since there in no measure of pain. There is the risk of implicit memory with pain, which has a severe effect on the patient and could lead to traumatic experiences and post-operative disorders. Therefore, the analgesic drug should be adequately combined with the anaesthetic drug to be of efficiency in general anaesthesia. In general, the analgesic drug is titrated according to the type of surgical procedure, the amount of surgical stimulus and the effects of the stimulus on the haemodynamic responses. An opioid with a rapid onset of action (such as remifentanil) allows for a rapid response to the stimulus effects. The analysis of the brain signals would improve the quality of analgesia, since there would be information about the arousal caused by the stimulus in the CNS and subsequent effects on the level of unconsciousness.

A simulation system would help to train the anaesthetist in different circumstances, reflecting the drug interactions. A monitoring and control system is of great value to process the information from the CNS, advising the anaesthetist about the DOA level and required infusion rate. The analysis of the signals from the CNS is crucial, since it can be done on-line in the operating theatre. Without this the anaesthetist has no information about the brain signals. In addition, such a structure would also work as an alarm system, alerting the anaesthetist to any event that could interfere with the infusion profiles and/or the patient safety, and any fault(s) in the equipment.

This project searches for a solution to the problems presented above and for a robust/reliable control system that could determine the optimal infusion rate of both drugs (anaesthetic and analgesic) simultaneously, and titrate each drug in accordance to its effects and interactions. Such a system would be a valuable assistant to the anaesthetist in the operating theatre.

1.1 Thesis Overview

This thesis is divided into seven chapters, references and bibliography, and five appendices. A brief explanation of the contents of each part is presented next.

Chapter 2 explains the concepts of anaesthesia and depth of anaesthesia (DOA). The methods of DOA assessment from clinical signals to evoked potentials, are presented. The chapter finishes with a review of the control and monitoring techniques used for DOA.

Chapter 3 deals with the classification of DOA using the auditory evoked potentials (AEP) and the haemodynamic parameters systolic arterial pressure (SAP) and heart rate (HR). Multiresolution analysis with wavelet transforms is used to extract meaningful features from the AEP relating to the classification of DOA. A fuzzy relational classifier (FRC) is developed and implemented using clinical data. The FRC uses fuzzy clustering and relational matrices to establish the link between the natural data clusters and the DOA levels. The results of the FRC are presented and compared with the results of a neural network and a neuro-fuzzy system.

Chapter 4 presents the clinical data gathered and used during this research, and the characteristics of the anaesthetic propofol and analgesic remifentanil, i.e. the two drugs focused upon in this project. The pharmacokinetic models of both drugs are presented with the concept and mathematical derivation of the effect concentration. In addition, a review of the effects of interactions of drugs relating to the simultaneous administration of anaesthetic and analgesic drugs, is presented. Special attention is given to the synergistic interaction of propofol and remifentanil.

In Chapter 5, a hybrid patient model is constructed using fuzzy logic techniques and nonlinear optimization. The data gathered in the operating theatre are used to construct and train the models. The cardiovascular parameters and wavelet extracted AEP features are modelled considering two different phases of general anaesthesia, i.e. induction and maintenance. The synergism between propofol and remifentanil is modelled using an Adaptive Network-Based Fuzzy Inference System (ANFIS). The effects of surgical stimulus on SAP and HR are modelled using the anaesthetist’s opinion translated into fuzzy rules.

Chapter 6 is the development of a multivariable control structure for DOA, with

simultaneous administration of propofol and remifentanil. The patient model is tested in open-loop simulations with different drug profiles. The closed-loop simulation system is presented in this chapter, linking the patient model, the FRC of DOA and the control structure. First, a single-output controller is developed, determining the infusion rate of the hypnotic drug and using the analgesic in a constant infusion rate. Second, a multivariable controller is constructed so as to determine the infusion rates of both drugs. The controllers are constructed using fuzzy logic techniques, and tested via a series of simulations with the developed patient model.

Finally, Chapter 7 presents the conclusions and recommendations for future work.

Chapter 2

Depth of Anaesthesia

2.1 Introduction

The word *anaesthesia* is derived from the Greek and means ‘without feeling’. It was first used by the Greek philosopher Dioscorides in the first century AD to describe the narcotic effect of the plant mandragora. In 1771 Encyclopedia Britannica defined anaesthesia as a ‘privation of the senses’. However, modern anaesthesia is considered to date from 1846, when W. Morton introduced ether anaesthesia for dental surgery (Stanski, 1994).

Anaesthesia can be defined as the lack of response or recall to noxious stimuli. General anaesthesia includes paralysis (muscle relaxation), unconsciousness (depth of anaesthesia) and analgesia (pain relief). The first two are concentrated in the operating theatre, whereas the third is also related to post-operative conditions. In addition, different surgical procedures require different proportions of the three components.

The assessment of depth of anaesthesia (DOA) during surgery under general anaesthesia has become a very difficult process since the introduction of balanced anaesthesia. In the early days of anaesthesia, when a single agent (e.g. ether) was used to control all the three components of anaesthesia, signs of inadequate anaesthesia could be obtained relatively easily from clinical measurements and from patient movement. The main concern was that muscular relaxation could only be provided at deep levels of anaesthesia. Therefore, the hypnotic and analgesic components were in excess of those required, resulting in long recoveries and other side effects. Postoperative respiratory and venous thrombotic complications were frequent (Carrie *et al.*, 1996; Newton, 1993). The point requiring most skill and care in the administration of anaesthetics was to determine when it has been

carried far enough, so as to avoid a too-deep stage of anaesthesia (Thornton and Jones, 1993).

The introduction of intravenous drugs as part of a balanced anaesthesia, (i.e. the use of a muscle relaxant, an analgesic, and an anaesthetic) made anaesthesia safer for the patient. The three components of anaesthesia could be more easily adjusted to individual requirements improving the patient's operative and post-operative well-being. However, this also meant that the measures of anaesthetic depth became obscured or even completely ablated, making the task of measuring DOA more difficult.

Several questions arise from balanced anaesthesia: the introduction of muscle relaxants meant that excellent relaxation could be obtained while the patient was only lightly anaesthetised. The degree of neuromuscular block can be monitored by observing the muscle response to nerve stimulation, commonly the ulnar nerve. Asbury and Linkens (1986) and Mahfouf (1994) are some of the researchers who designed automatic control systems of neuromuscular blockade. However, analgesia and unconsciousness are not so easy to measure. When a patient is unconscious it is not always clear how much analgesia is an agent providing or what is the patient's level of unconsciousness.

Jones (1994) reported several cases of conscious awareness occurring in apparently anaesthetised patients. Explicit memory of conscious awareness with pain during anaesthesia is different from the situation where there is explicit memory of intraoperative events but no pain (i.e. adequate analgesia but inadequate hypnosis). Conscious awareness with pain perception is the most worrying complication for patients and anaesthetists alike. This may cause post-traumatic stress disorder resulting in nightmares, anxiety, a preoccupation with dead and even bereavement conflict. Therefore, it is very important to establish an adequate method for measuring DOA.

Anaesthesiologists use a variety of observations, such as blood pressure, heart rate, lacrimation, movement, sweating, and pupil response, to make a judgement on the DOA (Shieh, 1994). However, agents such as neuromuscular blockers, β-blockers, anticholinergics or opioids obscure these signs of anaesthetic depth making them unreliable. This has prompted the search for methods for detecting awareness during anaesthesia and the graded changes that occur within the central nervous system (CNS) related to DOA.

Depth of anaesthesia can be considered as a balance between the depression of the CNS by the anaesthetic drug and the stimulation of surgery. A reliable monitor of DOA is of great

importance to establish effective control in the operating theatre.

2.2 Assessing Depth of Anaesthesia

Depth of anaesthesia is difficult to define and to measure accurately. ”Anaesthesia monitoring”, to assure that the level of anaesthesia is adequate, is of major importance for the anaesthetist, so that accidental conscious awareness during general anaesthesia can be avoided. If the event of conscious awareness occurs, it could lead to extreme psychological consequences for the patient and to a malpractice litigation against the anaesthetist.

The different monitoring methods that have been investigated for DOA can be divided into two groups: those that directly detect awareness and those that indirectly detect the level of consciousness by bioassays of anaesthetic depth (Doyle and Tong, 1996). The majority of monitoring methods used at present are indirect, meaning that the anaesthetist has to deduce the patient anaesthetic state based on the patient’s response.

The Tunstall’s isolated forearm technique is an example of the direct monitoring methods. One forearm is protected from neuromuscular block with a tourniquet and, at intervals, the patient is asked to squeeze the anaesthesiologist’s hand in a specified way (Doyle and Tong, 1996). However, if the patient is unconscious he will not able to respond to the anaesthetist’s command. It is worth noting that this technique may be suitable for surgical interventions where only analgesia and muscle relaxation is needed but not for general anaesthesia.

The isolated forearm technique has also been used in unconscious patients, but instead of the patient squeezing the anesthesiologist’s hand the response is analysed by the movement of the arm as a reaction to noxious stimuli. Thornton and Jones (1993) report that patients responding with the isolated arm during anaesthesia rarely recall this experience postoperatively, and they do not appear to experience pain at the time. These results raise the probability that very light anaesthesia is sufficient to abolish the sensation of pain to a range of surgical stimuli without any significant effect on conscious awareness but inhibiting explicit recall. Consequently, the patient is unconscious but the brain may be able to register information as shown by implicit memory of intraoperative events. This monitoring technique cannot be used during long periods of time, otherwise the patient may suffer from the effects of ischaemia. In addition, the tourniquet is an extra cause of pain for

the patient, making it an unsuitable technique altogether.

A review of the indirect monitoring methods is given here. These bioassays of anaesthetic depth include clinical signs, electroencephalogram, evoked potentials, and others.

2.2.1 Clinical Signs

Clinical signs of DOA derive directly from the patient. Haemodynamic responses such as heart rate (HR), systolic arterial pressure (SAP), mean arterial pressure (MAP), and diastolic arterial pressure (DAP) are widely used in current anaesthetic practice for DOA assessment, it is therefore likely that they carry useful information. However, the usefulness of clinical signs is reduced by drugs such as β-blockers or opioids, and conditions such as surgical haemorrhage, i.e. bleeding.

Anaesthetists use a variety of clinical signs, such as pupil response, sweating, lacrimation and haemodynamic responses. The relevance of these clinical signs has been widely discussed.

Thornton and Jones (1993) report that after the introduction of curare (Second World War), clinical signs such as pupil size, respiratory and peripheral movement were eliminated. In addition, it was very difficult to categorize the clinical signs of anaesthesia for one inhalational anaesthetic agent, let alone for agents in general.

Patient movement as an indicator of DOA is useless when the patient is paralysed via a muscle relaxant. Respiration cannot be used if a patient is under artificial ventilation. Pupil diameter is reduced artificially with the application of opioids. Nevertheless, the use of clinical signs is well spread in anaesthesia.

Greenhow *et al.* (1992) describe an expert system that provides decision-support for control of DOA by merging a number of qualitative clinical signs and quantitative on-line measurements. They use a measure of relevance and certainty to reflect the usefulness of clinical signs in different situations.

Linkens and Rehman (1992) use artificial neural networks to determine DOA, with isoflurane as the inhalational anaesthetic. Target values for HR, SAP and respiration rate are derived by the anaesthetist for individual patients undergoing surgery, and used as input to the system. They conclude that anaesthetic agents affect the respiratory system,

cardiovascular system, central nervous system and muscle.

The objective of Robb *et al.* (1993) was to determine if a clinically acceptable anaesthetic state could be achieved by altering isoflurane dosage to maintain SAP at a predetermined value. They suggest that SAP is a major component in the clinical assessment of DOA.

Shieh (1994) uses a hierarchical structure to monitor DOA, based on measurable data such as SAP and HR, and on non-numerical clinical signs such as sweating, lacrimation, and pupil response which are observed by the anaesthetist and input manually to the system.

Vefghi and Linkens (1999) use SAP, HR, respiration rate, age, weight, and sex to classify the anaesthetic state. Frei *et al.* (2000) used MAP regulation to maintain the patient in an adequate level of DOA. The overall control objective of Rao *et al.* (2000) was to maintain the haemodynamic variables MAP, cardiac output, and mean pulmonary arterial pressure at desired setpoints.

Haemodynamic responses are also used as a comparison when other measures of DOA are being investigated (Crabb *et al.*, 1996; de Beer *et al.*, 1996). Mortier *et al.* (1998) report on the complex nature of DOA when simple measures of the EEG correlate poorly with clinical parameters. In particular, haemodynamic parameters are used to determine the efficacy of opioids and evaluate total intravenous anaesthesia (TIVA) (Alexander *et al.*, 1999a; Hogue *et al.*, 1996; McAtamney *et al.*, 1998). Opioids are used to control haemodynamic changes in response to noxious stimulus (Casati *et al.*, 2001; Hall *et al.*, 2000; Joo *et al.*, 2001; Litman, 2000; O'Hare *et al.*,1999; Song *et al.*, 1999; Thompson *et al.*, 1998).

Wuesten *et al.* (2001) titrated the opioids to maintain HR and MAP within 20% of baseline, and defined inadequate analgesia as responses to surgical stimulus by hypertension and tachycardia. However, inadequate hypnosis was defined as the EEG bispectral index greater than 60 and was treated with propofol.

Satisfactory anaesthesia requires adequate cardiovascular and respiratory stability, no or minimal patient movement, and no awareness or recall of events during the procedure (Kenny, 2000). Therefore, it is acceptable that haemodynamic parameters should be used as an extra information to assess DOA. However, to rely only upon them will not reflect DOA in general anaesthesia.

2.2.2 Anaesthetic Concentration

Monitoring DOA using the concentration of the anaesthetic agent has been widely used in the case of inhalational drugs. The minimum alveolar concentration (MAC) of inhaled anaesthetic required to prevent 50% of patients from responding to painful stimulus has been used as a monitor of DOA (Stanski, 1994). MAC is measured by end-tidal concentration. The end-tidal concentration of anaesthetic in the alveoli is used as an indicator of the anaesthetic concentration in the brain. The MAC concept describes a concentration-versus-response relationship.

Chilcoat *et al.* (1984) used a control system to bring the tension of anaesthetic in the brain to any value specified in MAC units. One of the many researches in control of MAC of inhalational agents is by Nayak and Roy (1998) who use MAC and evoked potentials to estimate DOA.

The introduction of intravenous agents reduced the toxic effect of inhalational agents specially in the liver and kidneys but also in the operating room environment (Morgan, 1983; Zbinden and Luginbuhl; 1996). However, there is not an equivalent of MAC for intravenous agents.

The steady-state plasma concentration of intravenous anaesthetic required to prevent 50% of patients from responding, does not correspond to MAC for inhalational agents because it cannot be measured on-line. In addition, the relationship between infusion-rate and blood level concentration of intravenous drugs varies widely between patients.

The variability of pharmacokinetics for intravenous agents has been reported by several researchers (Glass, 1998; Vuyk, 1998). Similar infusion rates produce significantly different blood concentrations. For instance, the pharmacokinetics of propofol are affected by age, gender and weight (Hirota *et al.*, 1999; McFarlan *et al.*, 1999; Schuttler and Ihmsen, 1993; Vuyk *et al.*, 2001).

Davidson *et al.* (1993) reported that a 67% nitrous oxide dosage reduced the EC50 (effective concentration of propofol at which 50% of patients do not respond to a painful stimulus) by 30%. Furthermore, Vuyk (2000) analysed the reduction in the required concentration of propofol via opioids.

2.2.3 Electroencephalogram

The electroencephalogram (EEG) has been used to monitor the effects of general anaesthetics on the CNS, and is known to show graded changes with increasing concentrations of anaesthetics (Doyle and Tong, 1996; Thornton and Sharpe, 1998). Generated from within the CNS, the EEG is not affected by neuromuscular blocking agents and it has been used to monitor DOA.

The EEG represents cortical electrical activity derived from summated excitory and inhibitory postsynaptic activity, which are controlled and paced by subcortical thalamic nuclei. The EEG is a non-invasive indicator of cerebral function when the patient is unconscious and unresponsive (Stanski, 1994).

The unprocessed EEG is difficult to interpret, such a complex signal is of limited value (Mortier *et al.*, 1998). Therefore, several techniques involving frequency analysis of the EEG have been developed so that a reduced number of numerical parameters could be used on-line by the anaesthetist, and still reflect the descriptive properties of the EEG with respect to DOA.

Bispectral analysis is one of the techniques used to compress the information on the EEG. This is a method of signal processing that accommodates quadratic interactions between wave components making up the EEG trace, by quantifying phase coupling. Therefore, it determines the harmonic and phase relations among the various EEG frequencies (Jones, 1996; Kissin, 2000).

Mortier *et al.* (1998) use the bispectral index (BIS) as the control variable for the administration of propofol in 10 patients during spinal anaesthesia. The BIS describes the complex EEG pattern as a single variable, and similarly to the EEG the BIS behaves differently with different anaesthetics. For this reason, they developed BIS using a database of EEG data recorded with different anaesthetics. BIS was also used by Absalom and Kenny (1999) to control propofol infusion for anaesthesia in patient undergoing orthopaedic surgery.

Kissin (2000) states that BIS is promising as a monitor of unconsciousness. However, BIS should be derived statistically from a database which includes many types of anaesthetics and their combinations. If BIS is used with a new drug or new patient population that was not in the original database, it must be re-evaluated. In the same study, it is reported that the

accuracy of BIS is altered with the addition of opioids or nitrous oxide. The accuracy of BIS monitoring to prevent awareness is higher when a single anaesthetic is used.

Gajraj *et al.* (1999) compared the bispectral EEG analysis with auditory evoked potentials (AEP) for monitoring DOA during propofol anaesthesia. They reported that the BIS was unable to detect the transaction from unconscious to consciousness. Nevertheless, BIS appeared to measure the effect of the hypnotic at the time of unconsciousness.

Muthuswamy and Roy (1999) used fuzzy integrals and bispectral analysis of the EEG to predict movement under anaesthesia. They designed a methodology for estimating DOA in a canine model that integrates EEG derived parameters, haemodynamic parameters, and MAC of inhalational agents (isoflurane, halothane, and nitrous oxide). The EEG characteristics changed with the anaesthetic level and various other physiological parameters. As a result, they concluded that a single model may not be accurate at all times.

Singh (1999) reported that the utility of BIS depends on the anaesthetic technique being used. When isoflurane or propofol are used as the primary anaesthetic agents, changes in BIS correlate with the probability of response to skin incision. If opioids are used, the correlation of BIS values with movement response to skin incision becomes less significant. They conclude, that BIS is a monitor of sedation or hypnosis and cannot provide pre-emptive warning about inadequacy of all the components of anaesthesia.

Gentilini *et al.* (2001a, 2001b) are part of a research group that has been studying the use of BIS in closed-loop control of anaesthesia. They use BIS for modelling and closed-loop control of hypnosis with the volatile anaesthetic isoflurane. The controller is based on a model identified from experiments on 20 volunteers (Gentilini *et al.*, 2001b). The model is used to predict BIS from the measured endtidal isoflurane concentrations. The complex systems include artifact tolerance, respiratory system model, and a smooth transfer between manual and automatic control. The closed-loop system was tested on one patient and presented an acceptable performance. This study confirmed the usefulness of the BIS monitor for the titration of the drug. The authors state that this closed-loop system can be used with other volatile anaesthetics, as long as the appropriate pharmacokinetic and pharmacodynamic model is used. If intravenous anaesthetics are used the approach has to be completely changed, since the respiratory system will not be used and the concentrations cannot be measured online. This is a ongoing study which involves several researchers, such as Luginbuhl and Schinder (2002). They reported two case studies using BIS to detect awareness, when using the anaesthetic drug propofol and the analgesic remifentanil. The BIS monitoring proved to be a useful tool for early detection of an unintended decrease of

hypnotic drug effect. BIS correlates with both the incidence of explicit and implicit awareness. The use of DOA monitors is useful in prevention of awareness together with practice guidelines and continuous education of the anaesthetist.

Simanski *et al.* (2001) considered the control of neuromuscular blockade and control of DOA using BIS and the cardiac output as inputs to the system. They concluded that the main disadvantage of the EEG measurement is the variation with different anaesthetic agents.

Spectral edge frequency (SEF) (95% of the power) and the median frequency (MF) (50% of the power) of the EEG have also been investigated for the possibility of detecting awareness. Gajraj *et al.* (1998) showed that there was almost no separation between the MF and SEF values obtained in the awake and unconscious subjects, raising doubts about the adequacy of these measurements. The same study showed that BIS correlates well with predicted blood concentration of propofol during recovery of anaesthesia, but the auditory evoked potentials were better at distinguishing consciousness from unconsciousness.

Asteroth *et al.* (1997) used the MF as the control variable to adjust the vaporizer setting. They reported that MF alone does not include enough information to enable proper classification.

Graaf *et al.* (1997) use neural networks to extract features from the raw EEG. They use these features to design a decision support system in anaesthesia.

Kuizenga *et al.* (1998) studied the effects of propofol on the EEG in 10 healthy surgical patients under extradural analgesia. The EEG amplitude in six frequency bands was related to arterial blood propofol concentration and responsiveness to verbal commands. They observed a biphasic EEG amplitude response to an increasing blood concentration of propofol in all frequency bands. In the same research, it was reported that the study of EEG changes caused by hypnosis in the anaesthetised surgical patient are hindered by the effects of currently administered sedative and analgesic drugs.

Zhang and Roy (2001) use EEG derived parameters such as complexity, regularity, and spectral entropy to estimate DOA.

The EEG changes vary from different combinations of anaesthetic agents used, because different agents have different effects on the EEG (Thornton and Jones, 1993). In addition, Iselin-Chaves *et al.* (1998) report that each anaesthetic alters the EEG differently, making

precise correlation between EEG changes and DOA problematic.

2.2.4 Evoked Potentials

Evoked potentials (EP) are derived from the EEG in response to auditory, somatosensory, nociceptive and visual stimuli. They reflect the functional integrity of specific peripheral and CNS regions in humans (Thornton and Sharpe, 1998).

The EP are described in terms of the post-stimulation latency in ms (time between application of a stimulus and the occurrence of a peak in the EP waveform) and peak-to-peak amplitude (in mV or nV) of individual peaks in the waveform. These peaks and troughs arise from specific neural generators.

EP are sensitive to anaesthetic drugs. As a result, they have been investigated as possible measures of anaesthetic drug effect and DOA (Kumar *et al.*, 2000; Stanski, 1994; Thornton and Jones, 1993).

The change in EP is similar and uniform for potent inhalational and intravenous anaesthetics. This contrast with the EEG, in which different parameters must be examined depending on the anaesthetic being used.

According to the type of stimulus used, there are four main EP: auditory evoked potentials (AEP), somatosensory evoked potentials (SEP), movement evoked potentials (MEP) and visual evoked potentials (VEP). The advantages and disadvantages of SEP, VEP and MED are presented here. The AEP are described in greater detail in Section 2.3. The AEP have been greatly used to monitor DOA, the signal shows similar graded changes with different anaesthetics and reflects the subjective clinical signs used by the anaesthetist.

2.2.4.1 Visual Evoked Potentials

Visual evoked potentials (VEP) are recorded after monocular stimulation with recording electrodes over the occipital parietal and central scalp. The VEP are recorded in response to visual stimuli such as flashing lights or a checker board pattern. VEP have the disadvantage that the highly reproducible pattern of EP requires the subject to focus on the checker board, which is not possible for anaesthetised patients. In addition, VEP with flashing lights are variable between patients and trials, this has been described as qualitative rather than quantitative (Thornton and Sharpe, 1998). Kumar *et al.* (2000) states that VEP cannot be

reliably interpreted intra-operatively.

VEP have been used in neurology to confirm and localize sensory abnormalities, to identify silent lesion and to monitor changes, but little research exists with respect to anaesthesia (Nuwer, 1998).

2.2.4.2 Motor Evoked Potentials

Motor evoked potentials (MEP) are recorded by measuring compound muscle action potentials (with the help of fine wire electrodes) within muscles innervated by the motor nerve of surface electrodes, after direct stimulation of the nerve in the operative field. MEP assess the function of the motor cortex and descending tracts (Kumar *et al.*, 2000).

Pechstein *et al.* (1998) tested the influence of two anaesthetic techniques of general anaesthesia (isoflurane plus nitrous oxide or propofol) in the MEP. The MEP were monitored by transcranial and direct cortical high frequency repetitive electrical stimulation. They concluded, that high doses of isoflurane and nitrous oxide are not compatible with the recording of muscle activity, and that evaluation of muscular responses after transcranial stimulation is not feasible with balanced anaesthesia with isoflurane.

Motor function testing is not feasible during some operations and neuromuscular blocking drugs may obscure the responses completely.

2.2.4.3 Somatosensory Evoked Potentials

Somatosensory evoked potentials (SEP) are produced by stimulation of the sensory system. They can be recorded by stimulating almost any nerve trunk at various levels. The most frequent are those in response to median and ulnar nerve stimulation. The SEP elicited in response to cutaneous painful stimuli have a larger latency depending on the site and type of stimulus (Thornton and Sharpe, 1998).

Nuwer (1998) reviews the applications of SEP in neurology and in the operating room. He states that certain inhalational anaesthetics must be avoided when using cortical SEP monitoring, because the response can be abolished by them. However, SEP have been very useful in monitoring the spinal cord during scoliosis procedures and other surgical interventions in which it (the spinal cord) is at risk of damage. SEP tests are of better quality when the patient is tested asleep, and they have been used in the intensive care unit

(ICU) to assess prognosis for comatose patients.

Kumar *et al.* (2000) explain that both false-negative and false-positive results have been reported with intraoperative SEP monitoring. However, the reliability of SEP to predict post-operative somatic sensory function is very good. This supports the idea of SEP being used mainly in ICU.

Cortically generated SEP waves reflect the analgesic rather than the hypnotic action of anaesthesia. Thornton and Jones (1993) report observations that etomidate and propofol (which are devoid of analgesic action) failed to depress the response, whereas opioids like fentanyl, sufentanil, and morfine significantly suppress amplitudes of SEP. In contrast, Samra *et al.* (2001) report that there is large variability in SEP morphology with the introduction of opioids. They compare the effects of two opioids (remifentanil and fentanyl) on intraoperative monitoring of SEP during isoflurane anaesthesia, but it is not clear if the results presented are due to the analgesic action or to the interaction between the analgesic and the anaesthetic drugs.

2.2.5 Other Methods of DOA Assessment

The lower esophageal contractibility method measures contractions of the lower esophagus. The striated portion of the esophagus is innervated by reticular formation of the brain stem. Stanski (1994) explains how DOA might be measured by the degree of spontaneous contraction of the lower esophagus. Considering that increasing concentrations of potent inhalated anaesthetics decreased lower esophageal contractibility, it was inferred that the frequency of such contractions could predict movement in response to skin incision during anaesthesia.

Thornton and Jones (1993) state that there is large variability between patients, with different anaesthetic techniques. They also report that the dose response curve for provoked esophageal contractions was shallower than that for spontaneous contractions. Therefore, the method may be inappropriate for assessing cognitive function during anaesthesia. Furthermore, Thornton *et al.* (1989b) reported that there was no consistent relationship between esophageal contractions and evoked potentials. In addition, there was also no relation between lower esophageal contractibility and propofol blood concentration.

Bojanic *et al.* (2001) place the hypothesis of ocular microtremor (OMT) as a tool for measuring DOA. OMT is a fine high frequency tremor of the eyes caused by extra-ocular

muscle activity stimulated by impulses emanating in the brainstem. They studied the effect of general anaesthesia induced with propofol on the OMT in 22 patients. There were significant differences between the last awake OMT recording and the first recording at loss of consciousness. Further studies are needed to establish the efficacy of this method; OMT has an obvious measurement difficulty.

2.3 Auditory Evoked Potentials

The auditory evoked potentials (AEP) waveform with its series of peaks and troughs represents the passage of electrical activity from cochlea to cortex. The AEP are measured via electrodes on the surface of the scalp. They are responses on the EEG to clicks applied to both ears. Among all the EP the AEP are the most promising and most studied to monitor DOA (Abbod *et al.*, 1998; Backory, 1999; Elkfafi, 1995; Elkfafi *et al.*, 1998; Kenny, 2000; Kenny and Mantzaridis, 1999; Linkens *et al.*, 1997a; Nayak and Roy, 1998; Thornton and Sharpe, 1998; Thornton *et al.*, 1989a).

The AEP consist of three waves: the brainstem waves (1-10 ms), the middle latency waves (or early cortical, 10-100 ms), and the late latency waves (or late cortical, >100 ms). These waves are generated from different levels of the neuraxis, which are differentially sensitive to drugs and sensory stimuli. The AEP are not affected by neuromuscular blocking drugs.

The late cortical waves are attenuated and even abolished by general anaesthesia, sedation, and sleep. Therefore, they are not appropriate for clinical use.

The brainstem waves latencies have dose-related increases when inhalational agents are used. However, intravenous agents (such as propofol) have little or no effect on the brainstem waves. As a result, they cannot be used to measure DOA when intravenous agents are present (Thornton and Jones, 1993).

Middle latency evoked potentials (MLAEP) are able to distinguish between the aware and anaesthetised state and subsequent CNS depression, reflecting the balance between CNS depressions caused by anaesthetic drugs and arousal caused by surgical or other stimuli. Changes in the latency of the MLAEP correlate with the transition from awake to unconscious, and subsequent decreases and increases in the amplitude of these waves reflect the interplay of general anaesthetics, surgical stimulation and obtunding of the latter by analgesics (Thornton and Sharpe, 1998).

Figure 2-1 and Figure 2-2 show the MLAEP signal (peaks labelled Na, Pa, Nb, Pb) when the patient is awake and anaesthetised respectively (Backory, 1999). The difference in amplitude and latency of the peaks is clear between the two figures, reflecting the correlation between MLAEP and DOA.

Kumar *et al.* (2000) state that the change in the MLAEP reflects the hypnotic component of anaesthesia as opposed to an analgesic effect. The MLAEP are particularly helpful in understanding the central effects of various anaesthetic agents and in monitoring the concept of implicit memory, awareness and DOA. The AEP reflect the subjective clinical signs that anaesthetists use, and indicate the response of the CNS. However, AEP have the disadvantage of being susceptible to intraoperative disturbances (Simanski *et al.*, 2001).

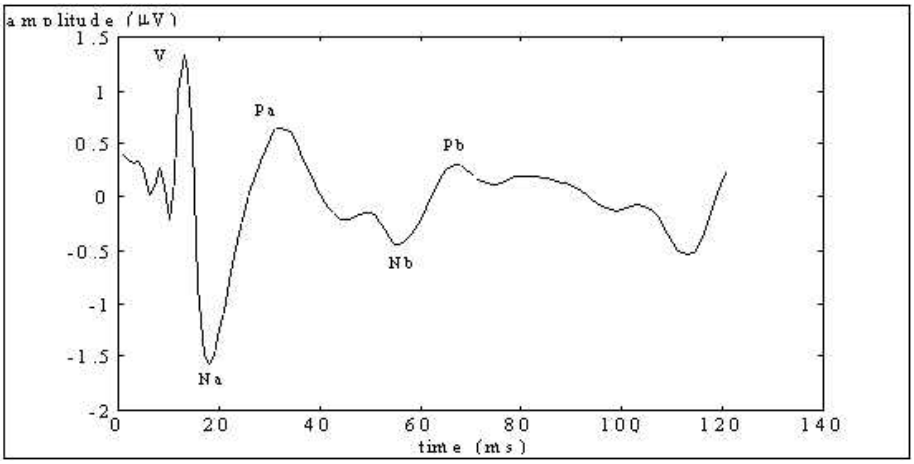

Figure 2-1: The AEP from an awake patient (Backry, 1999).

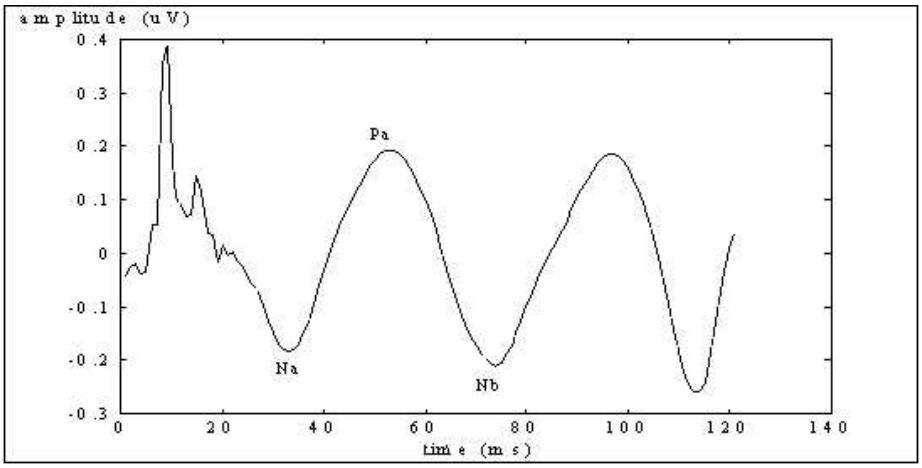

Figure 2-2: The AEP from an anaesthetised patient (Backory, 1999).

Considering the ability of the MLAEP to reflect the anaesthetic state, there are two studies based on the possibility of the MLAEP predicting movement during general anaesthesia. Schwender *et al.* (1997) reported that during intraoperative movement, amplitudes of the MLAEP increased and latencies decreased progressively. When movement was observed, the recorded MLAEP were similar to the awake state. This study was performed in 40 patients undergoing elective laparotomy under epidural analgesia, anaesthesia was produced with isoflurane or propofol. In contrast, Kochs *et al.* (1999) reported that none of the AEP or EEG variables were able to predict whether patients would move to surgical incision. However, data collected after skin incision, when the patient was actually moving, reflected significant changes in Pa and Nb amplitude from the pre-to-post incision. Of course the information is obtained too late to be of predictive value for the anaesthesiologist. Therefore, MLAEP may not predict movement in response to surgical stimuli, but they indicate inadequate anaesthesia by responding to movement.

Signal processing of the AEP is divided into two steps: extracting the AEP, and obtaining relevant features from the signal so as to assess DOA. Subsequent sections explain the extraction of the AEP from the EEG and also the different methods used for AEP feature extraction.

2.3.1 Signal Extraction

The AEP are responses in the EEG to auditory stimuli. Therefore, it is necessary to extract the AEP from the random background EEG or noise. Ensemble averaging is the most used tool in the analysis of evoked brain waves (Aunon *et al.*, 1981; Thornton and Sharpe, 1998).

This technique requires the stimulus to be applied at a known and precise point in time, and is straightforward for auditory, visual and electrical stimuli.

It is assumed that the measured waveform $f(t)$ is of the form:

$$f(t) = a(t) + n(t) \qquad 2\text{-}1$$

where $a(t)$ is the evoked potential and $n(t)$ is the noise (i.e. the ongoing EEG). Therefore, if the noise $n(t)$ is independent of the AEP and $a(t)$ repeats itself with each stimulus presentation, then an estimate of the AEP can be obtained by simple ensemble averaging (Aunon *et al.*, 1981).

Ensemble averaging decreases the noise in a manner inversely proportional to the square root of the number of replications, assuming that the signal component is deterministic, the expected value of $n(t)$ is zero, the noise in one epoch is not correlated to the noise in another, and that the average power is the same for each epoch of noise.

2.3.2 AEP Feature Extraction

The MLAEP show graded changes with anaesthetic concentrations and show similar changes for different agents in the time and frequency domains. Appropriate choice of signal features for data compression with acceptable classification performance is of primary concern in the design of automatic DOA monitors. Researchers have used a different number of discriminatory features extracted from the MLAEP. A review of these methods is presented next.

2.3.2.1 Pa and Nb Latencies

Several researchers reported that the Nb latency is associated with wakefulness and conscious awareness with explicit recall. As the latency increases, amnesia occurs, followed by loss of consciousness and ultimately loss of implicit memory (de Beer *et al.*, 1996; Kumar *et al.*, 2000; Newton *et al.*, 1989; Savoia *et al.*, 1988; Schwender *et al.*, 1997; Thornton and Jones, 1993; Webb *et al.*, 1996).

Increasing concentrations of propofol reduced amplitudes and increased latencies of waves Pa and Nb. These changes in the early cortical variables were related linearly to concentration. Researchers concluded that MLAEP reflect the hypnotic component of an anaesthetic drug (Schwender *et al.*, 1994; Thornton *et al.*, 1989a; White *et al.*, 1999).

Palm *et al.* (2001) investigated the dose-response relationship of propofol and MLAEP. They studied 100 patients in cardiac surgery with a propofol/sufentanil regimen. The MLAEP where evaluated using Pa/Nb amplitudes and Nb latencies. Propofol suppressed amplitude Pa/Nb in a dose dependent manner. In the same study, it was reported that AEP are less influenced by the application of opioids and benzodiazepines, whereas anaesthetics like isoflurane or propofol diminish MLAEP in a dose dependent manner. As a result, the preserved MLAEP during opioid-based anaesthesia allow the processing of auditory information.

2.3.2.2 AEP Index

The AEP index is a mathematical derivative which reflects the AEP waveform morphology, and is calculated from the amplitude difference between successive segments of the MLAEP.

Gajraj *et al.* (1998, 1999) used the AEP index to distinguish the transition from unconsciousness to consciousness. They reported that the AEP index was better than BIS at distinguishing consciousness from unconsciousness, while BIS correlated well with predicted blood concentration of propofol. They concluded that AEP index provides a measure of the overall balance between surgery, analgesia and hypnosis. This characteristic of the MLAEP is also supported by Thornton *et al.* (1988, 1989b). They reported that the amplitude of cortical waves in the AEP are sensitive not only to anaesthetic concentration but also to surgical stimulation.

Doi *et al.* (1997) also stated that the AEP index did not correlate with blood propofol concentration before eye opening. They observed that the AEP index reflects the level of consciousness rather than blood concentration of propofol. Schraag *et al.* (1999b) proved that the AEP index has more discriminatory power (describing the transition from conscious to unconscious state) than BIS.

2.3.2.3 AEP Feature Extraction using the Wavelet Transform

One of the methods used for detailed feature extraction from recorded AEP during anaesthesia, is the wavelet transform (WT) (Backory, 1999; Lee *et al.*, 1997, 1998; Miller *et al.*, 1998; Qin *et al.*, 1998; Thakor *et al.*, 1993). The WT has also been used for feature extraction of other biomedical signals such as the electrocardiogram (ECG) (Bahoura *et al.*, 1997; Li *et al.*, 1995). The power of the WT lies in its multiscale information analysis which can characterize a signal very well. The WT has potential for processing time-varying biomedical signals.

Multiresolution analysis (MRA) with WT was used to decompose the signal into approximations at different scales of resolution. The wavelet coefficients of the MLAEP detail components were used to calculate the average energy in each of the components (Abbod and Linkens, 1998b; Backory *et al.*, 1998; Linkens *et al.*, 1997a). These features were validated by Backory (1999) using data from 14 patients under general anaesthesia.

Stockmanns *et al.* (1997) investigated if the WT could be used for the quantification of the MLAEP signal. Their analysis was based on the consecutive extraction of the details from the original signal. The MLAEP of 7 healthy volunteers were processed by a one-dimensional discrete wavelet-decomposition. Only one parameter was obtained by combining significant coefficients. This wavelet parameter of the MLAEP could detect anaesthetised and awake with similar accuracy and over-all classification comparable to the Nb latency. This method was not used under clinical conditions, therefore no interference from noxious stimulus is present.

Nayak and Roy (1998) used the discrete time wavelet transform (DTWT) to compact the MLAEP. A step wise discriminant analysis was performed to obtain three features from the MLAEP that could separate responders from nonresponders. They reported that acceptable clinical performance was obtained in dogs.

Nayak and Roy (1995) compared the DOA prediction performance of the WT with power spectrum and the autoregressive parameter of the MLAEP. Results showed that WT parameters used in combination with anaesthetic concentration classified correctly all the testing data. The better performance of the WT was attributed to good localization in the time frequency domain and low sensitivity to signal-to-noise ratio. In this study, MLAEP data was collected from dogs under isoflurane anaesthesia.

2.3.2.4 Other Methods of AEP Feature Extraction

Munglani *et al.* (1993) used coherent frequency of the AEP as a measure of consciousness in isoflurane anaesthesia. The coherent frequency of AEP is derived using auditory clicks presented at frequencies in the range 5-47 Hz (after Fourier transform). They concluded that the coherent frequency reflects the likelihood of cognition during anaesthesia, as it showed consistent changes with anaesthetic administration and stimulation.

Elkfafi *et al.* (1997) processed the AEP using a parametric identification technique. The basis of this approach was a parametric model (ARX) provided for both the required signal (AEP) and the superimposed noise (EEG). Three factors were elicited to describe the changes in amplitudes and latencies of MLAEP. They compared the use of AEP with the use of classical cardiovascular parameters for monitoring DOA. AEP signals gave reliable results in all cases while sometimes SAP and HR did not represent DOA adequately for physiological reasons (e.g. blood loss, fluid loss).

Allen and Smith (2001) used a simple back-propagation neural network to extract pertinent features for the AEP signal. These features are used as input to a control system for administration of anaesthetic.

2.4 Monitoring and Control in Anaesthesia

The adequacy of a DOA monitor has been deeply discussed in the research area. Ideally, such a monitor should distinguish between the awake and the unconscious state and should not be affected by the haemodynamic status of the patient or by vasoactive drugs. A reliable monitor of DOA should present similar answers with different anaesthetic drugs administered to equal potency. Furthermore, it should have the ability to control anaesthesia in a closed-loop system.

A closed-loop control system for anaesthesia allows more frequent and more accurate adjustments to the DOA (i.e. automated and online measurement of DOA). As a result, better control is possible. The anaesthetic drug is titrated according to the individual patient, allowing for interpatient variability of pharmacokinetics and pharmacodynamics, and responding to changes of surgical stimuli. General anaesthesia would be safer for the patient as it helps to reduce the incidence of awareness and overdose, and optimizes the recovery times. If automated, the system would help the anaesthetist by reducing his workload and supplementing clinical signs (which the anaesthetist has access to) with information from within the CNS.

Absalom and Kenny (2000) commented on the usefulness of closed-loop control systems as a research tool in anaesthesia, for the study of the effects of drug interactions and different anaesthetic techniques. These systems can also be used as a supplementary training tool for anaesthetists (Schuttler and Schwilden, 1996).

A closed-loop control system in anaesthesia should be able to achieve and maintain an adequate level of DOA. In the previous section a review was carried out of the anaesthetic depth indicators used in anaesthesia. In this section, a general review about the control and monitoring systems used by researchers is presented.

Greenhow *et al.* (1992) described an expert system called RESAC (real time expert system for advice and control) that provides decision-support for control of anaesthetic depth by merging a number of qualitative clinical signs and quantitative on-line measurements.

RESAC uses fuzzy logic and Bayesian inference to cope with conflicting and uncertain evidence of the clinical signs. The system is an advisor to the anaesthetist as to the anaesthetic state. Linkens and Rehman (1992) demonstrated the ability of an artificial neural network (ANN) to replicate the advice from RESAC. They used target values of HR, SAP and respiration rate (desired by the anaesthetist for individual patients undergoing surgery) as inputs for the training of the program.

Webb *et al.* (1996) describes a preliminary study of automatic control of anaesthetic drug during surgery, in an attempt to improve the quality of control, to minimise drug usage, and to minimise the recovery time from surgery. The technique combines a fuzzy logic controller and a neural-based processing of the AEP.

An automatic model based control of volatile anaesthetics exploiting the MF was used by Asteroth *et al.* (1997) to adjust the vaporizer settings. However, an explicit invertible model is required to capture the dependence of control parameters and effects. Due to mathematical restrictions, this approach cannot be generalised to more than one narcotic.

Mortier *et al.* (1998) used BIS to control propofol administration by a patient individualized adaptive model-based controller incorporating target controlled infusion (TCI) technology combined with a pharmacokinetic-pharmacodynamic model. The closed-loop system was able to sedate patients undergoing surgery under spinal anaesthesia. This reduced the clinical workload and the amount of drug infused. Morley *et al.* (2000) also used BIS as the target of a proportional-integral-derivative (PID) controller algorithm for drug administration, so as to free the anaesthetist from the task of adjusting anaesthetic depth manually. No clinical utility beyond this was demonstrated. Furthermore, the closed-loop system worked well in clinical practice but it did not perform better than the anaesthetist manual control.

Neural networks constitute popular approaches for estimating DOA from MLAEP features. Nayak and Roy (1998) used this approach to control inhalational anaesthetic concentration (isoflurane) delivered to a patient, based on a fuzzy logic controller. The system had a clinically acceptable performance in dogs.

Huang *et al.* (1999) used a system that determines DOA by assessing the characteristics of the MLAEP which were extracted by WT. A four layer ANN was used to classify the MLAEP features coupled with the effect concentration of propofol into responders and nonresponders. The DOA as determined by the ANN is regulated by a fuzzy logic based controller for the scheduled decrementation or incrementation of propofol. This system was

implemented using experiments with dogs.

Kenny and Mantzaridis (1999) used the AEP index as the input of a control algorithm that sets the blood level of propofol to be achieved by a TCI pump. The algorithm calculates the required target concentration of propofol from the difference between the measured AEP index and a set AEP index target values selected by the anaesthetist. There was no incidence of intraoperative awareness and movement interfering with surgery was minimal in the 100 patients studied. Note that the anaesthetist needs to be familiar with values of the AEP index so as to be able to select an adequate target.

The AEP index is also used by Kenny (2000) in a closed-loop control system to administer propofol in 100 patients breathing spontaneously and also in patients who received a paralysing drug during surgery. The quality of anaesthesia was judged to be satisfactory as assessed by scores of automatic activity, cardiovascular stability and minimal movement during surgery. No occurrence of awareness was reported.

A simple back-propagation neural network can learn the AEP and provide a satisfactory input to a fuzzy logic infusion controller for the administration of anaesthetic drugs. This approach is used by Allen and Smith (2001). Neural networks were also used by Vefghi and Linkens (1999) to classify SAP, HR, respiration rate, age, weight and sex into three anaesthetic states (aware, relaxed and deep). The network accurately mapped the different variables into the corresponding anaesthetic states and dosage for different patients.

Decision support information in anaesthesia is becoming more and more popular. Lowe *et al.* (2001) developed an intelligent monitor with intuitive graphical presentation of decision-support information for the anaesthetist. Jones *et al.* (2001) used fuzzy trend templates to develop a sentinel anaesthesia monitor to lighten the cognitive load of the anaesthetist. There is a motivation for developing an automated (and therefore vigilant) system that would be able to detect the presence or onset of an undesirable state of health in the anaesthetised patient, and present a possible diagnosis to the attending anaesthetist. The fuzzy trend templates were a good representation of the anaesthetist diagnosis knowledge (Lowe *et al.*, 1999a, b) . Previously, Becker *et al.* (1997) designed an intelligent patient monitoring and alarm system for the operating theatre. This system evaluated the patient's haemodynamic state using a knowledge-based approach on the basis of a vital parameter database. This knowledge base is formed by evaluation rules expressed by the anaesthetist in natural language. The research prototype of the whole system was implemented and evaluated in the operating theatre. The evaluation of 684 events yielded a sensitivity and

predictability of the alarm recognition on more than 99%.

Zhang and Roy (1999, 2001) used an adaptive network-based fuzzy inference system (ANFIS) to integrate EEG extracted features for decision making in anaesthesia. By eliciting fuzzy IF-THEN rules the model provides a way to address the DOA estimation problem. This monitoring system was implemented in experiments with dogs under propofol anaesthesia.

A multitasked closed-loop control consisting of two additional controllers is presented by Gentilini *et al.* (2001a). They tried to control MAP and control hypnosis through BIS, for isoflurane anaesthesia. This is an advisor control system used with the anaesthetist close supervision. Another decision support system was designed by Graaf *et al.* (1997) and offers data processing to alert the anaesthetist.

Linkens and colleagues (Abbod *et al.*, 1998; Backory *et al.*, 1998; Elkfafi *et al.*, 1997; Linkens and Abbod, 1998; Linkens and Mahfouf, 2001; Linkens *et al.*, 1996b; Linkens *et al.*, 1998) have been engaged in research into modelling and control in biomedicine for many years. A hierarchical fuzzy monitor for DOA was developed by Shieh (1994). This hierarchical structure has two levels, the first level used numerical clinical signs (SAP and HR) to interpret a primary DOA based on a rule-base derived by the anaesthetist experience. The second level used non-numerical data, such as sweating, lacrimation and pupil response which was merged with the primary DOA from the first level to decide with more confidence. Linkens *et al.* (1996b) used a self-organizing fuzzy modelling approach to generate the rules from the hierarchical structure on-line using input and output data. After this approach using only clinical signs the group started to research signals from within the CNS. A quantitative feature extraction was implemented to extract the factors describing the changes in amplitudes and latencies of the MLAEP. As a result, three principal factors were obtained and then merged together using qualitative fuzzy logic to create a reliable index for monitoring depth of anaesthesia (Elkfafi, 1995; Elkfafi *et al.*, 1997; Elkfafi *et al.*, 1998). Furthermore, a multi-sensor fusion system for monitoring and control of DOA was designed (Abbod and Linkens, 1998a; Linkens and Abbod, 1998; Linkens *et al.*, 1998). This system used neuro-fuzzy and multiresolution wavelet analysis for monitoring the DOA based on the MLAEP signal. Another measure of DOA was based on the cardiovascular system status using a rule-based fuzzy logic classifier. The two measures were merged together using rule-based fuzzy logic data fusion to decide the final DOA. Backory (1999) used an artificial neural network to classify the MLAEP extracted features into DOA levels. DOA was used as the input to a predictive controller that set the desired target blood

propofol concentration.

2.4.1 Target Controlled Infusion

Target controlled infusion (TCI) is an infusion system which allows the anaesthetist to select the target blood concentration required for a particular effect, and then control DOA by adjusting the requested target concentration.

TCI systems are very much in use by anaesthetists, specially since infusion pumps incorporate 'Diprifusor' (TCI system for propofol). These pumps can be used to induce and maintain anaesthesia with propofol. If using such a system, the anaesthetist simply needs to set the initial target blood concentration required for an intravenous drug in a similar way to setting the percentage concentration of an inhalational agent with a vaporiser. The target concentration is achieved and maintained with no further intervention required by the anaesthetist. However, the anaesthetist can make changes to the target concentration at any time.

The rational administration of TCI requires an appropriate pharmacokinetic data set. Software is required to achieve and maintain a target blood concentration of an anaesthetic by balancing the rate of infusion with the process of distribution and elimination (Jacobs, 1990). Therefore, information about the pharmacokinetic properties of the drug in appropriate patients is required. The choice of pharmacokinetic model and infusion control algorithm are major determinants of the performance of a TCI system

In the classical approach, TCI devices consist of an infusion pump attached to a computer. The computer is programmed with a pharmacokinetic model as well as pharmacokinetic data. The computer translates predictions from the model into instructions to control the infusion pump. The required infusion rate to maintain the desired target plasma concentration is delivered by the infusion pump. Many research groups developed their own system (e.g. Alvis *et al.*, 1985a, b; Chaudhri *et al.*, 1992; Glass *et al.*, 1990; Shafer *et al.*, 1990; White and Kenny, 1989). Since 1996 TCI devices have been implemented in the infusion pumps by a number of manufacturers, such as the 'Diprifusor' by Zeneca.

Glass *et al.* (1989) reported the accuracy with which propofol was delivered using two different sets of pharmacokinetic parameters. They concluded that by using the newer set of parameters the accuracy of the predicted (by the TCI) and measured propofol levels would be better. White and Kenny (1989) also compared the predicted and measured blood

concentrations of propofol in 408 patients. They confirmed the overall validity of their TCI system.

Russell *et al.* (1995) compared a manual infusion with TCI of propofol in 160 patients. The TCI resulted in a more rapid induction of anaesthesia and allowed earlier insertion of a laryngeal mask airway. In addition, there was less response to surgical stimulus. TCI does not change the properties of drugs and the theoretical advantage over manually controlled infusions is increased controllability by the anaesthetist (van den Nieuwenhuyzen *et al.*, 2000).

TCI has also been investigated for use in analgesia by Milne and Kenny (1998). The synthetic opioids, such as alfentanil, remifentanil and sufentanil, all have shorter durations of action and are more suitable for use in TCI systems than opioids such as morphine, with a slow blood-brain equilibration. They reported a high degree of patient satisfaction when using patient-controlled analgesia (i.e. the patient controlled the target concentration using a push-button hand set).

Adjuvant agents such as sedative agents given for premedication, co-induction agents, nitrous oxide or one of the synthetic opioids, affect the required target propofol concentration during induction and maintenance of anaesthesia. The effects of these agents on the TCI system for propofol have been investigated by Vuyk (1998). He designed an infusion scheme so as to provide a good clinical performance of the TCI system in the presence of an optimal manually controlled infusion of an opioid.

The TCI systems are capable of creating a stable blood concentration. However, when the target concentration is changed the resulting effect correlates better with a theoretical effect site concentration. The efficacy of the TCI systems that can perform effect-site steering is still a process under investigation (Jacobs and Williams, 1993; van den Nieuwenhuyzen *et al.*, 2000).

2.5 Summary

Anaesthesia is a complex branch of the medical science profession. Depth of anaesthesia (DOA) (one of the three components of anaesthesia) offers a challenge in the areas of classification and control. In TIVA when different drugs are used to obtain hypnosis (i.e. DOA), muscle relaxation and analgesia, a reliable method of assessing DOA is of major

importance.

In this chapter a review of the advances in anaesthesia was presented, starting with the first time the word “Anaesthesia” was used, including the introduction of balanced anaesthesia, and finishing with the overall research projects dedicated to automated control systems. With all its advantages a closed-loop control system in anaesthesia needs a reliable numerical indicator of DOA before it can be successfully implemented in the operating theatre.

Initially, movement was used as a monitor for DOA. However, paralysis using neuromuscular relaxants prompted the search for other indicators. The next reasonable candidates were the qualitative clinical signs such as pupil diameter or respiratory movement, and the measurable haemodynamic parameters such as SAP or HR. Qualitative clinical signs are highly subjective and easily obscured by opioids, muscle relaxants and techniques such as artificial ventilation. Arterial pressure and HR are also affected by adjuvant agents such as β-blockers, but these signs are still useful and very must in use by anaesthetists. All these clinical signs are very useful in detecting inadequate anaesthesia, in the sense that if the patient moves or has high haemodynamic responses then DOA is not satisfactory. However, DOA may not be adequate even if the clinical signs do not present any evidence of this.

Unconsciousness should be measured from within the CNS, where the effect of the hypnotic drug occurs. The search for a signal from within the CNS started with the EEG. The EEG shows graded changes with increasing concentrations of anaesthetics, and it is not affected by neuromuscular agents. Nevertheless, EEG changes vary with different anaesthetic agents. As a result, researchers turned to the evoked potentials (EP) as the next candidates for investigation. Among all the EP, the AEP have been pointed out as the best signal for assessing DOA.

A signal which is able to reflect the hypnotic component of anaesthesia is the main objective of the AEP analysis. The MLAEP have been the focus of research in anaesthesia over recent years. MLAEP are known to distinguish the aware and unconscious state and the subsequent CNS depression. This signal provides a measure of the overall balance between surgery, analgesia and hypnosis. The techniques used to extract detailed features from the MLAEP were also discussed in this chapter. The WT appears to be the most promising for processing time-varying biomedical signals.

Closed-loop control systems in anaesthesia were presented. Different control algorithms

and classification techniques are used by researchers. All the above systems are used to control the administration of the anaesthetic drug (i.e. the hypnotic), while other adjuvant drugs such as the analgesic are administered by the anaesthetist. Most of these systems are advisors, except the ones tested in animals.

Artificial intelligent techniques such as ANN and fuzzy logic are mostly used, since direct measurements are unavailable, mathematical models are either unobtainable or too complex, and there is a large uncertainty in the process parameters (i.e. the patient).

Chapter 3

Development of a New Fuzzy Relational Classifier for Depth of Anaesthesia

3.1 Introduction

Fuzzy logic is no stranger to medicine. Lotfi A. Zadeh (1965) himself anticipated very early that the fields of pattern classification and information processing would be application domains of his theory.

Fuzzy set theory makes it possible to define inexact medical entities as fuzzy sets. It offers a linguistic approach that represents an excellent approximation to medical texts. Furthermore, fuzzy logic provides reasoning methods capable of making approximate inferences, since many uncertainties are present in medical or biological data as well as in the decision making process (Adlassing, 1986; Akay *et al.*, 1997).

The high complexity of biological systems, and the nonexistence of accurate mathematical models are some of the aspects that make fuzzy logic a well defined solution. The knowledge of experienced physicians and biomedical engineers is an important source of information for the design of intelligent machines in medicine. In Zadeh's own words (1994a):

"*The role model of fuzzy logic is the human mind.*"

Fuzzy logic has been widely used in diagnostic monitoring in anaesthesia and other areas of medicine. Several researchers have used fuzzy logic approaches for alarm and/or monitoring systems in anaesthesia (Becker *et al.*, 1997; Elkfafi *et al.*, 1998; Guez and Nevo, 1996; Lowe *et al.*, 1999a; Shieh, 1994). The basic concepts of fuzzy logic theory are

presented in Appendix B.

The classification of DOA is the first step when moving towards a closed-loop control system. As discussed in the previous chapter, different signals are used as indicators of anaesthetic depth. However, the main relevance is given to MLAEP as an indicator of the degree of hypnosis of a patient under anaesthesia.

Several methods have been used to classify MLAEP features into levels of DOA. Different researchers use different techniques. However, ANN and fuzzy logic based systems are already proving to be popular. From a simple four layer ANN (Huang *et al.*, 1999; Nayak and Roy, 1995, 1998) to a more complex Kohonen Self-Organizing Map (KSOM) (Backory, 1999), and including the back-propagation ANN (Allen and Smith, 2001), there are many examples of neural networks used in the area. Fuzzy logic has also been used in the classification of DOA; one of the fuzzy logic-based approaches is the adaptive network-based fuzzy inference system (ANFIS) used by Zhang and Roy (1999, 2001), and by Linkens and colleagues (Abbod and Linkens, 1998a, b; Linkens and Abbod, 1998; Linkens *et al.*, 1998). These classification methods are based on soft computing techniques, and although ANN have given fairly good results, they are still black box methods and it is not trivial to understand all the details behind the ANN final decision. Furthermore, to adequately train an ANN a large amount of clinical data is required, and these may in some cases be difficult to gather. As a result, some research on ANN has been carried-out using animals (Huang *et al.*, 1999; Nayak and Roy, 1995, 1998). The fuzzy logic-based classification systems appear to be more transparent as the anaesthetist's knowledge can be incorporated into the decision process.

In this chapter a Fuzzy Relational Classifier (FRC) for DOA is presented. This FRC uses features extracted from the AEP by multiresolution analysis (MRA) and wavelet transforms (WT), and cardiovascular parameters to enhance the overall decision making process. The FRC uses a combination of fuzzy clustering and fuzzy relations to establish an inference system. The classifier is trained by unsupervised fuzzy c-means clustering, then a fuzzy relation between cluster membership functions and the class identifiers is computed. The fuzzy relation specifies the existing relationship between the clusters and the classes (i.e. the different levels of DOA).

The FRC is described in detail throughout the chapter. First, an introduction to fuzzy clustering is presented, followed by the general structure of the classifier. Several aspects have to be considered when implementing the FRC to classify DOA including: the set of features used, the different levels of DOA, and how these are obtained and structured. The

classifier is trained and tested with different sets of clinical data. The results are presented and compared with the results of other classifiers.

3.2 Fuzzy Clustering

Cluster analysis intends to classify objects according to similarities among them, and to organize data into groups. The objective is to differentiate between classes in a manner which is simple and easy to visualize. As a result, solutions are restricted in an unknown way. The use of fuzzy sets is an attempt to resolve this problem.

In a 'hard' clustering algorithm, each object must be assigned to a single cluster. This restriction is not a realistic one, since many objects may have the characteristics of several classes. It is more natural to assign to each object a set of memberships, one for each class. This is the general idea of fuzzy clustering.

The first fuzzy clustering algorithm was presented by Ruspini (1969), as a method of representation of data, based on the idea of fuzzy sets. The objective was to avoid some of the problems of 'hard' clustering procedures and to provide a better insight into the structure of the original data. In 1973, Dunn developed the first fuzzy extension of the least-squared approach to clustering, and later in the year this was generalized by Bezdek to an infinite family of algorithms (Bezdek and Pal, 1991; Dunn, 1973). This approach conceived by Dunn is one of the most widely used algorithms within fuzzy clustering, the fuzzy c-means algorithm. This family of algorithms is based on an interactive optimization of a fuzzy objective function. They are popular due to their efficacy, simplicity and computational efficiency.

Different approaches to fuzzy clustering have been developed over the years. Gustafson and Kessel (1979) argued that the use of fuzzy covariances was a natural approach to fuzzy clustering. In addition, Karayiannis (1996) presented a new approach based on reformulation. He developed a new family of possibilistic c-means algorithms by selecting the natural logarithm as a generator function. In 1999, Hathaway *et al.* present an extended family of c-means type models, and attempts to empirically identify those which are least influenced by the presence of outliers (Hathaway *et al.*, 1999). In other study, Zahid *et al.* (1999) designed a clustering validity criterion and a fuzzy clustering algorithm based on the combination of the fuzzy c-means algorithm and the k-nearest neighbours decision rule.

Fuzzy clustering has been used for identification, modelling and monitoring in different areas. Tool condition monitoring in machining is one of the areas where fuzzy clustering has been successfully implemented (Fu *et al.*, 1998; Li and Elbestawi, 1996). Umayahara and Nakamori (1998) developed an elliptic type fuzzy modelling and simulation method using fuzzy clustering. The clustering algorithm is used to detect local linear varieties and implemented for prediction of water quality. Furthermore, Pal *et al.* (2000) used fuzzy clustering for extraction of rules from input-output data; this was implemented and tested in mathematical examples and in the inverted pendulum problem. Another application of fuzzy clustering is the medical diagnosis area, since biological systems are extremely complex and the boundaries between distinct medical diagnosis are not shapely defined (Steimann, 1997).

The mathematical structure of fuzzy clustering is presented next with a detailed description of the fuzzy c-means algorithm.

Each data observation consists of n measurable variables, grouped into an n-dimensional column vector $z_k = [z_{ik}, \ldots, z_{nk}]^T$, $z_k \in \Re^n$. A set of N observations is denoted by $Z = \{z_k | k = 1, 2, \ldots, N\}$, and is represented as an $n \times N$ matrix:

$$Z = \begin{bmatrix} z_{11} & z_{12} & \cdots & z_{1N} \\ z_{21} & z_{22} & \cdots & z_{2N} \\ \vdots & \vdots & \vdots & \vdots \\ z_{n1} & z_{n2} & \cdots & z_{nN} \end{bmatrix} \qquad 3\text{-}1$$

The columns of this matrix are called patterns (or objects), the rows are called the features (or attributes) and Z is called the data matrix. The meaning of the columns and rows depends on the context and will be defined when the method is applied (i.e. Section 3.4).

A cluster can be regarded as a group of objects that are more similar to one another than to members of other clusters. The objective is to partition the data set Z into c clusters (for the time being let's assume that c is known). Fuzzy clustering allows the objects to belong to several clusters simultaneously, with different degrees of membership (Bezdek and Pal, 1991; Babuska, 1998).

The next step is to define the fuzzy partition in terms of membership functions. Let us denote the membership function of z_k in the i cluster by $\mu_i(z_k) = \mu_{ik}$. A $c \times N$ matrix $U = [\mu_{ik}]$ represents a fuzzy partition if and only if its elements satisfy the conditions:

$$\mu_{ik} \in [0,1] \qquad 1 \le i \le c, 1 \le k \le N \tag{3-2}$$

$$\sum_{i=1}^{c} \mu_{ik} = 1 \qquad 1 \le k \le N \tag{3-3}$$

$$0 < \sum_{k=1}^{N} \mu_{ik} < N \quad 1 \le i \le c \tag{3-4}$$

Therefore, the fuzzy partitioning space of Z is the set:

$$M_{fc} = \left\{ U \in \Re^{c \times N} | \mu_{ik} \in [0,1], \forall i,k; \sum_{i=1}^{c} \mu_{ik} = 1, \forall k; 0 < \sum_{k=1}^{N} \mu_{ik} < N, \forall i \right\} \tag{3-5}$$

The i^{th} row of the fuzzy partition U contains values of the i^{th} membership function of the fuzzy subset i of Z. Equation 3-3 constrains the sum of each column to 1, and thus the total membership of each z_k in Z equals one.

Many of the fuzzy clustering algorithms are based on minimisation of the basic c-means objective function (Dunn, 1973), presented in Equation 3-6.

$$J(Z; U, v) = \sum_{i=1}^{c} \sum_{k=1}^{N} (\mu_{ik})^m \| z_k - v_i \|^2 \tag{3-6}$$

where

$$U = [\mu_{ik}] \in M_{fc} \tag{3-7}$$

is a fuzzy partition matrix of Z,

$$V = [v_1, v_2, \ldots, v_c] \qquad v_i \in \Re^n \tag{3-8}$$

is a vector of centres of clusters,

$$D_{ik}^2 = \| z_k - v_i \|^2 = (z_k - v_i)^T A (z_k - v_i) \tag{3-9}$$

is a squared inner-product distance norm ($A = I$ is the Euclidean norm), and

$$m \in [1, \infty) \tag{3-10}$$

is a weighting exponent, which determines the fuzziness of the resulting clusters. The value of Equation 3-6 can be seen as a measure of the total variance of z_k from v_i.

The fuzzy c-means algorithm is one of the most used fuzzy clustering algorithms, the details of this algorithm are presented in the next section.

3.2.1 Fuzzy c-means Algorithm

The minimization of the c-means functional (Equation 3-6) represents a nonlinear optimization problem that can be solved using a Picard iteration, for instance, through the first-order conditions for stationary points. This can be found by adjoining the constraint in Equation 3-7 to *J* using the Lagrange multipliers:

$$\overline{J}(Z;U,v) = \sum_{i=1}^{c}\sum_{k=1}^{N}(\mu_{ik})^{m}D_{ik}^{2} + \sum_{k=1}^{N}\lambda_{k}\left[\sum_{i=1}^{c}\mu_{ik} - 1\right] \qquad 3\text{-}11$$

and by setting the gradients of $\overline{J}$ with respect to *U*, *V* and λ to zero. If $D_{ik}^{2} > 0$, $\forall i$, *k* and $m > 1$, then $(U,V) \in M_{f_c} \times \Re^{n\times c}$ may minimize *J* only if:

$$\mu_{ik} = \frac{1}{\sum_{j=1}^{c}\left(\frac{D_{ikA}}{D_{jkA}}\right)^{\frac{2}{m-1}}},\ 1 \le i \le c \quad 1 \le k \le N \qquad 3\text{-}12$$

and

$$v_i = \frac{\sum_{k=1}^{N}(\mu_{ik})^{m}z_k}{\sum_{k=1}^{N}(\mu_{ik})^{m}},\ 1 \le i \le c. \qquad 3\text{-}13$$

Equation 3-13 gives v_i as the weighted mean of the data items that belong to a cluster, where the weights are the membership degrees. This is why the algorithm is called c-means. The general algorithm is presented next.

- First, given the data set *Z*, choose the number of clusters $1 < c < N$, the weighting exponent $m > 1$, the termination tolerance $\varepsilon > 0$ and the norm inducing matrix *A*.

- Second, initialize the partititon matrix $U^{(0)} \in M_{fc}$, then:

- **Repeat** for $l = 1, 2, \ldots$

Step 1: Compute the cluster prototypes (means):

$$v_i^{(l)} = \frac{\sum_{k=1}^{N}\left(\mu_{ik}^{(l-1)}\right)^{m}z_k}{\sum_{k=1}^{N}\left(\mu_{ik}^{(l-1)}\right)^{m}},\ 1 \le i \le c \qquad 3\text{-}14$$

Step 2: Compute the distances:

$$D_{ikA}^{2} = \left(z_k - v_i^{(l)}\right)^{T}A\left(z_k - v_i^{(l)}\right),\ 1 \le i \le c,\ 1 \le k \le N \qquad 3\text{-}15$$

Step 3: Update the partition matrix:

if $D_{ikA} > 0$ for $1 \le i \le c$, $1 \le k \le N$,

$$\mu_{ik}^{(l)} = \frac{1}{\sum_{j=1}^{c} \left(\frac{D_{ikA}}{D_{jkA}} \right)^{\frac{2}{m-1}}} \qquad 3\text{-}16$$

otherwise

$\mu_{ik}^{(l)} = 0$ if $D_{ikA} > 0$, and $\mu_{ik}^{(l)} \in [0,1]$ with $\sum_{i=1}^{c} \mu_{ik}^{(l)} = 1$

until $\| U^{(l)} - U^{(l-1)} \| < \varepsilon$.

3.3 Structure of the Fuzzy Relational Classifier

The objective is to identify structures in data similar to known structures. A fuzzy logic relation is used to establish the correspondence between structures in the features space and the class identifiers.

3.3.1 Training the Classifier

The training of the fuzzy relation classifier requires two steps. First, unsupervised fuzzy c-means clustering is performed in the feature space, then, from the obtained fuzzy partition and the labels of the training data set, a fuzzy relation is computed. Figure 3-1 shows a diagram explaining the training procedure.

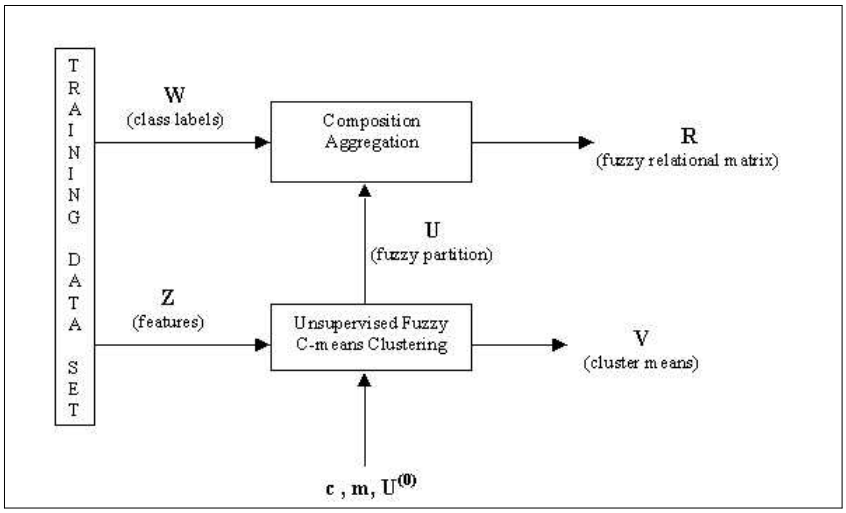

Figure 3-1: Training of the Fuzzy Relational Classifier.

3.3.1.1 Exploratory Data Analysis

The features space is partitioned to represent the natural structures in the data. These structures are discovered by unsupervised cluster analysis using the fuzzy c-means algorithm described in Section 3.2.1.

The data should be considered in the matrix form 3-1. The training data set *Z* is partitioned into *c* fuzzy subsets (clusters). The membership of the data samples in the clusters is described by the fuzzy partition matrix *U* and each cluster is characterized by its centre v_i, Equations 3-7 and 3-14 respectively.

Prior to clustering, several parameters have to be defined in the algorithm, i.e. *c* (number of clusters), *m* (fuzzy exponent) and ε (termination tolerance). The choice of *c* can be verified by assessing the validity of the obtained partition. The Xie-Beni index (Xie and Beni, 1991) is a commonly used validity criterion, of the form:

$$\chi(U,V;Z) = \frac{\sum_{i=1}^{c}\sum_{k=1}^{N}\mu_{ik}^{m}\|z_k - v_i\|^2}{N\left(\min_{i\neq j}\{\|v_i - v_j\|\}^2\right)} \qquad 3\text{-}17$$

The definition of $\chi(U,V;Z)$ is independent of the algorithm used to obtain μ_{ij}. Therefore, it is not internal to the clustering algorithm. The best partition is the one that minimises the value of $\chi(U,V;Z)$, since a smaller $\chi(U,V;Z)$ means a more compact and separate c-partition. The cluster algorithm is run for different values of *c* and *m*, and then several times for each of these settings with a different initialization matrix. The number of

clusters, which minimizes the measure, is finally set.

3.3.1.2 Fuzzy Relation

A fuzzy relation encodes the logical relation between the cluster membership and the class membership. This relation is computed from the information in the fuzzy partition matrix U and in the target vectors containing the membership of the pattern in the classes. The k^{th} target vector is denoted by:

$$w_k = [w_{1k}, w_{2k}, \ldots, w_{Lk}]^T \qquad 3\text{-}18$$

where $w_{jk} \in [0,1]$ and $L \in \aleph$ is the number of classes. For the training data, where the classification is exactly known, $w_{jk} \in \{0,1\}$. The target vector w_k is then a vector of all zeros except for a one at the place of the known class index.

For each of the training samples z_k, the vector of cluster membership degrees μ_{ik} is contained in the k^{th} column of U.

$$\mu_k = [\mu_{1k}, \mu_{2k}, \ldots, \mu_{ck}]^T \qquad 3\text{-}19$$

The binary fuzzy relation, R, is a mapping $R : [0,1]^c \times [0,1]^L \rightarrow [0,1]$. It can be represented as a $c \times L$ matrix:

$$R = \begin{bmatrix} r_{11} & r_{12} & \cdots & r_{1L} \\ r_{21} & r_{22} & \cdots & r_{2L} \\ \vdots & \vdots & \vdots & \vdots \\ r_{c1} & r_{c1} & \cdots & r_{cL} \end{bmatrix} \qquad 3\text{-}20$$

The relation R is obtained by aggregating the partial relations R_k, computed for the training samples (Pedrycz, 1994).

$$(r_{ij})_k = \min(1, 1 - \mu_{ik} + w_{jk}) \qquad j = 1,2,\ldots,L \qquad i = 1,2,\ldots,c \qquad 3\text{-}21$$

The aggregation of the relations R_k is computed by means of a fuzzy conjunction operator:

$$R = \bigcap_{k=1}^{N} R_k \qquad 3\text{-}22$$

implemented element-wise by the minimum function:

$$r_{ij} = \min_{k=1,2,\ldots,N} [(r_{ij})_k] \qquad 3\text{-}23$$

The relation matrix R is the basis of the FRC, since it is used to classify unseen patterns.

3.3.2 Classification of New Patterns

The main objective of any classifier is to determine the class of a new pattern. First, the cluster membership function μ is calculated from the distances to the cluster centres, v_k, as in the fuzzy c-means algorithm. Second, the class membership function vector w is computed by fuzzy relation composition using the Lukasiewicz implication:

$$w_j = \max_{1\le i\le c} [\max(\mu_i + r_{ij} - a, 0)] \quad j = 1, 2, \ldots, L \qquad 3\text{-}24$$

where a is considered to be one in the initial algorithm used by Setnes and Babuska (1999). Finally, defuzzification is applied to obtain a crisp decision, using the maximum method, i.e.:

$$y = \arg \max_{1\le j\le L} w_j \qquad 3\text{-}25$$

where y is the class index. Figure 3-2 illustrates this classification procedure.

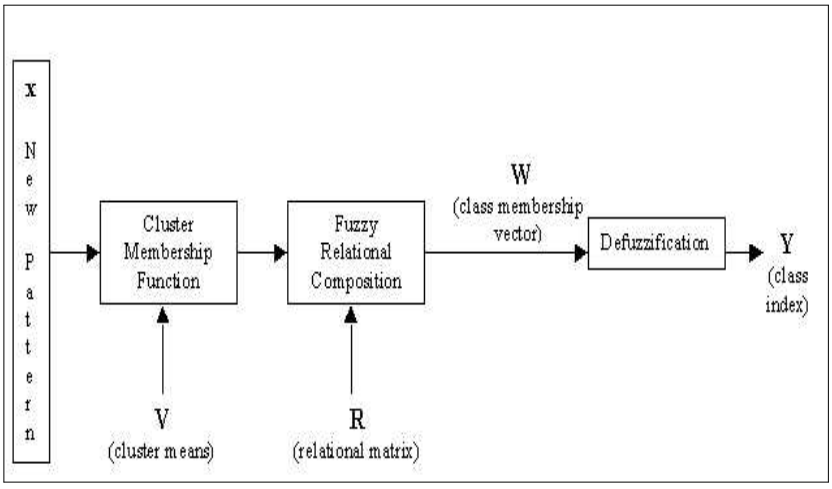

Figure 3-2: Classification of a new pattern by the FRC.

Note that the FRC can classify a new pattern well, wrongly, or not classify it at all. Unclassified cases happen when multiple j's satisfy Equation 3-25, meaning that a pattern

has the same membership value in more than one class. This could be due to noise in the features, misclassifications of training samples or inappropriate feature selection. Therefore it is necessary to select the best features so that no unclassified cases occur. Applying a fuzzy relation for classification will in general decrease the number of misclassifications. Furthermore, the FRC is not sensitive to the order in which training examples are presented and the risk of overtraining is eliminated.

3.4 Classification of Depth of Anaesthesia

The FRC is used to classify a set of features into different DOA levels. The computed fuzzy relation specifies the existing relationship between the clusters and the classes (i.e. levels of DOA).

The classifier will use two sets of features on the classification process. The first set is constituted from the AEP signal, and the second set is constituted from the cardiovascular parameters. These features are described in detail in the following sections.

3.4.1 Auditory Evoked Potentials Parameters

The AEP were recorded in the operating theatre using surface electrodes. The recording system used in this research was the one developed by the Intelligent Systems Group, in the Department of Automatic Control and System Engineering, the University of Sheffield. This system was used in previous researches (Abbod and Linkens, 1998a; Abbod *et al.*, 1998; Backory *et al.*, 1998; Linkens *et al.*, 1997a, b), it comprises an IBM-compatible PC (Intel PI 150 MHz) fitted with a Digital Signal Processing (DSP) board. A pre-amplifier is used to amplify the responses before they are transmitted to the DSP board where the signal is analogue-filtered and digitised.

The auditory stimulus in the patient's headphones is produced at a rate of 6.122Hz. The EEG is sampled at a frequency of 1kHz after passing through an analogue band-pass filter (0.5-400 Hz), for a sweep period of 120 ms after each click (i.e. 121 data points). The computer produces an average of 188 data sweeps plus calculation time, each 30 seconds. This time was judged to be short enough to assume that surgical and anaesthetic influences are static.

The system used to collect the AEP displays only the averaged AEP and its double differential value. The first step in the classification process is to consider the problem of what discriminatory features to select and how to obtain these features, as discussed in Chapter 2. In this research, the multiresolution analysis (MRA) using wavelet transforms (WT) is used to analyse the AEP during anaesthesia, so as to reflect the changes in amplitude and latency associated with DOA.

The WT is different from the Fourier transform, because it can zoom on arbitrary details of signals. The Fourier analysis is a mathematical technique for transforming our view of the signal from a time-based to a frequency-based one. In moving to the frequency domain, time information is lost. When looking at a Fourier transform of a signal, it is impossible to tell when a particular event took place. The wavelet analysis is a windowing technique with variable-sized regions. It allows the use of long time intervals where we want more precise low frequency information, and shorter regions where we want high frequency resolution (Hess-Nielsen and Wickerhauser, 1996). Therefore, wavelet analysis is capable of revealing aspects of data that other signal analysis techniques miss, aspects like trends and breakdown points. Also it compresses or de-noises a signal without appreciable degradation. All these positive points make wavelet analysis a good tool to analyse biomedical signals. The MRA technique and the WT are described further in Appendix C.

The signal, made of 121 samples (corresponding to the first 120 ms of the EP post-stimulus), is extended to 128 samples by padding the signal with extra zeros at the end, so that six levels of decomposition may be achieved using the multiresolution decomposition algorithm. The MRA decomposes the AEP into different resolutions allowing a detailed analysis of the behaviour of the signal in its different spectral bands (Rioul, 1993). The decomposed components were analysed for their energy content and used as an indicator of the DOA. The Daubechies Wavelet with 12 filter coefficients was used for decomposing the AEP signal (Mallat, 1999). Daubechies Wavelets have also been used by Abbod *et al.* (1998) and Backory (1999). This filter was found to produce good results and is of low order for the 121 discrete samples to be analysed.

Table 3-1 describes the different signal components obtained as a result of the MRA decomposition. There are 6 detail signals and a residual component.

Table 3-1: Table describing the different signal components obtained by MRA decomposition.

Signal Component	Samples in sequence
S1	64
S2	32
S3	16
S4	8
S5	4
S6	2
residual	2

Component S1 has the shortest analysis time of 2 ms, while the lowest frequency detail component S6 has an analysis time of 64 ms. However, the details in Table 3-1 contain the samples making up the brainstem and the late latency waves, which do not contain information related to DOA. Therefore, components in each detail regarding these waves were removed after the MRA. The component 6 which represents the low frequency range (8-16), and the residual contain a large amount of background EEG signal and are, therefore, not used.

The average energy contained in each detail signal is calculated as follows:

$$D_k = \frac{1}{n_k} \sum_{i=1}^{n_k} |S_k(i)|^2 \qquad 3\text{-}26$$

where

D_k is the energy contained in detail component k;
n_k is the number of samples in detail component k;
S_k is the detail sequence k;
i is the sample number.

Table 3-2 shows the features that have been analysed for correlation with DOA as well as the samples making up the components (Backory, 1999). D_1 is the energy contained in samples 9 to 56 in S_1, and is similar for S_2, S_3, S_4 and S_5. D_{31} is the energy contained in samples 3 to 6 in S_3, and is similar for the other features.

Table 3-2: Table describing the samples in each component used to create the features used in the validation process.

Energy Component	Samples used
D_1	9-56
D_2	5-28
D_{31}	3-6
D_{32}	7-10
D_{33}	11-13
D_{41}	2-3
D_{42}	4-5
D_{43}	6-7
D_{51}	2
D_{52}	3

Different sets of features are used in different research works with different classification methods, for example Abbod *et al.* (1998) and Linkens *et al.* (1997b) used 6 of these features (D_1, D_2, D_{31}, D_{32}, D_{33}, and D_4) while Backory (1999) used a different set (D_1, D_2, D_3, D_4, D_{51} and D_{52}). These features have given good results using an ANFIS classifier and a KSOM.

In this project 10 features are used in the classification process using the FRC. D_{41}, D_{42} and D_{43} are averaged to produce D_4, and similar for D_3 and D_5. Several combinations of AEP features were tested. However, the set of features D_1, D_2, D_3, D_{31}, D_{32}, D_{33}, D_4, D_5, D_{51} and D_{52} gave the best results considering the data available.

3.4.2 Haemodynamic Parameters

Anaesthetists have always used the cardiovascular system as an indicator of DOA, therefore, it is reasonable to use these measurements to enhance the overall decision making process.

The cardiovascular signals such as the heart rate (HR), the arterial pressure (i.e. systolic (SAP), diastolic (DAP) and mean (MAP)) and the pulse rate are measured on-line using a Datex-Engstrom AS/3 (anaesthesia monitor) connected to the computer through an RS232 port, at every 30 second interval.

SAP or MAP have been used for monitoring and control in anaesthesia. Robb *et al.* (1993) reported that a simple control system designed to maintain SAP at a predetermined value

produces a clinically acceptable state of anaesthesia (pattern of clinical signs). This supports the idea that SAP is a major component of the clinical assessment of the anaesthetic state. Other researchers use MAP as the indicator of cardiovascular stability when using inhalational agents (Gentilini *et al.*, 2001b) or intravenous agents such as propofol (Linkens *et al.*, 1993; Rao *et al.*, 2000). The most prominent effect of propofol in the haemodynamic responses is a drop in arterial pressure. During maintenance of anaesthesia SAP remains 20% to 30% below baseline values and similar changes can be seen in the mean pressure. This decrease in arterial pressure is associated with a decrease in cardiac output (Sasada and Smith, 2000).

The features used are the change of the individual patient baseline of HR, SAP and MAP, denoted by ΔHR, ΔSAP and ΔMAP. The use of the Δ values allows generalization, since the patient baselines are available before the operation and are considered as an input to the system. The variability between patients is high when considering haemodynamic parameters. For example, the normal ranges for SAP oscillate between 100 mmHg to 150 mmHg. As a result, the use of Δ values facilitates classification and reflects the cardiovascular depression independently of the patient baseline values.

3.4.3 Levels of Depth of Anaesthesia

According to the anaesthetist opinion the DOA was classified into five levels:

1- Awake;
2- OK/Light;
3- OK;
4- OK/Deep;
5- Deep.

Awake is when the patient response to surgical stimulus is not acceptable anymore. OK/Light is when there is a slight patient response, i.e. clinical signs demonstrating that the patient is getting lighter. OK is when no patient response is observed under surgical stimulus, i.e. the patient is in the adequate level of DOA. OK/Deep is when there is no patient response, but the patient is slightly deeper than necessary and still stable. Deep level is when the patient is clearly in a deep level of DOA, this is not safe for all patients and should be an indicator that something is wrong.

The OK and the OK/Deep levels are the most difficult to distinguish from one another and

are also the ones that occur more frequently during anaesthesia. A certain overlap between these two levels is expected through. While the arousal of clinical signs indicates that anaesthesia is getting lighter, the deeper depression of these signs may already indicate a Deep level of DOA. The OK/Deep level, which is often accepted by the anaesthetist as the interchange between OK and OK/Deep, is very frequent and also depends on the amount of surgical stimulation at the time. This is a very complex issue, since it is very difficult to measure analgesia and even if theoretically analgesia and DOA are two different entities. In practice, when confronted with a high surgical stimulus the anaesthetist tends to increase the concentration of both drugs (i.e. anaesthetic and analgesic), since the effects of surgical stimulation on the haemodynamic responses are the same as lighter anaesthesia (i.e. increases in HR and SAP). The information about the CNS depression is very useful in this situations, as it reflects the level of hypnosis. Therefore, the anaesthetist would easily distinguish if the arousal in the cardiovascular parameters is or is not caused by surgical stimulation, and if so, only the analgesic would be titrated accordingly.

In this research, the data were labelled by the anaesthetist based on the observed clinical signs during anaesthesia. This information was obtained at regular intervals and when a change in DOA level occurred, as to reflect the trend in anaesthetic depth of the patient. However, the anaesthetist uses only his experience and the patient clinical signs to establish the trend in anaesthetic depth. The information regarding AEP (i.e. depression in the CNS) during anaesthesia is not available to the anaesthetist.

3.5 Implementation and Results

The data used to train and test the FRC were obtained from two patients undergoing general surgery at the Royal Hallamshire Hospital in Sheffield. Anaesthesia was maintained using propofol as the anaesthetic drug and remifentanil as the analgesic drug. The drug profiles and the particular details of this surgical interventions are presented in Chapter 4. Figure 3-3 shows one of the AEP features from the data of patient Pat2 used to train and test the FRC, other graphs of the wavelet extracted AEP features are presented in Chapter 5.

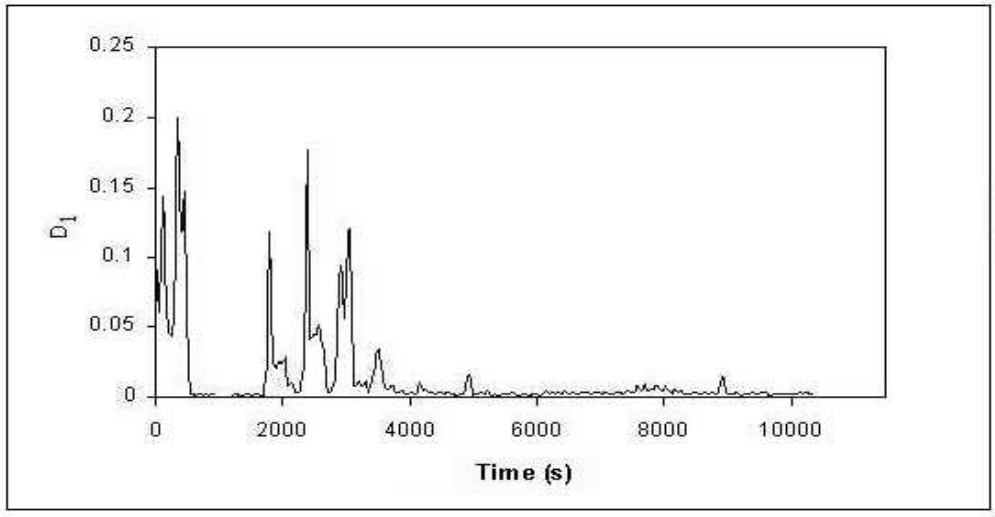

Figure 3-3: Wavelet extracted AEP feature D_1 from the data of patient Pat2.

The implemented FRC algorithm involves two distinct classifiers trained separately. The first FRC was trained using a set of wavelet extracted features from the AEP as the input pattern. In addition, the second FRC uses the cardiovascular parameters ΔHR and ΔSAP. Figure 3-4 presents the overall classification diagram.

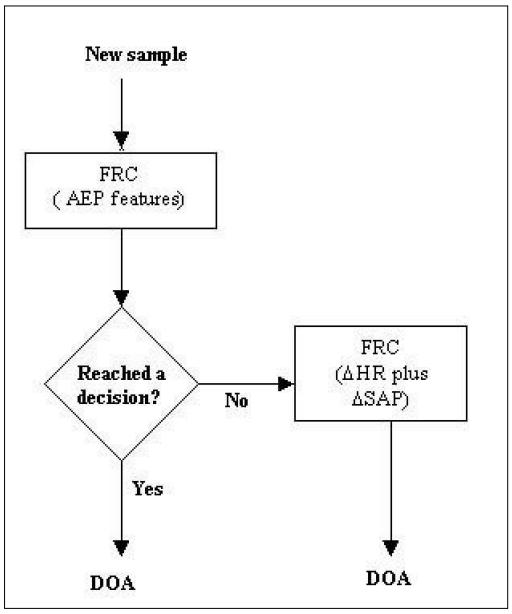

Figure 3-4: General classification algorithm.

Considering that the FRC may not reach a decision if multiple *j*'s satisfy Equation 3-22 or the vector in Equation 3-21 is all zeros, alternatives to the wavelet AEP features have to be considered. Therefore, the FRC is applied separately to the cardiovascular measurements

and trained to obtain a decision based only on these measurements. In conclusion, the two FRC's (the first using the AEP features and the second using ΔHR and ΔSAP) work separately. The main decision belongs to the AEP features classifier, if a decision is not reached then the cardiovascular parameters are used to determine DOA.

In the original algorithm, Setnes and Babuska (1999) use a value of $a = 1$ in Equation 3-21. The value of a makes the decision restricted, i.e. it forces the membership μ and the relational value to be both high. For example, is $\mu = 0.75$ and the associated relational value is 0.2 the classifier will not reach a decision; this was found to work well for well identified cluster/class groups. In the case of the AEP features where the feature space is of high dimension and the cluster classification is not distinct or obvious, using a value of $a = 1$ restricts the classification to the prototypes (training set) and hence impedes the generalization process. The objective is to obtain a general classifier that performs well for different patients considering that different patients have different characteristics. For the AEP there is no known baseline for the patient, therefore it is admissible that different patients respond in slightly different ways with respect to brain signals. The AEP FRC was tested for different values of a. The performance with the value of 0.75 proved to be better, by improving the classification percentage and reducing the number of unclassified cases, i.e. it helps to capture the variation between patients. Note that the value of a cannot be too small, e.g. a value of 0.5 makes the incorrect classified cases increase drastically. This change in the algorithm was applied only to the AEP classifier. When the cardiovascular parameters are used (ΔHR and ΔSAP), a is kept equal to 1 since the patient variability is expressed in the baseline and not in the parameters.

The training data for the FRC consisted of 2/3 of the available samples and the remaining 1/3 was used as the testing set. The number of samples used are presented in Table 3-3.

The samples of patient Pat1 used in the training data set correspond to the first part of the surgical procedure while from patient Pat2 the last data samples were used. This is to allow information of different scenarios in a surgical procedure (e.g. induction and recovery).

Table 3-3 Fuzzy relational classifier training and testing data sets.

	Training data	**Testing data**
Patient Pat1	134	67
Patient Pat2	142	71
Total	276	138

3.5.1 AEP Features Selection

The set of AEP features needed for classification depends not only on the correlation with the DOA level, but also on the type of classifier used and on the amount of data available. First, the correlation between each AEP feature and the DOA level was computed and from there different combinations of features were tested based on the performance of the FRC.

A correlation coefficient is a number between -1 and 1 which measures the degree to which two variables are linearly related. If there is a perfect linear relationship between the two variables with a positive slope, we have a correlation coefficient of 1; if there is a positive correlation, whenever one variable has a high (low) value, the other has a high (low) value. If there is a perfect linear relationship with a negative slope between the two variables, we have a correlation coefficient of -1; if there is a negative correlation, whenever one variable has a high (low) value, the other has a low (high) value. A correlation coefficient of 0 means that there is no linear relationship between the variables. The formula of the correlation coefficient (ρ_{xy}) between two variables (X and Y) is:

$$\rho_{xy} = \frac{\mathrm{cov(X,Y)}}{\sigma_x \sigma_y} \qquad 3\text{-}27$$

where $cov(X,Y)$ is the covariance between X and Y, σ_x and σ_y are the standard deviations of X and Y respectively. Table 3-4 shows the correlation coefficients of all the AEP features and the DOA level as classified by the anaesthetist.

Table 3-4: Correlation coefficient between the AEP features and the DOA level.

AEP Feature	Correlation Coefficient
D_5	-0.3732
D_{51}	-0.1765
D_{52}	-0.3764
D_4	-0.3954
D_3	-0.1757
D_{31}	-0.1956
D_{32}	-0.1077
D_{33}	-0.1414
D_2	-0.1602
D_1	-0.0299

The value of -0.3954 is the highest correlation coefficient amoung the AEP features. This is not a very high value. However, this does not mean that there is no correlation between the AEP features and DOA, only that there is a small linear correlation when comparing DOA with individual features. Different AEP features represent different levels of resolution, different frequencies and therefore different levels of information about the CNS. As a result, it is not expected that a simple linear relation using only one of the features can adequately describe the DOA level. All correlation coefficients in Table 3-4 have one common feature, which is that they all have a negative value. This demonstrates (as expected) that the lower values of the AEP are associated with deeper levels of DOA, i.e. the depression of the CNS. As the DOA level increases from Awake to Deep (i.e. 1 to 5) the MLAEP signal becomes more flat (Figures 1-1 and 1-2), this in accordance with the fact that increasing MLAEP latencies are associated with increasing CNS depression (Chapter 2).

The FRC was trained and tested with normalized AEP features. The AEP features vector (z) is normalized using the following equation:

$$z = \frac{z - \overline{z}}{\sigma_z} \qquad 3\text{-}28$$

where, $\overline{z}$ is the mean and σ_z the standard deviation of vector z. This type of normalization translates and scales the axes so that all the features have zero mean and unit variance. The data should be appropriately normalized before clustering, since distance norms are sensitive to variations in the numerical ranges of different features. The Euclidean distance, used in the c-means algorithm, assigns more weighting to features with wide ranges than to those with narrow ranges.

The Xie-Beni index (Equation 3-17) was used to determined the optimal values of c and m for the unsupervised c-means algorithm. Different sets of AEP features were used as to determine the best classification. Tables 3-5 to 3-10 show the results of the FRC using different sets of AEP features on the testing data set (i.e. 138 samples). A correct classification is assumed if the DOA level matches the anaesthetist classification. Selecting appropriate features is very important for the optimization of performance of FRC for inappropriate selection of features can lead to unclassified patterns.

Table 3-5 shows the performance of the FRC using AEP features with a higher correlation coefficient (Table 3-4). The results show that these features are not sufficient for the classification process. The number of unclassified cases is high and this suggests that the feature set could be inappropriate or not reflecting all the aspects of the data. The

complexity of DOA is not easy to detect and this may compromise the efficiency of any classifier.

Table 3-5: Performance of the FRC using the D_5, D_{52}, D_4 and D_{32} AEP features on the testing data set. Xie-Beni optimum values of $c = 11$ and $m = 2.6$.

	Correct	**Incorrect**	**Unclassified**
Number of samples	26	10	102
Percentage of samples	18.8%	7.2%	73.9%

Table 3-6: Performance of the FRC using the D_5, D_{52}, D_4, D_2 and D_1 AEP features on the testing data set. Xie-Beni optimum values of $c = 9$ and $m = 2.6$.

	Correct	**Incorrect**	**Unclassified**
Number of samples	26	19	93
Percentage of samples	18.8%	13.8%	67.4%

Table 3-7: Performance of the FRC using the D_{51}, D_{52}, D_4, D_{31} and D_1 AEP features on the testing data set. Xie-Beni optimum values of $c = 5$ and $m = 2.6$.

	Correct	**Incorrect**	**Unclassified**
Number of samples	36	23	79
Percentage of samples	26.1%	16.7%	57.2%

Table 3-8: Performance of the FRC using the D_5, D_{51}, D_{52} and D_4 AEP features on the testing data set. Xie-Beni optimum values of $c = 5$ and $m = 2.4$.

	Correct	**Incorrect**	**Unclassified**
Number of samples	37	20	81
Percentage of samples	26.8%	14.5%	58.7%

Table 3-9: Performance of the FRC using the D_{51}, D_{52}, D_{31}, D_{32} and D_1 AEP features on the testing data set. Xie-Beni optimum values of $c = 5$ and $m = 2.6$.

	Correct	**Incorrect**	**Unclassified**
Number of samples	67	27	44
Percentage of samples	48.55%	19.6%	31.9%

Table 3-10: Performance of the FRC using the D_5, D_{51}, D_{52}, D_4, D_3, D_{31}, D_{32}, D_{33}, D_2 and D_1 AEP features on the testing data set. Xie-Beni optimum values of $c = 11$ and $m = 2.6$.

	Correct	**Incorrect**	**Unclassified**
Number of samples	85	53	0
Percentage of samples	61.6%	38.4%	0%

The second set of AEP features (Table 3-6) gave the same results as the first set. The inclusion of more high frequency detail features proved to introduce more information, and as a result the percentage of correct classified samples increased (Table 3-7). These results are confirmed in Table 3-8, where all high frequency features are used. However, the percentage of correct classified cases is still low. In Table 3-9, the low frequency feature D_1 and the details D_{31} and D_{32} are included so as to provide information over a wider frequency range. The number of correct classified samples increased drastically. This result indicates that all the frequency bands should be used so as to grasp all the information regarding DOA.

Finally, the whole set of AEP features was used. The results are presented in Table 3-10. The percentage of unclassified samples was reduced to zero, and the percentage of correct classified samples was greater than before when using different combinations of features. The set of all the AEP features reflects the different levels of resolution of the AEP signal. All the frequency bands are covered and the AEP details are decomposed to obtain all the relevant information. In addition, the small number of data available can influence the necessary number of AEP features for an adequate classification. A larger number of features is necessary to describe the DOA levels.

The best classification performance was obtained using the 10 AEP features (D_5, D_{51}, D_{52}, D_4, D_3, D_{31}, D_{32}, D_{33}, D_2 and D_1) with $c = 11$ and $m = 2.6$. This will be the set of AEP features used throughout this project.

3.5.2 Cardiovascular Parameters Selection

The FRC using only the AEP features was able to classify all the samples. As a result, the cardiovascular parameters would not have been used in the classification process. Nevertheless, the FRC was trained and tested with different combinations of cardiovascular parameters so as to determined the best classification.

The cardiovascular parameters ΔHR, ΔSAP and ΔMAP were studied for their correlation

with DOA. Table 3-11 shows the correlation coefficients of the different parameters. ΔSAP has the highest correlation coefficient, a value of -0.7 shows that there is a high linear correlation between ΔSAP and DOA. The negative sign is common to all of the parameters, describing the increasing cardiovascular depression as DOA becomes deeper. ΔMAP presents a correlation coefficient of -0.6, which is still high. This result indicates that arterial pressure reflects more variation with different DOA levels. ΔHR does not have a high correlation coefficient, however, it may still introduce relevant information in the classification process.

The systolic and mean arterial pressures were the first candidates as the FRC classification features. However, both ΔSAP and ΔMAP alone did not give good classification results (Figure 3-5). Hence, the next step was to include ΔHR in the classification process, for the cardiovascular stability is one of the major concerns in anaesthesia and this is reflected in the heart rate as well as in the arterial pressure. The anaesthetist uses both measures to assess DOA and both must be regulated so as to ensure an adequate patient stability. Figure 3-5 shows the percentage of correct classified samples (testing data set) by the FRC using the different sets of cardiovascular parameters (ΔSAP plus ΔHR, ΔMAP plus ΔHR, ΔSAP or ΔMAP).

Table 3-11: Correlation coefficient between the cardiovascular parameters and the level of DOA.

Cardiovascular Parameter	**Correlation Coefficient**
ΔHR	-0.0526
ΔMAP	-0.6081
ΔSAP	-0.7001

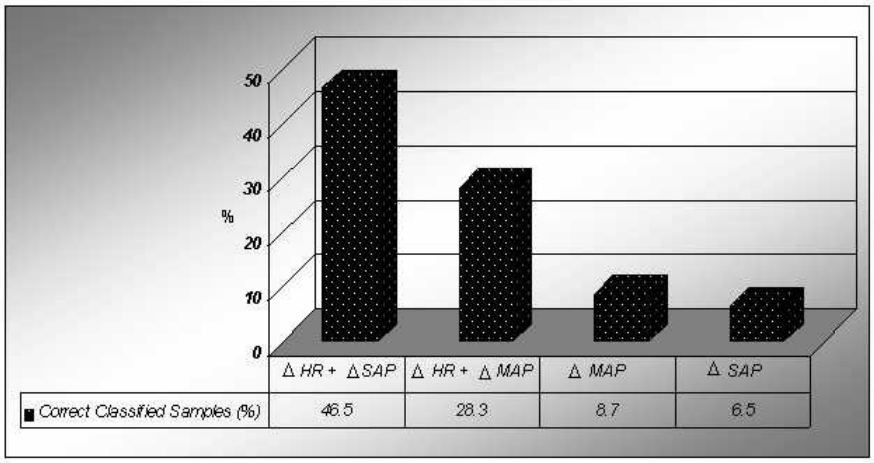

Figure 3-5: FRC percentage of correct classified samples (testing data set) using different parameters.

ΔHR plus ΔSAP performed better for classification. It was found that these parameters carry more relevant information considering the gradual changes in DOA levels.

The classifier which uses the cardiovascular parameters was able to classify 46.5% of the samples correctly with the Xie-Beni optimum values of $c = 13$ and $m = 2.6$. This result is hardly surprising since the AEP represent the brain depression of hypnosis. Nevertheless, a value of 46.5% is a reasonable percentage considering all that is involved in anaesthesia.

The cardiovascular system has always been an indicator of DOA for the anaesthetist. The use of these parameters is widely implemented, and the manual control of DOA is mainly based upon them when no information about the CNS is available.

The FRC which uses only the wavelet extracted AEP features was able to classify all the samples and as a result, the cardiovascular parameters were not used. However, they represent patient vital signs that should not be disregarded. The FRC using ΔSAP and ΔHR will remain as a reinforcement of the overall classifier.

3.5.3. General Results

The FRC using the AEP features was applied to the whole data of the two patients. Note that data from both patients were used to train and test the classifier. The results are presented in Table 3-12.

The percentage of correct classified samples is higher for patient Pat2 than for patient Pat1. However, both results are acceptable. Figures 3-6 and 3-7 show the FRC results for both patients Pat1 and Pat2 respectively. Analysing the figures, we can see that the majority of the incorrectly classified cases are between the OK/Deep and OK DOA levels. These are the two levels which were not easy to differentiate. In addition, there are less data from the Awake and OK/Light levels, nevertheless, these are more distinguishable from the other levels.

Table 3-12: Percentage of samples classified by the FRC using the AEP features.

Patient	Correct	Incorrect
Pat1	49.8%	50.2%
Pat2	59.6%	40.4%

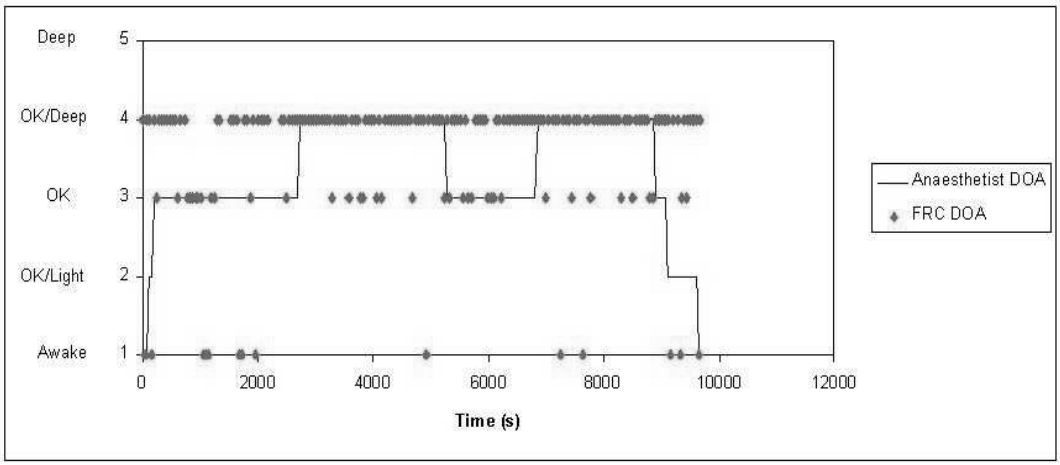

Figure 3-6: Results of the FRC using only the AEP features for the data of patient Pat1.

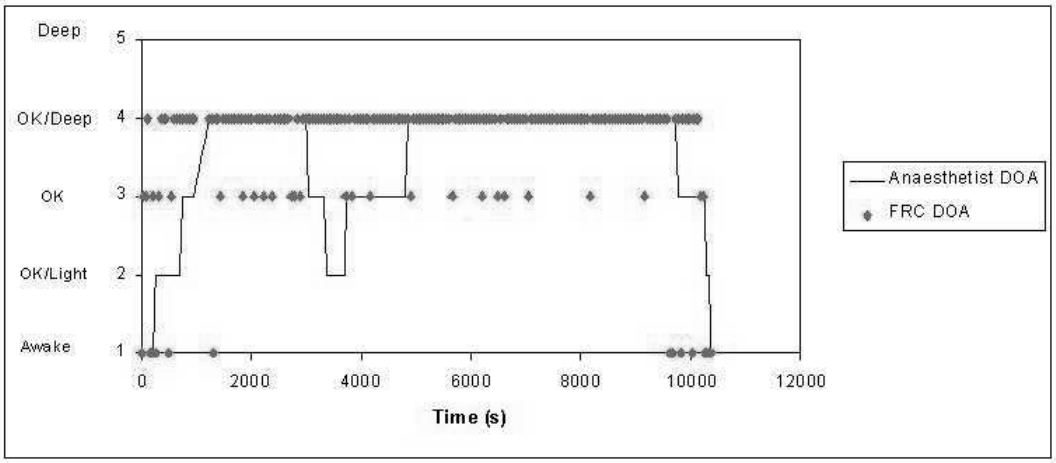

Figure 3-7: Results of the FRC using only the AEP features for the data of patient Pat2.

The FRC presents an acceptable performance and is capable of capturing the transition from awake to anaesthetised. Ideally, data from another patient should be used to analyse the overall efficiency of the classifier. However, this was not possible to gather due to circumstances beyond our control.

During both surgical procedures there were incidents of diathermy (use of electrical bisturi), which interfered with the recording of AEP. Diathermy is responsible for the samples classified as Awake after the induction of anaesthesia. This is more noticeable with patient Pat1. The electrical interference of diathermy on the AEP will be discussed in Chapter 5 with the modelling of the effects of surgical stimulus.

3.6 Comparison with other Classifiers

In this section, the results of the AEP features FRC are compared with the results of two other classifiers. First, a Kohonen Self-Organizing Map (KSOM) will be presented and secondly an Adaptive Network-Based Inference System (ANFIS) for the classification of DOA.

The KSOM was used by Backory (1999) to assess DOA from the AEP. The KSOM uses six of the AEP features presented in the previous section. This set of features was studied by the same researcher and proved to give acceptable results when using the KSOM. The KSOM developed by Backory (1999) will be applied to the data from patients Pat1 and Pat2, and later a KSOM will be trained and tested with the same data sets used for the FRC.

The ANFIS was used by Linkens and Abbod (1998) and Linkens *et al.* (1998) to assess DOA from a set of six wavelet extracted AEP features. The ANFIS uses a different set of features than KSOM. This classifier was applied to the data from patients Pat1 and Pat2. Finally, the ANFIS was trained and tested again with the same data sets used when developing the FRC. The results are compared with the ones from the FRC using the AEP features only.

3.6.1 Kohonen Self-Organizing Map

Kohonen Self-Organizing Map (KSOM) is an unsupervised learning method network. This type of network forms its own classifications of the training data. However, two basic assumptions about the network have to be made; the first is that class membership is broadly defined as input patterns that share common features, the other is that the network will be able to identify common features across the range of input patterns. KSOM works upon these assumptions, and uses unsupervised learning to modify the internal state of the network to model the features found in the training data. The learning algorithm organizes the nodes in the grid into local neighbourhoods that act as feature classifiers in the input data. The topographic map is autonomously organized by a cyclic process of comparing input patterns to vectors stored at each node. No training response is specified for any training input. Where inputs match the node vectors, that area of the map is selectively optimized to represent an average of the training data for that class. From a randomly

organized set of nodes the grid settles into a feature map that has local representation and is self-organized. Self-organization refers to the ability to learn without being given the corresponding output for an input pattern. Therefore, self-organizing networks modify their connection strengths based only on the characteristics of the input patterns. A training set has many input vectors that are similar, and the network should be trained to activate the same Kohonen neuron for each of them.

Backory (1999) developed a KSOM for DOA using the data of nine patients. These data were further balanced with data from three volunteers for the Awake and OK/Light levels. In addition, statistical generation of data for the OK and OK/Deep levels was used. This was necessary in order to achieve balanced training and testing data sets for the KSOM. This neural network classifier used a set of AEP features formed by: D_{51}, D_{52}, D_4, D_3, D_2 and D_1. The KSOM developed and used by Backory (1999) was applied to the data from patients Pat1 and Pat2, the classification results being presented in Table 3-13.

Table 3-13: Percentage of samples classified by the KSOM (Backory, 1999).

Patient	Correct	Incorrect
Pat1	9.5%	90.5%
Pat2	13.2%	86.8%

The KSOM has a very low performance, with a very low correct classification percentage. Figures 3-8 and 3-9 show the KSOM classification for the two patients. The KSOM was not able to correctly identify the DOA levels.

The data used by Backory (1999) was gathered during general anaesthesia with a different combination of drugs, i.e. fentanyl as the analgesic drug, while with patients Pat1 and Pat2 remifentanil was the analgesic drug used. The effect of analgesics on the AEP is a study under investigation and there are no clear results. However, some researches point out that remifentanil may depress AEP in a dose dependent manner (Crabb *et al.*, 1996; McGregor *et al.*, 1998). Therefore, the KSOM was trained again with the same data sets as for the FRC (Table 3-3), so as to reflect the remifentanil influence. The results of these new KSOM are presented in Table 3-14, considering the testing data set.

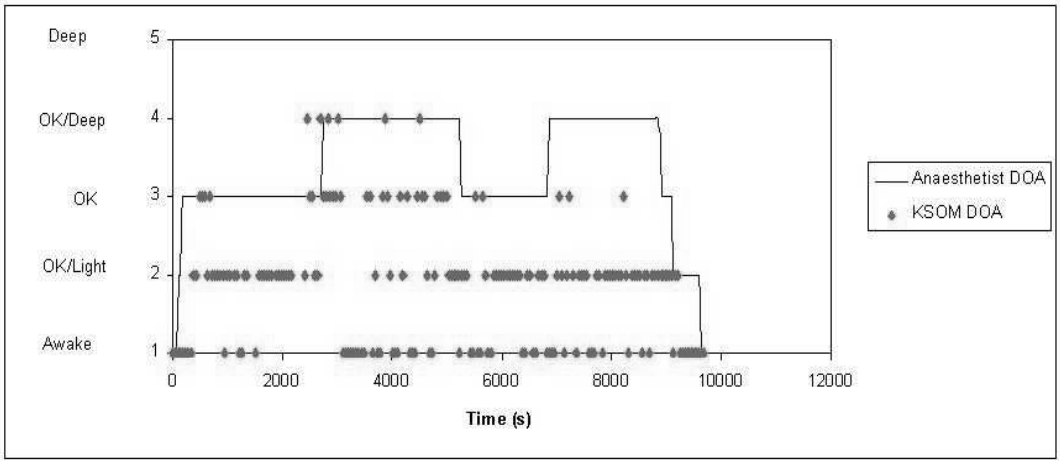

Figure 3-8: Results of the KSOM (Backory, 1999) for the data of patient Pat1.

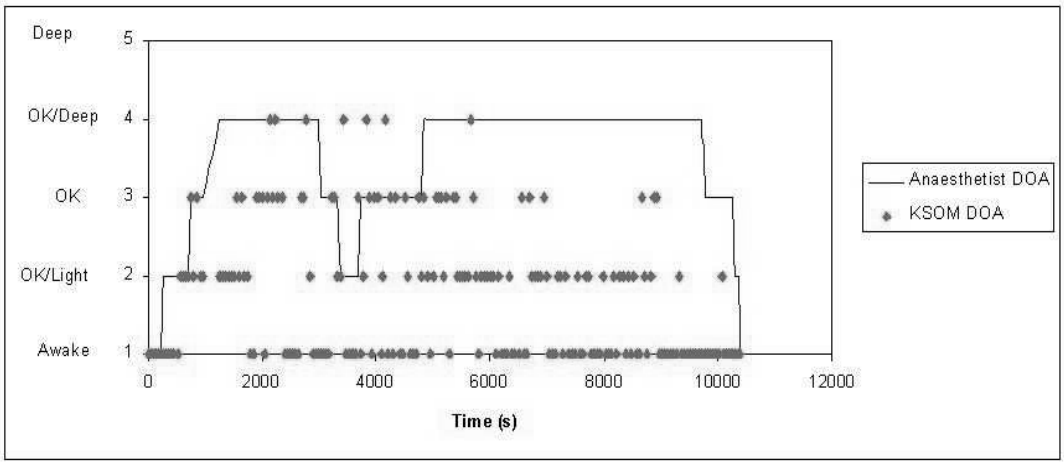

Figure 3-9: Results of the KSOM (Backory, 1999) for the data of patient Pat2.

Table 3-14: Performance of the new KSOM (trained with the data from patients Pat1 and Pat2) on the testing data set.

	Correct	**Incorrect**
Number of samples	97	41
Percentage of samples	70.3%	29.7%

Table 3-15: Percentage of samples classified by the new KSOM (using the same data set as the FRC).

Patient	Correct	Incorrect
Pat1	47.8%	52.2%
Pat2	64.3%	35.7%

Table 3-15 shows the results for patient Pat1 and Pat2 separately. The correct classification percentage for the new KSOM is very high. However, Figures 3-10 and 3-11 show that even with a high classification percentage the KSOM was not able to correctly classify the DOA changes. In fact, the KSOM has labelled all the data samples as OK/Deep, indicating that it is biased towards the OK/Deep level. This is due to the fact that the majority of the training data samples are from the OK/Deep level, which predominates.

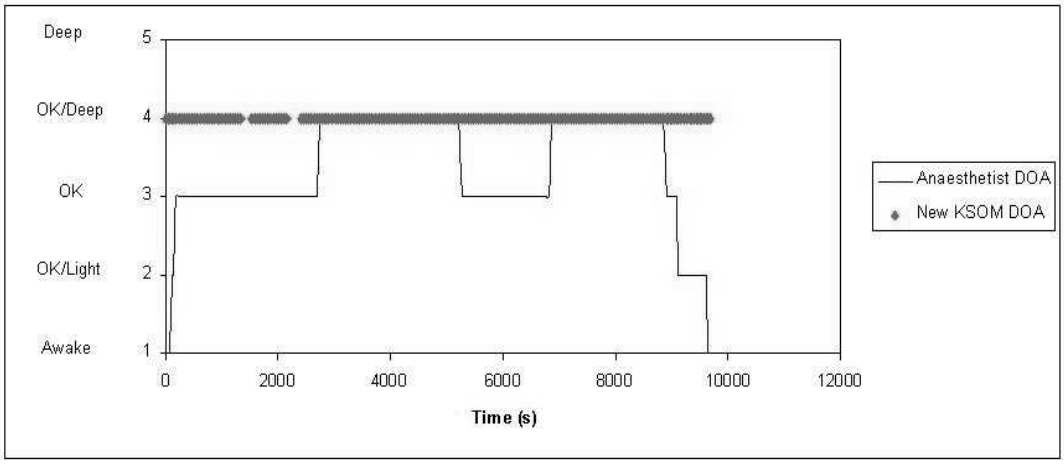

Figure 3-10: Results of the new KSOM (using the same data set as the FRC) for the data of patient Pat1.

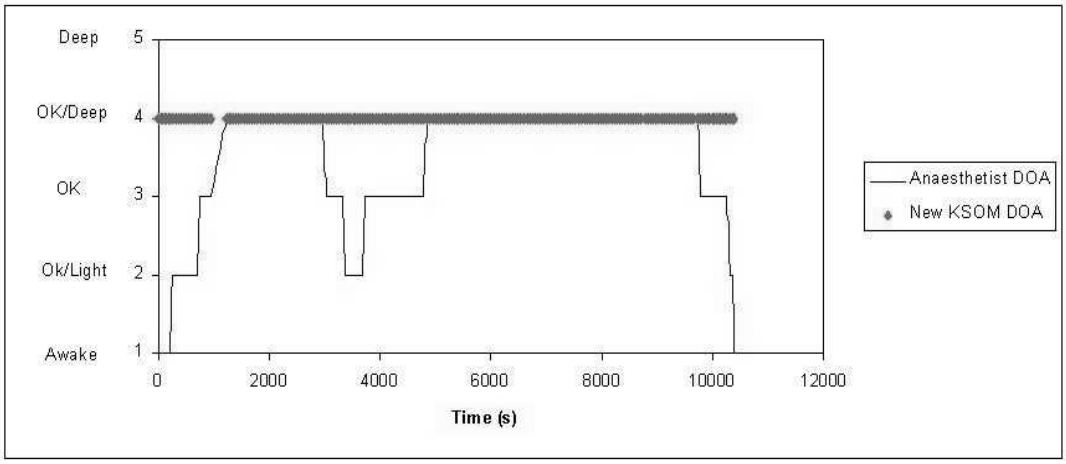

Figure 3-11: Results of the new KSOM (using the same data sets as the FRC) for the data of patient Pat2.

The KSOM needs a balanced training data set and a large number of samples, usually above 1000. The amount of data available is very small, and this will compromise the performance of any neural network; KSOM works best when the networks are very large, and the smaller the network, the less accurate the statistical model will be.

3.6.2 Adaptive Network-Based Fuzzy Inference System

Jang (1993) proposed an Adaptive Network-Based Fuzzy Inference System (ANFIS) that identifies a set of parameters through a hybrid learning rule combining the back-propagation gradient-descent and a least-squared method. ANFIS is a graphical network representation of Sugeno-Type fuzzy systems, endowed with neural learning capabilities. This allows the fuzzy system to learn from the data they are modelling. The membership function parameters are chosen so as to tailor the membership functions to the input/output data. Therefore, ANFIS is used for tuning the rules of fuzzy systems. The network is comprised of nodes and with duties collected in layers with specific functions. It constructs a network realization of fuzzy rules. ANFIS structure is shown in Figure 3-12. Layer 1 consists of membership functions with adaptable parameters. Layer 2 implements the fuzzy AND operator while layer 3 acts to scale the firing strengths. The output of layer 4 is comprised of a linear combination of the inputs multiplied by the normalized firing strength. Layer 5 is a simple summation of the outputs of layer 4.

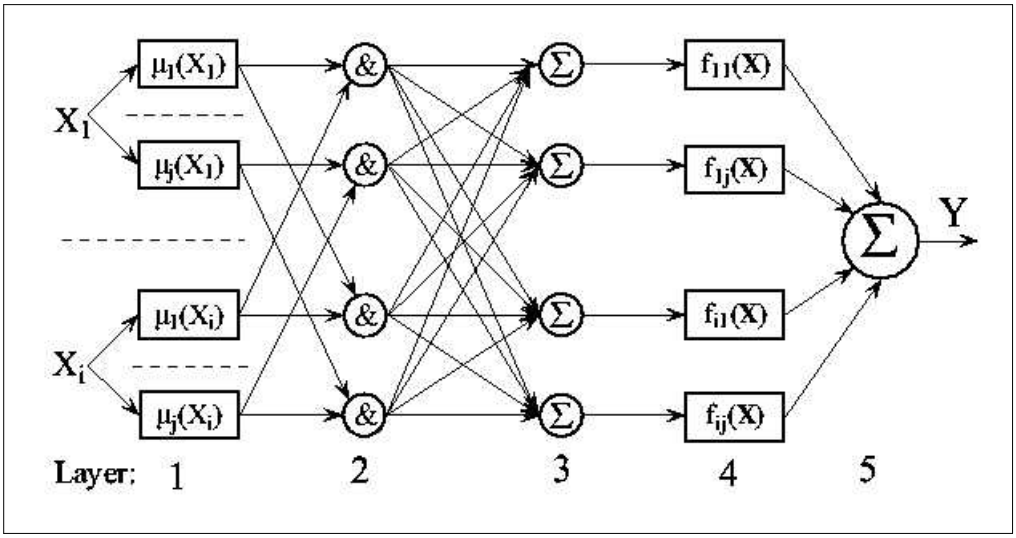

Figure 3-12: ANFIS structure.

Linkens and Abbod (1998) and Linkens *et al.* (1998) used the ANFIS to classify DOA

using six AEP features: D_4, D_{31}, D_{32}, D_{33}, D_2 and D_1. This set of features was studied for correlation with DOA and classification performance. The data from several patients were used to train the ANFIS, using the same drug combination as Backory(1999).

The classifier developed by these researchers was applied to the data of patients Pat1 and Pat2 (Table 3-16). The results show that the ANFIS classifier performs well with the data from patient Pat2. Patient Pat1 includes many DOA variations and incidents of Awake classification (Figure 3-13). These sporadic samples could be partly due to diathermy. However, many wrong classifications on the OK/Light level can induce the anaesthetist in error. In addition, the Deep DOA level classifications are also misleading, since this level is dangerous for the patient. Nevertheless, ANFIS performed better than the KSOM. Figure 3-14 shows the overall DOA classification for patient Pat2. The classifier performs reasonably and is capable of distinguishing between the lighter and deeper DOA levels.

Table 3-16: Percentage of samples classified by the ANFIS (Linkens and Abbod, 1998).

Patient	Correct	Incorrect
Pat1	33.3%	66.7%
Pat2	59.6%	40.4%

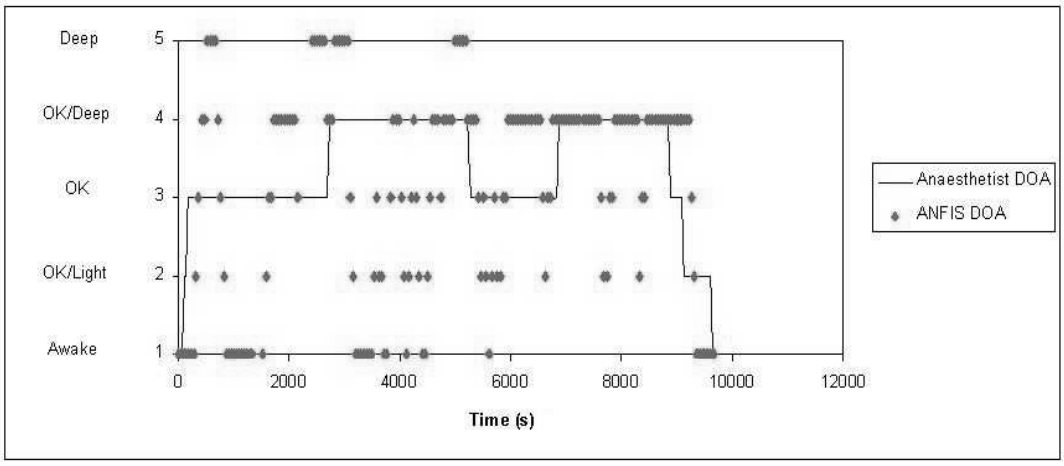

Figure 3-13: Results of the ANFIS (Linkens and Abbod, 1998) for the data of patient Pat1.

In Abbod *et al.* (1998) a second measure of DOA was used. A rule-based fuzzy logic using heart rate and arterial pressure is used to obtain another measure of DOA. This measure is fused (using fuzzy logic rules) with the ANFIS DOA measure to obtain a final assessment of DOA. The results with this data fusion of multi-anaesthetic depth measures improves the

overall classification results presented in the same study.

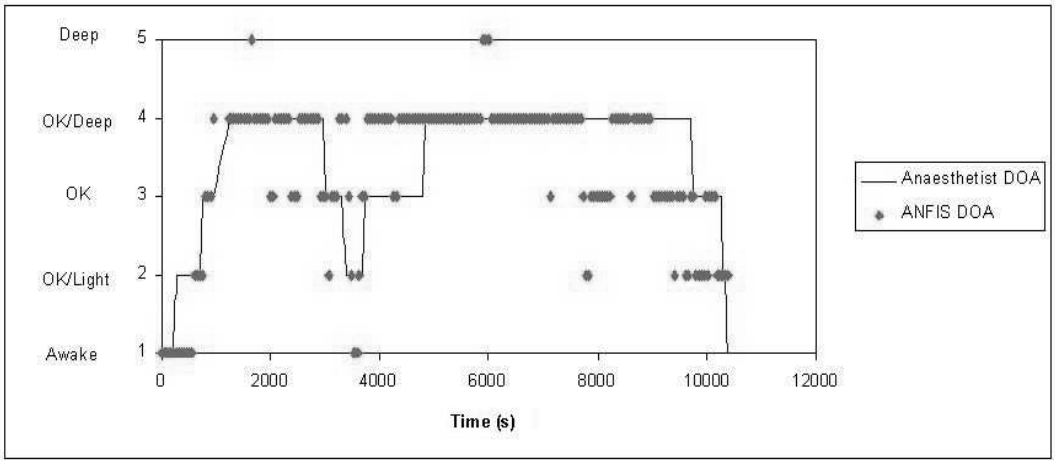

Figure 3-14: Results of the ANFIS (Linkens and Abbod, 1998) for the data of patient Pat2.

The ANFIS classifier using the AEP features was trained again with the same data groups as the FRC (Table 3-3). The objective was to compare the results with the results of the FRC using the same resources. Table 3-17 shows the results of the new ANFIS on the testing data set. The performance of the ANFIS is smaller than the FRC (Table 3-10).

Table 3-17: Performance of the new ANFIS (trained with the data from patients Pat1 and Pat2) on the testing data set..

	Correct	**Incorrect**
Number of samples	29	109
Percentage of samples	21%	79%

The new ANFIS was applied to the data of patients Pat1 and Pat2 separately (Table 3-18). The correct classification percentage has decreased for patient Pat2, but increased for patient Pat1 when comparing with Table 3-16.

Table 3-18: Percentage of samples classified by the new ANFIS (using the same data set as the FRC).

Patient	**Correct**	**Incorrect**
Pat1	41.8%	58.2%
Pat2	28.2%	71.8%

Figures 3-15 and 3-16 show the overall classification results for patient Pat1 and Pat2 respectively. The ANFIS is able to distinguish between lighter and deeper DOA levels. The

majority of the samples are classified in the OK DOA level. Notice that OK and OK/Deep levels are most difficult to distinguish. Nevertheless, the ANFIS developed by Linkens and Abbod (1998) has a better performance with the data from patient Pat2 than with the data from Pat1.

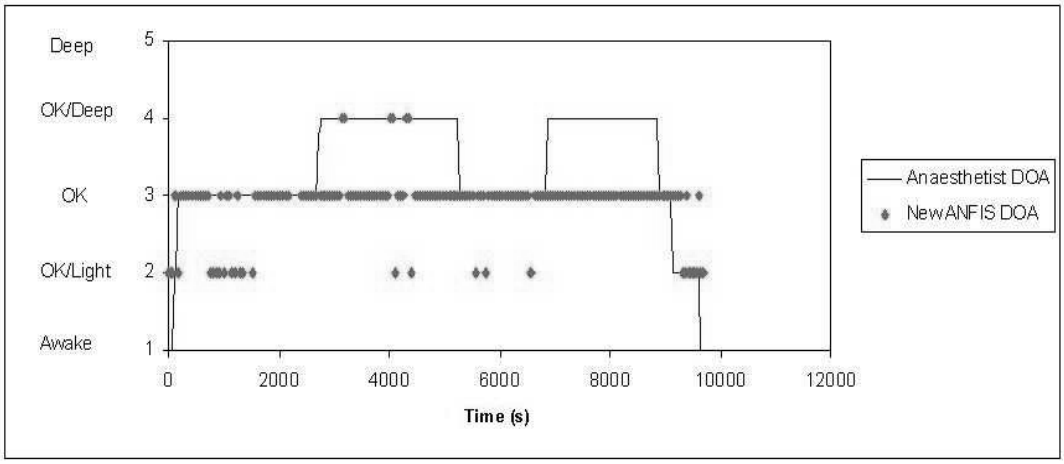

Figure 3-15: Results of the new ANFIS (using the same data set as the FRC) for the data of patient Pat1.

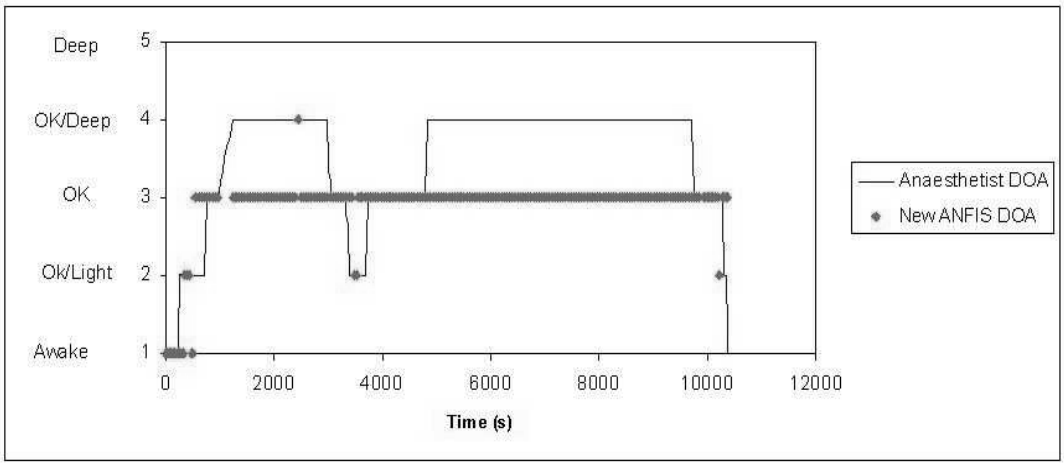

Figure 3-16: Results of the new ANFIS (using the same data set as the FRC) for the data of patient Pat2.

3.6.3 General Results

Figure 3-17 shows the classification results of the classifiers presented previously, the KSOM developed by Backory (1999) and the ANFIS developed by Linkens and Abbod (1998). The ANFIS matches the performance of the FRC when considering patient Pat2.

However, the ANFIS was not trained with data from this patient and such a high correct classification percentage indicates the efficiency of the classifier. The KSOM has a poor performance with the data from both patients.

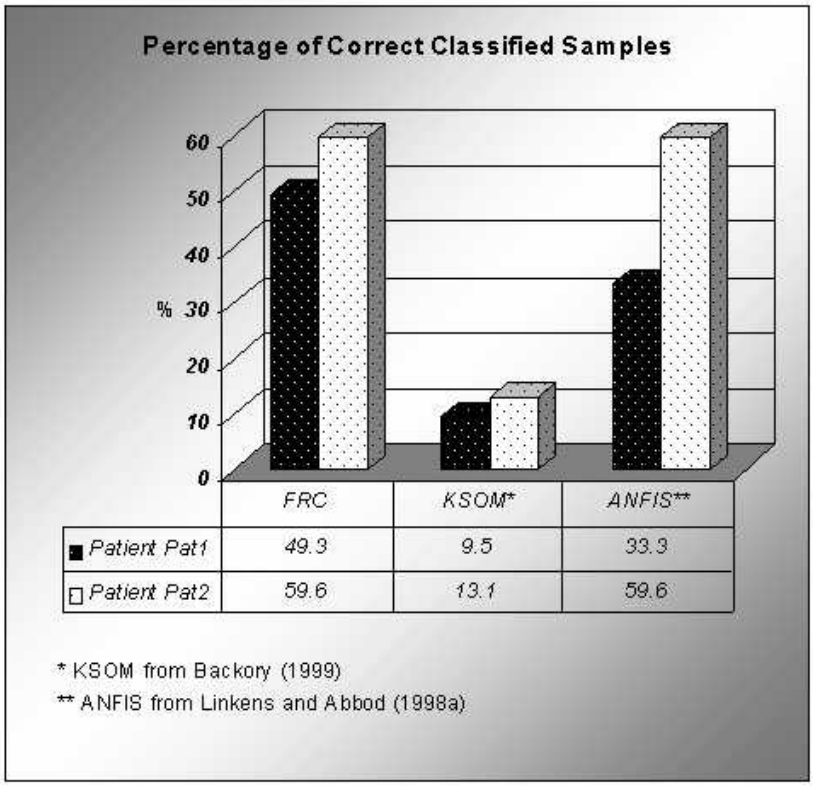

Figure 3-17: Classification results using the FRC, the KSOM and the ANFIS.

The data used by these researchers to develop these two classifiers were gathered during general anaesthesia when using a combination of propofol and fentanyl. While the FRC was trained with the data from patients Pat1 and Pat2 which was obtained under general anaesthesia with a combination of propofol and remifentanil. The two analgesics, i.e. fentanyl and remifentanil, have different characteristics. Remifentanil is more potent than fentanyl and it is known for reducing the cardiovascular parameters more than the other analgesics. Whether remifentanil can influence the AEP is still a matter of debate, but it is not unreasonable to think so.

It was discussed in Chapter 2 that the AEP show similar results with different anaesthetic agents, reflecting the hypnotic effect. The synergistic interaction of propofol and remifentanil will be discussed in Chapter 4. Remifentanil potentiates propofol, therefore, the degree of unconsciousness will be different when using propofol alone and when the same dose of propofol is combined with remifentanil. Consequently, the KSOM and the

ANFIS were trained again with the same data as the FRC. Table 3-19 shows the percentage of correct classified samples of the three classifiers on the same testing data set.

Table 3-19: Percentage of correct classified samples on the testing data set by the three classifiers.

	FRC	**New KSOM**	**New ANFIS**
Testing data set	61.6%	70.3%	21%

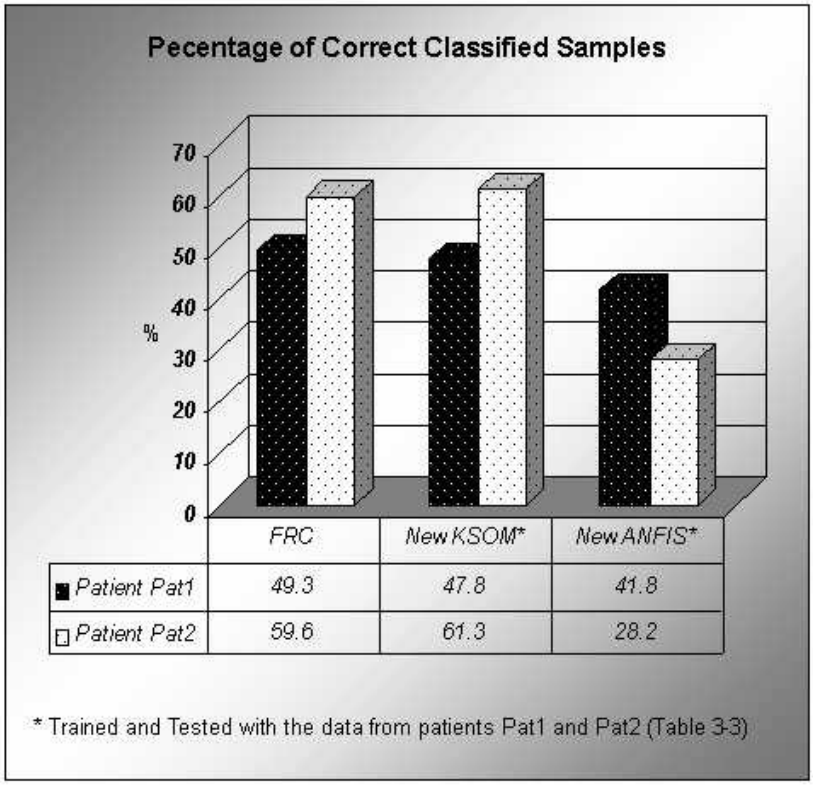

Figure 3-18: Classification results using the FRC, the new KSOM and the new ANFIS.

Analysing Table 3-19 and recalling Figures 3-10 and 3-11, it is obvious that the KSOM is biased to the OK/Deep level and that even with 70.3% of correct classified samples, the classifier has a poor performance. Figure 3-18 shows the results of the classifiers on the data from both patients. The ANFIS performs better than the KSOM, because it is not biased. Overall, the FRC led to an acceptable performance and proved to work better than the other classifiers on the available data.

3.7 Summary

The classification of DOA is a complex task, but essential to develop efficient closed loop control systems. However, direct measurements are unavailable and signal processing techniques are required to determine the DOA level.

Research on MLAEP led to the investigation of feature extraction techniques and of classifiers, so as to obtain a clear indicator of DOA. Any pattern that can be recognised and classified, possesses a number of discriminatory features. The measured values do not necessarily carry much discriminatory information; the data may even complicate the classification scheme because of this deficiency. The first step in the classification task is to consider the problem of what discriminatory features to select and how to obtain these features. The use of MRA with WT proved to be very efficient in extracting relevant features from the AEP. The MRA decomposes the AEP into different resolutions allowing a detailed analysis of the behaviour of the signal in its different spectral bands. The decomposed components were analysed for their energy content and these are used as an indicator of the DOA. The next step is how to classify these detailed features into different anaesthetic depths. The complexity of biomedical systems makes it a favourable space for fuzzy logic based applications. In this specific case, there is a small amount of data available; this can be proved useful when choosing an adequate type of classifier.

Neural networks are very popular as classifiers and have proved to be efficient in some cases. However, they need a large number amount of data to be effective. Balanced training data sets, representing all the classification classes with a similar amount of samples is essential for a non-biased neural network classifier. This is reflected in the KSOM performance, where there is also the risk of overtraining.

The trained FRC was used to classify a set of wavelet extracted AEP features into DOA levels. The FRC uses fuzzy relations to establish the connection between natural data clusters and the class identifiers. The nature of the FRC makes it adequate for high dimension vector features and complex classification processes, when a small amount of data is available; this is reflected in the classification results.

The ANFIS led also to acceptable results, however, these were no better than those of the FRC. Note that ANFIS uses neural network training techniques allied to fuzzy logic

decision making.

The results of the AEP features classifier have to be carefully analysed, since the anaesthetist based his decision about DOA level on the clinical signs and his own experience. Considering that the sampling time was 30 seconds, it was possible that changes in the DOA level from OK to OK/Deep could go unnoticed to the anaesthetist. Therefore, some samples attributed to a wrong classification could in fact be correct. Nevertheless, the anaesthetist's opinion is taken as the correct classification for there is no other precise analysis to evaluate DOA. In conclusion, this is not an easy classification problem where one knows the correct classification and the performance of the classifier can only be judged on the percentage of the correct classified samples; the overall trend of classification has to be accounted for. It is important that the classifier is able to distinguish between the different levels of DOA, and specially to reflect the trend of anaesthetic depth changes.

The FRC will be used throughout this project as the classifier of DOA from the wavelet extracted AEP features. A second FRC was also trained with a set of cardiovascular parameters, and will be used as a reinforcement to the overall decision scheme. The AEP FRC did not present any unclassified cases.

Chapter 4

Patients and Drug Pharmacology

4.1 Introduction

The concepts of DOA and AEP were presented in the previous chapters. However, in anaesthesia the adopted drug profile plays an important role (i.e. anaesthetic and analgesic drugs). The interaction of different drugs has also an influence on the overall efficacy and efficiency of anaesthesia. The anaesthetist has to be aware of the drug effects and interactions.

Anaesthesia involves the use of three drugs, a muscle relaxant, an anaesthetic (hypnotic) and an analgesic. Since the main concern is the monitoring and control of DOA, and as explained in Chapter 2 the muscle relaxant has no influence on the degree of hypnosis. The analgesic drug is of more importance since it affects the pharmacodynamics of the anaesthetic drug and there is no clear indicator of the degree of pain. The analgesic and anaesthetic drugs are interconnected, since they interact with each other so as to achieve an adequate level of DOA and analgesia.

The intravenous anaesthetic drug propofol is used in this project. The drug propofol can be used as a sole anaesthetic agent. However, the required propofol concentration is associated with severe haemodynamic responses. As a result, propofol is combined with specific analgesic agents so as to reduce the dose requirements and diminish the side effects during anaesthesia. The intravenous analgesic drug remifentanil is the analgesic agent used in this project. Remifentanil is a new rapid-acting μ-opioid that can be titrated to patient's needs.

In this chapter, the patient's demography is presented and the properties of the anaesthetic (propofol) and analgesic (remifentanil) drugs used are explained in detail. In addition, a review of research on drug interactions and its importance in balanced anaesthesia is

presented. The different types of drug interactions are explained and main focus is given to the drugs combination used in this project (i.e. propofol/remifentanil).

4.2 Patients Demography

The data used in this project were gathered during surgical interventions in the Royal Hallamshire Hospital in Sheffield, with the supervision of Dr. J. Peacock, a senior anaesthetist in the Department of Anaesthesia of the same hospital. The patients had an ASA I or II status and gave previous explicit consent to be included in this study.

The data collection was restricted to patients who received the same anaesthetic/analgesic drug profile, and to surgical interventions that did not need other drugs that could interact with this particular drug profile. For instance, obese patients could not be used for the data gathering, since these patients have different pharmacokinetic properties, and patients having serious health problems and previously medicated with other drugs were also excluded, since these could interfere with normal drug profile/interaction. In addition, surgical procedures that require electrical equipment that could interfere heavily with the AEP recording were excluded.

A clear profile of both drugs is of great importance when the interaction between the drugs and its effects on DOA are being studied, hence, it was not easy to gather suitable data. In addition, the Royal Hallamshire Hospital operation theatres were being restructured during the course of this project, limiting even more the number of suitable cases.

The surgical data relating to three patients were collected for the project. In one of the surgical interventions there was a fault in the AEP recording equipment. Therefore, patient Pat3 was excluded from the study. The two other patients profiles are presented in Table 4-1.

The data from both patients were used to train and test the DOA classifier (Chapter 3). However, when modelling the drug effects only the data from patient Pat1 will be used. Patient Pat2 was excluded from the modelling part because of the drug profile used and its possible implications. The use of a bolus of morphine could have added an extra interaction with propofol, since the level of analgesia is not only provided by remifentanil. In addition, there are some controversial results (Sasada and Smith, 2000) about the use of atracurium (muscle relaxant) with propofol, indicating a possible physical incompatibility. This means

that both drugs cannot be mixed together in the same syringe. However, when administered separately into different veins there is little risk of incompatibility, considering that atracurium was used in bolus doses and the speed of the blood flow. These facts could interfere with the analysis of the interaction of propofol and remifentanil and lead to an inadequate model. Therefore, it was considered best to exclude the data from patient Pat2 and only use the coherent data (i.e. Pat1) for the modelling part (Chapter 5).

Table 4-1: Particulars of the patients forming part of this study. The drugs used are partitioned in three categories: muscle relaxant (vecuronium and atracurium), anaesthetic (propofol) and analgesic (remifentanil and morphine).

Patient	Date	Age	Sex	Weight (kg)	Surgical Procedure	Drugs Used
Pat1	14/06/2000	75	M	82	Incision Retroperitoneal Sarcoma	Vecuronium Propofol Remifentanil
Pat2	21/02/2001	66	F	61	Right Mastectomy and Axillary Node Clearance	Atracurium Propofol Remifentanil Morphine

Two GRASEBY 3500 anaesthesia syringe pumps from Graseby Medical Limited were used. One for the infusion of propofol and the other for remifentanil. Both infusion profiles were controlled by the anaesthetist. The GRASEBY 3500 incorporates a “Dipifusor” TCI for propofol. Therefore, the anaesthetist targeted the propofol plasma concentration and the TCI infusion algorithm decided upon the necessary infusion rate. Figure 4-1 shows the syringe pump used, which has an RS232 output port for the interface with a computer.

Figure 4-1: GRASEBY 3500 anaesthesia syringe pump used for propofol and remifentanil.

4.3 The Anaesthetic Propofol

Propofol (Diprivan) is used mainly for the induction and maintenance of general anaesthesia, and also for sedation during intensive care and regional anaesthesia. It has also been used for the treatment of refractory nausea and vomiting in patients receiving chemotherapy and in the treatment of status epilepticus, but these are secondary uses of propofol (Sasada and Smith, 2000). The effects of propofol are controlled by rapid hepatic metabolism. A significant proportion of the drug is metabolised as soon as it passes through the liver. Because of the rapid hepatic metabolism of propofol, accumulation does not occur and so the waking time should be the same irrespective of the duration of the normal maintenance infusion; recovery is pleasant, nausea and vomiting are rare (Carrie *et al.*, 1996).

Propofol is presented as a white oil-in-water emulsion containing 1% or 2% weight/volume of propofol in sybean oil and purified egg phosphatide. Propofol is administered intravenously in a bolus dose of 1.5-2.5 mg/kg for induction and as an infusion of 4-12 mg/kg/h for maintenance of anaesthesia. These doses are for normal patients, when considering children or elderly the doses have to be adjusted according to the group drug sensitivity. Children require higher doses of propofol to maintain adequate anaesthesia (Marsh *et al.*, 1991). Generally an increase of 25-50% is necessary. McFarlan *et al.* (1999) explains that children require higher infusion rates than adults due to altered pharmacokinetics in this age group. Some practical guidelines for the use of propofol in paediatric anaesthesia are also presented in the same study. The influence of age on the propofol requirements has been studied by several researchers (Peacock *et al.*, 1990; Schnider, 2000; Schnider *et al.*, 1999; Schuttler and Ihmsen, 1993). When considering elderly patients, gender also influences the pharmacokinetics of propofol. Vuyk *et al.* (2001) reports that female elderly patients require approximately a 10% higher propofol infusion rate than male patients, in order to ensure the same blood propofol concentration. Female patients will regain consciousness more rapidly than male patients when they experience similar propofol infusion schemes, in the presence of a similar pharmacodynamic profile.

Propofol is a useful drug for induction and maintenance of hypnosis during total intravenous anaesthesia. The drug's fast distribution and rapid metabolism result in a short plasma half-life. This explains the fast and clear-headed recovery after its use and makes it

an ideal drug for use in continuous infusions.

Propofol produces a 15-25% decrease in blood pressure and systemic vascular resistance, and a 20% decrease in cardiac output. This is one of the side effects of propofol. Profound bradycardia and asystole may complicate the use of the drug (Chaudhri *et al.*, 1992; Sasada and Smith, 2000; Schulze *et al.*, 1999).

Propofol decreases the amplitudes of the AEP due to its hypnotic effect (Chassard *et al.*, 1989; Palm *et al.*, 2001). Kuizenga *et al.* (1998) studied the effects of propofol on the EEG, when infused at a rate of 0.5 mg/kg/min for 10 minutes. They concluded that propofol exerts a biphasic effect on the EEG amplitude in all frequency bands.

Computerized propofol infusion systems have been used in anaesthesia for some time. Researchers like Russell *et al.* (1995) and White and Kenny (1989), evaluated the use of manual versus TCI of propofol. Overall, controlled infusion of propofol have performed as accurately as manual infusions. Roberts *et al.* (1988) developed a simple scheme for manual control of a propofol infusion so as to approximate the program used by a computer controller. This scheme proved to be efficient when the anaesthetist did not have access to a microprocessor controller or a computer enabled volumetric infuser.

A drug general pharmacology is divided in pharmacokinetics and pharmacodynamics. Pharmacokinetics are generally described as: “what the body does to a drug”, while pharmacodynamics are described as: “what the drug does to the body” (Shieh, 1994). In the next section the pharmacokinetics of propofol will be discussed.

4.3.1 Pharmacokinetic Model

Pharmacokinetics is the quantitative study of the absorption, distribution, metabolism and elimination of chemicals in the body and the rate of these effects. Most drugs exhibit multicompartment pharmacokinetic behaviour (Sheiner *et al.*, 1979). A three-compartment model best describes the distribution and elimination of propofol. This model is used to predict the plasma concentrations. Figure 4-2 shows the general diagram of a three-compartment model.

The pharmacokinetics of propofol appear to be linear within clinical dosage ranges. This is necessary for the compartmental model to adequately describe the metabolism of propofol. The shape of the drug concentration decay is unaffected by dose and the derived

pharmacokinetic parameters are similar for the different doses used (Gepts, 1998).

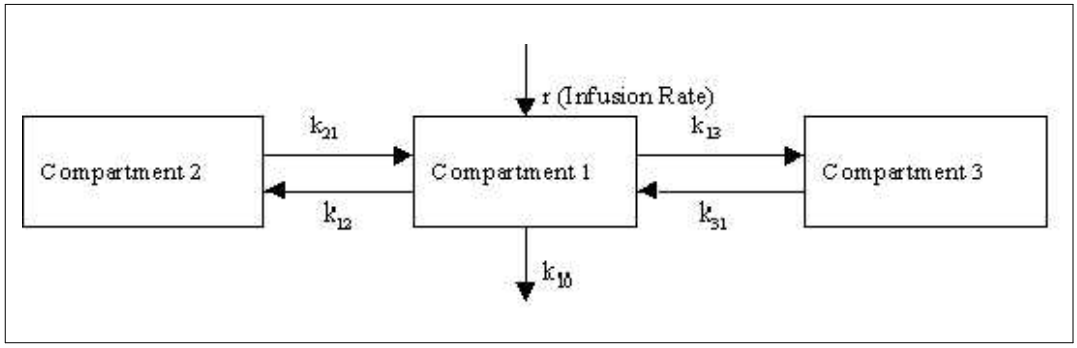

Figure 4-2: The three-compartment model. The k_{ij} are the inter-compartmental rate constants that govern drug distribution and k_{10} is the rate constant of elimination. Compartment 1 is defined as the central compartment.

The pharmacokinetic constants used in the propofol linear three-compartment model (Figure 4-2) are shown in Table 4-2, and were used by Marsh *et al.* (1991). V_c is the central compartment volume per kg of patient's weight. V_c is used to derive V_1 the volume of the central compartment from the mass of the patient, using $V_1 = V_c * mass$. The pharmacokinetic parameters describing the flow-rate of the drug between the various compartments are as follows: k_{ij} is the rate constant for drug transfer from compartment *i* to compartment *j*; k_{10} is the rate constant of elimination from the central compartment (i.e. compartment 1).

Table 4-2: Pharmacokinetic parameters for propofol described by Marsh *et al.*, (1991) reflecting the three-compartment patient model.

V_c (l kg^{-1})	k_{10} (min^{-1})	k_{12} (min^{-1})	k_{13} (min^{-1})	k_{21} (min^{-1})	k_{31} (min^{-1})
0.228	0.119	0.112	0.0419	0.055	0.0033

Following a propofol injection to the central compartment, elimination and inter-compartmental distribution can be defined by the following systems of equations, considering $m_1(t)$, $m_2(t)$ and $m_3(t)$ as the masses at time t in compartment 1, 2 and 3 respectively, and $r(t)$ as the drug infusion rate at time t.

$$\left\{ \begin{array}{l} \dot{m_1}\ (t) = k_{21}m_2(t) + k_{31}m_3(t) - (k_{12} + k_{13} + k_{10})m_1(t) + r(t) \\ \dot{m_2}\ (t) = k_{12}m_1(t) - k_{21}m_2(t) \\ \dot{m_3}\ (t) = k_{13}m_1(t) - k_{31}m_3(t) \end{array} \right\} \qquad 4\text{-}1$$

Assuming zero initial conditions and using the Laplace transform, the system in Equation

4-1 becomes:

$$\left\{\begin{array}{l} sM_1(s) = k_{21}M_2(s) + k_{31}M_3(s) - (k_{12} + k_{13} + k_{10})M_1(s) + R(s) \\ sM_2(s) = k_{12}M_1(s) - k_{21}M_2(s) \\ sM_3(s) = k_{13}M_1(s) - k_{31}M_3(s) \end{array}\right\} \quad 4\text{-}2$$

Finally

$$\frac{M_1(s)}{R(s)} = \frac{s^2+(k_{21}+k_{31})s+k_{21}k_{31}}{s^3+p_1s^2+p_2s+p_3} \quad 4\text{-}3$$

where

$$p_1 = k_{31} + k_{21} + k_{12} + k_{13} + k_{10} \quad 4\text{-}4$$

$$p_2 = k_{21}k_{31} + k_{12}k_{13} + k_{13}k_{21} + k_{10}k_{31} + k_{10}k_{21} \quad 4\text{-}5$$

$$p_3 = k_{21}k_{31}k_{10} \quad 4\text{-}6$$

The plasma concentration (i.e. concentration in compartment 1) is described as:

$$C_p = \frac{M_1}{V_1} \quad 4\text{-}7$$

Equation 4-3 is discretised using a ZOH (zero-order-hold) and a sampling rate of 30 seconds.

The values of the pharmacokinetic parameters are average population values. The individual pharmacokinetic variability produces different pharmacological responses, when patients are given identical doses of a drug. Therefore, the dose required to produce a specific response may vary between individuals. Age, body weight and disease are some factors that affect more the pharmacokinetic variability. Propofol infusion rates should be set according to total body weight (Hirota *et al.*, 1999). Plasma concentration of propofol is dependent on the body weight during a fixed rate infusion (Equation 4-7). Special care is necessary with obese patients, since the pharmacokinetic parameters are largely affected by this.

The accuracy of the different sets of parameters was analysed by Glass *et al.* (1989). It was found that, if the parameters are coherent then the compartmental model is valid.

In conclusion, the pharmacokinetics is the mathematical analysis of the drugs matabolite levels in the body. The changes in drug concentration in relation to time are used to derive

the pharmacokinetic constants that adequately account for the behaviour of drugs in the body.

4.3.2 Effect Compartment

There is a temporal delay between changes in the plasma drug concentration and the measured effect, because some drugs act at the sites which maybe remote from the blood stream. This delay is a consequence of the finite time needed for drugs molecules to equilibrate with the effect site. The effect site is modelled by adding an additional compartment, linked to the central compartment of the three-compartment pharmacokinetic model (Figure 4-2) by the single first-order process shown in Figure 4-3.

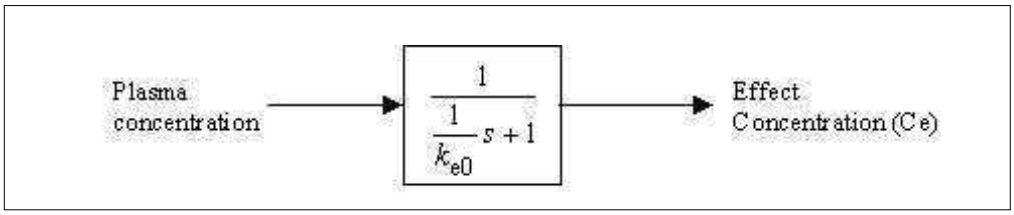

Figure 4-3: Effect compartment model. k_{e0} is the rate constant of drug elimination.

More accurately, the effect compartment is connected to the central compartment by a first-order rate constant, k_{1e}, while the drug dissipation from the effect compartment occurs by means of a second first-order rate constant, k_{e0} (Sheiner *et al.*, 1979). However, the effect compartment is defined as being negligibly small and k_{1e} is an arbitrary small fraction of k_{e0}. The hypothetical concentration in the effect compartment can only be calculated if the value of k_{e0} is known, since k_{e0} will precisely characterize the temporal effects of equilibration between the plasma concentration and the corresponding drug effect (Mortier and Struys, 2000).

Bovill (2000) reports that a consequence of the delay in equilibration is that a plot of pharmacodynamic response (effect) against plasma concentration measured during and after a short i.v. infusion, will show an anticlockwise hysteresis loop. The underlying effect site concentration and the blood-effect delay (i.e. the value of k_{e0}), can be estimated by manipulating the hysteresis loop so that the loop collapses.

The pharmacodynamic parameter k_{e0} for propofol was set by Linkens *et al.* (1993) as being 0.1 min^{-1}. In the same study, these researchers used the same pharmacokinetic parameters

shown in Table 4-2. The value of $k_{e0} = 0.1\ \text{min}^{-1}$ will be used in this project.

The concentration of drug at the effect site (C_e), not the plasma concentration, governs the drug effect. Therefore, it is more accurate to use the effect concentration to model the drug effect (Jacobs and Williams, 1993; Morita *et al.*, 2000; Shafer and Varvel, 1991; Weiss, 2000).

Wakeling *et al.* (1999) compares the targeting of the effect compartment or central compartment concentration of propofol for predicting the loss of consciousness. The median time to loss of responsiveness was 3.02 minutes in the group targeted to a predicted plasma concentration versus a 1.23 minutes in the group targeted to a predicted effect compartment concentration. The effect site is the theoretical compartment in which a drug exerts its action and thus the concentration at this site is a direct determination of the effect of the drug.

4.4 The Analgesic Remifentanil

Opioids provide the analgesia required in balanced and total i.v. anaesthesia techniques to block autonomic nervous system and somatic responses to noxious surgical stimuli. Remifentanil (GI87084B) is one of the opioids used to provide the analgesic component of general anaesthesia. It is a new synthetic opioid that exhibits classic μ-agonist pharmacologic effects including analgesia, sedation and respiratory depression. Remifentanil is presented as a clear, colourless solution for injection, containing remifentanil hydrochloride in a glycine buffer (Sasada and Smith, 2000).

A metabolism by nonspecific esterases gives remifentanil a pharmacokinetic profile unlike that of any other opioid. The clinical advantage of this drug lies in its extremely rapid clearance, and offset of effect, which is independent of excretory organ function. Remifentanil can be closely titrated to patient need and could provide new methods of combining large-dose opioid anaesthesia with risk reduction strategies (Camu and Royston, 1999).

Remifentanil is generally administered by continuous infusion because intermittent bolus doses are inconvenient for all but shortest procedures. A continuous infusion approaches steady-state concentration in only 10 minutes (Rosow, 1999). The titration of drug doses according to each patient's needs is facilitated by the rapid offset of action combined with a

rapid onset of action (Westmoreland *et al.*, 1993).

Accurate dosing of remifentanil is not quite so critical as with other opioids, because rapid recovery is effectively dose-independent. Its clearance is unaffected by variables such as hepatic or renal function, gender, drug interaction and duration of infusion. Hoke *et al.* (1997) concluded that remifentanil elimination was independent of renal function (renal disease). The other parameters that have been demonstrated to alter remifentanil clearance such as age and weight, do not produce great changes in drug duration. Therefore, an infusion of remifentanil produces a consistent steady-state blood concentration and the rate of disappearance is more uniform within a patient population (Minto *et al.*, 1997a; Rosow, 1993). However, Minto *et al.* (1997b) showed that age-related pharmacodynamic changes occur in the peak effect site concentrations; because EEG showed an increase in brain sensitivity to opioids with increasing age.

The reduction in pharmacokinetic variability with remifentanil is one of its major advantages. Peacock *et al.* (1998) show that remifentanil can be used for a diverse patient population as part of a balanced anaesthesia.

Reves (1999) suggests that practitioners should be educated about remifentanil. The unique pharmacokinetic profile of remifentanil gives it unparalleled flexibility, but vigilance is required to avoid problems. The rapid onset of analgesia can be accompanied by an equally rapid onset of side effects if the dose given is too large if it is given too rapidly.

Remifentanil infusions have been evaluated by Williams (2000) for cardiac and vascular anaesthesia. He presents a new method for calculating the remifentanil infusion rate based on weight. This method was accompanied by Cort (2000), who presented an easy dilution technique to simplify the administration of remifentanil by infusion to supplement anaesthesia during cardiac surgery. Nevertheless, remifentanil is possible to use safely in patients undergoing cardiac surgery (Michelsen, 2000).

Remifentanil has one major side effect: respiratory depression (Woods *et al.*, 1999). In fact, dose-dependent increases in analgesic efficacy and respiratory depression are reported by Glass *et al.* (1993). Furthermore, remifentanil decreases mean arterial pressure and heart rate by 20%. Myocardial contractibility and cardiac output may also decrease (Sasada and Smith, 2000). Kallar *et al.* (1994) reported that remifentanil caused dose-dependent reductions in blood pressure and heart rate. In the same study, remifentanil was found to be more effective than alfentanil in attenuating the responses to anaesthetic and surgical stimuli. Prakash *et al.* (2001) reports incidents of hypotension and bradycardia when using

remifentanil during rigid bronchoscopy. Glass *et al.* (1999b) reports that remifentanil in the presence of isoflurane, resulted in a 10-40% decrease in SAP and similar changes in heart rate. They suggest that bradycardia could be prevented by pretreating patients with glycopyrrolate.

Lower values of blood pressure and heart rate are reported with the use of remifentanil than with other opioids, such as alfentanil and fentanyl (Natalini *et al.*, 1999; Ng *et al.*, 2000; Peacock and Philip, 1999; Sneyd *et al.*, 1998). However, the major difference between remifentanil and other opioids is the smaller recovery time (Bekker *et al.*, 2000; Dershwitz *et al.*, 1995; Egan *et al.*, 1996; Fleisher *et al.*, 2001; Monk *et al.*, 1994). Ahonen *et al.* (2000) reports that the times to awakening and tracheal extubation where more predictable in patients receiving remifentanil compared with patients receiving alfentanil. Loop and Priebe (2000) studied the recovery after anaesthesia with remifentanil combined with different anaesthetics. They concluded that the use of remifentanil was characterized by predictably rapid early and complete recovery with all the anaesthetics studied (i.e. propofol, desflurane and sevoflurane).

Remifentanil has also been reported by its sedative effects. Sneyd (1999) states that monitored anaesthesia care sedation with remifentanil is an effective technique which worked reasonably well in clinical trials. However, this is not the primary action of the opioid and should be considered as a side effect.

Remifentanil is also used as a sole agent, when only analgesia is required. Blair *et al.* (2001) uses remifentanil in a patient-controlled analgesia system for labour. Litman (2000) also used remifentanil for conscious sedation during painful medical procedures. Remifentanil safely provides analgesia.

Glass *et al.* (1999a) used ventilatory depression as the measure of opioid effect, when determining the potency of remifentanil. They concluded that remifentanil is approximately 40 times more potent than alfentanil, when remifentanil and alfentanil whole-blood concentration are compared. In fact, remifentanil is also more potent than fentanyl and sufentanil.

Remifentanil is not only used in combination with propofol. Several studies have been published using different anaesthetics. Drover and Lemmens (1998), and Monk *et al.* (1994) used remifentanil as a supplement to nitrous oxide (a volatile anaesthetic with good analgesic properties) anaesthesia. Casati *et al.* (1999) used midazolam (i.v. anaesthetic) with remifentanil, although, this is not a common combination, since midazolam is mainly

used as a sedative for minor surgeries, as a premedication or to induce general anaesthesia. Remifentanil has also been used as a supplement to isoflurane anaesthesia (Bekker *et al.*, 2000; Glass *et al.*, 1999b; Maguire *et al.*, 2001).

According to Egan *et al.* (1993) the potential advantages of an ultra-short acting opioid, such as remifentanil, are:

- The ability to rapidly decrease the drug effect to an appropriate level intraoperatively,
- a decreased likelihood of undesirable opioid side effects postoperatively,
- the lack of drug accumulation with repeated bolus injections or prolonged i.v. infusion,
- the absence of a prolonged metabolism with hepatic or renal disease.

The theoretical disadvantages include:

- The necessity for administration by infusion techniques,
- the lack of prolonged opioid effect when such effects are desirable (e.g. postoperative analgesia).

4.4.1 Pharmacokinetic Model

Remifentanil pharmacokinetics have been investigated following bolus doses and continuous infusions. A three-compartment model (Figure 4-2) best describes the pharmacokinetics of remifentanil, reflecting more closely the drug metabolism in the body (Egan *et al.*, 1996; Glass *et al.*, 1999a, b; Mertens *et al.*, 1999; Minto *et al.*, 1997a, b).

The pharmacokinetic parameters used in this project for remifentanil are presented in Table 4-3 and were used by Egan *et al.* (1993).

Table 4-3: Pharmacokinetic parameters for remifentanil described by Egan *et al.*, (1993) reflecting the three-compartment patient model.

V_c (l kg^{-1})	k_{10} (min^{-1})	k_{12} (min^{-1})	k_{13} (min^{-1})	k_{21} (min^{-1})	k_{31} (min^{-1})
0.0899	0.3955	0.3234	0.0222	0.1468	0.0155

The striking feature of the pharmacokinetics of remifentanil is the very rapid decay in remifentanil blood concentration after termination of an infusion. Therefore, remifentanil presents a new pharmacokinetic class of opioids. Remifentanil has a context-sensitive half-time plateaus of 3-4 minutes in humans, and its effects are fully reversible by naloxone antagonism (Dershwitz *et al.*, 1995).

The calculations in Equations 4-1 to 4-7 have also been used for remifentanil, since the same structure of a three-compartmental model was used.

4.4.2 Effect Compartment

Even for remifentanil, which has a rapid effect site equilibration, there is a small, but appreciable, benefit from targeting the effect site (Bovill, 2000). The peak effect of the drug occurs within 1-3 minutes. The offset is rapid and predictable, even after prolonged infusions.

The pharmacodynamic parameter k_{e0} for remifentanil was set by Vuyk *et al.* (1997) as being 0.9242 min^{-1}. These researchers used the same pharmacokinetic parameters as in Table 4-3. The value of $k_{e0} = 0.9242\ \text{min}^{-1}$ will be used throughout this project.

4.4.3 Effect of Remifentanil on the DOA Indicators

Remifentanil possesses minimal hypnotic or sedative activity. It produces EEG effects similar to those of the other opioids, i.e. high-amplitude and low frequency activity. The remifentanil effects on the AEP and BIS have been studied by several researches. A review of this results will be presented next.

The addition of remifentanil to anaesthetics affects the CNS signals in the presence of a painful stimulus. Crabb *et al.* (1996) studied the effect of remifentanil on the AEP and SEP during isoflurane anaesthesia. Pa amplitude correlated inversely with remifentanil blood concentrations before and after intubation and incision.

Guignard *et al.* (2000) studied the effect of remifentanil on the BIS change (ΔBIS) and haemodynamic responses to orotracheal intubation. Remifentanil attenuated or abolished increases in BIS after intubation in a dose-dependent fashion. Significant reduction of ΔBIS was reported. They concluded that ΔBIS was as sensitive as changes in the haemodynamic variables after a painful stimulus to detect a deficit in the analgesic component of anaesthesia.

The effect of the combination of opioids and hypnotics on BIS was also studied by Strachan and Edwards (2000). They combined different infusion doses of remifentanil with a steady infusion of propofol. It was shown that BIS was reduced by increasing infusion rates of

remifentanil, and that there was a strong correlation between BIS and sedation with this combination of drugs. There was clearly a dose-related effect of remifentanil upon BIS, which suggests that opioids reduce BIS when combined with propofol.

Lysakowski *et al.* (2001) studied the effect of several opioids (including remifentanil) on the loss of consciousness and BIS during propofol induction of anaesthesia. The effect-site concentrations of propofol required for loss of consciousness depend on the simultaneous administration of opioids. They concluded that remifentanil, when added to propofol, did not affect BIS before stimulation. However, there was a significant decrease in BIS value after intubation.

The AEP reflect the balance between CNS depression, caused by anaesthetic drugs and arousal caused by surgical stimulus. McGregor *et al.* (1998) reported that remifentanil was able to abolish the response to laryngoscopy, intubation or incision, as measured by the AEP. This is the main characteristic of a potent analgesic like remifentanil.

Remifentanil has a greater effect on the haemodynamic parameter compared with other opioids. Howie *et al.* (2001) compared the use of fentanyl with remifentanil in an isoflurane/propofol regimen. They reported that remifentanil study group had lower values of HR and MAP than the fentanyl study group. In fact, HR was kept below baseline from induction until the end of the remifentanil infusion, while in the fentanyl group there were significant values above the baseline; the same was also true for MAP. Cafiero *et al.* (2000) also evaluated the effects of remifentanil versus fentanyl on the haemodynamic response to orotracheal intubation. Significant decreases in SAP at induction and 4 minutes after intubation were recorded in the remifentanil group, while significant increases were recorded in the fentanyl group. HR decreased significantly at induction in the remifentanil group, while there was an increase in the fentanyl group. The values of HR were kept below or on the baseline in the remifentanil groups while in the fentanyl groups, HR is always above the baseline.

Kallar *et al.* (1994) compared remifentanil with alfentanil for outpatient surgery. They reported that remifentanil caused dose-dependent reduction in HR and blood pressure. These results are supported by Crabb *et al.* (1996). They also reported dose-related decreases in SAP, DAP and HR after administration of remifentanil. In another study by Thompson *et al.* (1998) it was observed that when using remifentanil blood pressure and HR never went above baseline. For example, MAP increased significantly after intubation, but in the remifentanil groups this increase was quantitatively less than with other

analgesics and did not exceed the pre-induction values.

In conclusion, when added to a hypnotic an opioid prevents the somatic and autonomic responses to noxious stimulus. Remifentanil has a depressive effect on HR, blood pressure, and on the AEP and BIS. This is due to the potency of remifentanil, i.e. its pharmacodynamic characteristics. Lower values of all variables are reported when using remifentanil compared with other opioids. Therefore, the range of expected value during anaesthesia is changed when using remifentanil. Special care is necessary to avoid bradycardia and hypotension. In addition, remifentanil depressed the AEP, indicating that deeper levels of anaesthesia will be reached. Loss of consciousness is achieved faster when remifentanil is used.

4.5 Drug Interactions

General anaesthesia on the basis of a single agent is associated with significant side effects, compromising haemodynamic and/or respiratory function, reducing operating conditions, or postponing postoperative recovery. Another therapeutic advantage of combining an anaesthetic with an analgesic is to achieve the analgesic component of anaesthesia. For an hypnotic to be able to provide pain relief it has to be administered at a very high concentration, which can be dangerous for the patient. Furthermore, general anaesthesia is a process requiring a state of unconsciousness of the brain. If only unconsciousness is achieved, a noxious stimulus will cause arousal/awakening as a result of the intensity of the stimulus. The analgesic is used to prevent arousal, inhibiting the noxious stimulus from reaching the brain (Glass, 1998).

One of the major concerns, when using a combination of drugs is the possible interactions between them. Interactions are generally described as being synergistic or antagonistic. According to Berenbaum (1989), synergy means “working together” and antagonism means “working against each other”, and these terms imply the existence of some intermediate, zero-interactive state in which agents do neither of the above. Formally, the combination is termed (d_a, d_b) where d_a and d_b are the doses (or concentrations) of the two drugs *A* and *B*, respectively. The effect is treated as a mathematical function *E*; thus, $E(d_a, d_b)$ is the effect of the combination. *E* is expressed as a fractional effect. D_a and D_b are the doses of *A* and *B* separately that are isoeffective with the combination. Commonly, isoboles are used for analysing interactions. Isoboles are iso-effect curves, in which the combination (d_a, d_b) is

represented by a point on a graph, the axes of which are the dose-axes of the individual agents. It is expected that, if the agents do not interact, the isobole joining the point representing the combination to those on the dose-axes representing doses isoeffective with the combination (D_a and D_b) will be a strait line. Figure 4-4 shows the isobolar diagram presenting the different interactions.

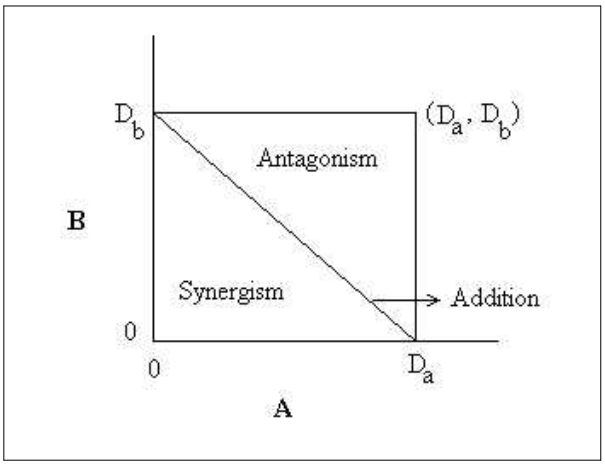

Figure 4-4: Isobolar diagram from Berenbaum (1989). A and B are two different drugs. D_a and D_b are the doses of A and B separately, that are isoeffective with the combination.

The three different classes of pharmacodynamic interactions are defined as (Minto *et al.*, 2000; Vuyk, 2000):

- Zero-interaction or additive interaction: the effect of the combination of the two drugs is exactly the sum of the effects of the individual agents, the two agents simply provide their action next to one another without influence;
- Synergistic or potentiation (the isobole bows towards the origin): the effect of the combination is greater than that expected as based on the concentration effect relationships of the individual agents;
- Antagonistic or infra-additive (the isobole bows away from the origin): the effect of the combination is less than the sum of the effects of the individuals, it could even be less than that of one of its constituents.

If the interaction is synergistic, smaller amounts of both drugs are needed to produce the drug effect when administered together. On the other hand, if the interaction if antagonist, greater amounts of both drugs are needed to produce the effect when administered together. This approach is used to describe pharmacodynamic drug interactions, while pharmacokinetic interactions are described by the interaction-induced changes on the pharmacokinetic parameters.

Pharmacokinetic drug interactions can be divided into interactions that occur during absorption, distribution or elimination. According to Olkkola and Ahonen (2001), pharmacodynamic interactions are far more common and have greater significance in anaesthetic practice than pharmacokinetic interactions. In fact, modern balanced anaesthesia is based on pharmacodynamic interactions, they can be regarded as desirable and the variety of potential pharmacodynamic interactions is limitless. Pharmacodynamic variability is typically quite large, reproducible, and often substantially exceeds the relative magnitude of pharmacokinetic variability (Levy, 1998).

The incidence of adverse reactions increases exponentially as the number of drugs prescribed rises, and this is probably at least partly caused by drug interactions (Olkkola and Ahonen, 2001). Chyka (2000) compared the number of deaths attributed to adverse drug reactions by death certificates and by the food and drug administration's spontaneous postmarketing surveillance system (MedWatch), in order to characterize national mortality statistics in the United States of America in 1995. According to death certificates, 206 deaths were attributed to adverse drug interactions, whereas MedWatch tabulated 6894 deaths. These values were far below what was estimated by extrapolation from surveillance programmes. It was estimated that the number of deaths attributed to adverse drug reactions could be as high as 200,000 deaths per year. Of course, these numbers are more related to normal patient medication or emergence procedures than to interactions during general anaesthesia. However, this study is a clear indicator of the importance of defining drug interactions for the patient's safety.

In general anaesthesia it is clinically important to recognize the pharmacokinetic and pharmacodynamic interaction between propofol (hypnotic) and the analgesic. The improved knowledge of these interactions can be used to optimize the quality of intravenous anaesthesia and to develop practical guidelines for optimal drug dosing.

Intravenous anaesthetic agents affect each other's distribution and elimination. Vuyk (1998) states that for propofol and the opioids, the relationship between dose and blood concentration changes by approximately 10-20% due to these pharmacokinetic interactions. He concludes that, this small variability is unlikely to be recognizable in clinical practice, since the interindividual pharmacokinetic variability of simple agents is on the order of 70-80% and interindividual pharmacodynamic variability is 300-400%. The large pharmacodynamic variability means that such interactions are of much greater importance from a clinical point of view compared with pharmacokinetic interactions.

The hypnotic should be administered to concentrations, which at a minimum, equal the

concentration producing loss of consciousness. To inhibit somatic and autonomic responses to noxious stimuli of surgery, an opiate should be added, thereby lowering the concentration of the hypnotic. However, a ceiling effect on the reduction of the hypnotic by the opioid is reached, thus showing that opioids cannot be used as a sole anaesthetic agent (Glass, 1998).

The pharmacodynamic interaction between propofol and the synthetic opioids is synergistic (Vuyk, 1997, 1999). The pharmacodynamic synergistic interaction strengthens the action of both agents even more. The optimal propofol concentration is affected by the choice of opioid. The longer acting the opioid is, the lower the concentration of opioid one should provide in the presence of equivalent higher propofol concentration.

Vuyk *et al.* (1997) evaluated the implication of opioid selection and duration of infusion on the rate of recovery for combination with propofol. With a longer infusion duration, the optimal target propofol concentration increases when combined with alfentanil, sufentanil and fentanyl, but decreases when combined with remifentanil. Longer infusions increase the time to awakening after termination of the infusion, more for the combination of propofol with alfentanil, sufentanil and fentanyl, than for the combination of propofol and remifentanil, due to a rapid recovery from effects of remifentanil and the possibility of using lower target propofol concentrations.

Fentanyl and alfentanil have been shown to decrease the propofol requirements for induction and maintenance of anaesthesia in a synergistic manner (Smith *et al.*, 1994; Vuyk *et al.*, 1993, 1995, 1996). For both these analgesics the magnitude of the interaction with propofol increases with the strength of the stimulus. The concavity of the isobole for loss of eyelash reflex and consciousness < skin incision < intraabdominal surgery. The major pharmacodynamic differences between these opioids are potency and rate of equilibration between the plasma and the site of drug effect. The half-time of equilibration between the effect site and the plasma for fentanyl is 5-6 minutes (same as for sufentanil) and for alfentanil is of 1.5 minutes. For the three opioids, fentanyl, sufentanil and alfentanil, the time required for recovery increases with the duration of the infusion (Shafer and Varbel, 1991). However, the decay in the effect site remifentanil concentration is much steeper than that of the other opioids and that of propofol. Remifentanil also affects propofol in a synergistic manner (Mertens *et al.*, 2001).

The optimal propofol concentration is much lower when combined with remifentanil compared with the other three opioids. Whereas the optimal propofol concentration when combined with alfentanil is in the order of 3.5 μg/ml, when combined with remifentanil the

optimal propofol concentration is in the order of 2.5 μg/ml. For a infusion duration of 15-600 minutes the context-sensitive half times of the opioids decrease in the order of fentanyl > alfentanil > sufentanil >> remifentanil. Therefore, the optimal propofol concentration decreases in the order of fentanyl > alfentanil > sufentanil >> remifentanil (Vuyk, 2000).

For all concentration combinations of propofol and remifentanil and all durations of infusion, recovery after propofol/remifentanil anaesthesia is much faster than when propofol is combined with one of the other opioids at equipotent doses (Vuyk *et al.*, 1997).

Vuyk (1999) gives the following guidelines:

- fentanyl should be combined with a relatively high propofol dosage;
- alfentanil and sufentanil with an intermediate propofol dosage;
- remifentanil in a relatively high concentration, should be combined with a low propofol infusion regimen.

Recovery after prolonged infusion is rapid, even at suboptimal propofol/remifentanil concentrations. Return of consciousness after propofol/remifentanil anaesthesia is much more caused by the decrease in the effect site concentration of the opioid than that of propofol, since the effect site propofol concentration drops much slower than that of remifentanil. The 60% decrement curve of remifentanil runs more or less parallel to the 25% decay curve of propofol (Vuyk, 2000).

The pharmacodynamic interaction between propofol and remifentanil as measured by effects on BIS, was analysed by Ropcke *et al.* (2001), using a BIS of 50 as a measure of "adequate" DOA. They concluded that the two drugs have a synergistic interaction for maintenance of a BIS value between 45 and 55 during surgery. This was true, regardless of whether concentrations or infusion rates were used as model input.

Minto *et al.* (2000) suggested the use of a response surface model for anaesthetic interactions. The model is based on the assumption that there is a sigmoid relationship between the effect and drug concentration at the site of action. The response surface model considers any ratio of two drugs given simultaneously as behaving as a new drug. This model is empirical and only assumes that the concentration-response relation for each of the interacting drugs is described by a pharmacodynamic model. They apply the model using data from a study of the interaction of midazolam, propofol, and alfentanil with loss of consciousness. This is a recent and new approach in this research area and the work is still under development. They propose to apply this model to a control system in

anaesthesia.

Propofol also interacts with inhalational analgesics like nitrous oxide. Davidson *et al.* (1993) reported that nitrous oxide reduced the blood propofol concentration at which 50% of patients moved by approximately 30%. In fact, propofol has a synergistic relation with other sedative agents and not just the synthetic opioids (Vuyk, 1998).

4.6 Simultaneous Administration of Propofol and Remifentanil

In the recent years, general anaesthesia with propofol and remifentanil has become more popular. Because of its pharmacokinetic characteristics, remifentanil, a short-acting opioid agonist, may be the ideal opioid to use in combination with propofol for continuous i.v. administration (Olivier *et al.*, 2000).

The use of this combination of drugs has been reported as efficacious (Bagshaw, 1999; Domaingue, 2001; Grundmann *et al.*, 2001; Kulkarni, 2000; Lehmann *et al.*, 1999; Rowbotham *et al.*, 1998). The studies on anaesthetic drug interactions showed that the optimal propofol concentration decreases more significantly with remifentanil as compared with other opioids and recovery is much faster than when propofol is combined with other opioids. For this reason, remifentanil has specific advantages over the other opioids.

Holas *et al.* (1999) studied the use of remifentanil, propofol or both for conscious sedation during eye surgery under regional anaesthesia. The goal was a sedation level at which patients were calm and comfortable but obeyed vocal commands during the entire surgical procedure. When total anaesthesia is not considered the drug requirements are different. However, they concluded that the combination of propofol and remifentanil, provided a smooth haemodynamic profile and lacked untoward effects. Therefore, a continuous infusion of remifentanil with propofol seems to be a useful and cost effective technique for conscious sedation under regional anaesthesia. Smith *et al.* (1997) also compared the use of propofol versus remifentanil for monitored anaesthesia care. However, the propofol group lacked analgesia and the remifentanil group offered a low sedation level and was associated with greater respiratory depression. A combination of both drugs seems to be preferable.

Olivier *et al.* (2000) used a continuous infusion of remifentanil and a TCI of propofol for patients undergoing cardiac surgery. This combination resulted in haemodynamic stability and good postoperative analgesia. The optimal infusion rate of propofol when combined

with remifentanil is less than that normally used for maintenance of anaesthesia with other opioids. The major impetus for low-dose propofol administration is decreasing the haemodynamic effects of this drug (Hogue *et al.*, 1996). This technique allowed physicians to schedule the time of extubation in patients undergoing cardiac anaesthesia. Intraoperative low-dose propofol associated with high-dose remifentanil should promote rapid awakening as a result of the short, context-sensitive half-time of these drugs (Vuyk, 1997).

The use of this drug combination was also studied for elective non-cardiac surgery by Pelosi *et al.* (1999). When combined with propofol, remifentanil effectively provided for profound analgesia during surgery, stable anaesthetic conditions, simplicity of use and predictable recovery. They concluded that, for an adequate level of anaesthesia low doses of propofol are adequate if combined with remifentanil in a high dose range (0.25-0.5 μg/kg/min) according to noxious stimulation; if signs of light anaesthesia are recorded, remifentanil rescue could be the first choice solution.

Duce *et al.* (2000) evaluated the combination of propofol and remifentanil for short painful procedures in children. Both drugs were given in bolus injection. This technique was found simple, effective and predictable for procedures lasting less than 10 minutes. Propofol and remifentanil are a simple alternative to inhalational anaesthesia for short painful procedures. Inhalational agents are associated with postoperative nausea, vomiting and agitation. The technique with propofol and remifentanil has a low incidence of these side-effects. Another study in paediatric patient can be found in Grundmann *et al.* (1998). They compared TIVA with propofol and remifentanil versus a desflurane-nitrous oxide inhalational anaesthesia. They demonstrated that a combination of remifentanil/propofol is suitable for children. It is a well-tolerated anaesthesia method, which can provide rapid smooth induction of anaesthesia, intraoperative haemodynamic stability, a fast emergence and a short postoperative recovery period. Keidan *et al.* (2001) studied the effect of adding remifentanil to propofol anaesthesia in children. Remifentanil resulted in: a lower total amount of propofol to prevent patient movement; a lower time interval to eye opening; an improvement in the conditions during the procedure; fewer movements in response to the insertion of the aspiration needle and required significant fewer additional doses of propofol; and a significantly higher decrease in HR.

There are several studies evaluating the effects of this combination of drugs as measured by the BIS. Hoymork *et al.* (2001) evaluated the accuracy of TCI systems for propofol and remifentanil in a clinical surgical setting, with these two drugs as the only anaesthetics used

for hypnosis and analgesia. BIS was not sensitive enough for evaluating drug effects to pick out patients with deviating drug concentration at the deep level of anaesthesia. There was no correlation between measured plasma concentrations and BIS, for both drugs. The same conclusion was reached in a previous study when measuring serum drug levels (Hoymork *et al.*, 1999). BIS registration was not able to pick-out patients with highly deviating serum levels from the others. Other researchers, such as Finianos *et al.* (1999a, b) and Hans *et al.* (2000), concluded that BIS measured the level of sedation and did not correlate with effect-site concentrations of the hypnotic propofol. This is not surprising, since remifentanil potentiates propofol and the level of unconsciousness is different when different concentrations of remifentanil are used with the same concentration of propofol.

Philip *et al.* (1997) compared remifentanil with alfentanil for ambulatory surgery using propofol for TIVA. Remifentanil used with propofol was effective as the primary opioid in TIVA. In this study, remifentanil provided better intraoperative haemodynamic stability than alfentanil, because remifentanil was dosed to higher levels of opioid. For ambulatory patients, short-acting drugs are needed for TIVA so as not to delay recovery.

O'Hare *et al.* (2001) examined recovery with the use of remifentanil to supplement anaesthesia maintained with different preselected target plasma concentrations of propofol. The results showed that adequate anaesthesia could be maintained by using different proportions of the hypnotic and the opioid. It was also evident that the use of a short-acting opioid, when given at a higher dose results in a more rapid, early recovery. Regardless of the duration of infusion, the decrease in remifentanil plasma concentration to 50% has a time of 3.6 minutes. This characteristic allows uncomplicated changes in infusion rates with rapid effect, making remifentanil an ideal adjunctive for i.v. anaesthesia. These results are also supported by Papilas *et al.* (1999).

The interaction of the remifentanil and propofol doses required to prevent patient response during surgery was studied in patients undergoing arthroscopic surgery with a median anaesthesia duration of 1 hour by Peacock and Philip (1999). They concluded that remifentanil can be administered in comparatively larger doses as the opioid component of ambulatory anaesthesia, which will reduce patient's responses to surgery but will not delay recovery. Remifentanil is also appropriate to use for patients or procedures that require a brief, variable, or rapidly terminating intense opioid effect.

Space prohibits mentioning all other researches in this area but the following are worth mentioning: Doyle *et al.*, 2001; Fragen and Fitzgerald, 2000; Haughton *et al.*, 1999;

Kazmaier *et al.*, 2000; Milne and Kenny, 1999; Peacock *et al.*, 1998; Twersky *et al.*, 2000.

4.7 Summary

General anaesthesia with intravenous drugs, is gaining increasing acceptance because of the availability of short-acting hypnotics and opioids and improved infusion systems. With TIVA, the analgesic and hypnotic components of anaesthesia can be titrated separately to control DOA despite changing surgical stimulus.

The hypnotic propofol is the most suitable intravenous anaesthetic agent, and it is frequently used in combination with synthetic opioids. The introduction of remifentanil, an ultra short-acting opioid with a rapid onset and offset of action, leads to more stable operating conditions. Remifentanil potentiates the effects of propofol, i.e. a decrease in the haemodynamic parameters and depression of the CNS, which is reflected in the AEP. Therefore, when combined with remifentanil the adequate propofol concentration is largely reduced. The use of remifentanil provides a faster recovery without side effects (e.g. nausea), enhancing the quality of anaesthesia. Due to its potency, remifentanil provides an adequate analgesia and was proved to be suitable for various types of surgery, from cardiac surgery to short interventions needing only regional anaesthesia, in adults or in children.

The combination of propofol and remifentanil is becoming more popular with anaesthetists. However, the study of the pharmacodynamic interaction of these two drugs is necessary so as to assure an adequate DOA level and pain relief. Remifentanil has a synergistic interaction with propofol and this can be used to an advantage, which is titrating propofol to lower infusion rates and speeding up recovery. However, special care is necessary because if propofol is used to achieve high concentrations, the simultaneous administration of remifentanil will increase drastically propofol side effects, leading to situations of bradycardia or hypotension. It is of major importance to consider the pharmacodynamic interaction of the two drugs.

Drug interactions can interfere with the anaesthetic conditions and patient safety. The anaesthetist should be aware of these interactions and use this information to combine properly the infusion doses of both drugs.

General anaesthesia techniques could take advantage of the pharmacodynamic interaction between the hypnotic and the opioid to determine the optimal infusion profiles, controlling

the amount of drug administered based on the level of DOA, and also on the haemodynamic parameters. These parameters can be used to obtain simulation models for the effects of the drug combination (propofol/remifentanil). The modelling of the patient's vital signs, based on the interaction of these drugs will be discussed in the next chapter. In addition, effect concentrations will be used to model the effect of the two drugs. The effect concentration governs the drug effects, since it is in the effect site that the drug exerts its action.

Chapter 5

A Hybrid Patient Model

5.1 Introduction

A patient model is necessary to construct and test a closed-loop control system in anaesthesia prior to any transfer of the design to the operating theatre. In Chapter 3, a fuzzy relational classifier (FRC) for depth of anaesthesia (DOA) was presented. The FRC uses a set of wavelet extracted auditory evoked potentials (AEP) features, and the cardiovascular parameters change of heart rate (ΔHR) and change of systolic arterial pressure (ΔSAP), to classify DOA into five different levels. This set of parameters is considered to be the effect of the combination of the two drugs used (i.e. propofol and remifentanil) and of the surgical stimulus.

The next step is to model the ΔHR, ΔSAP and the AEP features using the drug effect concentrations and the surgical stimulus level. The effect concentrations are obtained using the pharmacokinetic compartmental models combined with an effect compartment, as explained in Chapter 4. The objective of this exercise is to model the pharmacodynamic properties of both drugs and the interactions between them.

Overall, the patient model includes the pharmacokinetic compartmental models of both drugs, and a pharmacodynamic model constituted by the effect compartment and by a model describing the relationship between the effect concentrations and the different effects. Furthermore, the patient model is different considering the two main phases of a surgical procedure, i.e. induction and maintenance of anaesthesia. These two phases present different characteristics, not just in the amount of drug used, but also in the degree of stimulus. The absence of stimulus in the induction phase (except intubation) affects the pharmacodynamic interaction between propofol and remifentanil (Chapter 4). In the

maintenance phase, the surgical stimulus is a continuous event, from incision until suture, with different degrees of intensity.

The induction phase was considered to be the initial 1500 seconds (25 minutes), when the patient is still in the anaesthetic room. The maintenance phase was considered to be from 1500 seconds (assuming that the patient is stable and is already in the operating room) until the infusion of propofol stops and recovery begins. In this project, the recovery phase is not considered, since the major objective is the control of DOA using a combination of the two drugs. In the recovery phase, the infusion of both drugs is usually stopped and there is no control, however, this drug combination is notorious for providing a rapid recovery.

This chapter presents the different pharmacodynamic models for the induction and maintenance phase, considering ΔHR, ΔSAP and the AEP features. The effect concentrations of the two drugs are used to model the pharmacodynamic interaction of remifentanil and propofol on the cardiovascular parameters, and on the AEP. Fuzzy Takagi-Sugeno-Kang (TSK) models are used in the maintenance phase, which are trained using the Adaptive Network-Based Fuzzy Inference System (ANFIS). In addition, a stimulus model is used to establish the effects of the surgical stimulus on the cardiovascular parameters, according to the level of analgesia. This stimulus model is constructed into a Mamdani type fuzzy model, using the anaesthetist knowledge described by fuzzy IF-THEN rules.

The hybrid patient model is constructed using the data from one surgical intervention (patient Pat1). This model represents a typical procedure using the combination of propofol and remifentanil. The limited amount of data available, restricts the choice of models and the possibility of a wider generalization.

5.2 Patient Data

The data from patient Pat1 were used to obtain the pharmacodynamic patient models. These data were gathered during a surgical procedure lasting 9685 seconds, approximately 2 hours, 41 minutes and 25 seconds. The infusion profiles of both drugs were determined by the anaesthetist, according to his experience and the nature of the surgical stimulus present at the time. Figure 5-1 shows the infusion profiles for propofol and remifentanil.

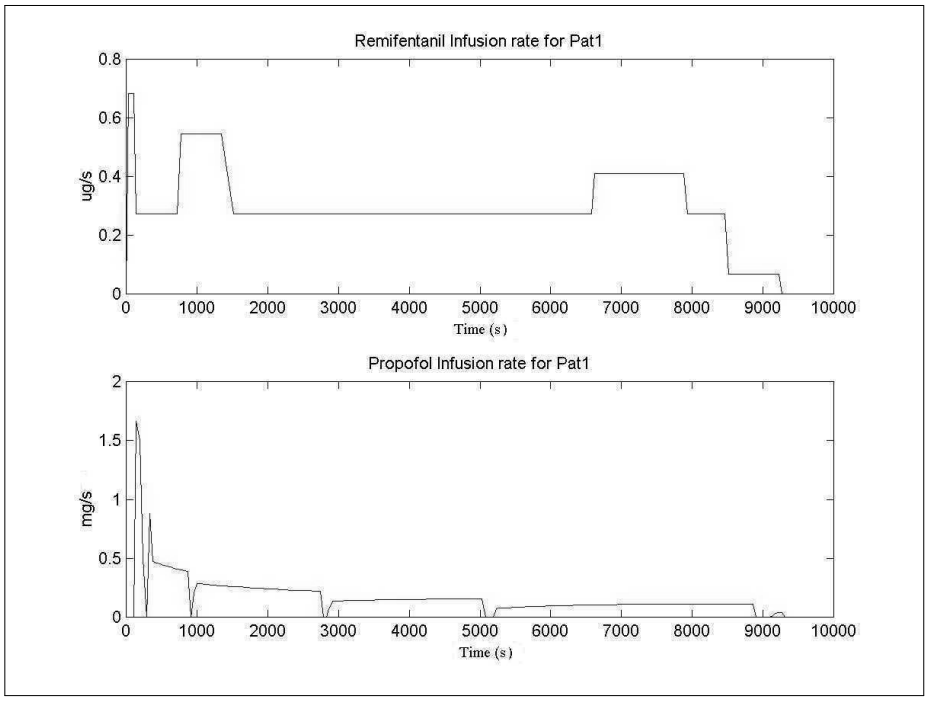

Figure 5-1: Remifentanil and propofol infusion rate profiles used in the surgical procedure of patient Pat1.

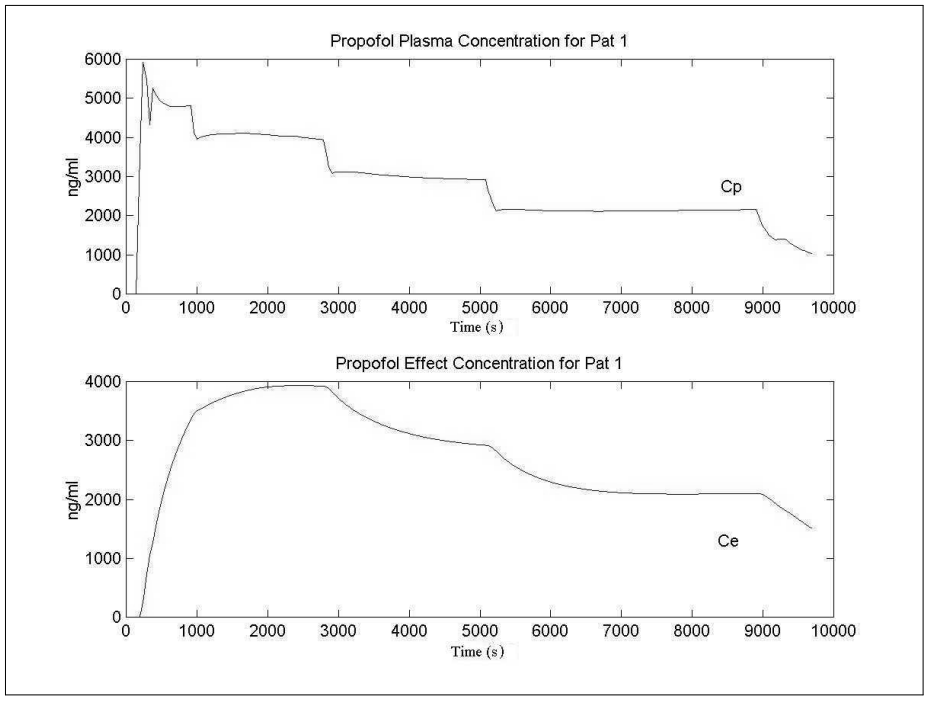

Figure 5-2: Propofol plasma (C_p) and effect (C_e) concentrations obtained from the infusion profile used in the surgical procedure of patient Pat1 (Figure 5-1).

The plasma concentration of both drugs was obtained using the infusion rates in Figure 5-1 and the pharmacokinetic compartmental models described in Chapter 4, with the mean population pharmacokinetic parameters. The effect compartment was used to establish the effect concentration of propofol and remifentanil, using the parameter k_{e0}. The

pharmacokinetic interactions of the two drugs were not studied. Therefore, the concentrations of propofol and remifentanil are determined separately. Figures 5-2 and 5-3 show the plasma and effect concentrations for propofol and remifentanil, respectively.

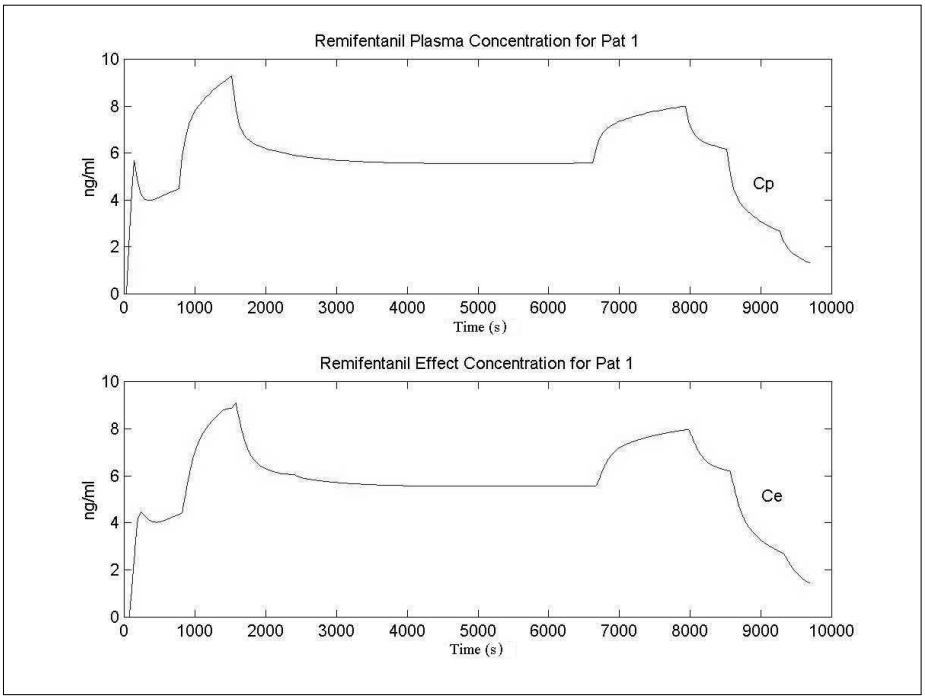

Figure 5-3: Remifentanil plasma (C_p) and effect (C_e) concentrations obtained from the infusion profile used in the surgical procedure of patient Pat1 (Figure 5-1).

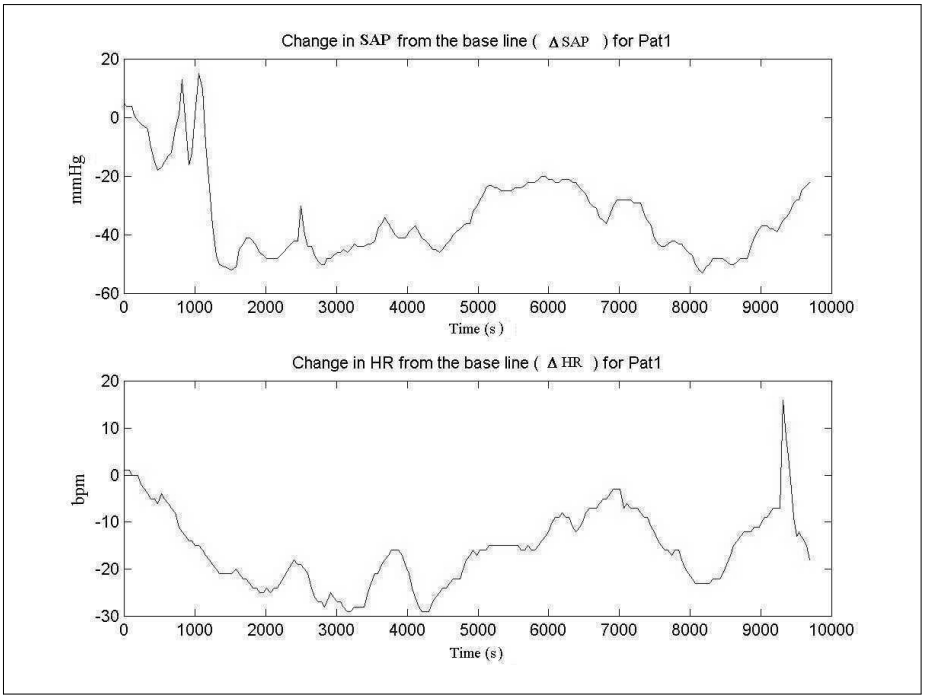

Figure 5-4: Cardiovascular parameters, ΔSAP and ΔHR, recorded during the surgical procedure of patient Pat1.

The effect concentrations of remifentanil and propofol will be used to model the effect of both drugs on the cardiovascular parameters, ΔSAP and ΔHR and on the AEP features. Figure 5-4 shows the parameters ΔSAP and ΔHR recorded during the surgical procedure with patient Pat1. The SAP and HR baselines were 130 mmHg and 90 bpm respectively.

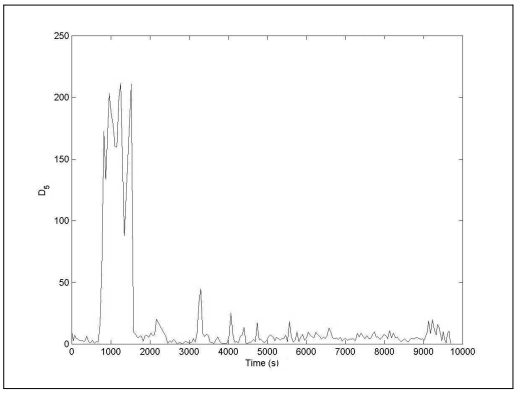

Figure 5-5: AEP feature D_5.

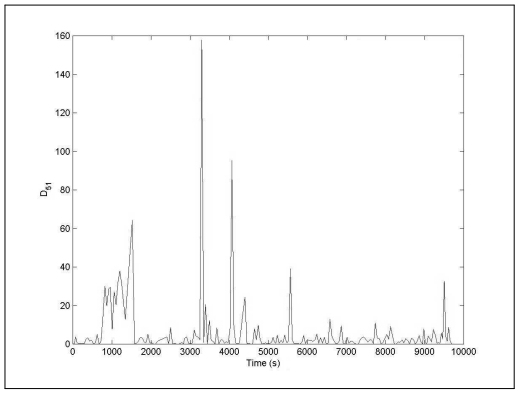

Figure 5-6: AEP feature D_{51}.

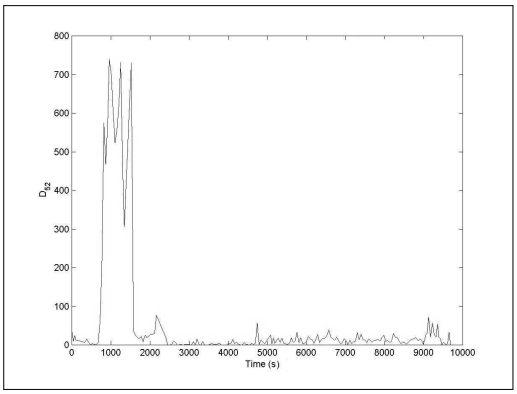

Figure 5-7: AEP feature D_{52}.

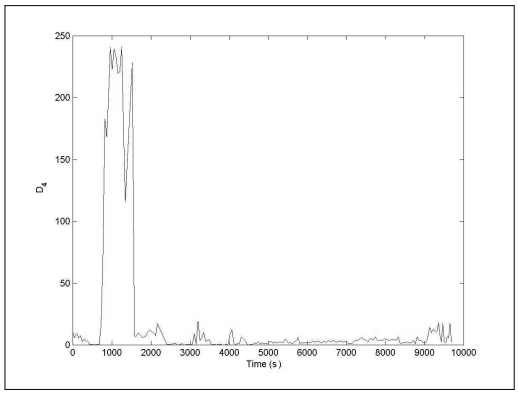

Figure 5-8: AEP feature D_4.

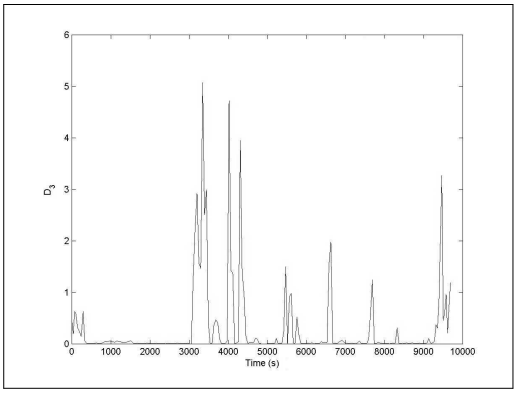

Figure 5-9: AEP feature D_3.

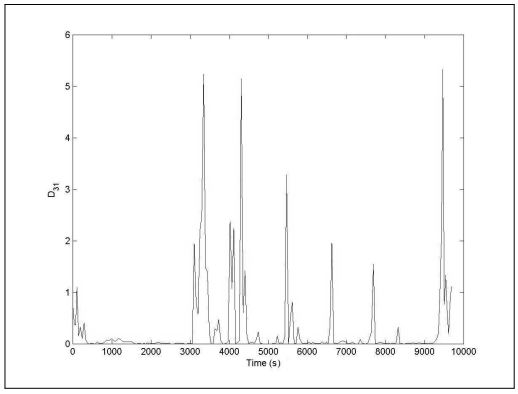

Figure 5-10: AEP feature D_{31}.

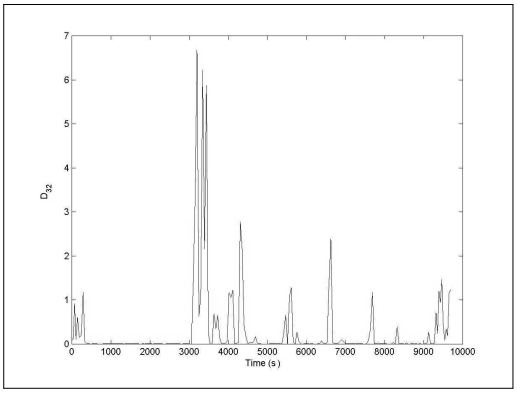

Figure 5-11: AEP feature D_{32}.

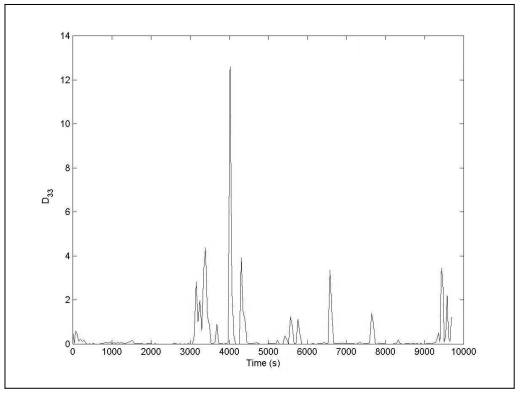

Figure 5-12: AEP feature D_{33}.

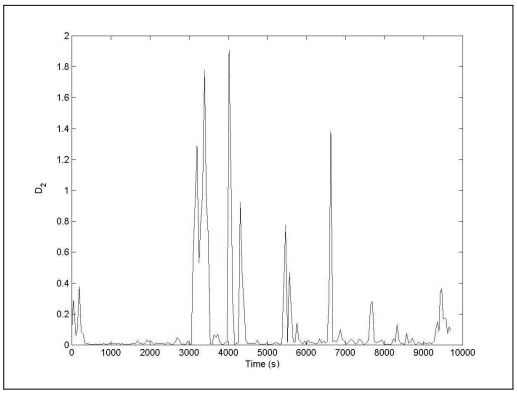

Figure 5-13: AEP feature D_2.

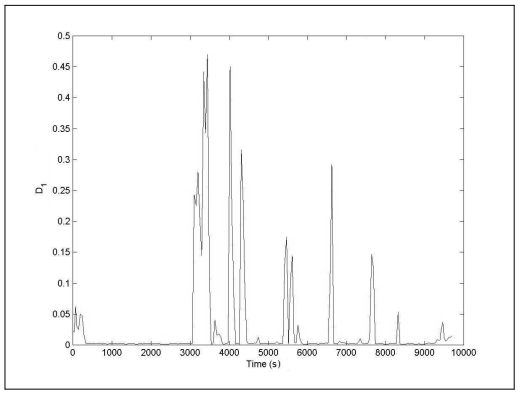

Figure 5-14: AEP feature D_1.

The ten wavelet extracted AEP features, D_5, D_{51}, D_{52}, D_4, D_3, D_{31}, D_{32}, D_{33}, D_2 and D_1, were obtained from the AEP sweeps recorded (204 sweeps in total) during the surgical procedure, and are presented in Figures 5-5 to 5-14. Analysing the figures, the different characteristics of the several AEP features are clear; they represent different frequency bands and carry different information. However, some of them present a similar profile, specially when comparing the low frequency components to the high frequency, e.g. D_2 and D_1 with D_5 and D_4.

The DOA profile for patient Pat1 is presented in Figure 5-15, as classified by the anaesthetist during the intervention. This is based on the anaesthetist experience and the observed clinical signs.

The data gathered in the operating theatre are used to model the different parameters, considering the induction and maintenance phase of anaesthesia. The data from patient Pat1 are used to train and test the different pharmacodynamic models, presented in the next sections. The final patient model describes a typical surgical intervention with the combination of propofol and remifentanil. This model will be used in Chapter 6, to

substitute the patient when simulating a closed-loop control system for DOA.

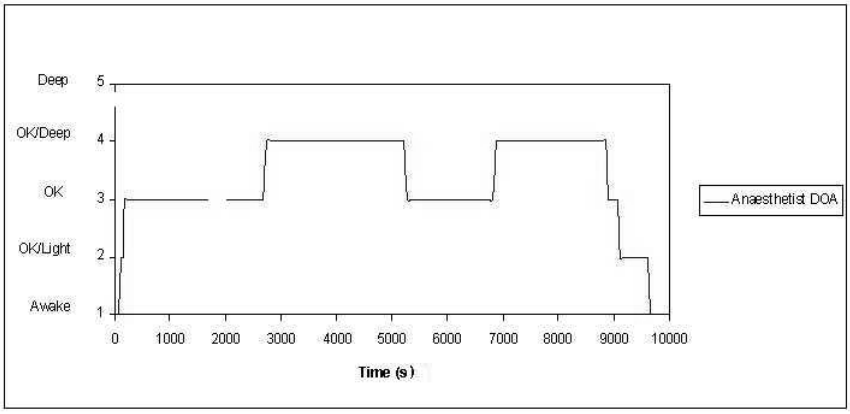

Figure 5-15: Depth of anaesthesia (DOA) as classified by the anaesthetist, for Patient Pat1.

5.3 Induction-Phase Model

The surgical procedure is divided into induction and maintenance phases. The induction phase was established as being the first 1500 seconds (25 minutes) of the whole procedure. This is usually the time spend by the patient in the anaesthetic room, where the induction of anaesthesia and the intubation of the patient takes place.

During induction of anaesthesia, high effect concentrations of the hypnotic are targeted. A rapid intravenous bolus injection or a continuous infusion of a high dose for a limited short time are usually used. Depth of anaesthesia increases rapidly causing loss of consciousness, and then decreases as the hypnotic concentration declines.

The rapidly changing concentrations during induction cause a corresponding fluctuation in the degree of CNS depression. The CNS depression lags behind the plasma concentration, represented by hyteresis on curves plotting the effect against the concentrations. The non-steady-state conditions produced by rapid administration of a drug, make assessment of the relationship of the drug concentration and DOA difficult, if not impossible (Stanski, 1994).

The AEP latency appears erratic at the induction of anaesthesia, since the calibration of the AEP waveform in an awake patient is difficult in the time available in the anaesthetic room. In addition, the increase in latency at induction of anaesthesia is followed by a decrease due to intubation of the trachea, which causes a stress response manifested by an increase in

blood pressure and a decrease in latency (Allen and Smith, 2001).

The AEP signal is not normally used for the monitoring of DOA during the induction of anaesthesia. However, immediately after induction of anaesthesia and tracheal intubation, the AEP display a characteristic pattern (Thornton *et al.*, 1989a). The AEP features displayed in Figures 5-5 to 5-8 (the high frequency components) show the discrepancy between the values at induction and during maintenance of anaesthesia. For these reasons, the AEP will not be used during the induction phase. The patient model will only reflect the changes in SAP and HR during this phase.

Induction agents, such as propofol, show a much stronger interaction with opioids for suppression of responses intraoperatively, compared with the minor interaction seen during the induction of anaesthesia (Vuyk, 1998). In addition, several researchers stated that the influence of remifentanil on the haemodynamic parameters during the induction phase is reflected on the response to intubation, the only strong stimulus during induction (Cafiero *et al.*, 2000; Casati *et al.*, 2001; Grewal and Samsoon, 2001; Joo *et al.*, 2001; McGregor *et al.*, 1998; Song *et al.*, 1999).

Significant haemodynamic changes are associated to tracheal intubation. This response is attenuated by the use of opioids such as remifentanil (Alexander *et al.*, 1999a; Lee *et al.*, 2001). The effect of different doses of remifentanil on the cardiovascular response to intubation, has been the focus of several researches (Grant *et al.*, 1998; Hall *et al.*, 2000). Remifentanil prevents the movement and the increases in haemodynamic variables associated with intubation is a concentration dependent fashion. Remifentanil has a more significant reduction in the increases of MAP and HR after intubation compared to other opioids (Guignard *et al.*, 2000; Thompson *et al.*, 1998).

The induction phase patient model is presented in Figure 5-16, including the pharmacokinetic and pharmacodynamic models. Section 5.3.1 shows how ΔSAP and ΔHR can be modelled using the propofol effect concentration, and Section 5.3.2 presents the effect of intubation on the cardiovascular parameters and the action of remifentanil.

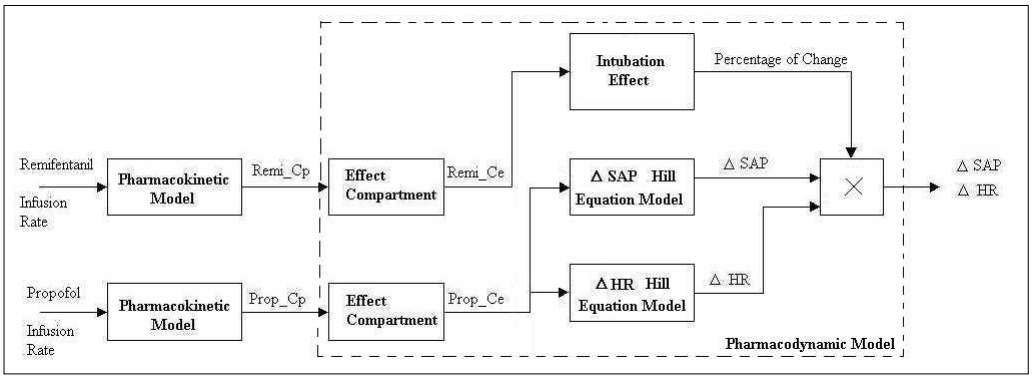

Figure 5-16: Block diagram of the induction phase model. *Prop_Cp* and *Remi_Cp* are the plasma concentrations of propofol and remifentanil, respectively, whereas *Prop_Ce* and *Remi_Ce* are the effect concentrations.

5.3.1 Cardiovascular Parameters

The cardiovascular parameters ΔSAP and ΔHR were modelled using a set of data from patient Pat1. The data set used is presented in Figure 5-17 and represents the time period from 2018 seconds to 6576 seconds (termed Group1). During this time, the remifentanil infusion rate and effect concentration were constants (Figures 5-1 and 5-3). Therefore, only the effect of the changes in propofol infusion rate are considered.

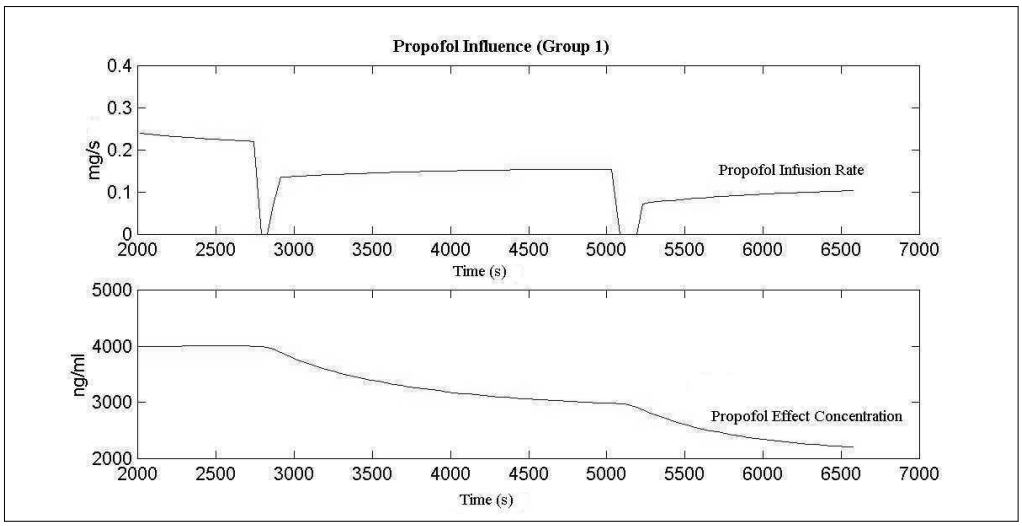

Figure 5-17: Propofol infusion rate and effect concentration, of the time period in Group1.

A Hill equation model (described by Sheiner *et al.* (1979)) was used to model the influence of propofol on ΔSAP and ΔHR. The Hill equation used is of the form:

$$Effect = E_{\max}\frac{C_e^{\alpha}}{C_e^{\alpha}+C_{p50}^{\alpha}} \qquad 5\text{-}1$$

where $E_{\max}$, α and C_{p50} are constants, C_e is the propofol effect concentration, and *Effect* represents ΔSAP or ΔHR.

The Nonlinear Control Design (NCD) MATLAB Toolbox was used to optimize the parameters of Equation 5-1. The NCD is a time-domain-base optimization approach to system design. It automatically converts time-domain constraints and time responses into an optimization problem, and then solves the problem using a gradient method with a modified line-search algorithm. Successive simulations and sequence quadratic programming solve the optimization problem. Monte Carlo methods can also be used to increase the system robustness.

The difference between the Hill equation value and the actual effect (ΔSAP or ΔHR) during the time period of the data set was used as the signal to be constraint to a minimum (ideally zero). The parameters $E_{\max}$, α and C_{p50} were automatically tuned based on the performance constraint. Several simulations were performed with different initial values, uncertainty and error margins, so as to obtain the best approximation to the values of ΔSAP and ΔHR of patient Pat1, using the specified data set (Group1, Figure 5-17).

5.3.1.1 Systolic Arterial Pressure

After several interactive optimizations, the NCD allowed the following values to be obtained

$$E_{\max} = -69.61$$
$$\alpha = 3.18$$
$$C_{p50} = 2999.4$$

Therefore the ΔSAP Hill equation model is:

$$\Delta SAP_{model} = -69.61\frac{C_e^{3.18}}{C_e^{3.18}+2999.4^{3.18}} \qquad 5\text{-}2$$

where C_e is the propofol effect concentration.

The model results on the training data set (Group1) are presented in Figure 5-18. The mean absolute error of the model was of 3.37 mmHg, this low value represents a reasonable model approximation. This set of parameters captures well the ΔSAP changes. However, the value of SAP is not the result of the drug effect only, but surgical stimulus is also

responsible for the SAP variations. Therefore, a model using only the effect concentration of the drug will not reproduce the data exactly.

Equation 5-2 was applied to the data of the induction phase and the result is shown in Figure 5-19. The model has a reasonable performance when modelling the induction phase. This result shows that the propofol effect concentration is sufficient to describe the behaviour of ΔSAP during the induction phase. The high ΔSAP values (peaks) at approximately 810 seconds and 1025 seconds were caused by tracheal intubation.

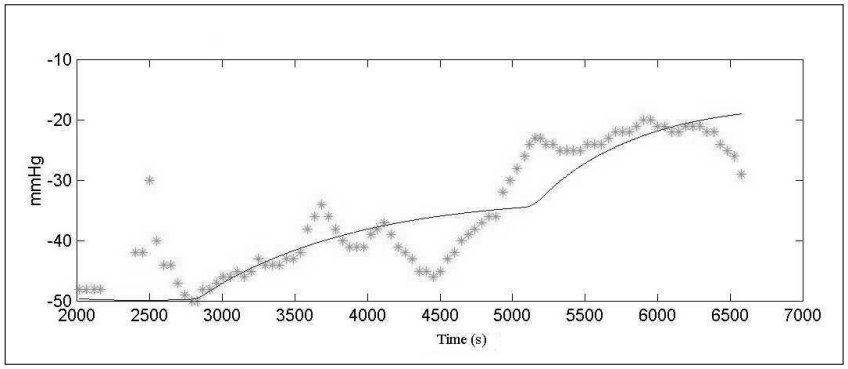

Figure 5-18: ΔSAP from patient Pat1 (*) and the result of the Hill equation model (solid line), considering the data of Group1.

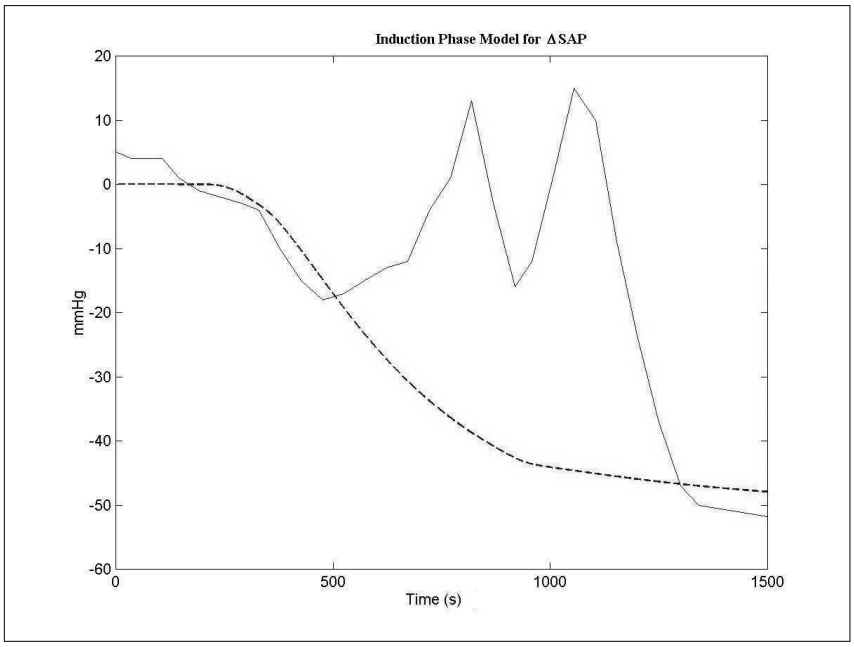

Figure 5-19: ΔSAP from patient Pat1 (solid line) and ΔSAP from the Hill equation model (dashed line), considering the induction phase.

5.3.1.2 Heart Rate

The optimized parameters of Equation 5-1, when considering ΔHR, where established by the NCD blockset as:

$$E_{\max} = -40.91$$
$$\alpha = 1.84$$
$$C_{p50} = 2990.8$$

Therefore the ΔHR Hill equation model is:

$$\Delta HR_{model} = -40.91 \frac{C_e^{1.84}}{C_e^{1.84} + 2990.8^{1.84}} \qquad 5\text{-}3$$

where C_e is the propofol effect concentration.

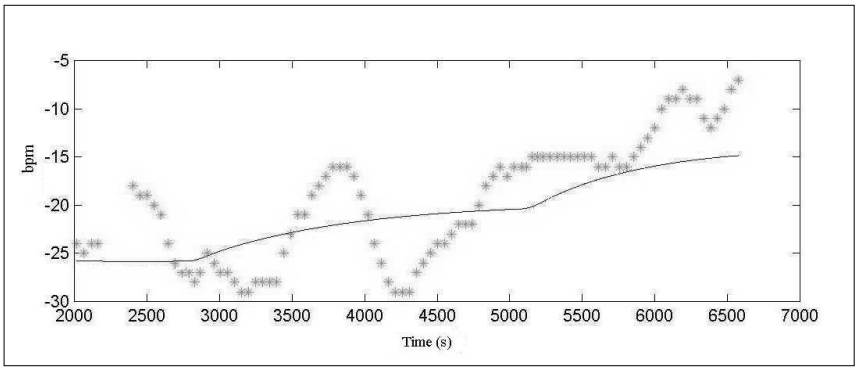

Figure 5-20: ΔSAP from patient Pat1 (*) and the result of the Hill equation model (solid line), considering the data of Group1.

Figure 5-20 shows the model results and the ΔHR of patient Pat1, considering the data set Group1. The mean absolute error of the model for this set of data was of 3.66 bpm. The reasonable model approximation and low error, show that the Hill equation is suitable to model the effect of propofol on the ΔHR, when remifentanil is kept at a constant level.

The Hill equation model of Equation 5-3 was applied to the induction phase data, and the result is presented in Figure 5-21. The model of ΔHR has an acceptable performance, representing the ΔHR trend during the induction phase.

Propofol has a depressive effect on both ΔHR and ΔSAP, and this is reflected when using the Hill equation models. However, it is necessary to note that the pharmacokinetic parameters and the k_{e0} value used to model the plasma and effect concentrations of propofol are mean population values. Therefore, it is expected that small changes may occur between the modelled concentrations and the real concentrations that lead to the

observed effect (ΔSAP or ΔHR). The plasma propofol concentration was not measured, therefore, the model results are the best available approximation.

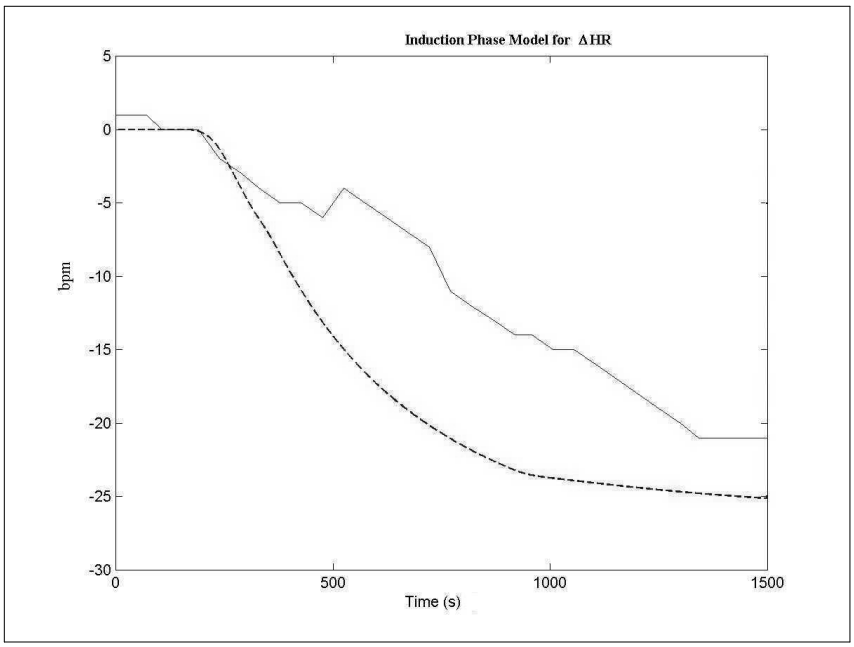

Figure 5-21: ΔHR from patient Pat1 (solid line) and ΔHR from the Hill equation model (dashed line), considering the induction phase.

The peak in ΔHR present in the patient data (Figure 5-21) was diagnosed by the anaesthetist as being related to intubation. The haemodynamic response to intubation is more predominant in the blood pressure than in the heart rate, this is discussed in detail in the following subsection.

5.3.2 Remifentanil and the Haemodynamic Response to Intubation

Remifentanil interacts with propofol in the presence of surgical stimulus. However, in the induction phase the only stimulus was tracheal intubation. This is a very strong stimulus which is associated with haemodynamic changes. Opioid drugs are administered at the time of induction of anaesthesia in an attempt to attenuate the cardiovascular response to intubation.

Guignard *et al.* (2000) reported that remifentanil attenuated or abolished increases in MAP and HR after intubation in a comparable dose-dependent fashion. Thompson *et al.* (1998) also assessed the effect of remifentanil on the ΔSAP and ΔHR after intubation. They reported that intubation had no significant effect on HR in the remifentanil groups and SAP increased significantly in all groups, but in the remifentanil groups this increase was

quantitatively less than with other opioids, and did not exceed pre-induction values.

The influence of remifentanil in ΔSAP and ΔHR could be described as a function of the effect concentration at the time of intubation. Considering that the remifentanil effect is dose/concentration dependent. In order to obtain the relation between remifentanil effect concentration and the effect in ΔSAP and ΔHR, the data from two researches was used (McAtamney *et al.*, 1998; O'Hare *et al.*, 1999). These researches reported the effects of remifentanil bolus doses on the haemodynamic responses to tracheal intubation.

Figures 5-22 and 5-23 show the percentage of change in mean SAP and HR respectively, compared with the baseline values for the data in McAtamney *et al.* (1998). Three different remifentanil bolus doses were used: 0.25, 0.5 and 1 μg/kg administered at induction over a period of 30 seconds. Tracheal intubation occurred 1 minute after induction. A group of 80 patients were assigned by random allocation to one of four treatment groups, receiving: 0.25, 0.5 or 1.0 μg/kg of remifentanil or placebo (10 ml 0.9% saline). Analysing the figures, it is clear that the major effect is observed 1 minute after intubation (i.e. 2 minutes after induction). At minute 4, the SAP and HR values seem to go back to normal values.

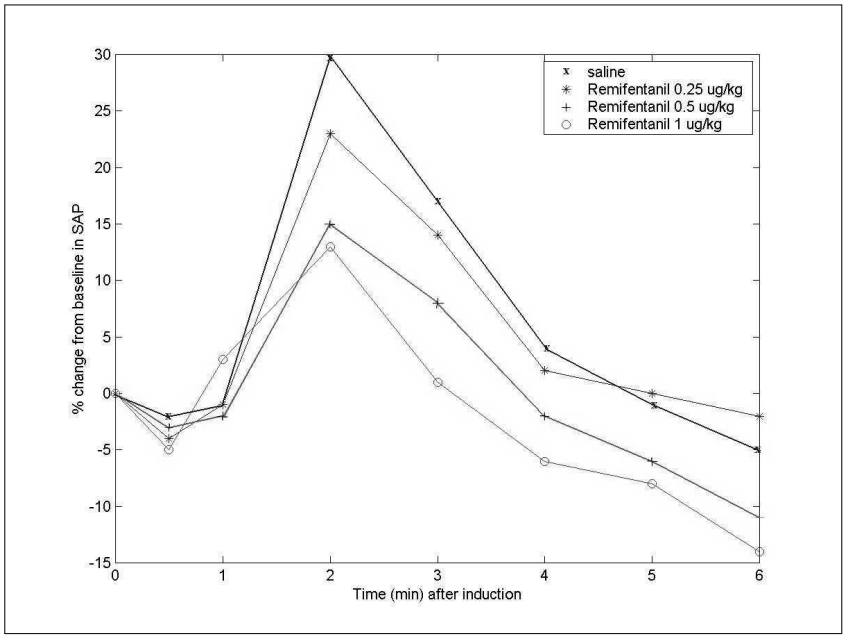

Figure 5-22: Percentage of change from baseline in mean SAP, after induction of anaesthesia. Data from McAtamney *et al.* (1998). Intubation was performed 1 minute after induction.

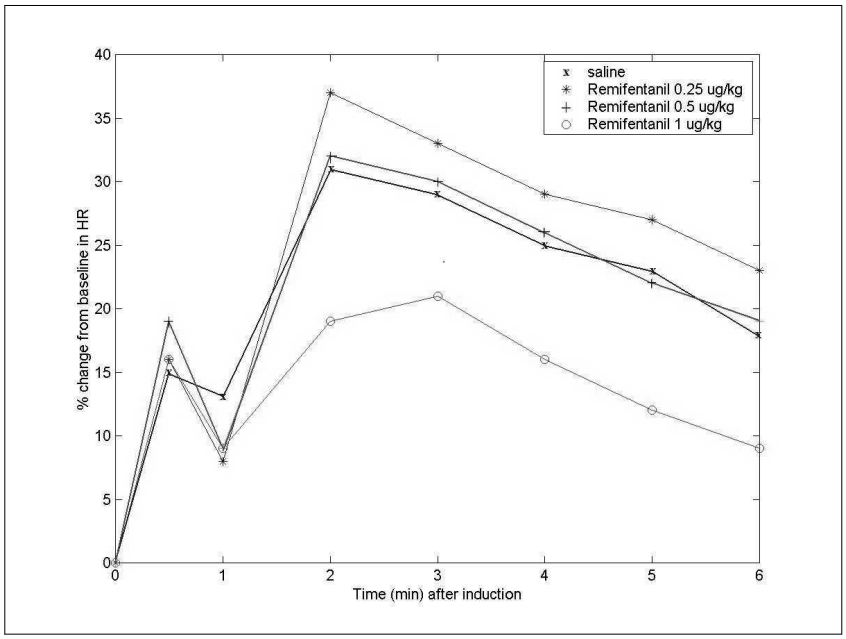

Figure 5-23: Percentage of change from baseline in mean HR, after induction of anaesthesia. Data from McAtamney *et al.* (1998). Intubation was performed 1 minute after induction.

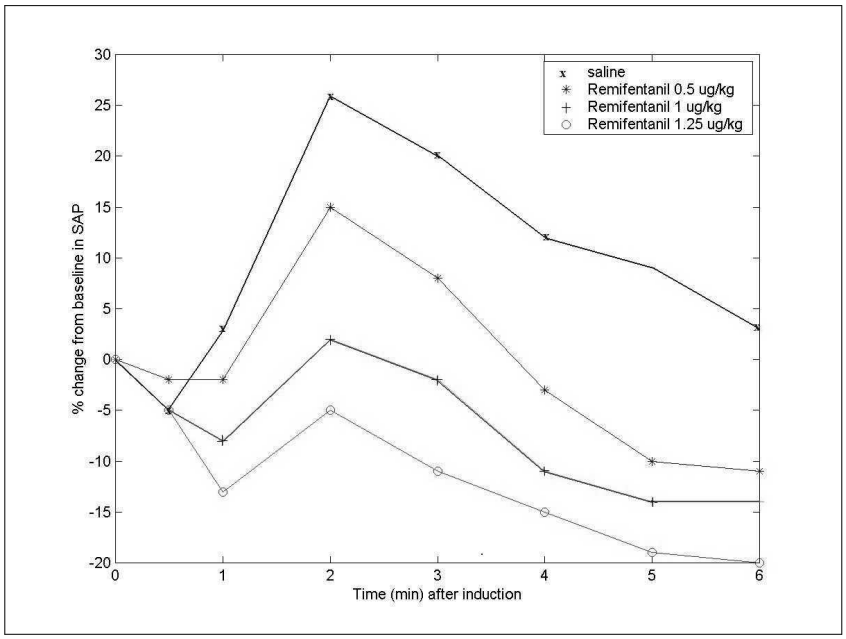

Figure 5-24: Percentage of change from baseline in mean SAP, after induction of anaesthesia. Data from O'Hare *et al.* (1999). Intubation was performed 1 minute after induction.

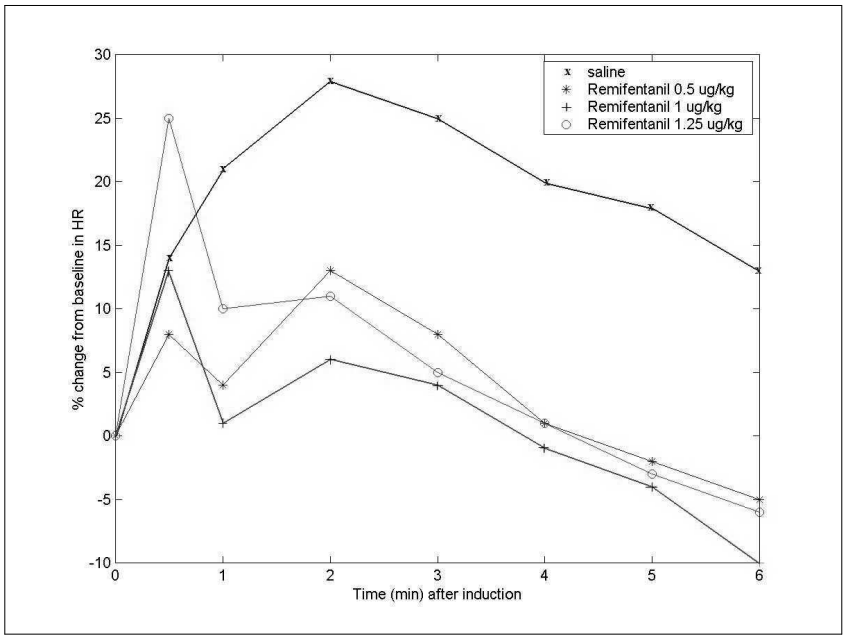

Figure 5-25: Percentage of change from baseline in mean HR, after induction of anaesthesia. Data from O'Hare *et al.* (1999). Intubation was performed 1 minute after induction.

Figures 5-24 and 5-25 show the percentage of change in mean SAP and HR respectively, compared with baseline values for the data in O'Hare *et al.* (1999). The same profile as in McAtamney *et al.* (1998) was used by O'Hare *et al.* (1999). However, the remifentanil bolus doses used were 0.5, 1 and 1.25 μg/kg. The same number of patients was analysed (i.e. 80 patients) considering four different groups, the three different doses of remifentanil and a saline group. In this study, they concluded that the remifentanil dose of 0.5 μg/kg was ineffective in controlling the increase in HR and arterial pressure after intubation but the 1 and 1.25 μg/kg doses were effective in controlling the response.

Remifentanil seems to have a possible linear dose/effect relationship when considering the SAP signal 2 minutes after induction (1 minute after intubation). The reduction on the SAP increase to intubation is notorious. In the saline group there is a change of 25-30% of baseline, while in the remifentanil groups there is a smaller increase. The amplitude of the SAP change decreases as the remifentanil dose increases. In the remifentanil group of 1.25 μg/kg the increase in SAP is minor, in fact the SAP values remain below the baseline. However, there does not seem to be a linear relation between dose/effect when considering HR. In Figure 5-25, there is a reduction in the HR response to intubation when remifentanil is used compared with the saline group, but this reduction is not linear. In order to establish a clear relationship between remifentanil and haemodynamic effect, the remifentanil effect concentrations were calculated using the pharmacokinetic compartmental model and effect compartment model described in Chapter 4. Tables 5-1 and 5-2 show the remifentanil effect concentration for all the time samples and data of McAtamney *et al.* (1998) and a

O'Hare *et al.* (1999), respectively.

Table 5-1: Remifentanil effect concentration (ng/ml) for the data in McAtamney *et al.* (1998). In the following order: at baseline, pos-induction, pre-intubation, 1 to 5 minutes after intubation.

Group	baseline	pos-ind.	pre-int.	1 min	2 min	3 min	4 min	5 min
0.25 μg/kg	0	0.3416	0.9739	1.1062	0.8301	0.5698	0.3949	0.2893
0.5 μg/kg	0	0.6833	1.9478	2.2123	1.6603	1.1396	0.7897	0.5785
1 μg/kg	0	1.3665	3.8955	4.4247	3.3206	2.2792	1.5794	1.157

Table 5-2: Remifentanil effect concentration (ng/ml) for the data in O'Hare *et al.* (1999). In the following order: at baseline, pos-induction, pre-intubation, 1 to 5 minutes after intubation.

Group	baseline	pos-ind.	pre-int.	1 min	2 min	3 min	4 min	5 min
0.5 μg/kg	0	0.6833	1.9478	2.2123	1.6603	1.1396	0.7897	0.5785
1 μg/kg	0	1.3665	3.8955	4.4247	3.3206	2.2792	1.5794	1.157
1.25 μg/kg	0	1.7081	4.8694	5.5308	4.1507	2.849	1.9743	1.4463

In this research, the effect concentration of remifentanil is in the range 0-10 ng/ml, in accordance with the anaesthetist and the drug profile used (remifentanil/propofol). Alexander *et al.* (1999b) reported that a remifentanil effect concentration of 12 ng/ml at 1 minute after intubation (bolus doses of 3 μg/kg at induction) block the haemodynamic changes to intubation. This value of 12 ng/ml will be used as the limit of the remifentanil effect concentrations, since it is known that there is a ceiling effect.

The O'Hare *et al.* (1999) data for the bolus doses of 0.5, 1 and 1.25 μg/kg and saline group (i.e. zero effect concentration of remifentanil), and the information from Alexander *et al.* (1999b) (i.e. at a concentration of 12 ng/ml there is 0% of effect) were used to described the relationship between effect concentration and percentage of change in SAP and HR from intubation time to 1 minute after intubation. A 1^{st} and 2^{nd} order polynomials were fitted to the data using the least-squares method.

Figures 5-26 and 5-27 show the percentage change in SAP and HR , respectively, versus the remifentanil effect concentration at 1 minute after intubation. The 2^{nd} order polynomial approximation (solid line) has a better fit to the data from both variables. It seems to capture the ceiling effect in remifentanil and presents a smaller error. The relationship for HR is not so clear as for SAP, and the 1^{st} and 2^{nd} order polynomials have poorer approximations. Nevertheless, considering the patient variability and smaller change in HR values, the 2^{nd} order polynomial was considered to be reasonable.

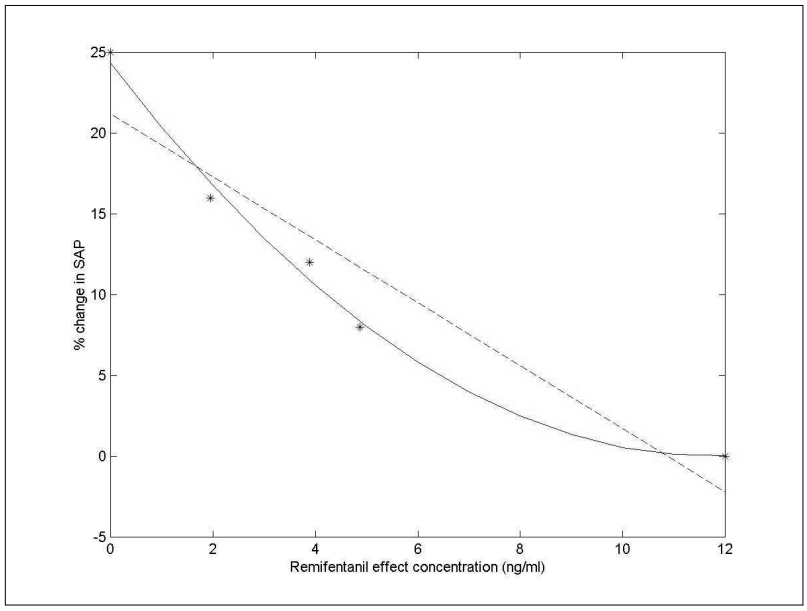

Figure 5-26: Percentage of change in SAP and the remifentanil effect concentration at 1 minute after intubation: 1^{st} order polynomial (dashed line); 2^{nd}order polynomial (solid line); (*) data from O'Hare *et al.* (1999) and Alexander *et al.* (1999b).

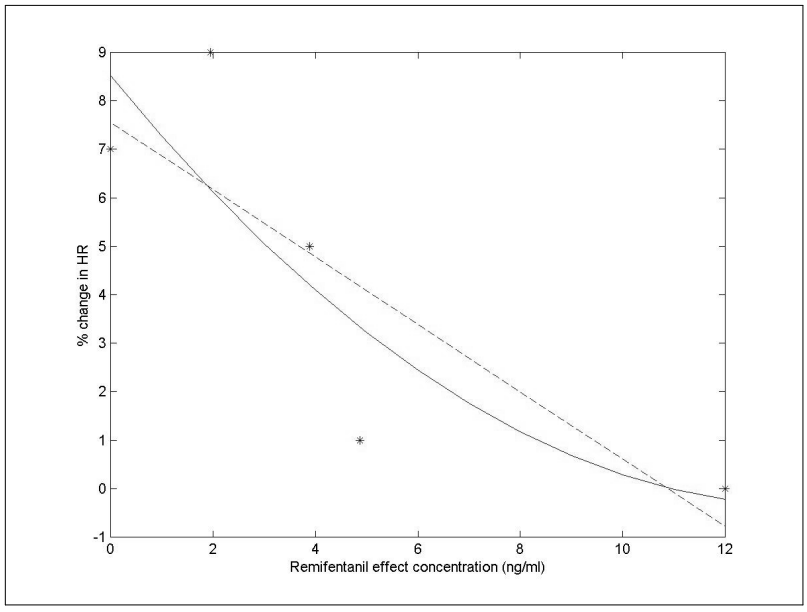

Figure 5-27: Percentage of change in HR and the remifentanil effect concentration at 1 minute after intubation: 1^{st} order polynomial (dashed line); 2^{nd}order polynomial (solid line); (*) data from O'Hare *et al.* (1999) and Alexander *et al.* (1999b).

Comparing with the 1^{st} order polynomials, the 2^{nd} other polynomials gave smaller error and a better fitness to the overall data. The expressions for these functions are as follows:

- SAP

$$\%\ \text{Change (SAP)} = 0.1346C_e^2 - 3.6388C_e + 24.3267 \qquad 5\text{-}4$$

- HR

$$\% \text{ Change (HR)} = 0.029C_e^2 - 1.0787C_e + 8.458 \qquad 5\text{-}5$$

where C_e is the remifentanil effect concentration. The above functions represent the effect of remifentanil on the haemodynamic changes at 1 minute after intubation. The influence of intubation is reflected during approximately 3 minutes, after which the haemodynamic parameters return to the normal values.

5.4 Maintenance-Phase Model

The maintenance phase starts at 1500 seconds, after which the patient is stable in the operating room and the surgical procedure is about to start.

The interaction between propofol and remifentanil is of crucial importance during the maintenance phase, due to the continuous presence of stimulus and the properties of the two drugs. It is known that remifentanil potentiates the effects of propofol, therefore, reducing the required propofol effect concentration. The cardiovascular parameters ΔHR and ΔSAP, and the wavelet extracted AEP features are the result of the drugs concentration, the surgical stimulus and the patient's individual parameters. Therefore, it is necessary to use simultaneously the effect concentrations of both drugs to establish the effect on the different parameters.

Figure 5-28 shows the block diagram of the proposed maintenance phase patient model. The pharmacodynamic model for the maintenance phase, describing the effect of the drugs in the body, is divided into two parts. First, Takagi-Sugeno-Kang (TSK) fuzzy models are used to describe the relationship between the effect concentrations of both drugs (including the drug interactions) and ΔHR, ΔSAP and the AEP features. Secondly, a stimulus model is used to establish the stimulus perceived by the patient and its effect on the cardiovascular parameters. The stimulus model is described in Section 5.5. In the following sections the TSK fuzzy models will be explained in more details.

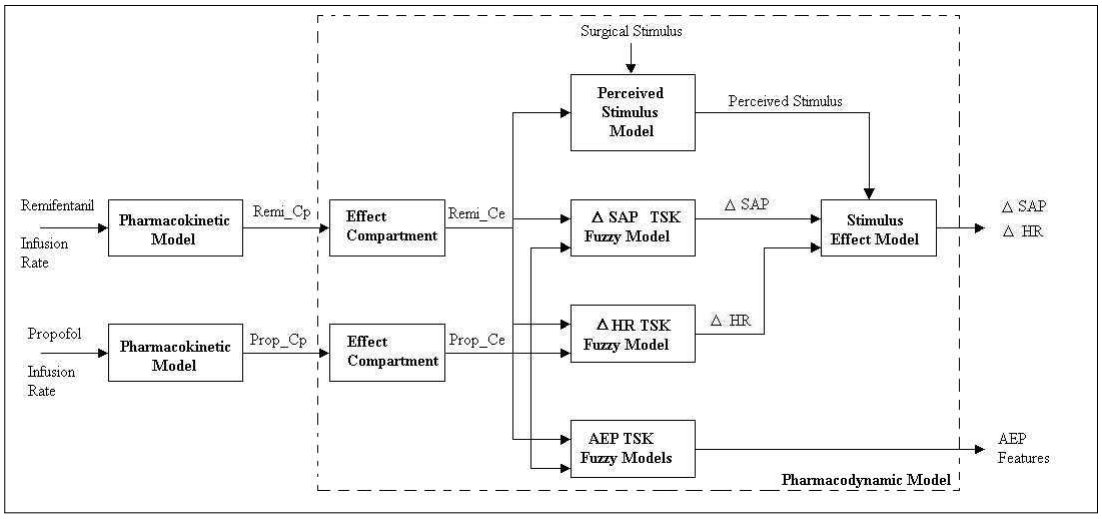

Figure 5-28: Block diagram of the maintenance phase model. *Prop_Cp* and *Remi_Cp* are the plasma concentrations of propofol and remifentanil, respectively, whereas *Prop_Ce* and *Remi_Ce* are the effect concentrations.

The maintenance phase of anaesthesia has different characteristics than induction. The drug profiles used are aimed to maintain a stable DOA level considering the surgical stimulus present. Before automatic or TCI systems, a steady continuous infusion of anaesthetic was administered during maintenance of anaesthesia, supplemented with bolus doses of the analgesic when required. At the moment, the anaesthetist targets the propofol plasma concentration according to his knowledge about the patient's conditions and the surgical procedure. However, when remifentanil is used the anaesthetist also has to establish the adequate dose for a continuous infusion of analgesic. In addition, the interaction of the two drugs will alter the required amount of each of them. As studied by different researchers, the presence of different doses, therefore different concentrations, of remifentanil alters the optimal propofol concentration to adequately maintain DOA (Peacock and Philip, 1999; Peacock *et al.*, 1998; Vuyk *et al.*, 1997).

Figure 5-29 shows a data density diagram for the combination of effect concentrations of propofol and remifentanil, during the surgical procedure of patient Pat1 (Figures 5-2 and 5-3). Analysing this graph, it is clear that the existent data is concentrated in certain areas, and these do not cover the whole space. In fact, several combinations of the two drugs effect concentrations are not used during the maintenance phase. For example, low concentrations of remifentanil are only obtained in the end of the surgical procedure (recovery), since there is only a minimal, if any, surgical stimulus. A medium to high concentration of remifentanil is used to provide the analgesic component of anaesthesia, considering the continuous stimulus present. At the same time, very high concentrations of remifentanil would increase the effects of propofol leading to a probable Deep level of

DOA, and undesired side effects.

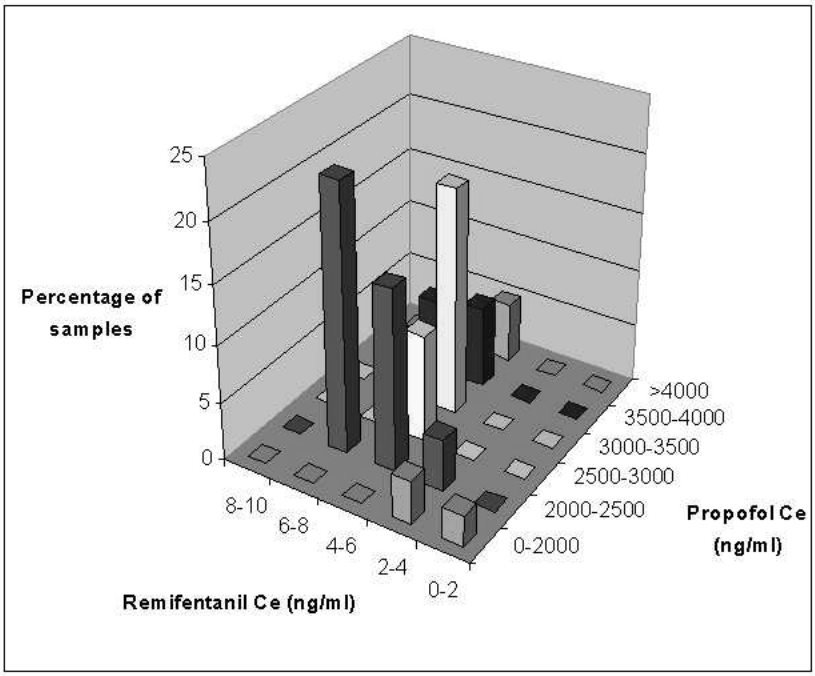

Figure 5-29: Data density graph for the data of patient Pat1 (combination of propofol/remifentanil effect concentrations).

The propofol effect concentration during the maintenance phase does not reach the same high values used for induction (Figure 5-2), the maximum value does not reach the 4000 ng/ml. Low effect concentrations of propofol (<2000 ng/ml) are not combined with high remifentanil concentrations, since a minimum amount of propofol is required throughout the maintenance phase, so as to produce unconsciousness. In conclusion, the data gathered during the maintenance phase are limited not only by the existence of a single patient, but also by the specific anaesthetic requirements during this phase of the procedure.

The maintenance phase is a very important phase, if not the most important, of anaesthesia. It is during this time that the surgical procedure takes place. The objective is, therefore, to model the effect of the existent combinations of propofol and remifentanil effect concentrations on the ΔHR, ΔSAP and the AEP features, i.e. on the patient's cardiovascular and CNS.

The Adaptive Network-Based Fuzzy Inference System (ANFIS) was used to construct TSK models for ΔHR, ΔSAP and the AEP features (Figure 5-28). The TSK fuzzy system comprises of the following rules:

$$\text{If } x_1 \text{ is } C_1^l \text{ and ... and } x_n \text{ is } C_n^l, \text{ then } f_l = c_0^l + c_1^l x_1 + \ldots + c_n^l x_n \qquad 5\text{-}6$$

where C_i^l are fuzzy sets, c_j^l are constants, $l = 1,\ldots,m$, $i = 1,..,n$ and $j = 0,\ldots,n$. The antecedent parts of the rules are the same as in the ordinary fuzzy IF-THEN rules, but the consequent parts are linear functions of the input variables (see Appendix B).

Given an input $x = (x_1,\ldots,x_n)^T \in U \subset \Re^n$, the output $f(x) \in V \subset \Re$ of the TSK fuzzy system is computed as the weighted average of the f_l's in Equation 5-6, i.e.:

$$f(x) = \frac{\sum_{l=1}^{m} f_l w^l}{\sum_{l=1}^{m} w^l} \qquad 5\text{-}7$$

where the weights w^l are computed as:

$$w^l = \prod_{i=1}^{n} \mu_{C_i^l}(x_i) \qquad 5\text{-}8$$

$\mu_{C_i^l}(x_i)$ are the input membership functions of x_i (Takagi and Sugeno, 1985). Therefore, the output of each rule is a linear combination of input variables plus a constant term, and the final output is the weighted average of each rule's output.

The ANFIS designed by Jang (1993), constructs a TSK Fuzzy Inference System (FIS) using a given input/output data set. See Figure 3-12 in Chapter 3 for the general ANFIS structure diagram.

The membership function parameters are tuned using a hybrid learning rule, which combines the gradient method and the least-squares estimator for fast identification of parameters (Jang and Sun, 1995). This allows the fuzzy systems to learn from the data they are modelling.

The ANFIS was built through the Fuzzy Toolbox available for MATLAB. The following properties were used when running ANFIS:

- Subtractive clustering was used to generate the initial FIS structure;
- Gaussian input membership functions;
- Hybrid optimization method (i.e. back-propagation gradient-descent and least squares method).

These properties were found to provide the best results for the models. Since, subtractive clustering determines the initial FIS based on the training data set and the natural clusters in it, this method is deemed to be the safest option when no information is available so as to determine adequately the initial FIS, or the data is not equally distributed in the input space (such as in this case, Figure 5-29).

The TSK models use as input the effect concentrations of remifentanil and propofol and as output ΔSAP, or ΔHR, or one of the AEP features. The available data were divided into training and checking data sets, 2/3 and 1/3 of the data respectively.

The detailed TSK models for the cardiovascular parameters and the AEP features will be presented in the next sections.

5.4.1 Cardiovascular Parameters

The cardiovascular parameters ΔHR and ΔSAP were modelled separately, using the same ANFIS structure. The available data from patient Pat1 were divided into training and checking data sets. The training data set should represent the features of the data that the trained TSK system is intended to model. Therefore, the checking data set consists of four different pieces of the data, making up 1/3 of the total number of samples, the remaining samples are used as the training data set. This choice of checking and training data sets, was necessary to assure that both sets were balanced and representative of the data, but distinct.

5.4.1.1 Systolic Arterial Pressure

Figure 5-30 shows the input membership functions for the effect concentrations of propofol and remifentanil of the trained TSK model for ΔSAP.

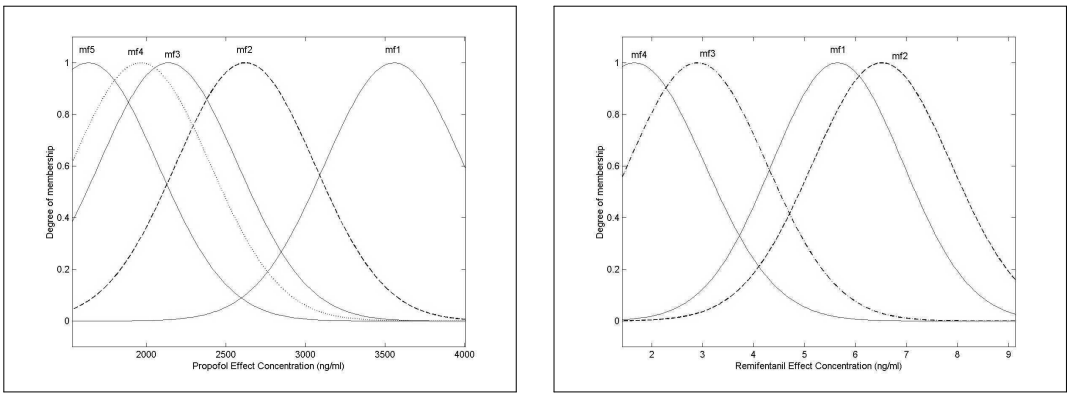

a) b)

Figure 5-30: Input membership functions describing the propofol effect concentration (a)) and the remifentanil effect concentration (b)), for the ΔSAP TSK fuzzy model.

The input membership functions parameters were tuned by ANFIS after determining the

initial FIS using subtractive clustering. Table 5-3 shows the rule-base of the ΔSAP TSK model.

Table 5-3: Rule-base table for the fuzzy TSK model of ΔSAP. RC_e is the remifentanil effect concentration, PC_e is the propofol effect concentration. f_i is the i output membership function, $i = 1,\ldots,5$.

PC$_e$	**RC**$_e$			
	mf1	**mf2**	**mf3**	**mf4**
mf1	f_1			
mf2	f_2			
mf3		f_3		
mf4			f_4	
mf5				f_5

The output membership functions $f_1,\ldots,f_5$ are static linear functions of the inputs (i.e. propofol and remifentanil effect concentrations). The tuned output membership functions are:

$$\begin{aligned} f_1 &= 0.0223PC_e + 2.0627RC_e - 149.7138 \\ f_2 &= 0.4169PC_e - 159.467RC_e - 566.9308 \\ f_3 &= PC_e - 78.3RC_e - 1418 \\ f_4 &= -0.2486PC_e - 74.2046RC_e + 832.3579 \\ f_5 &= -0.0366PC_e - 138.4659RC_e + 99.3317 \end{aligned} \qquad 5\text{-}9$$

The output surface of the ΔSAP TSK fuzzy model is presented in Figure 5-31. The input space was restricted to the maintenance phase values. Analysing the figure, one can notice that in the areas where there are not data (recall Figure 5-29), the TSK model surface presents distorted peaks or valleys. For example, around a remifentanil effect concentration of 8 ng/ml with a corresponding low effect concentration of propofol, the TSK model gives positives values of ΔSAP (i.e. SAP is above baseline), which was not present in the data from patient Pat1. It is not expected that SAP would raise above baseline during the surgical procedure under general anaesthesia with this drug profile. The peak in the output surface is due to the non existence of data in that area of the input space. ANFIS cannot model the response to unseen data, therefore, the TSK model is only valid in the accepted effect concentration ranges for the maintenance phase. If for any abnormal reason the effect concentrations of the two drugs would be outside the typical maintenance phase ranges, then an alarm is activated to advise and warn the anaesthetist of the invalid (i.e. not accurate) model responses.

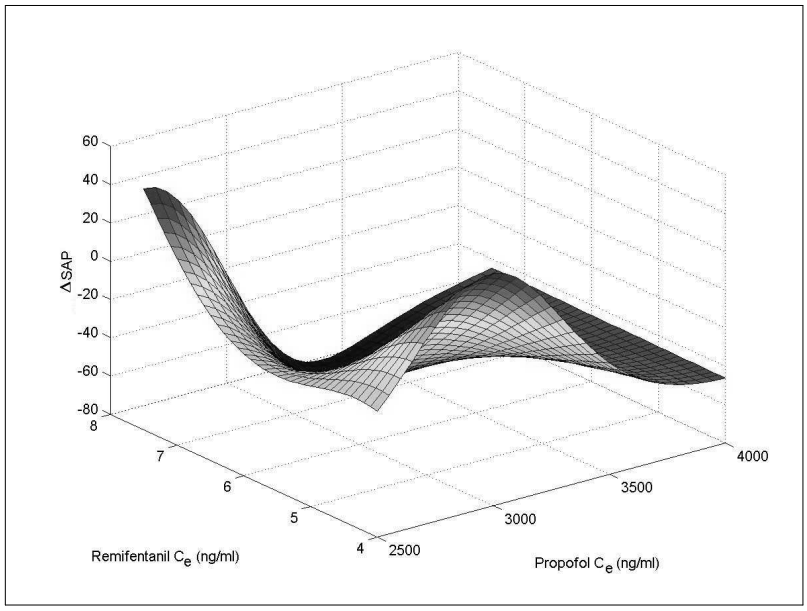

Figure 5-31: Output surface for ΔSAP TSK fuzzy model, considering the maintenance phase.

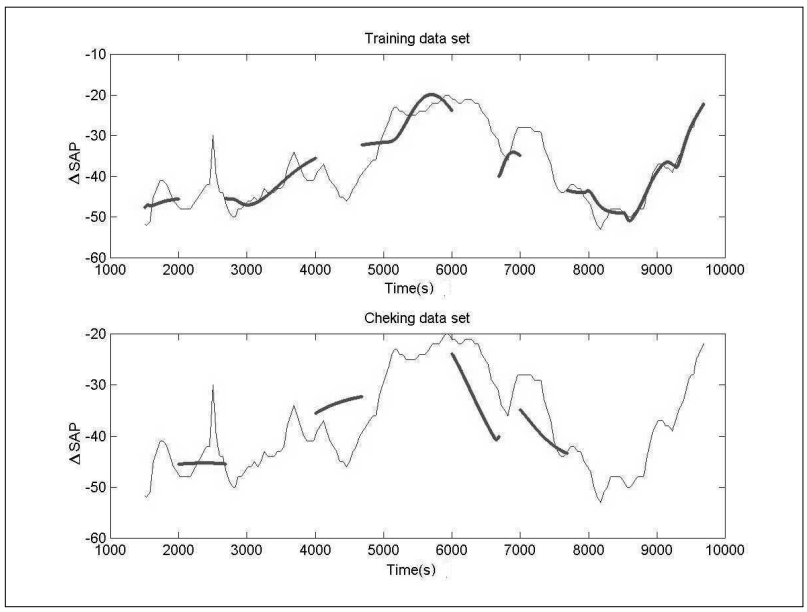

Figure 5-32: Results of the ΔSAP TSK fuzzy model on the training and checking data set (strong solid line) and ΔSAP from patient Pat1 (solid line), considering the maintenance phase.

The results of the ΔSAP TSK model on the training and checking data sets are presented in Figure 5-32. The mean absolute errors on the training and checking data sets were 2.26 and 6.53 mmHg, respectively. As expected, the model has a reasonable performance on the training data set with a low error. The results on the checking data set reflect the ΔSAP trend and appear to smooth out the disturbances due to stimulus.

Figure 5-33 shows the results of the ΔSAP TSK model on the whole data of patient Pat1 (i.e. training and checking data sets). The TSK model reflects the ΔSAP trend in response

to the effect concentrations. The smooth response reflects the smooth changes in the concentrations. Overall, the model presents an acceptable performance.

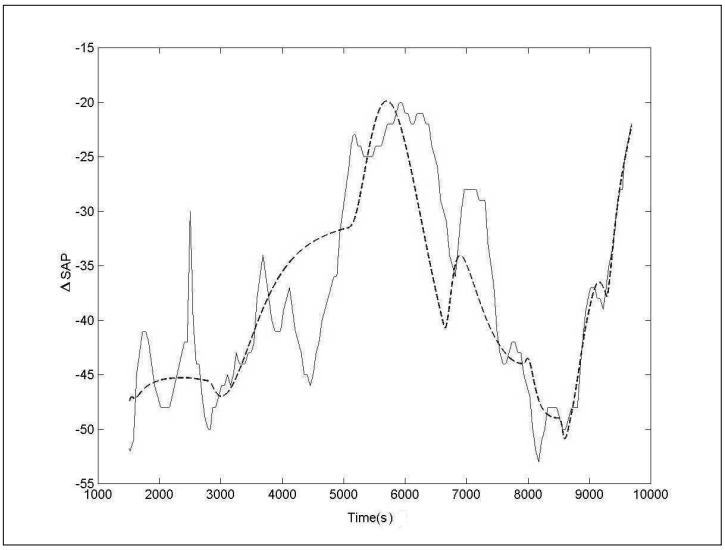

Figure 5-33: Results of the ΔSAP TSK fuzzy model (dashed line) and ΔSAP from patient Pat1 (solid line), considering the maintenance phase.

5.4.1.2 Heart Rate

The ΔHR TSK model was also trained using 2/3 of the data. The remaining 1/3 was used as the checking data set, which represented four different pieces of data. Figure 5-34 shows the model input membership functions for the propofol and remifentanil effect concentrations.

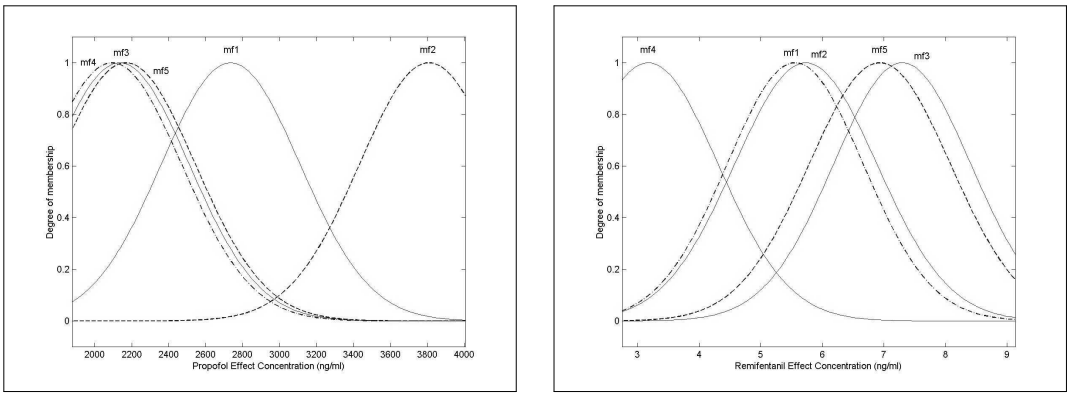

a) b)

Figure 5-34: Input membership functions describing the propofol effect concentration (a)) and the remifentanil effect concentration (b)), for the ΔHR TSK fuzzy model.

The ΔHR TSK model rule-base is presented in Table 5-4. The output membership functions are the following:

$$
\begin{aligned}
f_1 &= -0.1PC_e + 433.6RC_e - 2231 \\
f_2 &= 0.014PC_e + 0.1826RC_e - 83.1286 \\
f_3 &= 4.4PC_e - 436.7RC_e + 1327.4 \\
f_4 &= -0.0502PC_e + 58.5949RC_e - 72.8725 \\
f_5 &= -1.5PC_e - 1645.8RC_e + 7312.6
\end{aligned}
\qquad 5\text{-}10
$$

Table 5-4: Rule-base table for the fuzzy TSK model of ΔHR. RC_e is the remifentanil effect concentration, PC_e is the propofol effect concentration. f_i is the i output membership function, $i = 1,\ldots,5$.

PC$_e$	**RC$_e$**				
	mf1	**mf2**	**mf3**	**mf4**	**mf5**
mf1	f_1				
mf2		f_2			
mf3			f_3		
mf4				f_4	
mf5					f_5

Figure 5-35 shows the output surface of the ΔHR TSK model, considering the maintenance phase. As in ΔSAP, the TSK model surface presents distortions in the areas where there are no data.

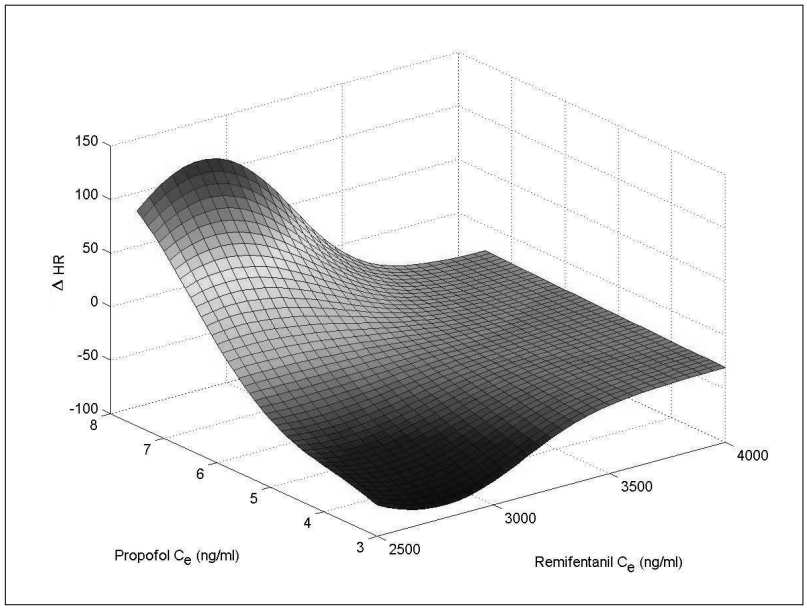

Figure 5-35: Output surface for ΔHR TSK fuzzy model, considering the maintenance phase.

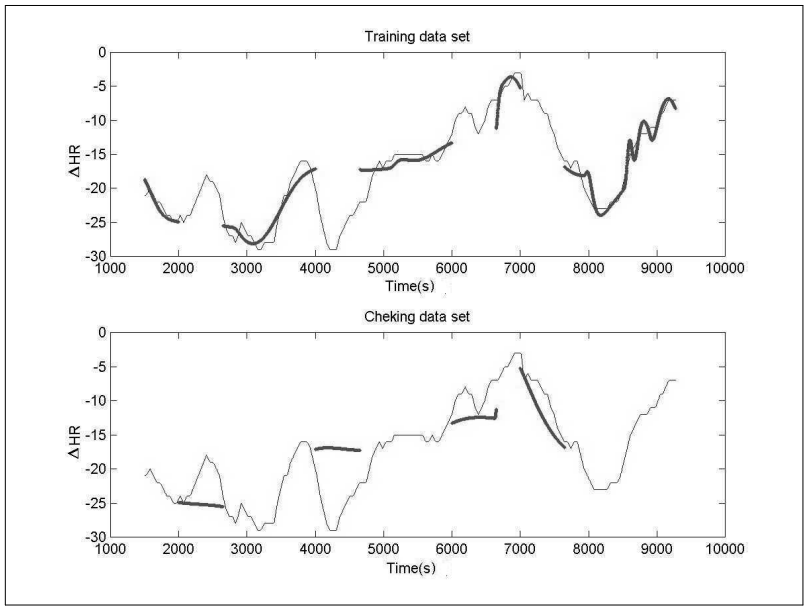

Figure 5-36: Results of the ΔHR TSK fuzzy model on the training and checking data set (strong solid line) and ΔHR from patient Pat1 (solid line), considering the maintenance phase.

Figure 5-36 shows the results of the ΔHR TSK model on the training and checking data sets. Note that the peak in the ΔHR at approximately 9200 seconds (Figure 5-4) was removed from the training data set. According to the anaesthetist, this outlier in the data was caused by an external disturbance, and would damage the modelling procedure. The mean absolute errors on the training and checking data set were of 1.12 and 4.54 bpm respectively.

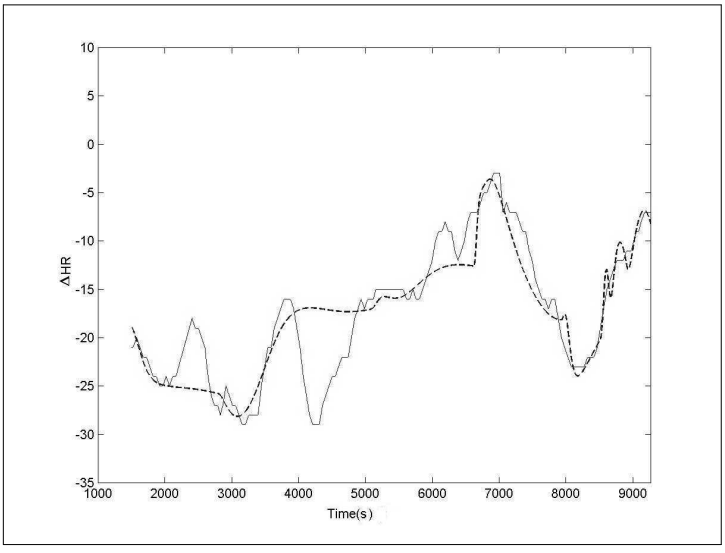

Figure 5-37: Results of the ΔHR TSK fuzzy model (dashed line) and ΔHR from patient Pat1 (solid line), considering the maintenance phase.

The ΔHR model results on the whole data of patient Pat1 (training plus checking data sets) are presented in Figure 5-37. The model reflects the trend in ΔHR and has a reasonable

overall performance. Note that the models reflect the changes in effect concentrations and interaction between the two drugs, therefore, the changes in ΔHR and ΔSAP due to outside disturbances (including surgical stimulus) are not reflected in the results. For example the deep valley in ΔHR at about 4200 seconds is not the result of the drugs, since there is no drastic change in the effect concentrations.

5.4.1.3 Comparison with a Linear Model

A linear model was developed using the Nonlinear Control Design (NCD) MATLAB Toolbox (mentioned in Section 5.3.1) and genetic algorithms optimization to describe ΔSAP and ΔHR. These models were obtained using selected pieces of the data where the concentration of one of the drugs was constant and the other varied, and vice versa.

The data in Group1 (Section 5.3.1, Figure 5-17) were used to consider the effect of the changes in propofol concentration. The data in the time period from 5998 to 8905 seconds (termed Group2) were used to analyse the influence of remifentanil. During this period the propofol concentration was constant, therefore, the effect of remifentanil on the cardiovascular parameters can be analysed (Figures 5-2 and 5-3).

Considering ΔSAP, the following equations were obtained with the NCD blockset:

- Influence of propofol (Group1):

$$\Delta SAP_{propofol} = 11.2254 - 0.0153 PC_e \qquad 5\text{-}11$$

- Influence of remifentanil (Group2):

$$\Delta SAP_{remifentanil} = -26.2855 - 1.7622 RC_e \qquad 5\text{-}12$$

where PC_e and RC_e are the propofol and remifentanil effect concentrations, respectively.

Figure 5-38 shows the results of the linear model for $\Delta SAP_{propofol}$ (Equation 5-11) on the data of Group1. The mean absolute error is of 3.93 mmHg, reflecting the reasonable approximation of the model to the data in this group.

Figure 5-39 shows the results of the linear model for $\Delta SAP_{remifentanil}$ (Equation 5-12) on the data of Group2. The mean absolute error is 9.52 mmHg, reflecting the poor results. The remifentanil effect concentration does not seem to reflect the ΔSAP changes, this is not surprising since remifentanil is used for clinical stability, therefore very small changes in

ΔSAP are expected. According to the anaesthetist, remifentanil blocks the response (i.e. the effect), whereas propofol reflects the changes in ΔSAP and ΔHR.

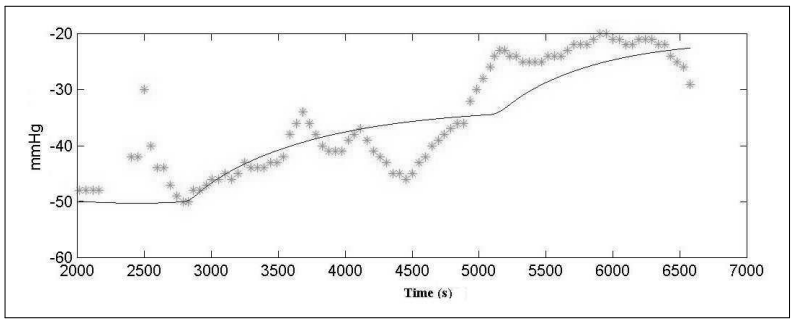

Figure 5-38: ΔSAP from patient Pat1 (*) and the result of the linear model from Equation 5-11 (solid line), considering the data of Group1.

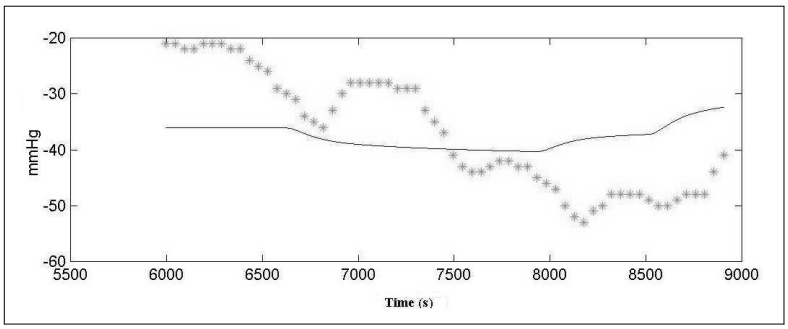

Figure 5-39: ΔSAP from patient Pat1 (*) and the result of the linear model from Equation 5-12 (solid line), considering the data of Group2.

Considering ΔHR the following equations were obtained with the NCD blockset:

- Influence of propofol (Group1):

$$\Delta HR_{propofol} = -1.8727 - 0.0061 PC_e \qquad 5\text{-}13$$

- Influence of remifentanil (Group2):

$$\Delta HR_{remifentanil} = -23.3519 + 2.1674 RC_e \qquad 5\text{-}14$$

where PC_e and RC_e are the propofol and remifentanil effect concentrations, respectively.

Figure 5-40 shows the results of the linear model for $\Delta HR_{propofol}$ (Equation 5-13) on the data of Group1. The mean absolute error is of 3.66 bpm, reflecting the reasonable approximation of the model to the data in this group.

Figure 5-41 shows the results of the linear model for $\Delta HR_{remifentanil}$ (Equation 5-14) on the data of Group2. The mean absolute error is 6.47 bpm, reflecting the poor results. The $\Delta HR_{remifentanil}$ model results are fairly flat, with very small changes. From Figures 5-39 and

5-41 it appears that the two effects are not linked to the changes in the effect concentrations of remifentanil.

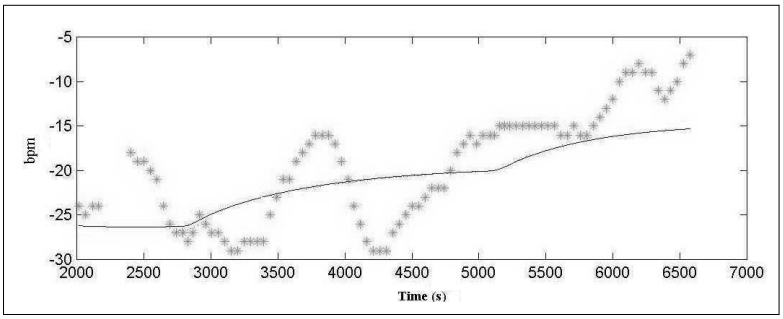

Figure 5-40: ΔHR from patient Pat1 (*) and the result of the linear model from Equation 5-13 (solid line), considering the data of Group1.

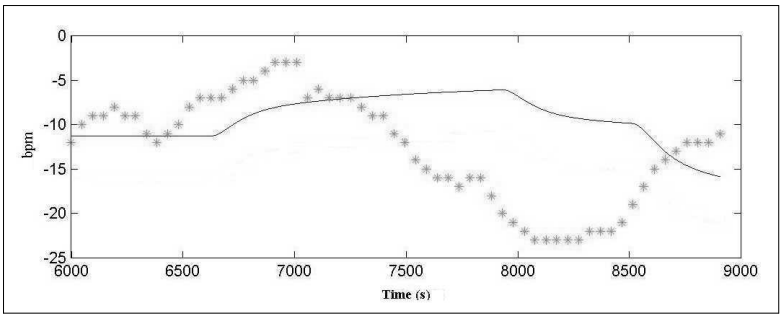

Figure 5-41: ΔHR from patient Pat1 (*) and the result of the linear model from Equation 5-14 (solid line), considering the data of Group2.

The effects of the two drugs have to be accounted for, when modelling the cardiovascular parameters. Remifentanil alone seems to have little influence on ΔHR and ΔSAP, however remifentanil has an interaction with propofol. A linear combination of these models (Equations 5-11 to 5-14) was obtained using a genetic algorithm, which optimized the contribution of the two drugs to the values of the cardiovascular parameters. The results of the optimization were as follows:

$$\Delta SAP_{linear} = 0.7036\Delta SAP_{remifentanil} + 0.3945\Delta SAP_{propofol} \qquad 5\text{-}15$$

$$\Delta HR_{linear} = 0.0575\Delta HR_{remifentanil} + 0.8453\Delta HR_{propofol} \qquad 5\text{-}16$$

The results of these optimized linear models are presented in Figures 5-42 and 5-43, considering ΔSAP and ΔHR respectively. The results of the linear models are compared with the results of the TSK fuzzy model (described in the previous subsections), and plotted versus the data of patient Pat1. The objective is to analyse the performance of the two

models with respect to the maintenance phase data.

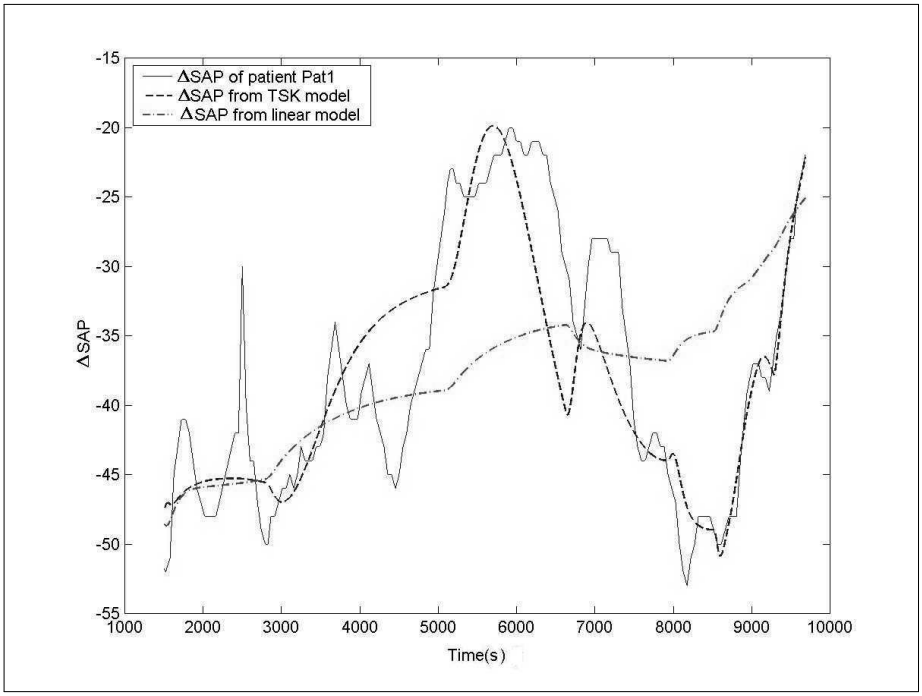

Figure 5-42: ΔSAP from patient Pat1 (solid line) and the results of the TSK fuzzy model (dashed line) and the results of the linear model (dash-dot line), considering the maintenance phase.

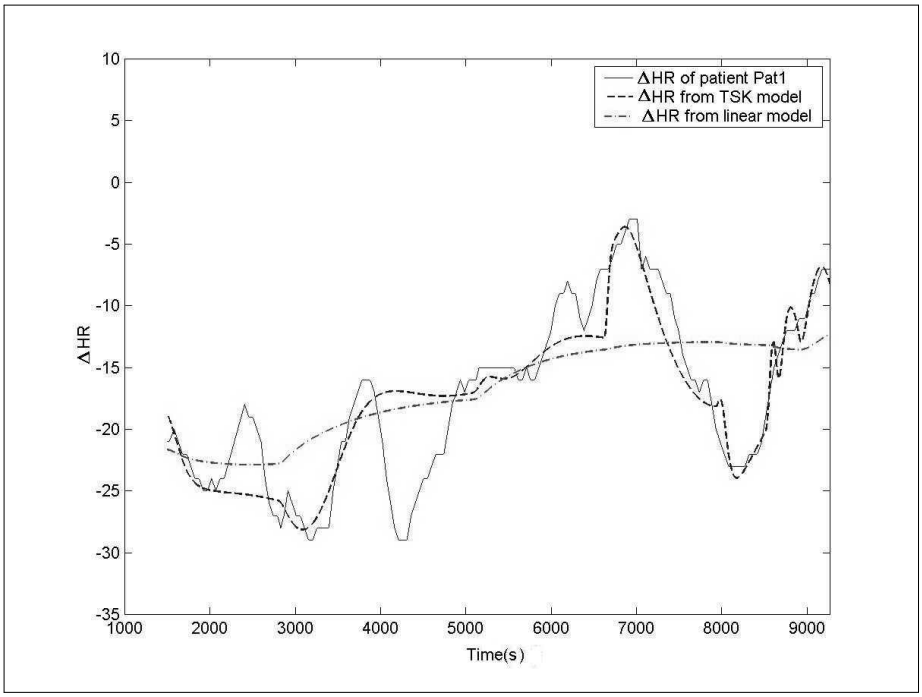

Figure 5-43: ΔHR from patient Pat1 (solid line) and the results of the TSK fuzzy model (dashed line) and the results of the linear model (dash-dot line), considering the maintenance phase.

Analysing Figures 5-42 and 5-43, it is clear that the two drugs interact. The linear model does not perform well, nevertheless, it reflects the relation between the effect

concentrations of the drugs and the cardiovascular parameters, assuming that there is no interaction between them. The TSK model seems to capture the synergism between propofol and remifentanil. This is more evident, when considering the time period of 7000-8000 seconds. Indeed, the decrease in ΔSAP and ΔHR is not due to an increase in propofol concentration. In fact, the propofol effect concentration is almost constant during this time. The depression in the cardiovascular parameters is associated with the increase in remifentanil concentration which potentiates the effect of propofol. If propofol would be used alone during this time, there would be a clear relation between effect concentration and effect. Therefore, an increase in the remifentanil effect concentration increases the depressive effect of propofol on the cardiovascular parameters.

In conclusion, ANFIS was able to optimize the parameters of the TSK models, leading to an adequate description of the effects and interaction of the two drugs. It is important that the model reflects the synergistic interaction between propofol and remifentanil, to be an adequate representation of the body's behaviour.

5.4.2 Wavelet Extracted AEP Features

The wavelet extracted AEP features were modelled using the same ANFIS structure (i.e. same properties) as the cardiovascular parameters. Ten TSK models were obtained, one for each of the AEP features, using the propofol and remifentanil effect concentrations as inputs. The training and checking data sets are 2/3 and 1/3 of the whole data, respectively. Considering the characteristics of the AEP features (Figures 5-5 to 5-14), the checking data set is represented by one sample in every three. The approach used with the cardiovascular parameters, i.e. the checking data set represented by four different pieces of data, was not suitable for these type of data. The AEP features are a set of spikes and they do not reflect trends. The nature the AEP features signal is very different from the cardiovascular parameters, as reflected in the AEP features graphs (Figures 5-5 to 5-14) and Figure 5-4.

The AEP features D_1, D_3, D_5 and D_{51} TSK models will be presented in the next sections. These features were selected to show the models behaviour and details, considering different frequency features. The TSK models for the other six features, D_2, D_{31}, D_{32}, D_{33}, D_4 and D_{52}, were obtained in the same way and are presented in Appendix D.

5.4.2.1 AEP Feature D_1

Figure 5-44 shows the input membership functions for the effect concentrations of propofol and remifentanil of the trained D_1 TSK model. The model rule-base in presented in Table 5-5.

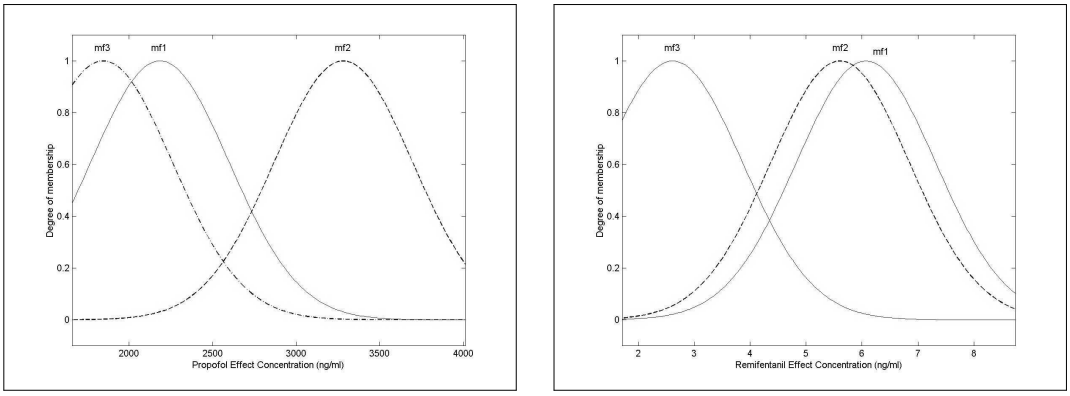

a) b)

Figure 5-44: Input membership functions describing the propofol effect concentration (a)) and the remifentanil effect concentration (b)), for the AEP feature D_1 TSK fuzzy model.

Table 5-5: Rule-base table for the fuzzy TSK model of the AEP feature D_1. RC_e is the remifentanil effect concentration, PC_e is the propofol effect concentration. f_i is the i output membership function, $i = 1,\ldots,3$.

PC$_e$	**RC$_e$**		
	mf1	**mf2**	**mf3**
mf1	f_1		
mf2		f_2	
mf3			f_3

The output membership functions are the following:

$$\begin{aligned} f_1 &= 0.0007PC_e - 0.0182RC_e + 0.4700 \\ f_2 &= -0.0001PC_e - 0.0294RC_e + 0.4792 \\ f_3 &= 0.0001PC_e - 0.0504RC_e - 0.0834 \end{aligned} \qquad 5\text{-}17$$

The D_1 TSK model output surface is presented in Figure 5-45. The surface presents a sharp decrease into negative values in the area of high remifentanil effect concentrations versus low propofol effect concentrations. As explained in the previous sections with the cardiovascular parameters, this is due to the lack of data in that area. Note that D_1 decreases as the propofol and the remifentanil effect concentrations increase, showing the depression of the CNS at deeper levels of DOA (i.e. higher concentration of propofol and

the synergistic effect of remifentanil).

Figure 5-46 shows the results of the model on the training and checking data sets. The mean absolute errors for the training and checking data sets were 0.055 and 0.043, respectively. The lower error on the checking data sets shows the efficiency of the model and demonstrates that there was no overtraining.

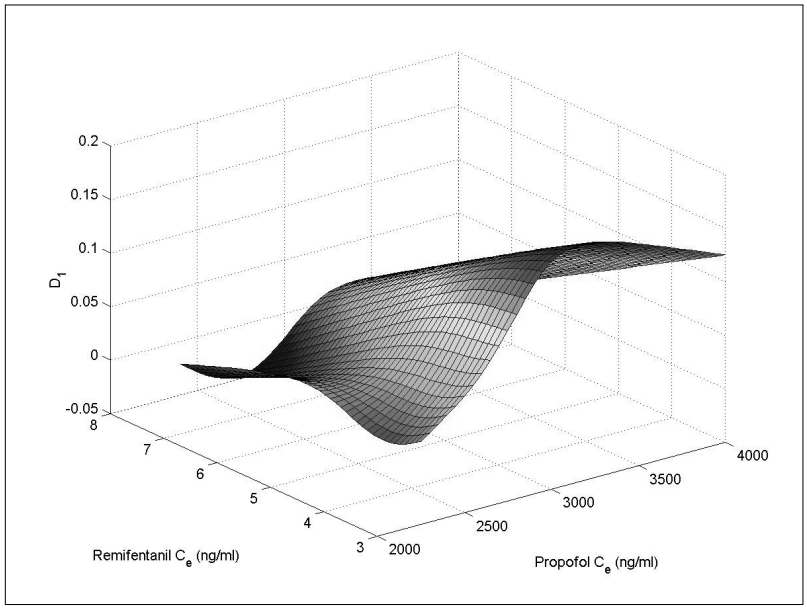

Figure 5-45: Output surface of the AEP feature D_1 TSK fuzzy model.

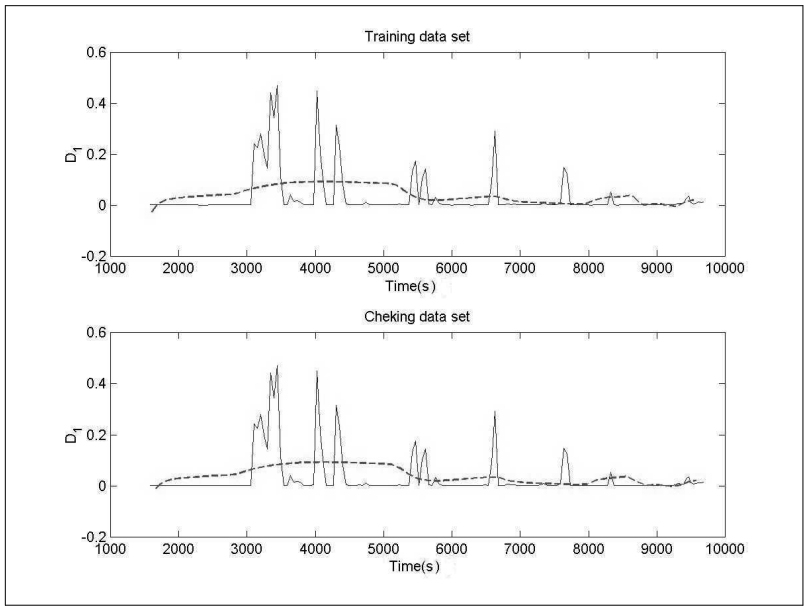

Figure 5-46: Results of the AEP feature D_1 TSK fuzzy model on the training and checking data sets (dashed line) and the AEP feature D_1 from patient Pat1 (solid line), considering the maintenance phase.

The TSK model does not reflect the highest spikes in the data, there is an increase in the D_1

value as a result of the concentrations. However, an external disturbance (probably surgical stimulus) is affecting the values of D_1.

5.4.2.2 AEP Feature D_3

Figure 5-47 shows the input membership functions for the propofol and remifentanil effect concentrations of the trained D_3 TSK model. The rule-base of the model is presented in Table 5-6.

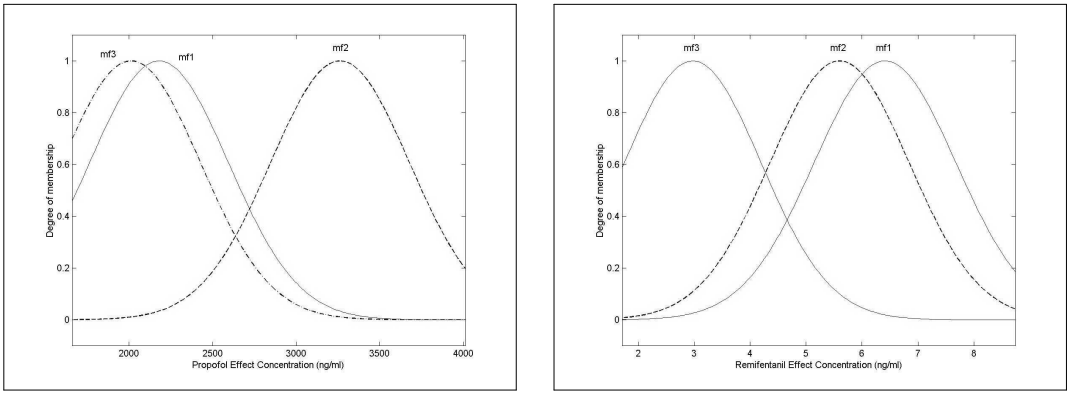

a) b)

Figure 5-47: Input membership functions describing the propofol effect concentration (a)) and the remifentanil effect concentration (b)), for the AEP feature D_3 TSK fuzzy model.

Table 5-6: Rule-base table for the fuzzy TSK model of the AEP feature D_3. RC_e is the remifentanil effect concentration, PC_e is the propofol effect concentration. f_i is the i output membership function, $i = 1,\ldots,3$.

PC$_e$	**RC$_e$**		
	mf1	**mf2**	**mf3**
mf1	f_1		
mf2		f_2	
mf3			f_3

The output membership functions are the following:

$$\begin{aligned} f_1 &= -0.0021PC_e - 0.2615RC_e + 6.5268 \\ f_2 &= -0.0006PC_e - 0.2793RC_e + 4.4771 \\ f_3 &= -0.001PC_e - 0.3518RC_e + 3.1850 \end{aligned} \qquad 5\text{-}18$$

Figure 5-48 shows the output surface of the D_3 TSK model, considering the maintenance phase. The shape of the surface is similar to the one from D_1, representing a similar trend in the data when the effect concentrations change.

The model was applied to the training and checking data sets, the results are presented in Figure 5-49. The mean absolute errors of the training and checking data sets were 0.52 and 0.41, respectively. Once more the checking error is smaller than the training error.

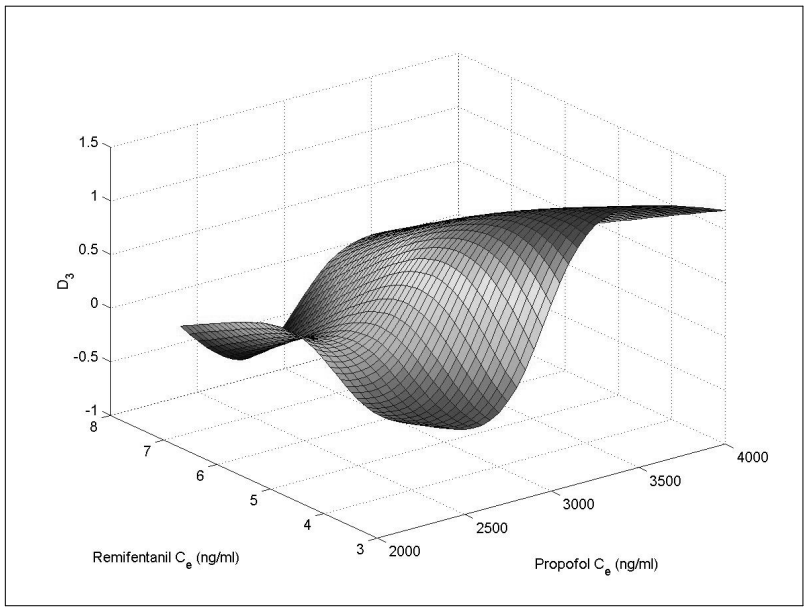

Figure 5-48: Output surface of the AEP feature D_3 TSK fuzzy model.

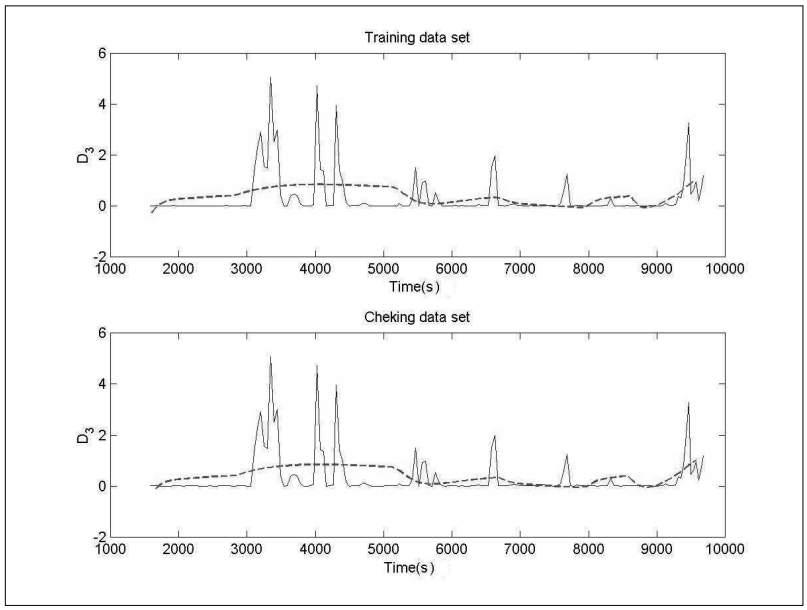

Figure 5-49: Results of the AEP feature D_3 TSK fuzzy model on the training and checking data sets (dashed line) and the AEP feature D_3 from patient Pat1 (solid line), considering the maintenance phase.

The D_3 feature appears to have the same high spikes as feature D_1. In fact, the overall data is similar in trend but with different amplitude values. These are both low frequency features.

5.4.2.3 AEP Feature D_5

Figure 5-50 shows the input membership functions for the propofol and remifentanil effect concentrations of the trained D_5 TSK model. Table 5-7 presents the rule-base of the model.

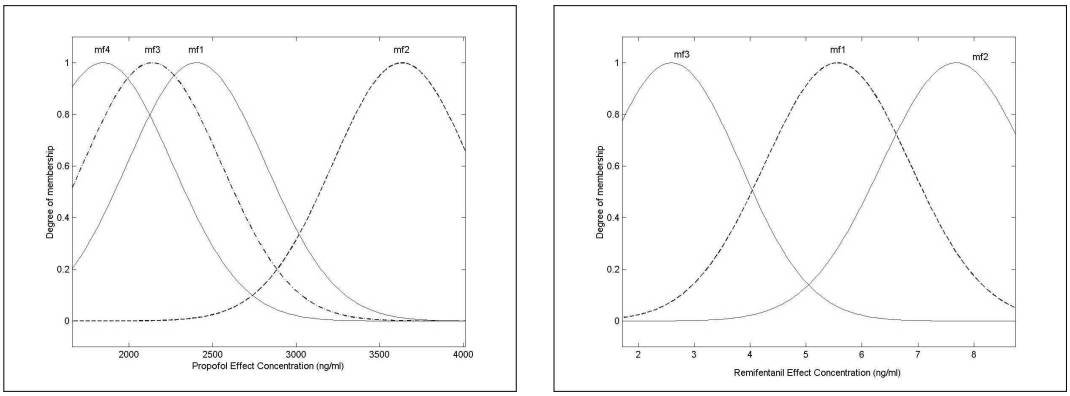

a) b)

Figure 5-50: Input membership functions describing the propofol effect concentration (a)) and the remifentanil effect concentration (b)), for the AEP feature D_5 TSK fuzzy model.

Table 5-7: Rule-base table for the fuzzy TSK model of the AEP feature D_5. RC_e is the remifentanil effect concentration, PC_e is the propofol effect concentration. f_i is the i output membership function, $i = 1, \ldots, 4$.

PC$_e$	**RC$_e$**		
	mf1	**mf2**	**mf3**
mf1	f_1		
mf2	f_2		
mf3		f_3	
mf4			f_4

The output membership functions are the following:

$$\begin{aligned} f_1 &= -0.0315PC_e + 20.2944RC_e - 22.7108 \\ f_2 &= -0.008PC_e + 1.3529RC_e + 28.4694 \\ f_3 &= 0.0906PC_e + 19.1609RC_e - 349.0115 \\ f_4 &= -0.0179PC_e + 9.6614RC_e + 20.5424 \end{aligned} \qquad 5\text{-}19$$

Figure 5-51 shows the output surface of the D_5 TSK model. The surface presents a different shape than the previous models (Figures 5-45 and 5-48), showing the different nature of the AEP feature. There is a distortion in the surface around 3000 ng/ml propofol effect concentration versus low remifentanil effect concentrations, this is, once more, due to the lack of data in that area.

The D_5 TSK model was applied to the training and checking data sets. The results are presented in Figure 5-52. The mean absolute errors on the training and checking data set are 3.09 and 3.41, respectively. In contrast with the previous two features, the error on the checking data set is slightly higher than on the training data set.

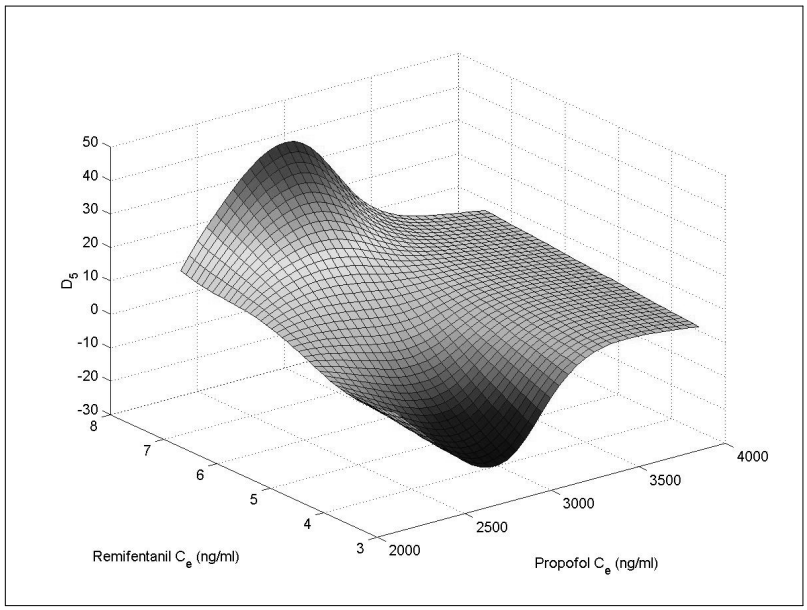

Figure 5-51: Output surface of the AEP feature D_5 TSK fuzzy model.

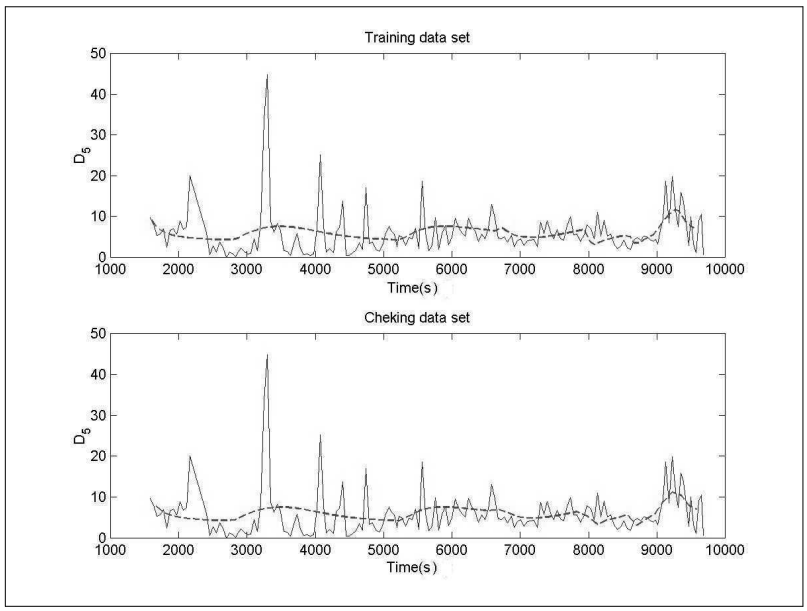

Figure 5-52: Results of the AEP feature D_5 TSK fuzzy model on the training and checking data sets (dashed line) and the AEP feature D_5 from patient Pat1 (solid line), considering the maintenance phase.

The high frequency D_5 AEP feature is more oscillatory than the low frequency features. Analysing Figure 5-52, one can see that the TSK model is capturing the fluctuation of the signal. The high spikes in the data are less predominant than with the low frequency

features, presenting a smaller amplitude change compared with the rest of the signal.

5.4.2.4 AEP Feature D_{51}

Figure 5-53 shows the input membership functions for propofol and remifentanil effect concentrations of the TSK model of the AEP feature D_{51}. Table 5-8 presents the rule-base of the model.

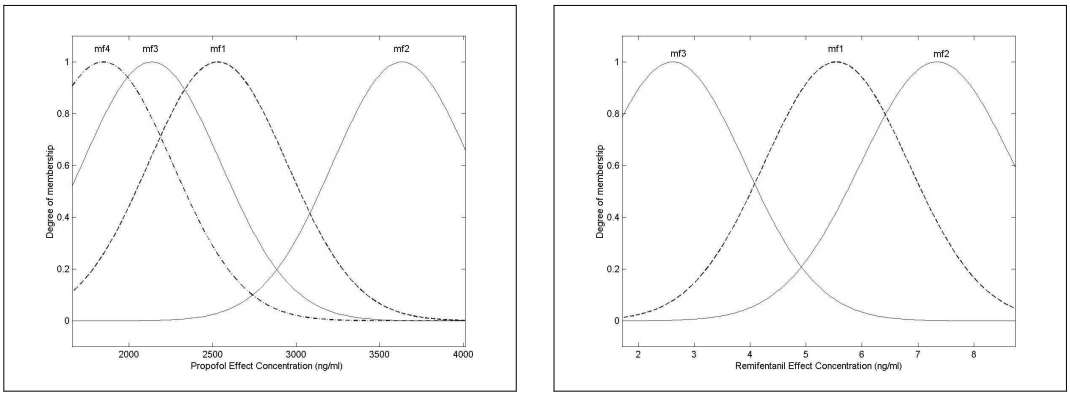

a) b)

Figure 5-53: Input membership functions describing the propofol effect concentration (a)) and the remifentanil effect concentration (b)), for the AEP feature D_{51} TSK fuzzy model.

Table 5-8: Rule-base table for the fuzzy TSK model of the AEP feature D_{51}. RC_e is the remifentanil effect concentration, PC_e is the propofol effect concentration. f_i is the i output membership function, $i = 1,\ldots,4$.

PC_e	**RC_e**		
	mf1	**mf2**	**mf3**
mf1	f_1		
mf2	f_2		
mf3		f_3	
mf4			f_4

The output membership functions are the following:

$$\begin{aligned} f_1 &= -0.0439PC_e - 10.7005RC_e + 157.5113 \\ f_2 &= -0.0418PC_e - 2.2590RC_e + 182.4764 \\ f_3 &= 0.1638PC_e + 2.1645RC_e - 360.4773 \\ f_4 &= 0.0196PC_e - 17.4224RC_e + 11.3201 \end{aligned} \qquad 5\text{-}20$$

In contrast with the low frequency features (D_1 and D_3), the features D_5 and D_{51} are modelled using more rules and membership functions, this may represent the higher variability of these features. Figure 5-54 shows the output surface of the D_{51} TSK model.

The results of the model on the training and checking data sets are presented in Figure 5-55. The mean absolute errors were 6.5 and 4.6 on the training and checking data sets, respectively.

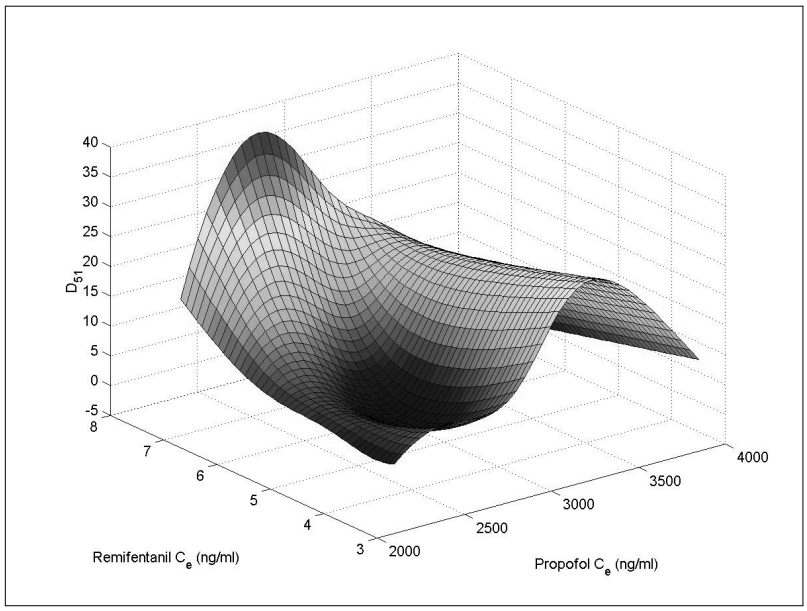

Figure 5-54: Output surface of the AEP feature D_{51} TSK fuzzy model.

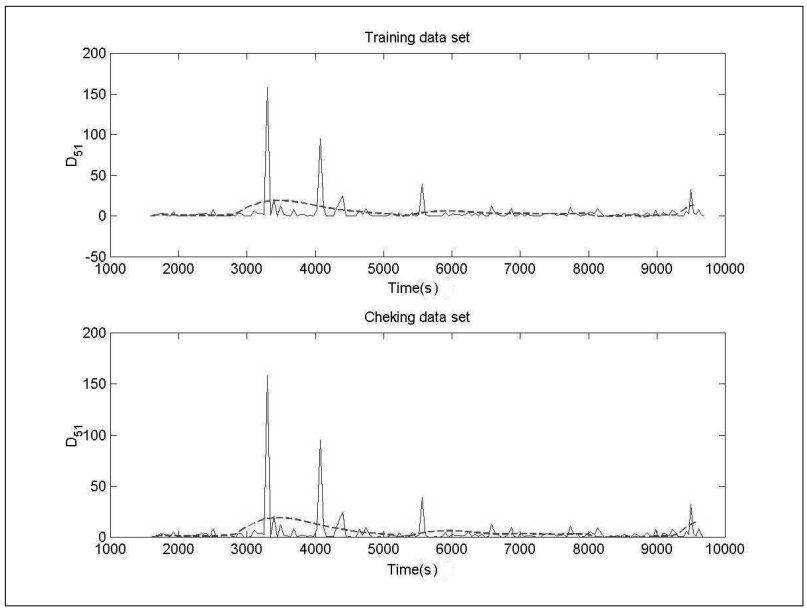

Figure 5-55: Results of the AEP feature D_{51} TSK fuzzy model on the training and checking data sets (dashed line) and the AEP feature D_{51} from patient Pat1 (solid line), considering the maintenance phase.

The detailed feature D_{51} is clearly influenced by some factor, not related with the effect concentrations. The very sharp peaks at approximately 3200 seconds and 4000 seconds have very high amplitudes compared with the rest of the signal. The D_{51} values are generally below 25, however this disturbances are of values greater than 100. As a result,

the model is not able to cope with these very high values.

In conclusion, the TSK models obtained from the wavelet extracted AEP features describe the relationship between the effect concentrations and the AEP features. The models have different characteristics according to the high and low frequency features. The AEP features are affected by other factors besides the effect concentrations. In general, the sharp peaks in the AEP features are the responses to surgical stimulus, this is discussed in detail in the next section.

5.5 Stimulus Model

Surgical stimulus increases the value of SAP and HR. Tassorelli *et al.* (1995) reported on the haemodynamic responses to stimulation, using a cold-pressor test. Increases in both blood pressure and HR were observed throughout the test. Schwender *et al.* (1994) reports changes in HR, SAP and DAP after skin incision as well as sternotomy, with different anaesthetised groups. In addition, Pinerua-Shuhaibar *et al.* (1999) demonstrated the cardiovascular modulation of pain perception in humans.

The final value of the cardiovascular parameters is the result of the effect of the two drugs and of the surgical stimulus present. Propofol provides unconsciousness, while remifentanil provides pain relief. Remifentanil action can be viewed as a reduction on the patient's perception of surgical stimulus. In fact, remifentanil effect concentration determines the quality of analgesia and therefore the level of stimulus perceived by the patient. In the previous section, the interaction of propofol and remifentanil was modelled, considering the effect on ΔSAP, ΔHR and the AEP features. In this section, the objective is to model the surgical stimulus effect on the cardiovascular parameters, considering the analgesic component of anaesthesia (i.e. the remifentanil effect concentration). Figure 5-56 presents a diagram illustrating the overall stimulus model scheme. Note that only the effect of stimulus during the maintenance phase is modelled. The stimulus effect present in the induction phase (i.e. intubation) was analysed according to the remifentanil action in Section 5.3.2.

In Figure 5-56, the Fuzzy Model 1 describes the analgesic component of remifentanil in reducing the level of stimulus perceived by the patient (i.e. the perceived stimulus). Fuzzy Model 2 comprises two fuzzy models describing the effect of the perceived stimulus on

SAP and HR, respectively.

The surgical stimulus also affects the AEP (Thornton *et al.*, 1988). However, modulation of such effect is an unexplored subject. The effect of stimulation on the wavelet extracted AEP features will be discussed in Section 5.5.4. First, the perceived stimulus model will be presented (Fuzzy Model 1 in Figure 5-56). Secondly the fuzzy model for the changes in SAP will be presented, followed by the fuzzy model for HR, using the perceived stimulus. The overall stimulus model comprises three Mamdani type fuzzy models based on the anaesthetist knowledge and presented in IF-THEN rules. Details of the Mamdani type fuzzy systems are presented in Appendix B.

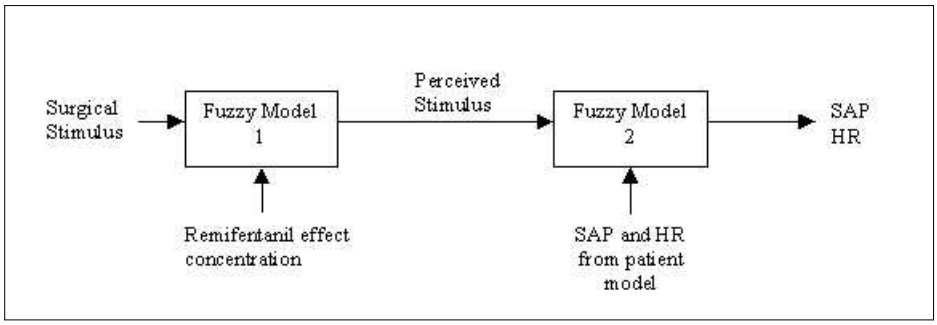

Figure 5-56: Block diagram of the stimulus model.

5.5.1 Perceived Stimulus

The surgical stimulus intensity was described as Zero, Low, Medium and High, considering the following events as labelled by the anaesthetist:

Intubation - high intensity stimulus
Incision - high intensity stimulus
Retractors - high intensity stimulus
Cutting - medium intensity stimulus
Diathermy - low to medium intensity stimulus
Suture - low intensity stimulus.

The remifentanil effect concentration was established as being between 0-10 ng/ml throughout the procedure. However, in the maintenance phase this is more restrict. The remifentanil effect concentration was labelled by the anaesthetist as Zero, Low, Medium, High and VeryHigh.

The surgical stimulus and the remifentanil effect concentration are the inputs to the fuzzy model. The output is the perceived stimulus, obtained using the rule-base in Table 5-9. The

perceived stimulus is labelled Zero, VeryLow, Low, Medium and High.

Table 5-9: Perceived stimulus fuzzy rule base. Surgical stimulus $\in [0,1]$, remifentanil effect concentration $\in [0, 10 \text{ ng/ml}]$ and perceived stimulus $\in [0,1]$.

Surgical	**Remifentanil Effect Concentration (ng/ml)**				
Stimulus	**Zero**	**Low**	**Medium**	**High**	**VeryHigh**
Zero	Zero	Zero	Zero	Zero	Zero
Low	Low	VeryLow	Zero	Zero	Zero
Medium	Medium	Low	VeryLow	Zero	Zero
High	High	Medium	Low	VeryLow	Zero

Figures 5-57 and 5-58 show the membership functions for the remifentanil effect concentration and surgical stimulus, respectively. Figure 5-59 shows the perceived stimulus membership functions. The output surface of the perceived stimulus fuzzy model is presented in Figure 5-60. The centre of gravity defuzzifier was used as the defuzzification method (details of this method are presented in Appendix B).

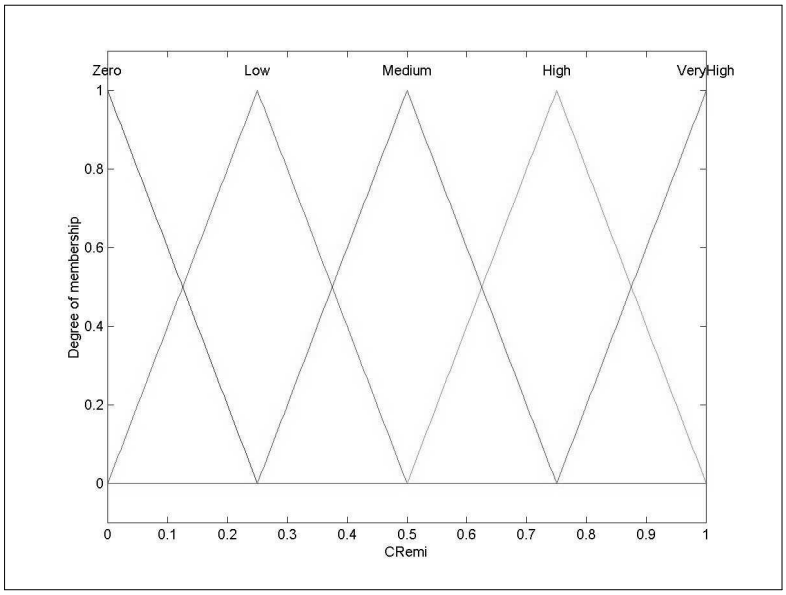

Figure 5-57: Remifentanil effect concentration (CRemi) membership functions, normalised between 0 and 1, scaling factor of 0.1 (0 to 10 ng/ml).

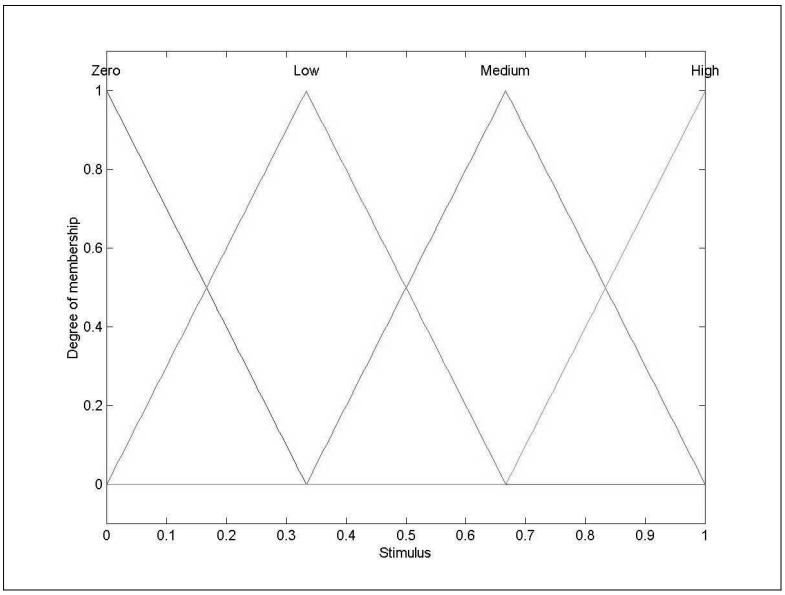

Figure 5-58: Surgical stimulus membership functions.

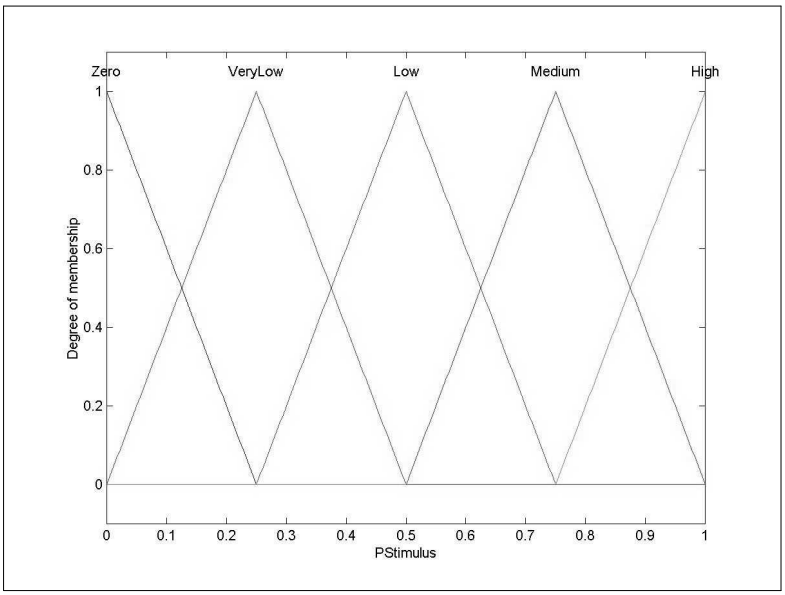

Figure 5-59: Perceived stimulus membership functions.

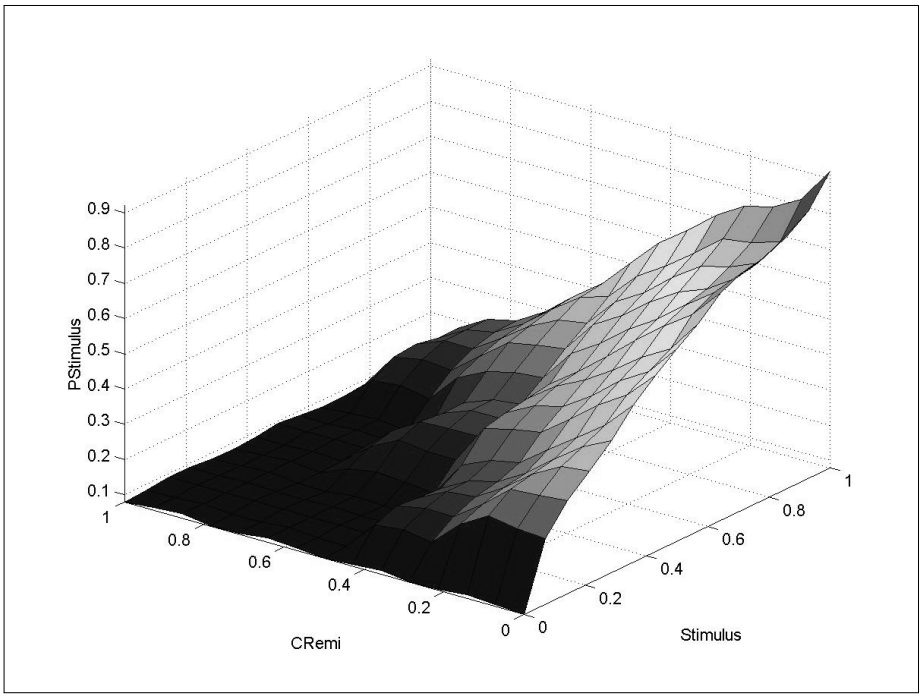

Figure 5-60: Perceived stimulus fuzzy model output surface. CRemi is the remifentanil effect concentration and PStimulus is the perceived stimulus.

The membership function VeryLow for the perceived stimulus, is necessary so as to describe the effect of a low surgical stimulus in the presence of a low remifentanil effect concentration. In other words, a low remifentanil concentration does not suppress completely a low stimulus.

The model output surface reflects the smooth decrease in the perceived stimulus as the remifentanil concentration increases. The stimulus profile present in the procedure of patient Pat1, was labelled by the anaesthetist and stored in a data file. This file will be used in the simulation system, Note that during the maintenance phase of anaesthesia the surgical stimulus is continuous, with different degrees of intensity.

The perceived stimulus model was applied to the data profile from patient Pat1 (i.e. the remifentanil effect concentration in Figure 5-3). The result is presented in Figure 5-61. The surgical stimulus profile (solid line) from the data file was transformed into the perceived stimulus (dashed line) according to the remifentanil effect concentration. Note that sometimes the perceived stimulus is slightly above the surgical stimulus when it is of very low intensity. This is due to the defuzzification method used, since the centre of gravity defuzzifier uses the centre of area of the triggered membership functions, hence providing smoother outputs. However, at such low intensity the difference is not significant, considering its effect on the cardiovascular parameters and that the stimulus is continuous

throughout the maintenance phase (i.e. after incision until suture).

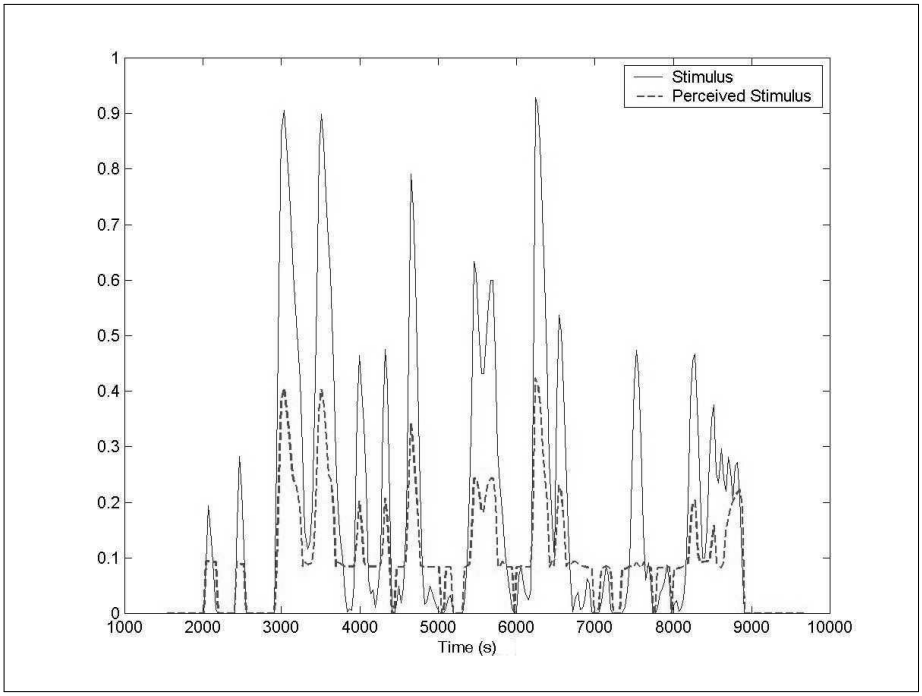

Figure 5-61: Surgical stimulus (solid line) and perceived stimulus (dashed line) in the maintenance phase, using the surgical profile of patient Pat1.

5.5.2 Systolic Arterial Pressure

The effect of the perceived stimulus on the SAP values is modelled using the anaesthetist knowledge described by IF-THEN rules. Figure 5-62 presents the block diagram for the fuzzy model describing the effect of the perceived stimulus on SAP. The inputs to the model are: *PrevSAP*, the value of SAP (i.e. baseline SAP plus ΔSAP) from the maintenance phase model described in Section 5.4 (Figure 5-28); and *PerStimulus*, the perceived stimulus level obtained from the perceived stimulus fuzzy model described in the previous section (Fuzzy Model 1 in Figure 5-56).

After considering the effect of the perceived stimulus the value of SAP is described using the rule base in Table 5-10, constructed with the cooperation of the anaesthetist. The perceived stimulus was labelled as Zero, Low, Medium and High, according to the membership functions of Figure 5-63.

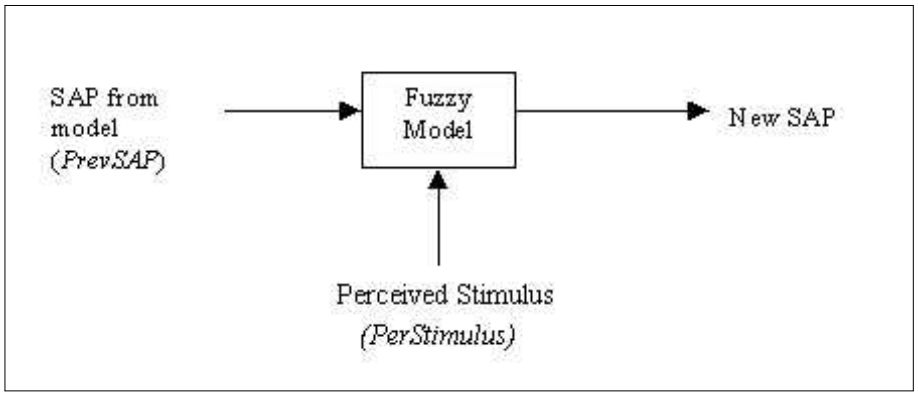

Figure 5-62: Block diagram of the fuzzy model describing the effect of surgical stimulus on SAP.

Table 5-10: Rule base for the new value of SAP after the stimulus. *PrevSAP* is the value of SAP from the maintenance phase model.

Perceived	**Previous value of SAP (*PrevSAP*)**		
Stimulus *(PerStimulus)*	**Low**	**Medium**	**High**
Zero	Low	Medium	High
Low	Low	Medium	High
Medium	Medium	High	VeryHigh
High	High	VeryHigh	VeryHigh

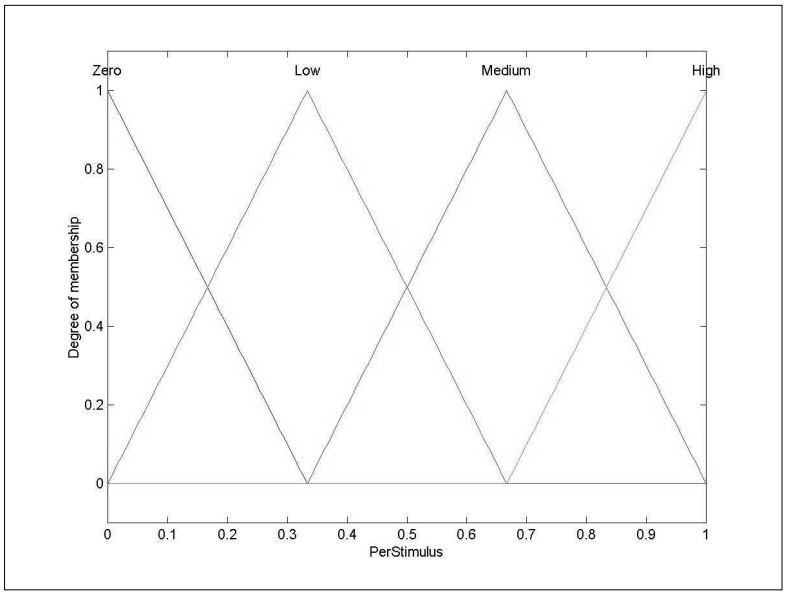

Figure 5-63: Input membership functions describing the perceived stimulus (*PerStimulus*).

The values of the different SAP classes are described as follows:

- **Situation A:** baseline SAP > 130 mmHg

  Low: SAP < 70% of baseline;

  Medium: SAP between 70-80% of baseline;

High: SAP > 80% of baseline.

- **Situation B:** baseline SAP between 120-130 mmHg

  Low: SAP < 75% of baseline;
  Medium: SAP between 75-85 % of baseline;
  High: SAP > 85% of baseline.

- **Situation C:** baseline SAP < 120 mmHg

  Low: SAP < 90 mmHg;
  Medium: SAP between 90-120 mmHg;
  High: SAP > 120 mmHg.

This class division was established by the anaesthetist and also used by Shieh (1994) and Linkens *et al.* (1996b).

The membership functions for the previous value of SAP (*PrevSAP*) are presented in Figure 5-64, taking into account Situations A and B. These two situations can be modelled together considering a normalized range between [0,1], and using different scaling factors. In Situation A, the SAP range is 50-120% of baseline value, and for Situation B a range of 55-125% is considered.

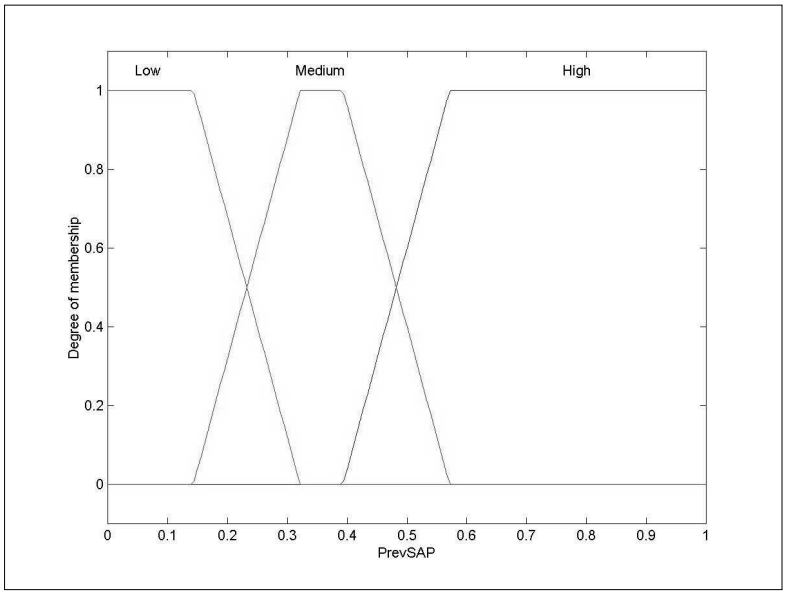

Figure 5-64: Input membership functions describing the previous value of SAP (*PrevSAP*), considering situations A and B. The range is normalised between [0,1].

After considering the perceived stimulus effect, the new value of SAP (i.e. output of the fuzzy system) is labelled Low, Medium, High and VeryHigh according to the membership functions in Figure 5-65, for Situations A and B. The SAP output surface is presented in

Figure 5-66. The center of gravity defuzzifier was used as the defuzzification technique.

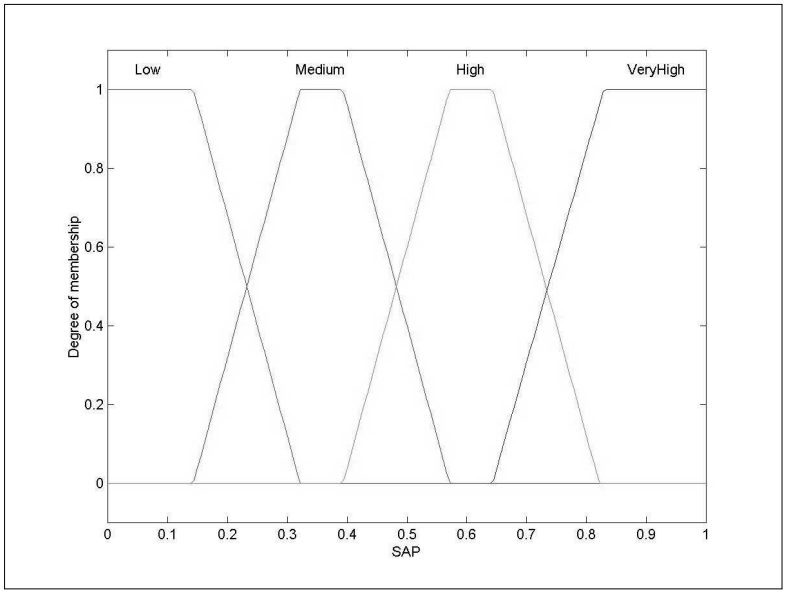

Figure 5-65: Output membership functions describing the new value of SAP, considering situations A and B. The range is normalised between [0,1].

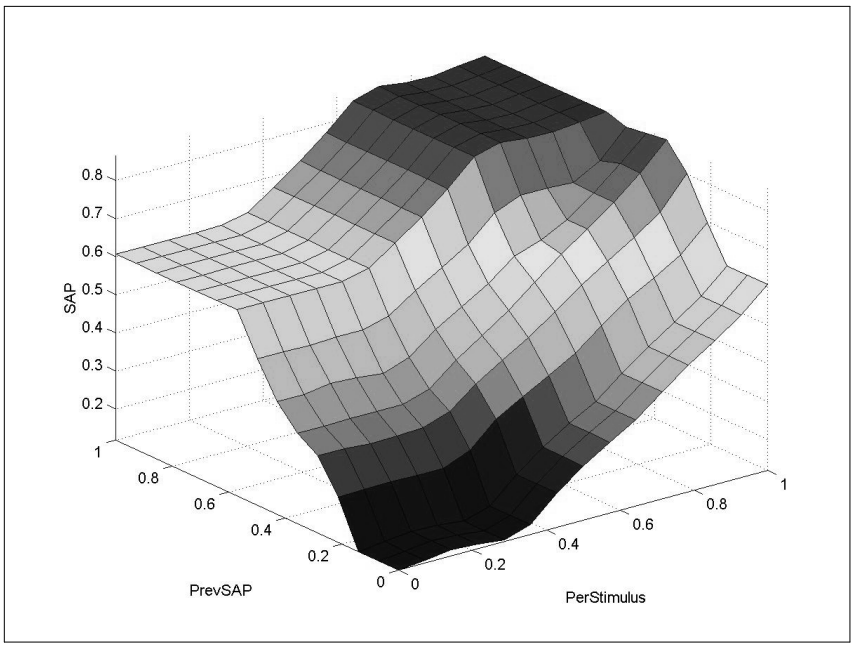

Figure 5-66: Output surface for SAP fuzzy model, situations A and B. *PerStimulus* is the perceived stimulus and *PrevSAP* is the previous value of SAP.

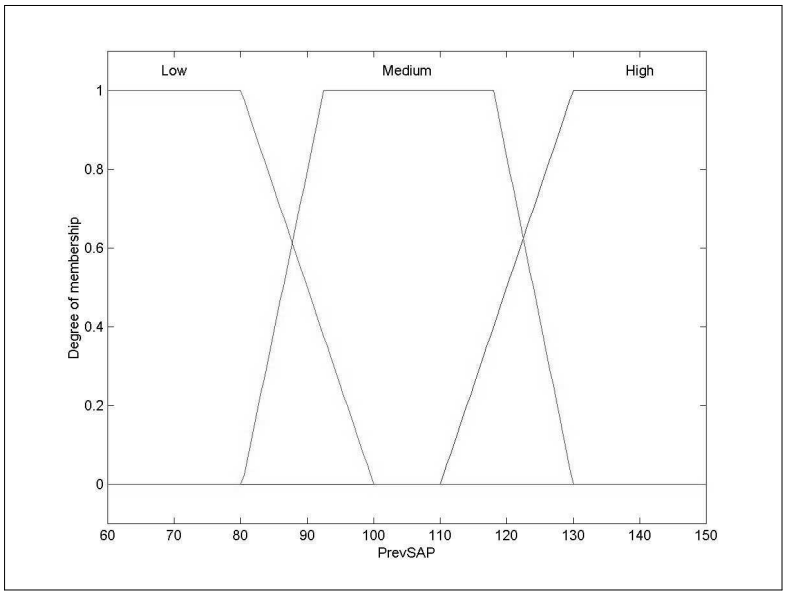

Figure 5-67: Input membership functions for the previous value of SAP (*PrevSAP*), considering situation C.

Situation C is treated separately, since it is not expressed in terms of a percentage from the baseline. Figure 5-67 shows the membership functions for the previous value of SAP, and Figure 5-68 shows the membership functions of the output value of SAP, considering Situation C. Note that, the input and output ranges are not normalized, i.e. they are represented in mmHg. The output surface for SAP is presented in Figure 5-69, considering Situation C. The output surface is different from the one obtained for Situations A and B (Figure 5-66), but reflects the same change trend.

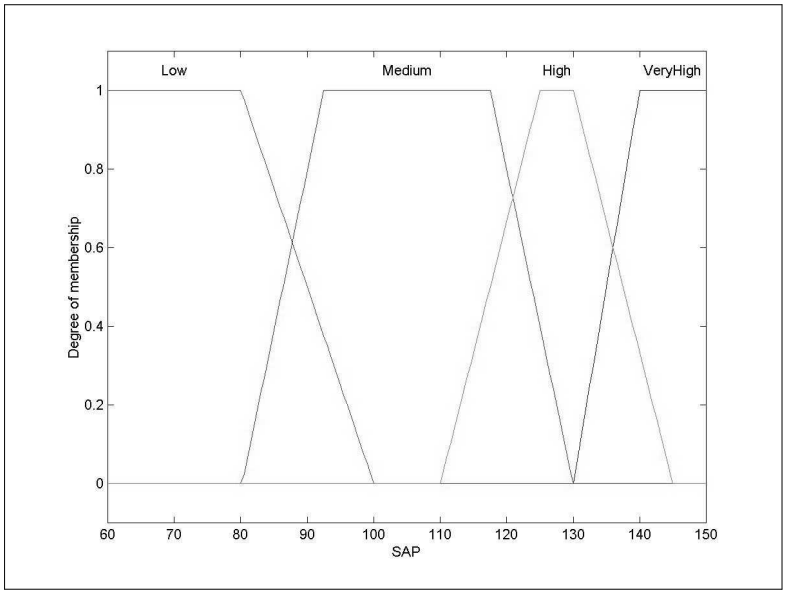

Figure 5-68: Output membership functions for the new value of SAP, considering situation C.

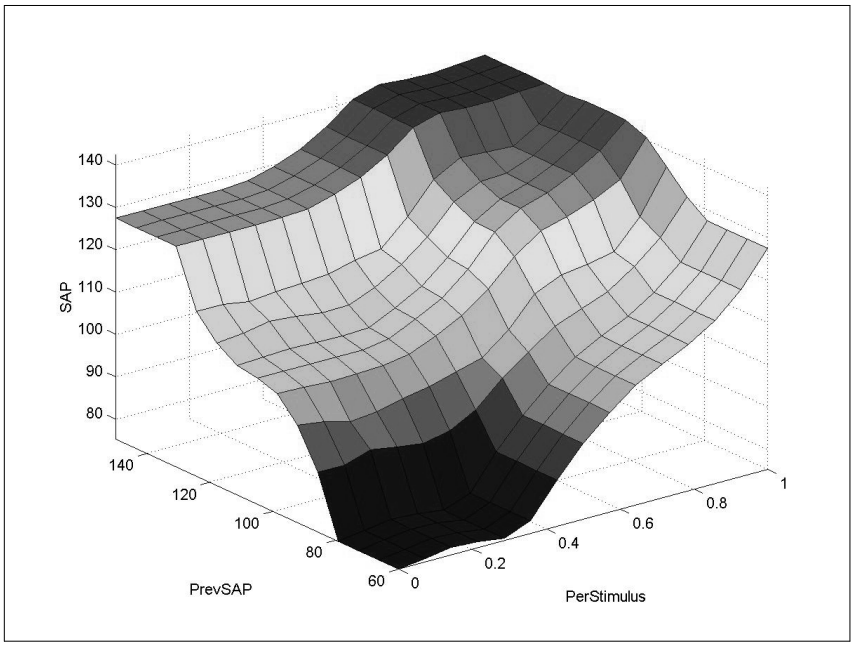

Figure 5-69: Output surface for SAP fuzzy model, considering situation C. *PerStimulus* is the perceived stimulus and *PrevSAP* is the previous value of SAP.

The shape and values of the membership functions were chosen so as to reproduce the anaesthetist knowledge reflected in the classification of SAP.

The fuzzy model was applied to the results of the simulation using the maintenance phase model for the profile of patient Pat1. Figure 5-70 shows the SAP value before and after the stimulus model, solid and dashed line respectively. Note how the presence of the stimulus is affecting the value of SAP, introducing changes and peaks to the smooth output of the maintenance phase model.

Figure 5-71 shows the observed SAP from patient Pat1 (solid line) versus the value of SAP after the stimulus model (dashed line). The results of the model including the stimulus effect have a reasonable approximation to the observed value of SAP. This was expected, since the stimulus level affects the cardiovascular responses. However, there is a small delay between the model results and the observed SAP. This happens because in reality it takes 2-5 minutes for the stimulus effect to be reflected in the SAP value; meaning that the influence of the stimulus is not instantaneous. This time-delay has not been included in the SAP model. Therefore, the stimulus model responds immediately to the stimulus, altering the SAP value. The existing time-constant is different for SAP and HR, and to our knowledge there are no studies defining its value. In addition, it was not considered adequate to estimate the time-delay based only on the data of a single patient, knowing the high variability between patients.

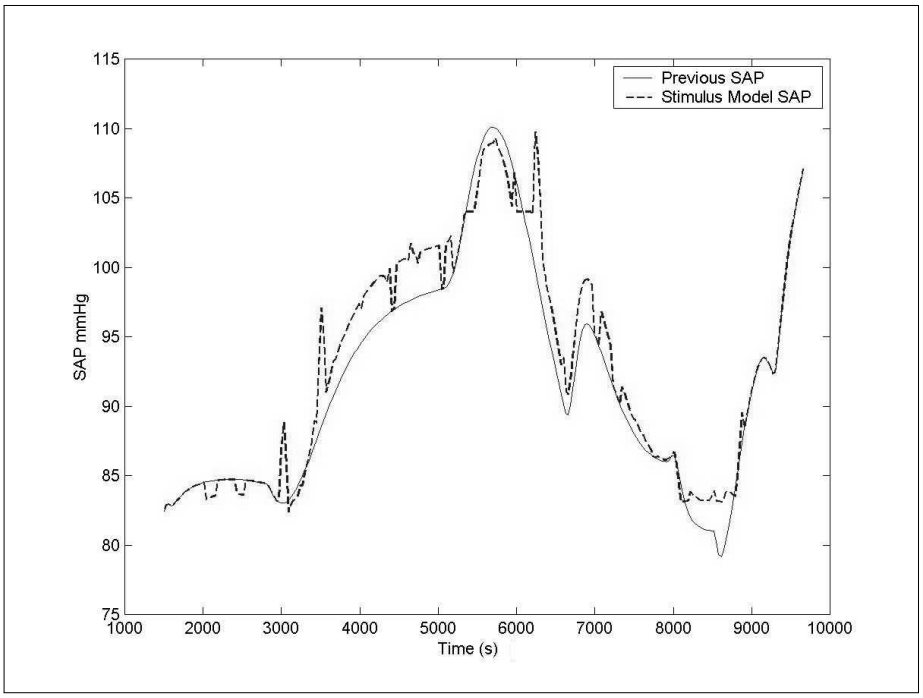

Figure 5-70: SAP from patient model without stimulus (solid line) and SAP after the stimulus model (dashed line). The profile of patient Pat1 was used for the simulation, considering the maintenance phase.

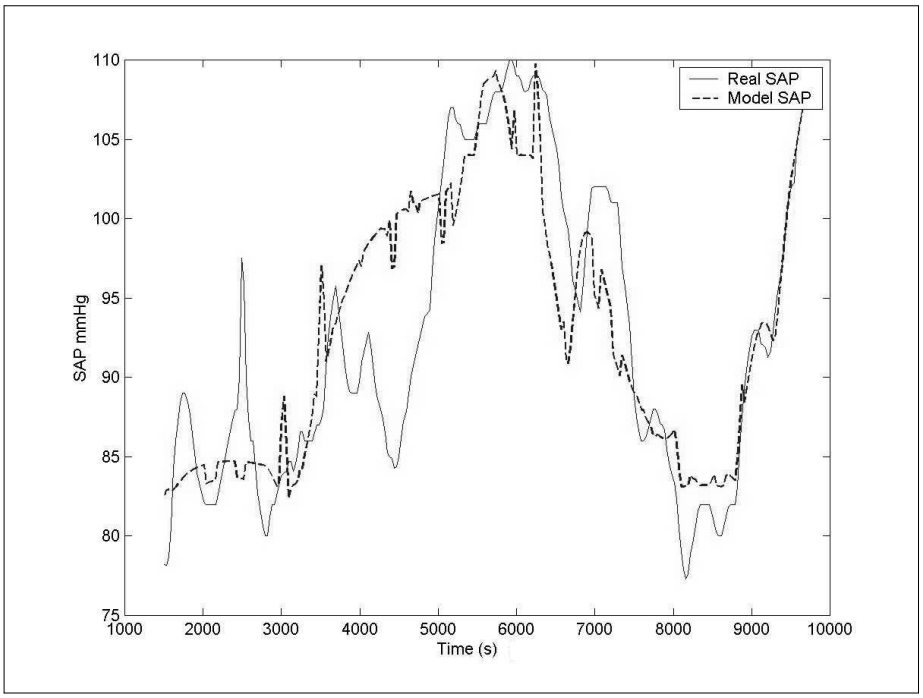

Figure 5-71: SAP from patient Pat1 (solid line) and SAP from patient model including the stimulus model (dashed line), in the maintenance phase.

5.5.3 Heart Rate

The effect of the perceived stimulus on the HR values is modelled using the anaesthetist knowledge by describing the change in HR using fuzzy rules. Figure 5-72 shows the block diagram describing the change in HR as a result of the perceived stimulus. *PrevHR* is the HR value from the maintenance phase model (HR baseline plus ΔHR); *PerStimulus* is the perceived stimulus value. The effect of the perceived stimulus on the HR is described as a change in its value. This change in HR is labelled as Zero, Little and Large according to the anaesthetist opinion. A little change represents a change of 5% of the previous value, and a large change could be as big as 10%. Therefore, the value of HR after the stimulus model will be increased by a certain percentage.

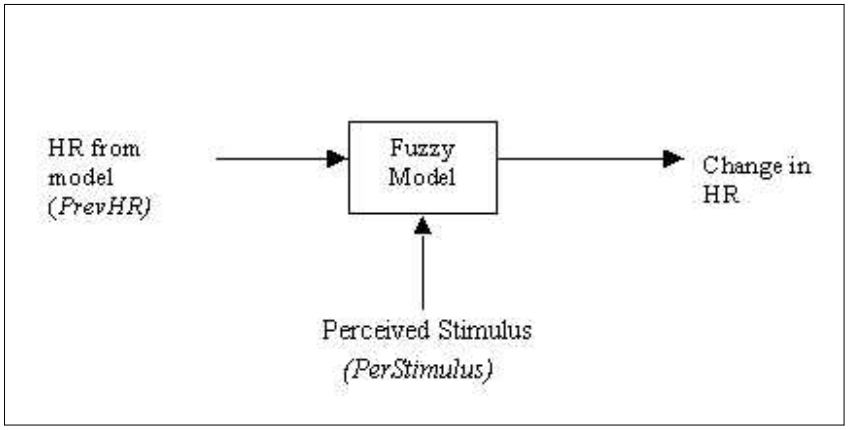

Figure 5-72: Block diagram of the fuzzy model describing the effect of surgical stimulus on HR.

The change in HR is modelled using the rule-base in Table 5-11, with the previous value of HR (*PrevHR*) and the perceived stimulus (*PerStimulus*) as the inputs of the fuzzy model.

Table 5-11: Rule base for the change in HR after the stimulus. *PrevHR* is the value of HR from the maintenance phase model.

Perceived	**Previous value of HR (*PrevHR*)**		
Stimulus *(PerStimulus)*	**Low**	**Medium**	**High**
Zero	Zero	Zero	Zero
Low	Zero	Zero	Little
Medium	Zero	Little	Large
High	Little	Little	Large

The perceived stimulus membership functions are the same as the ones used for SAP (Figure 5-63), labelled Zero, Low, Medium and High. The HR class values were classified by the anaesthetist as follows:

Low: HR < 70% of baseline;
Medium: HR between 70-90% of baseline;
High: HR > 90% of baseline.

The *PrevHR* membership functions according to this description, are presented in Figure 5-73. The HR has lower normal values when using remifentanil than with other opioids, due to its depressive effect. This was taken into consideration when establishing the HR ranges. Note that in Figure 5-73 the HR range represents 50-110% of baseline.

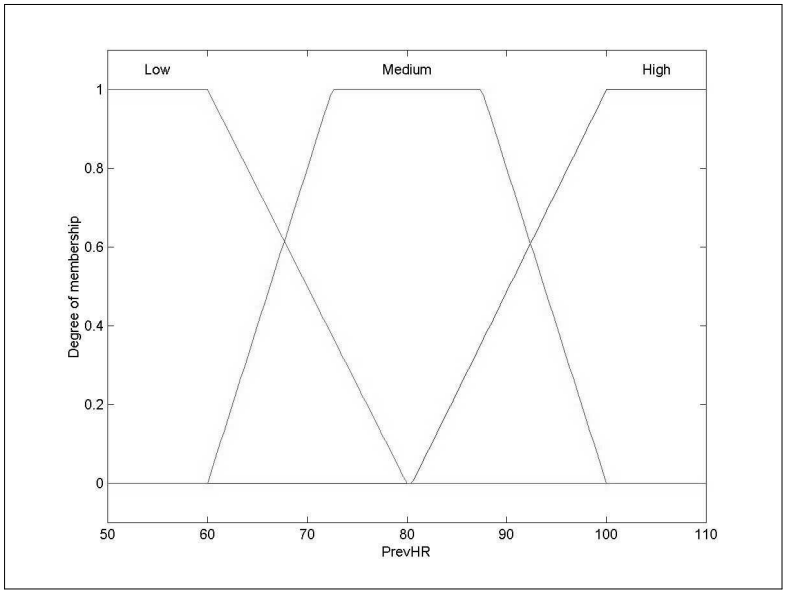

Figure 5-73: Input membership functions describing the previous value of HR (*PrevHR*).

Figure 5-74 shows the output membership functions for the change in HR. The change in HR is presented as a percentage of the previous value (i.e. *PrevHR*). The output surface for the change in HR fuzzy model is presented in Figure 5-75. The center of gravity defuzzifier was used as the defuzzification method.

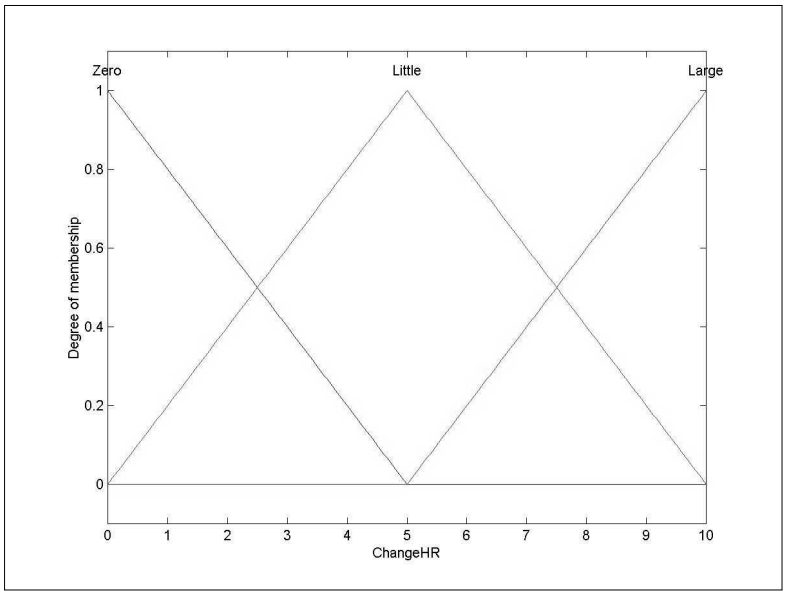

Figure 5-74: Output membership functions for the change in HR (effect of stimulus). The range of 0-10 represents 0-10% change.

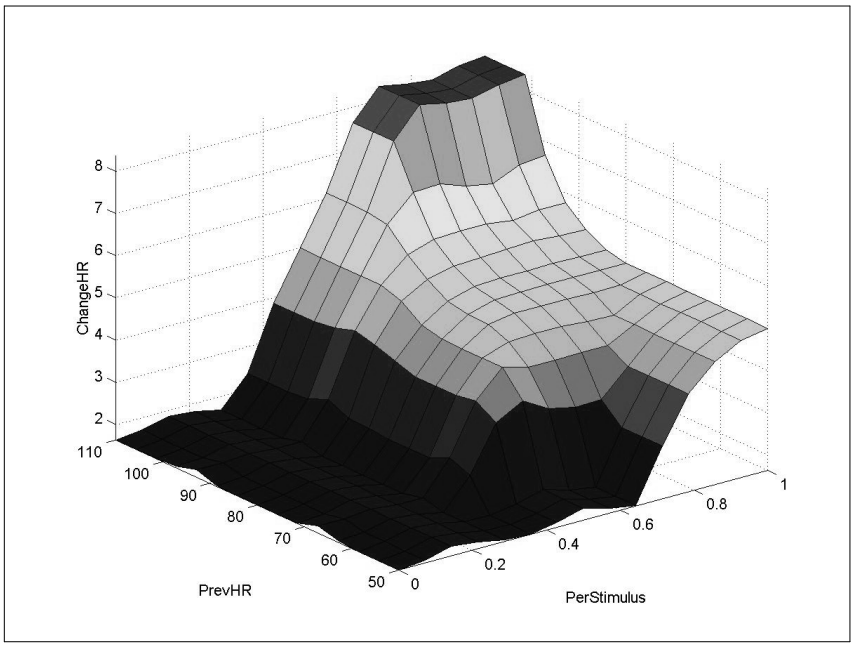

Figure 5-75: Output surface for the change in HR fuzzy model. *PerStimulus* is the perceived stimulus and *PrevHR* is the previous value of HR from the maintenance phase model.

The described fuzzy model was applied to the results of the simulation using the maintenance phase model for the profile of patient Pat1. Figure 5-76 shows the HR value before the stimulus model (solid line) versus the HR after considering the change resulting from the stimulus model (dashed line). The HR value was increased throughout due to the stimulus effect. The peaks resulting from the stimulus are quantitatively less than the ones on SAP, which demonstrates that HR is a more stable variable.

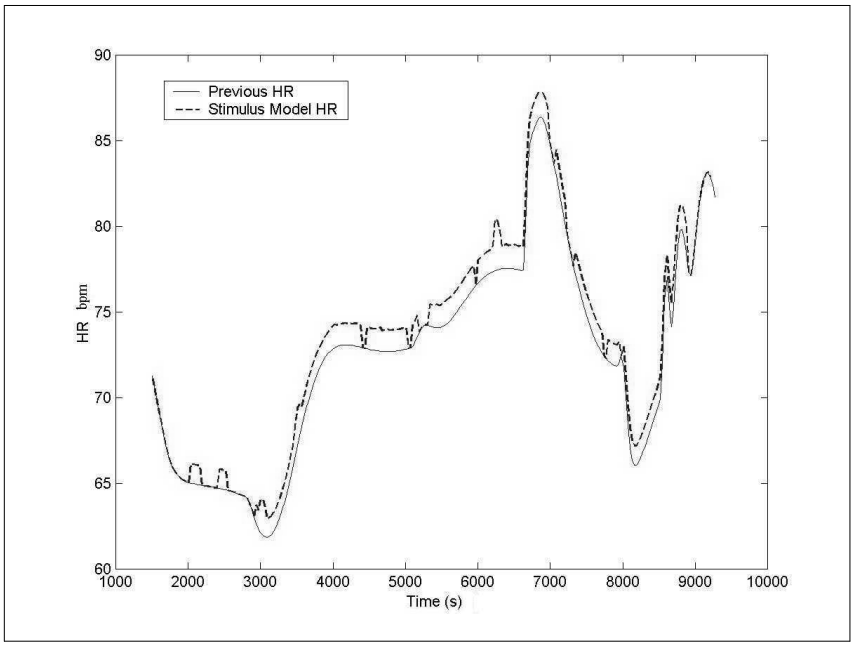

Figure 5-76: HR from patient model without stimulus (solid line) and HR after the stimulus model (dashed line). The profile of patient Pat1 was used for the simulation, considering the maintenance phase.

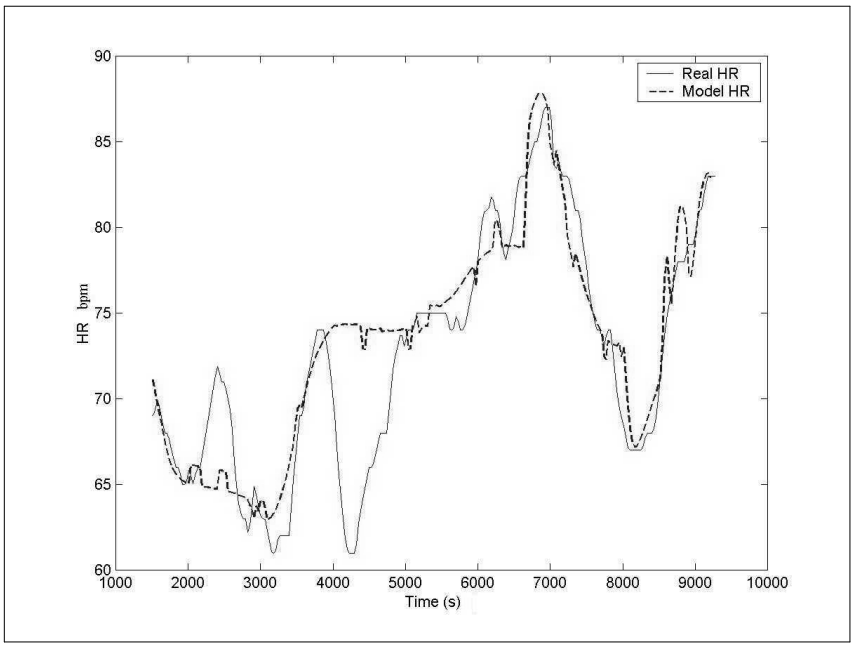

Figure 5-77: HR from patient Pat1 (solid line) and HR from patient model including the stimulus (dashed line), in the maintenance phase.

Figure 5-77 shows the HR observed for patient Pat1 (solid line) versus the HR from the patient model after the inclusion of the stimulus effect. The model approximation has improved, considering the result before the stimulus model. This reflects the appropriateness of a stimulus model. In addition, the HR model seems to be averaging-out disturbances in the HR signal. When considering the time period of 4000 to 6000 seconds, the model HR is reflecting the HR trend but smoothing the sharp "valley" in the data.

Overall, the model has an adequate performance.

The time-delay for HR is different from the one for SAP. It appears that the HR reacts faster than SAP to the stimulus. Due to the same reasons as for SAP, no time-constant was included in the HR model. In contrast, the AEP respond faster to the stimulus effect, this is demonstrated in the following section.

5.5.4 Auditory Evoked Potentials

The surgical stimulus affects the auditory evoked potentials (AEP) and, hence, the wavelet extracted AEP features. However, the effect of different surgical stimuli (i.e. different intensity) is not trivial to analyse. The anaesthetist has not enough knowledge to describe this effect on the AEP. Figures 5-78 to 5-83 show several AEP features in contrast with the existence of different surgical stimuli.

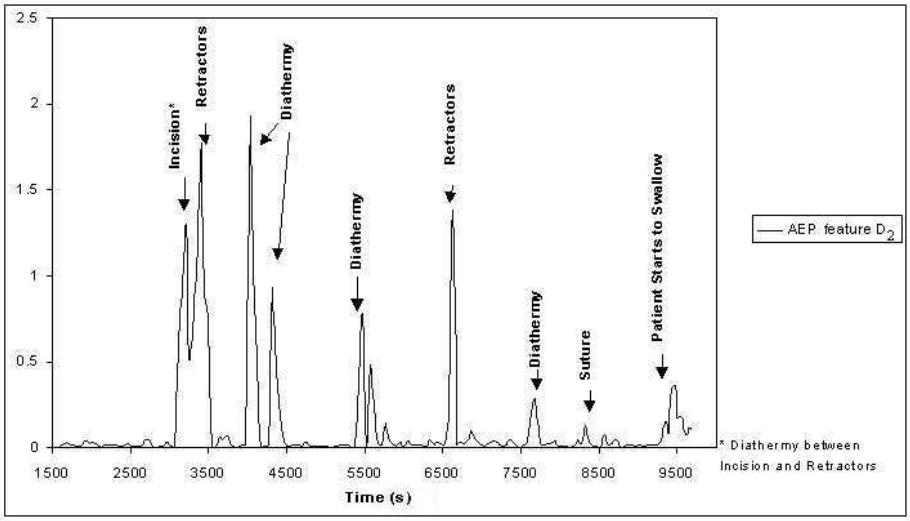

Figure 5-78: Wavelet extracted AEP feature D_2 from the data of patient Pat1, considering the maintenance phase and the different surgical stimulus.

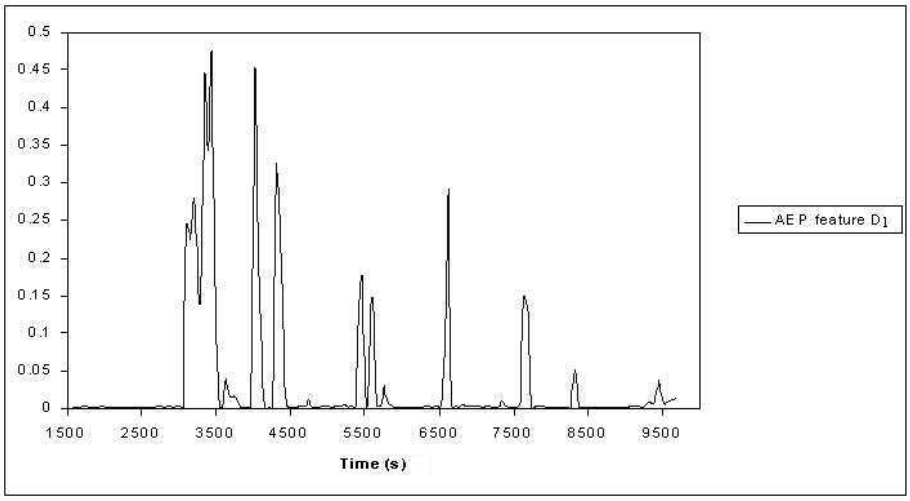

Figure 5-79: Wavelet extracted AEP feature D_1 from the data of patient Pat1, considering the maintenance phase.

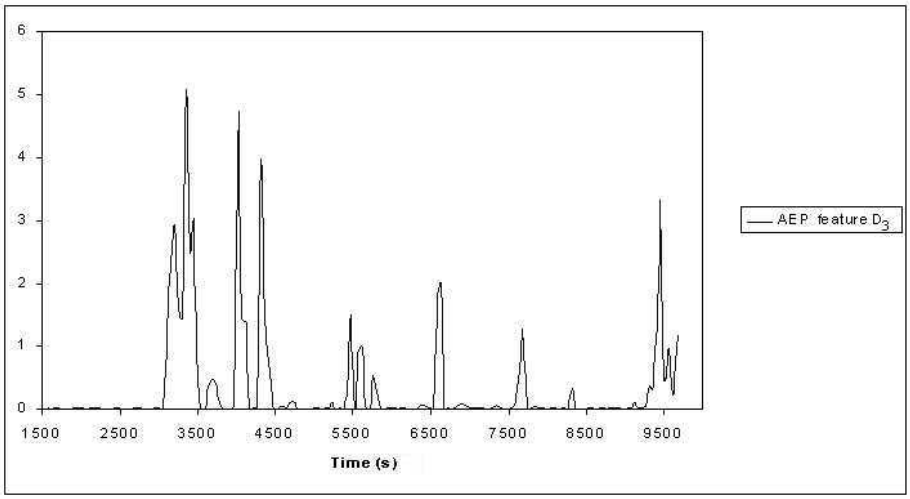

Figure 5-80: Wavelet extracted AEP feature D_3 from the data of patient Pat1, considering the maintenance phase.

The low frequency AEP features D_2, D_1 and D_3 present similar changes to the same stimulus (Figures 5-78 to 5-80). The amplitude of the AEP features response to stimulus is different according to the different features, nevertheless, these features (D_2, D_1 and D_3) seem to reflect the same trend. The surgical stimulus produces clear peaks, and the amplitude of these peaks is related with the intensity of the stimulus. The response of D_2 (Figure 5-78) to the use of retractors is notorious compared with the response to a low stimulus such as a suture. When the surgical procedure is at the end and the patient starts to swallow (i.e. awaking), the AEP feature rises to higher values. In fact, they have a similar response to recovery and to stimulus. This leads to the conclusion that surgical stimulus could lead to an arousal of the patient.

Figures 5-81 to 5-83 show some of the high frequency AEP features, D_5, D_{51} and D_4. The

effect of surgical stimulus is different in the low and high frequency AEP features. In the detailed feature D_{51} (Figure 5-82), is clear the effect of diathermy. In fact, the change produced by diathermy obscures all the effects of other stimuli, considering the amplitude of the change.

The AEP features D_5 and D_4 present a greater variability during the surgical procedure than the low frequency features (Figures 5-81 and 5-83). The effect of the surgical stimulus is not easy to detect. For example, the use of retractors at approximately 6500 seconds does not have a great effect on the feature D_5, and is not detected in features D_{51} and D_4. However, this stimulus has a clear effect on the low frequency features.

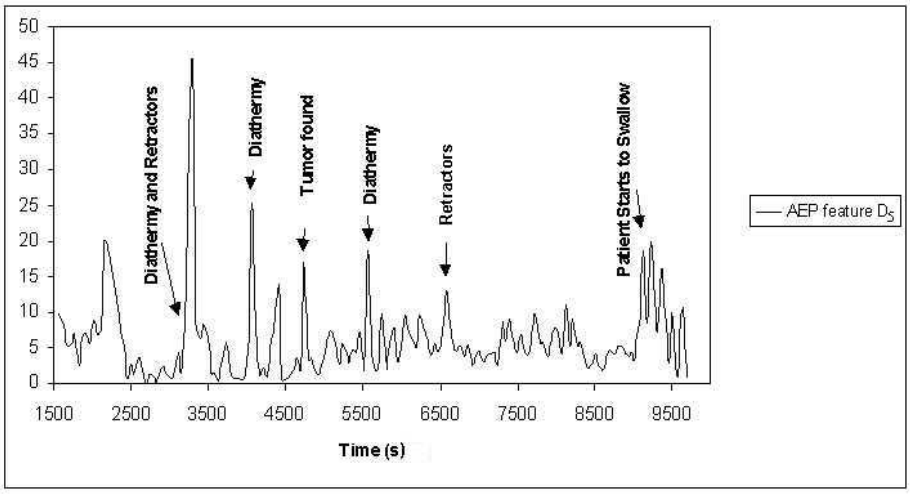

Figure 5-81: Wavelet extracted AEP feature D_5 from the data of patient Pat1, considering the maintenance phase and the different surgical stimulus.

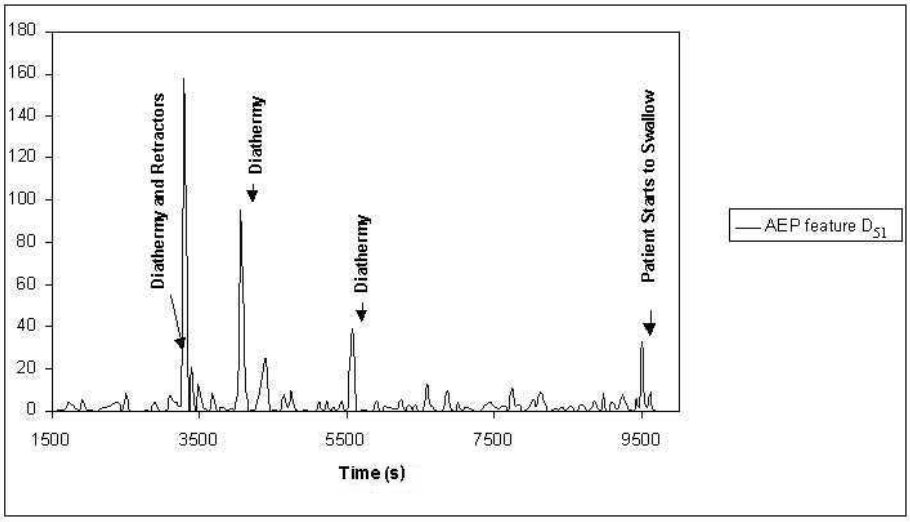

Figure 5-82: Wavelet extracted AEP feature D_{51} from the data of patient Pat1, considering the maintenance phase and the different surgical stimulus.

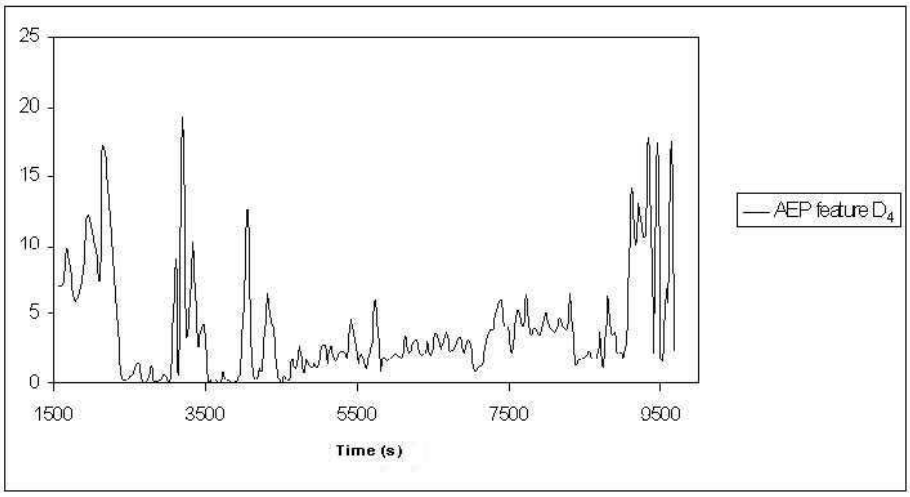

Figure 5-83: Wavelet extracted AEP feature D_4 from the data of patient Pat1, considering the maintenance phase.

In conclusion, the AEP features react to stimulus with an increase in amplitude and this appears to be an instant reaction, i.e. there is no time-delay as was observed with the cardiovascular parameters.

The low frequency AEP features, D_1, D_2 and D_3, show a clear effect of the surgical stimulus. This could be used to quantify the stimulus effect if more data would be available, since there are no previous studies on the subject, and the anaesthetist knowledge cannot be used. In addition, the remifentanil analgesic action, when preventing the response to surgical stimulus, is not clear when considering the CNS. It is not possible to compare these results with experiments without the use of remifentanil, therefore, the relationship between surgical stimulus cannot be reasonably modelled.

The high frequency AEP features, D_4, D_5 and D_{51}, are not affected by surgical stimulus in the same way as the low frequency features. The effect of several stimuli cannot be identified clearly, and there is no trend between the response and the stimulus intensity.

A future study on the relationship between surgical stimulus, analgesia and the CNS, would be challenging and promising when considering data from several patients under different conditions. In this research, the effect of surgical stimulus on the AEP features will not be considered further.

5.6 Summary

The effects of the analgesic and anaesthetic drugs on the cardiovascular and central nervous systems, were modelled using different techniques according to the two main phases of a surgical procedure, i.e. induction and maintenance.

The induction phase of anaesthesia was modelled using the optimized Hill equation models, and characterizing the influence of remifentanil on the haemodynamic responses to intubation. In this phase, only the cardiovascular parameters ΔHR and ΔSAP were modelled, since the AEP cannot be monitored adequately during induction.

The maintenance phase was modelled using TSK fuzzy models which were trained using ANFIS. These models reflect the effect and interaction of the two drugs on ΔSAP, ΔHR and the wavelet extracted AEP features. The synergistic interaction between propofol and remifentanil has a major importance on the drugs effect, in the presence of surgical stimulus. During the maintenance phase, the surgical stimulus can be considered continuous, therefore, the responses of the patient are heavily influenced by the drugs interaction.

The ΔSAP and ΔHR TSK models were compared with optimized linear models, which model the effects of propofol and remifentanil independently. The results show that there is a synergistic interaction between the two drugs, which is reflected in the results of the TSK models.

The TSK models performed adequately with all the parameters (i.e. ΔSAP, ΔHR and the AEP features) presenting small errors and reflecting the drugs effect. However, these models are only valid in the specified drug ranges for the maintenance phase. The drug infusion rates during maintenance of anaesthesia follow a specific profile, so as to maintain a stable DOA in the presence of surgical stimulus.

The effect of surgical stimulus on the cardiovascular parameters was modelled via Mamdani type fuzzy models, using the anaesthetist knowledge expressed with IF-THEN rules. First, the stimulus perceived by the patient was modelled, in order to reflect the analgesic action of remifentanil. Finally, the change on the value of SAP and HR was modelled so as to reflect the effect of the perceived stimulus.

The response of the AEP features to surgical stimulus was also studied. The AEP features have different responses to the different stimuli, according to its nature and intensity. There is a major difference between the behaviour of the low frequency versus the high frequency AEP features. The effect of the stimulus on the AEP features was not modelled due to the lack of information and data. In addition, it was found that there is a time-delay in the cardiovascular responses to stimulus, while the AEP features respond immediately.

In conclusion, the patient model is constituted by an induction phase model plus a maintenance phase model, describing the difference between these two phases of anaesthesia. The models presented an adequate performance on the training and checking data sets, and seem to reflect the effect of the drugs and surgical stimulus. This patient model describes a typical patient's behaviour during a surgical procedure.

Chapter 6

Fuzzy Control of Depth of Anaesthesia

6.1 Introduction

The infusion rate of the anaesthetic drug is titrated according to the patient's requirements, so as to maintain a certain level of depth of anaesthesia (DOA). The patient's clinical signs and/or brain signals are used by the anaesthetist to determine the adequate infusion rate. In addition, the anaesthetist also establishes the required infusion rate of the analgesic drug, based on the patient's response to surgical stimulus.

A closed-loop control system of DOA will help the anaesthetist, adjusting simultaneously the infusion rates of the anaesthetic and analgesic drugs. The majority of the researches in the area are mainly concerned with the automatic control of the anaesthetic drug, whereas the analgesic is controlled manually by the anaesthetist. However, in this research the objective is a multivariable control structure for both drugs.

The patient model presented in Chapter 5, described adequately the effects and interactions of the two drugs in the presence of surgical stimuli. This model will be used to construct a control algorithm relating to the administration of both drugs. The study of the interactions between propofol and remifentanil helps to determine the ideal combination of infusion rates. This study will also represent a practical guide for the anaesthetist, which would help him/her learn how to adjust the amount of drug infused and hence improve the patients comfort.

In this chapter, a multivariable fuzzy controller will be developed to establish the required infusion rates of propofol and remifentanil. First, the patient model will be tested using a series of open-loop simulations with different infusion profiles. Second, the closed-loop structure will be presented, showing the links between the patient model, the DOA

classifier (i.e. the fuzzy relational classifier presented in Chapter 3) and the controller. Third, a SISO (single-input-single-output) fuzzy PI controller of DOA is developed. This controller adjusts the infusion rate of propofol according to the level of DOA with the infusion rate of remifentanil kept constant. The results of the fuzzy PI controller are compared with the results of a conventional PI controller. The parameters of both controllers are optimized using a genetic algorithm (GA).

Finally, a multivariable fuzzy controller developed with the anaesthetist's cooperation, is presented. This controller establishes the infusion rates of propofol and remifentanil simultaneously based on the level of DOA, the concentrations of the drugs and the surgical stimuli. The performance of the controller is tested under different conditions.

6.2 Open-Loop Simulation Results

The patient model developed in Chapter 5 was tested in open-loop simulations with different infusion profiles for propofol and remifentanil. The open-loop results with three different infusion profiles are presented in the following sections.

The simulations were performed for 7200 seconds (120 minutes) with a sampling time of 30 seconds. The first 1500 seconds relate to the induction phase, followed by the maintenance phase. It is worth noting that the recovery phase is not simulated.

The fuzzy relational classifier (FRC) for DOA developed in Chapter 3 is applied to the wavelet extracted AEP features, as determined by the maintenance phase model. In the induction phase, the FRC uses only the cardiovascular parameters ΔSAP and ΔHR for the classification of DOA, since the AEP features are not modelled during this phase.

6.2.1 Infusion Profile 1

Figure 6-1 shows the infusion rate profiles for propofol and remifentanil used in the first simulation, and denoted as Infusion Profile 1. The propofol infusion rate is very similar to the profile of patient Pat1, while the remifentanil infusion rate follows a typical profile during a surgical procedure (i.e. high at induction and constant during maintenance).

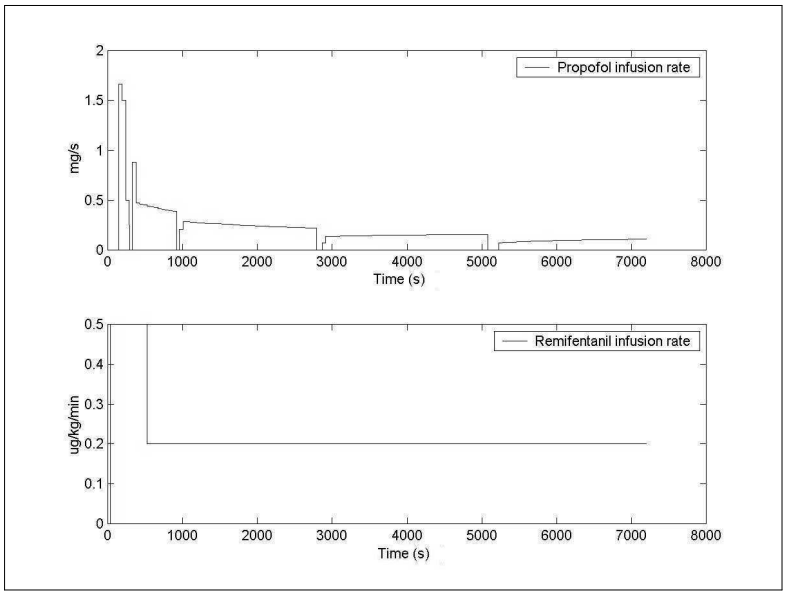

Figure 6-1: Propofol and remifentanil infusion rate profiles (Infusion Profile 1).

Figure 6-2 shows the effect concentration of propofol as determined by the effect compartment model using mean population parameters (see Chapter 4). As expected, the effect concentration of propofol is similar to that of patient Pat1 (Figure 5-2).

The effect concentration of remifentanil for this infusion profile is presented in Figure 6-3. The constant concentration level during the maintenance phase leads to a steady level of analgesia.

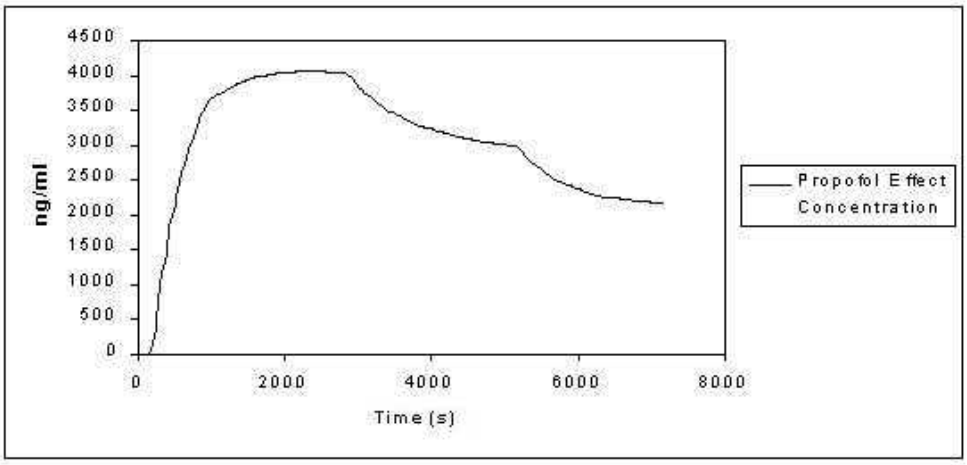

Figure 6-2: Propofol effect concentration for the infusion rate profile in Figure 6-1.

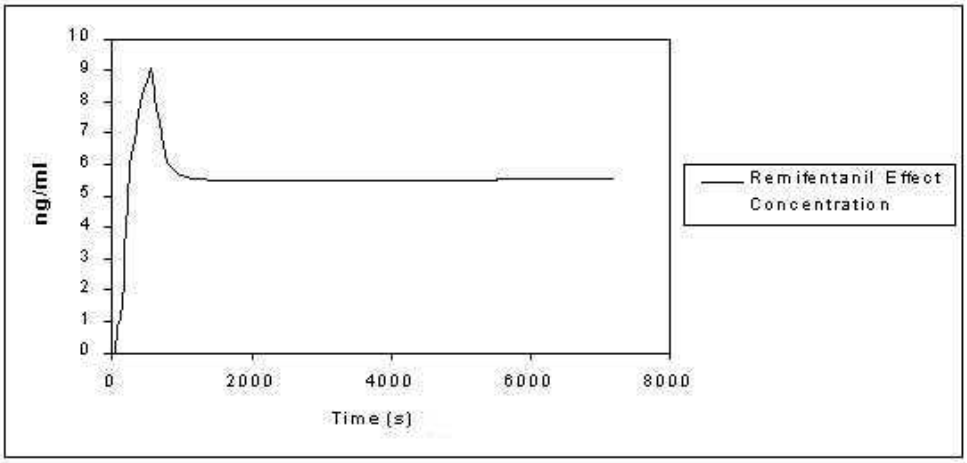

Figure 6-3: Remifentanil effect concentration for the infusion rate profile in Figure 6-1.

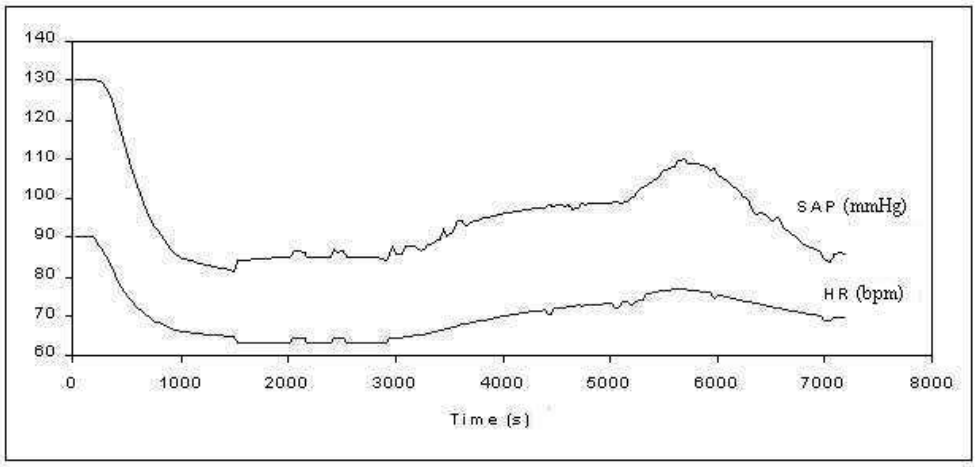

Figure 6-4: Systolic arterial pressure (SAP) and heart rate (HR) as determined by the patient model, using the infusion profiles in Figure 6-1.

Figure 6-4 shows the HR and SAP as simulated by the patient model, using the Infusion Profile 1. The perceived stimulus level, according to the stimulus model and the remifentanil effect concentration, is presented in Figure 6-5.

The wavelet extracted AEP features as simulated by the patient model are used to classify the DOA level by the FRC during the maintenance phase. The DOA level is shown in Figure 6-6.

The model performs adequately, describing the effects of the stimulus level on SAP and HR. The effect concentrations are within the ranges of the maintenance phase and this is reflected in the model's response.

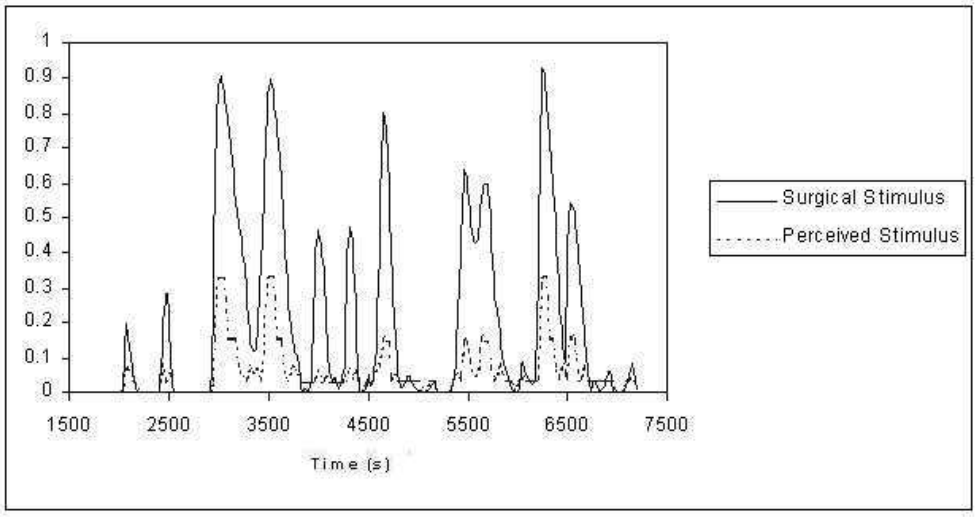

Figure 6-5: Surgical stimulus (solid line) and perceived stimulus (dashed line) for the remifentanil effect concentration in Figure 6-3, during the maintenance phase.

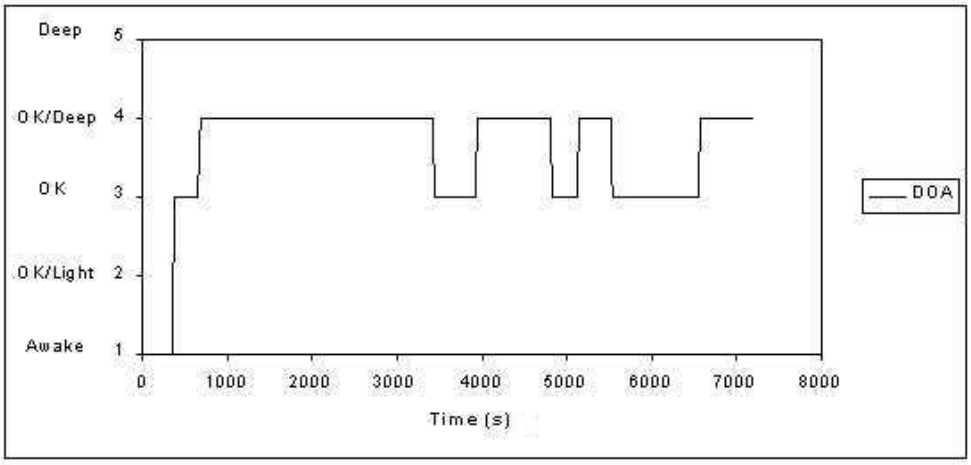

Figure 6-6: Depth of anaesthesia (DOA) as classified by the Fuzzy Relational Classifier (FRC) using the wavelet extracted AEP features (Infusion Profile 1).

The DOA level as determined by the FRC cannot be compared with the anaesthetist's classification, since this is a simulated infusion profile. However, the classification is not unreasonable as it reflects the AEP features from the model.

6.2.2 Infusion Profile 2

Figure 6-7 shows the infusion rate profiles used in the second simulation, and will be referred to as Infusion Profile 2. It is worth noting that the remifentanil infusion rate profile is the same as in the previous simulation (Figure 6-1). The propofol infusion rate profile includes more changes than the one used in the previous section. Therefore, the model

response can be analysed according to the different propofol changes.

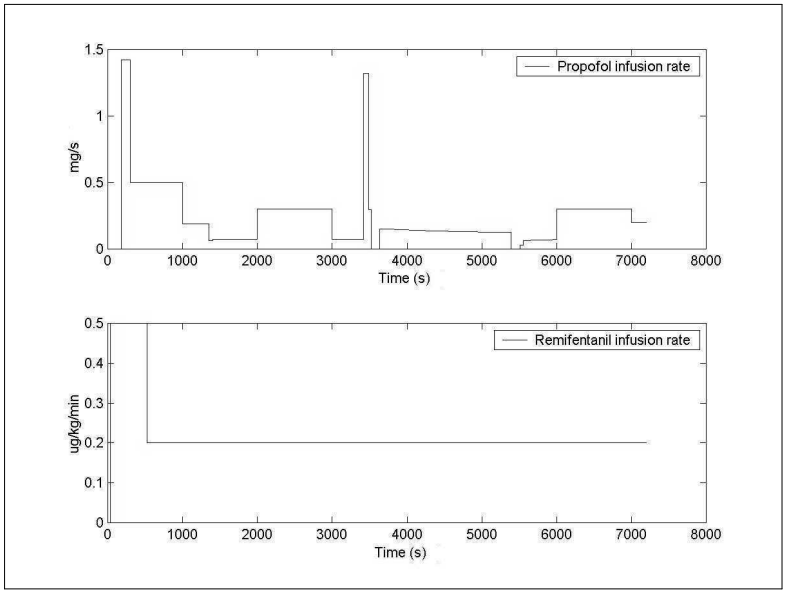

Figure 6-7: Propofol and remifentanil infusion rate profiles (Infusion Profile 2).

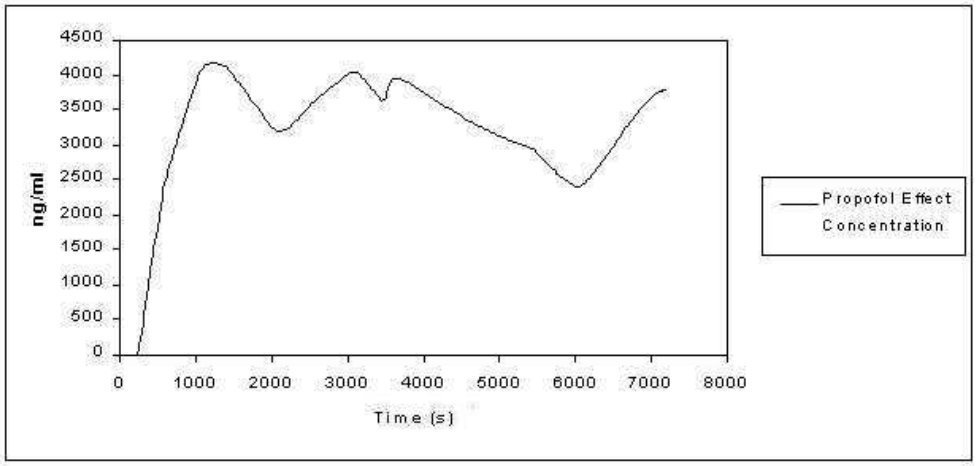

Figure 6-8: Propofol effect concentration for the infusion rate profile in Figure 6-7.

Figure 6-8 shows the effect concentration of propofol, reflecting the changes in infusion rate. The remifentanil effect concentration is the same as in Figure 6-3. Therefore, the perceived stimulus is the same as in Figure 6-5, since the same surgical stimulus profile is used.

The cardiovascular parameters SAP and HR are presented in Figure 6-9. Analysing the figure, one can see the first increase in SAP and HR in response to the decrease in the propofol effect concentration, and the subsequent decrease in SAP due to the increase in concentration. This is also noticeable after 6000 seconds, when the increase in the propofol

concentration leads to a decrease in the cardiovascular parameters. Therefore, the patient model reflects the propofol effect concentration trend, if one considers the constant remifentanil effect concentration. It is also worth noting that the different simulations use different baseline for SAP and HR, proving that the model is not dependent on the baseline values since it uses Δ values.

The DOA level, as classified by the FRC using the modelled AEP features, is shown in Figure 6-10.

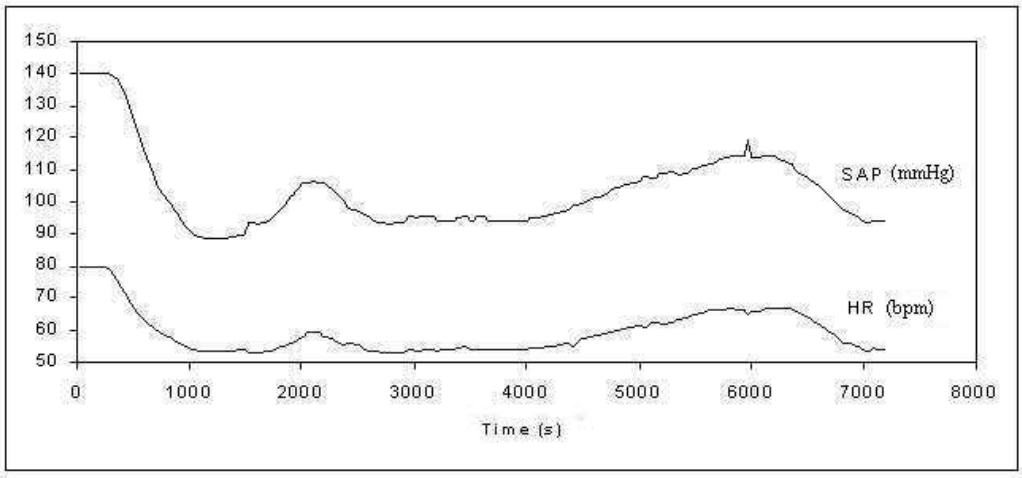

Figure 6-9: Systolic arterial pressure (SAP) and heart rate (HR) as determined by the patient model, using the infusion profiles in Figure 6-7.

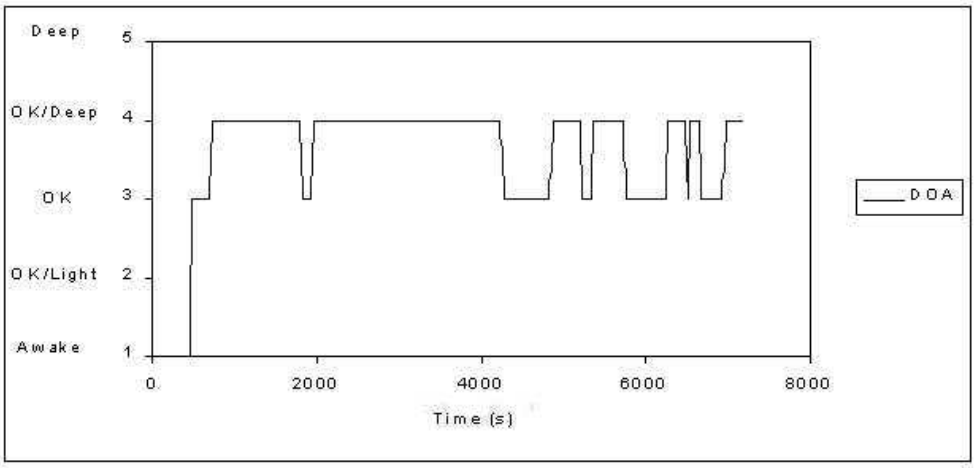

Figure 6-10: Depth of anaesthesia (DOA) as classified by the Fuzzy Relational Classifier (FRC) using the wavelet extracted AEP features (Infusion Profile 2).

6.2.3 Infusion Profile 3

Figure 6-11 shows the infusion rate profiles of propofol and remifentanil for the third simulation, which will be referred to as Infusion Profile 3. In contrast with the other simulations, the remifentanil profile is not constant here. The propofol infusion rate is the same as in the Infusion Profile 2 (Figure 6-7), with the respective effect concentration in Figure 6-8.

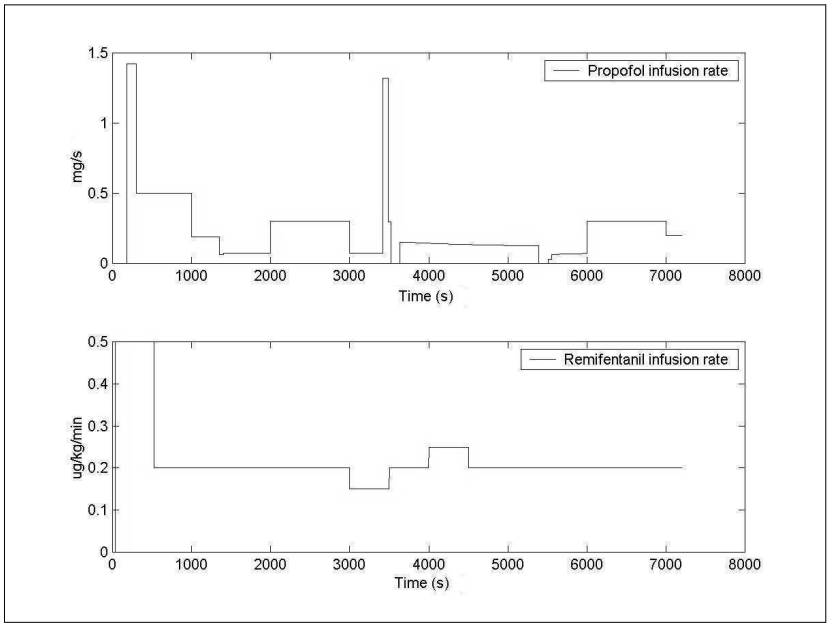

Figure 6-11: Propofol and remifentanil infusion rate profiles (Infusion Profile 3).

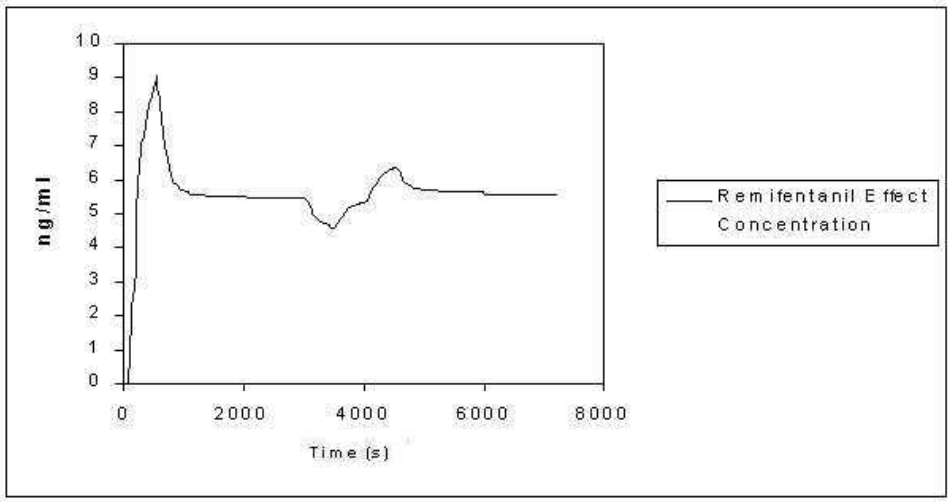

Figure 6-12: Remifentanil effect concentration for the infusion rate profile in Figure 6-11.

The remifentanil effect concentration for this infusion profile is presented in Figures 6-12. The changes in the remifentanil infusion rate produce variations in the effect concentration. The effect of such variations will be analysed by comparing the model results using Infusion Profile 3 with the results using Infusion Profile 2.

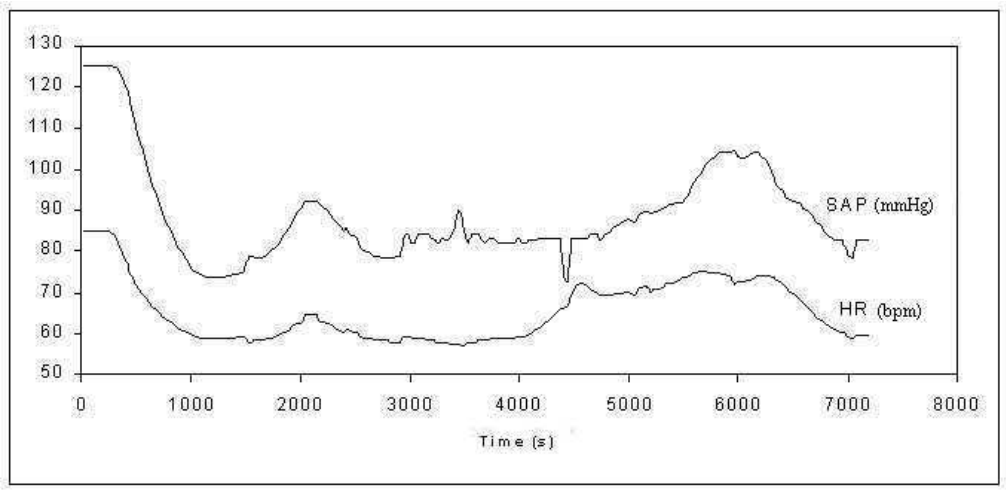

Figure 6-13: Systolic arterial pressure (SAP) and heart rate (HR) as determined by the patient model, using the infusion profiles in Figure 6-11.

Figure 6-13 shows the cardiovascular parameters SAP and HR as determined by the patient model using Infusion Profile 3. The increase in SAP and HR at approximately 2000 seconds is due to the decrease in the propofol effect concentration. There is a gradual change in the values of SAP representing the gradual decrease in propofol concentration (see Figure 6-8). The change in HR is more moderate, this is expected since HR is less sensitive to such changes. The remifentanil effect concentration shows a rapid trend compared with propofol, due to the rapid onset and offset of the action of the analgesic. These sharp variations in the remifentanil concentration result in abrupt changes in SAP. For example, the sharp decrease in SAP at approximately 4400 seconds is due to the increase in the remifentanil concentration, potentiating the effect of propofol at a medium concentration. This is also noticeable at approximately 3400 seconds when the remifentanil effect concentration reaches the lowest value, and there is an increase in SAP. As expected, the effect of propofol is predominant and reflected in the gradual changes of SAP and HR following the increases and decreases of the effect concentration (see the time between 5500 and 7000 seconds).

Figure 6-14 shows the perceived stimulus and the surgical stimulus, determined by the stimulus model according to the effect concentration of remifentanil for Infusion Profile 3. The perceived stimulus is similar to that obtained with the constant remifentanil profile (see

Figure 6-5), since the remifentanil effect concentration is still within the Medium range of the stimulus model (see Figure 5-57).

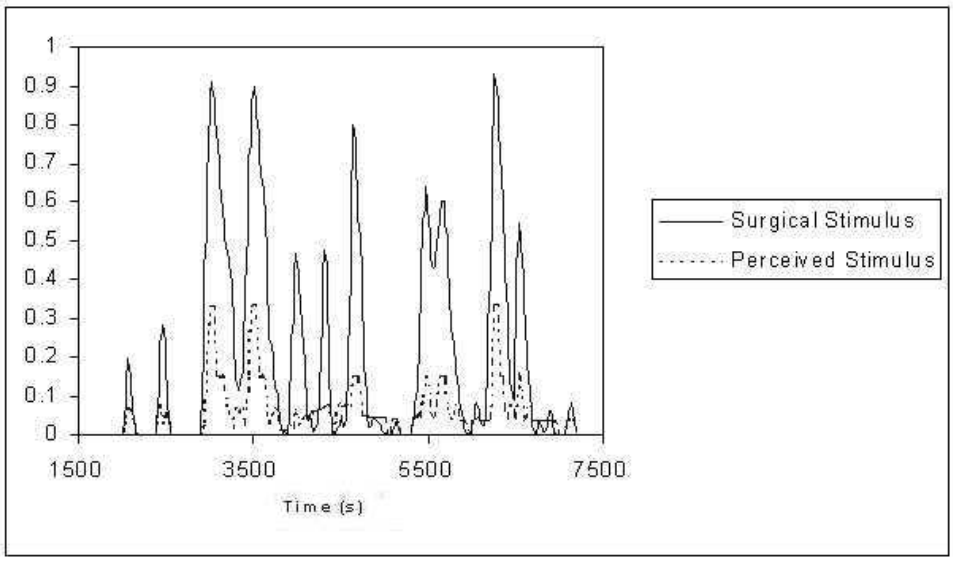

Figure 6-14: Surgical stimulus (solid line) and perceived stimulus (dashed line) for the remifentanil effect concentration in Figure 6-12, during the maintenance phase.

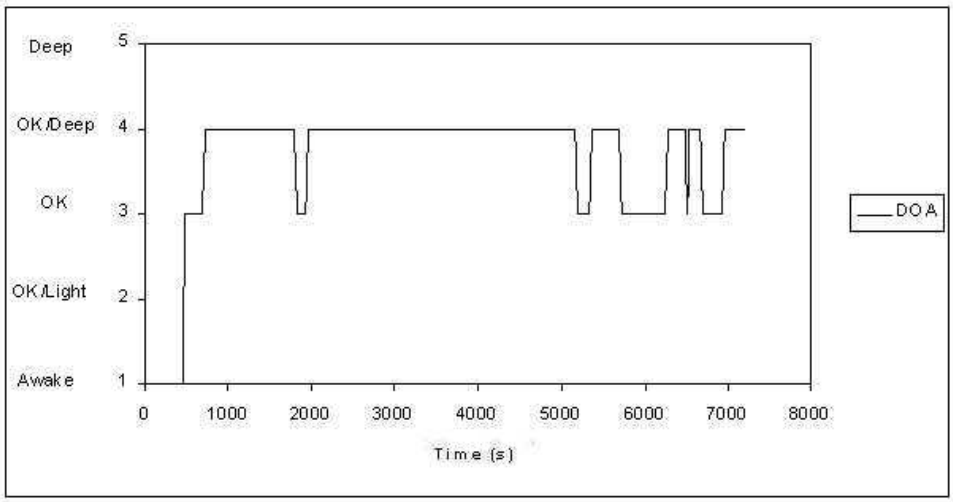

Figure 6-15: Depth of anaesthesia (DOA) as classified by the Fuzzy Relational Classifier (FRC) using the wavelet extracted AEP features (Infusion Profile 3).

The wavelet extracted AEP features as determined by the patient model, were used by the FRC to classify the DOA level during the maintenance phase. The result is presented in Figure 6-15. The DOA profile is the same as in the previous simulation (Figure 6-10) until approximately 4100 seconds due to the effect of propofol. However, the DOA level using Infusion Profile 3 returns to the OK level later than that of Infusion Profile 2. This is due to the higher remifentanil concentration that potentiates the effect of propofol. The level of DOA reaches the OK level at approximately 4900 seconds, when the remifentanil effect

concentration stabilizes.

6.3 Closed-Loop Structure

The final objective of an advisor system in anaesthesia is to determine the infusion rate of the anaesthetic and analgesic drugs, in order to achieve and maintain an adequate level of DOA. Figure 6-16 shows the implementation diagram of the advisor system in the operating theatre. The system (implemented on a PC) gathers information from the AEP amplifier and the anaesthesia monitor (in this case the Datex-Engstrom AS/3) which measures the cardiovascular parameters.

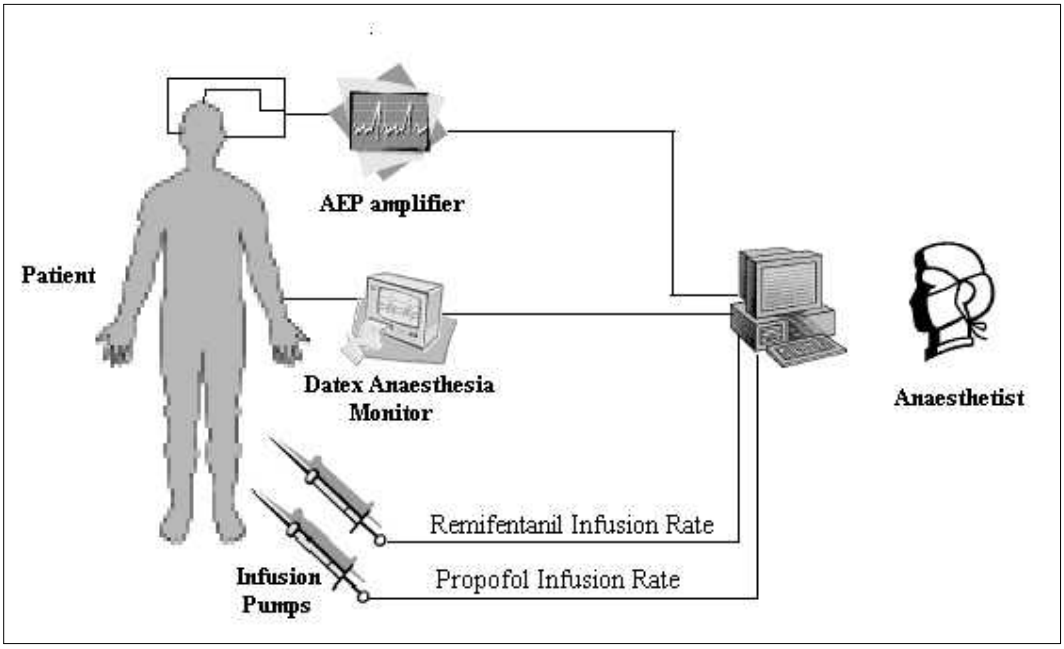

Figure 6-16: Implementation diagram of the advisor system in the operating theatre.

The AEP are processed by averaging and filtering, after which multiresolution wavelet analysis is used to extract a set of features. This set of wavelet extracted AEP features and the cardiovascular parameters ΔHR and ΔSAP are used by the fuzzy relational classifier (FRC) to determine the DOA. The DOA level in addition to the information about the surgical stimulus introduced to the system by the anaesthetist, are used to determine the adequate infusion rate of the two drugs (i.e. propofol and remifentanil). In other words, a multivariable controller would advise the anaesthetist about the required changes in the infusion rate of both drugs. This information would be transmitted to the two infusion

pumps (Graseby 3500), which administer the drugs to the patient.

An advisor system needs to be developed and tested in simulations before transfer to the operating theatre. Therefore, an adequate patient model is paramount for such real-time software development.

The closed-loop simulation system links the patient model, the FRC of DOA and the control algorithms. Figure 6-17 shows the block diagram comprising of the different components of the closed-loop system during the maintenance phase of anaesthesia. The patient model is divided into pharmacokinetic and pharmacodynamic models. The compartmental pharmacokinetic models, which use the mean population parameters, determine the plasma concentration of both drugs independently. The pharmacodynamic model comprises the effect compartments of the two drugs and a structure of fuzzy models. This fuzzy structure models the wavelets extracted AEP features and the cardiovascular parameters from the effect concentrations and the surgical stimulus, according to the drugs interaction and the effects of the different stimuli intensity. These modelled parameters are then used by the FRC to classify DOA. Finally, a control structure maintains an adequate DOA level by adjusting the infusion rates of propofol and remifentanil, which are the inputs to the patient model.

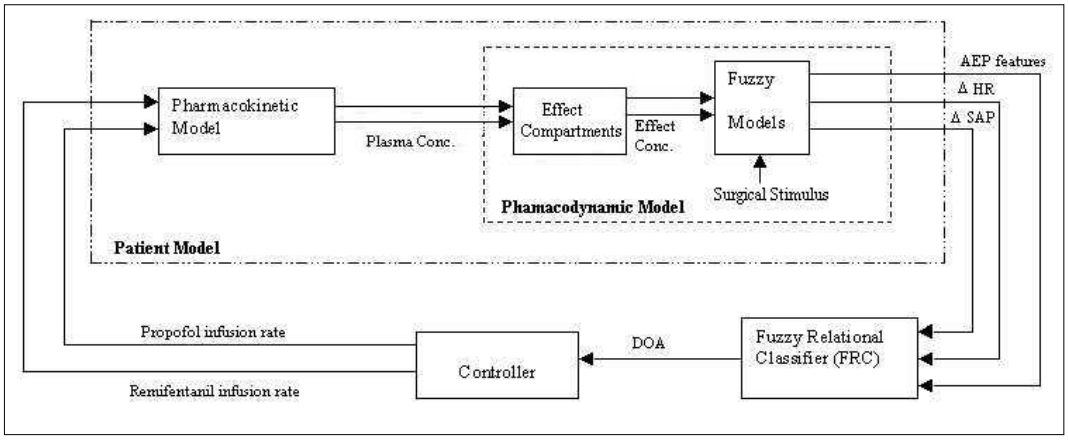

Figure 6-17: Block diagram of the closed-loop simulation system.

The following sections focuses on the development of the DOA controller. First, a SISO fuzzy PI controller is developed using only the infusion rate of propofol, and by assuming that the analgesic drug is manually controlled by the anaesthetist. Second, a multivariable control structure is developed, which establishes the infusion rate of both drugs simultaneously. It is worth noting that the control action concerns only the maintenance

phase due to the differences between induction and maintenance as explained in Chapter 5.

6.4 SISO Fuzzy PI Controller

Feedback control has proved to be an effective and convenient clinical tool for optimizing the routine delivery of anaesthetics (Westenskow, 1997). Control systems should reduce the induction time, deliver a minimum amount of drug, and avoid costly delays from failing to keep the patient in a desired state.

A fuzzy logic controller may be regarded as a means of emulating a skilled human operator. It provides a means of converting a linguistic control strategy based on expert knowledge into and automatic control strategy (Lee, 1990a, b). Appendix B presents the basic concepts of fuzzy logic and fuzzy logic based control.

A fuzzy proportional-integral (PI) controller is designed to control the change in the infusion rate of the anaesthetic drug propofol, in order to achieve and maintain a steady level of DOA and to reduce the amount of drug infused. Figure 6-18 shows the closed-loop system diagram with the implementation of the fuzzy PI controller.

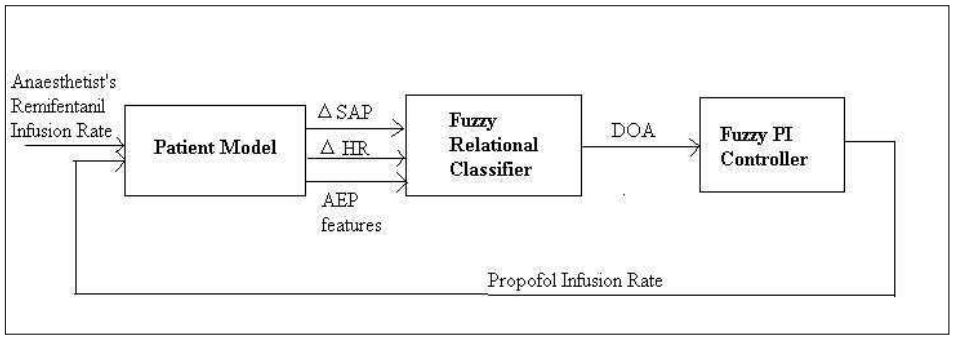

Figure 6-18: Implementation diagram of the fuzzy PI controller of DOA.

The controller is activated only at the start of the maintenance phase. The propofol infusion profile, during the induction phase, was set by the anaesthetist. In other words, the loop remains open during induction but is closed during maintenance. The recovery phase is not simulated here for during this phase no drugs are administered.

The analgesic drug remifentanil is administered at a fixed profile as set by the anaesthetist according to a typical surgical procedure. Figure 6-19 shows the remifentanil infusion rate

used in closed-loop simulations. The corresponding remifentanil effect concentration is presented in Figure 6-20. The steady effect concentration of remifentanil during the maintenance phase provides a constant level of analgesia.

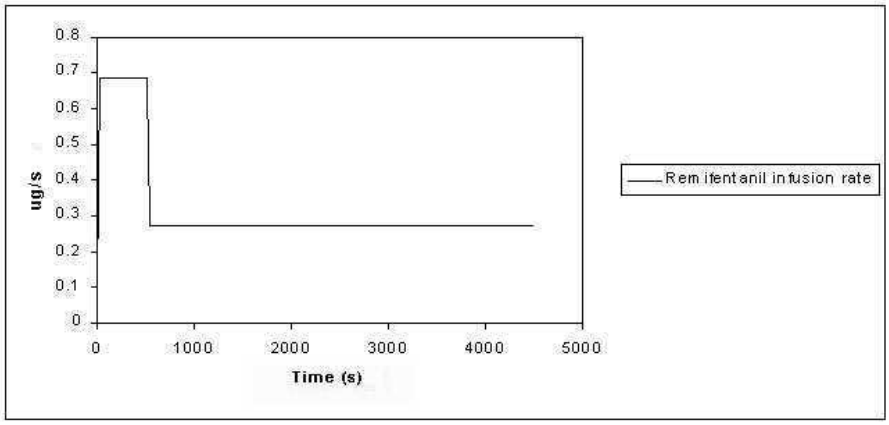

Figure 6-19: Remifentanil infusion rate set for a typical surgical procedure.

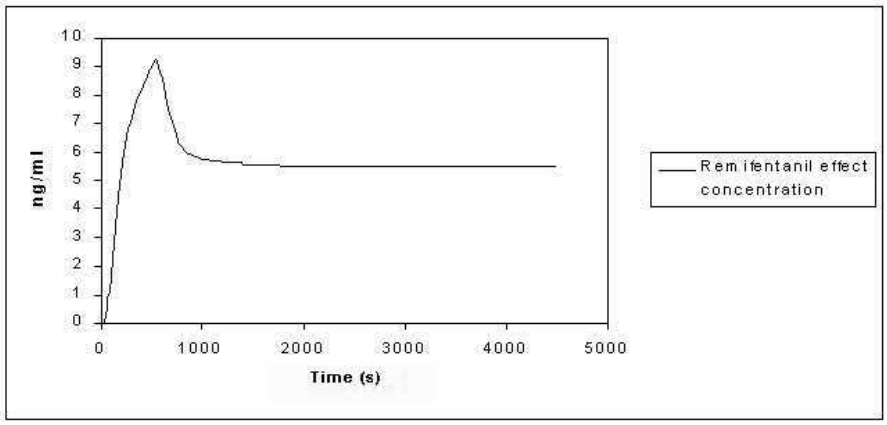

Figure 6-20: Remifentanil effect concentration for the infusion profile in Figure 6-19.

In general, researchers are only concerned with the control of the anaesthetic drug, developing different types of complex controllers (Asteroth *et al.*, 1997; Backory, 1999; Gentilini *et al.*, 2001a; Linkens and Rehman, 1992). However, simple fuzzy logic controllers have been proven to give also good control (Allen and Smith, 2001; Huang *et al.*, 1999; Mortier *et al.*, 1998; Webb *et al.*, 1996).

In this research, a fuzzy PI controller determines the infusion rate of propofol during the maintenance phase based on a patient model which considers the drug's interaction with remifentanil. The structure of the fuzzy PI controller is presented in the next section.

6.4.1 Fuzzy PI Controller Structure

The fuzzy PI controller uses the error (target DOA minus measured DOA) and the change of error as inputs. The output of the controller is the change in propofol infusion rate. Figure 6-21 shows the structure of a fuzzy PI controller: w is the target DOA level (i.e. the OK level =3); e is the error; Δu is the change in infusion rate; u is the infusion rate and y is the DOA level (output of the FRC). G_1 and G_2 are the scaling factors for the error and the change of error, respectively. As mentioned previously, five DOA levels are considered and represented as: 5-Deep; 4-OK/Deep; 3-OK; 2-OK/Light and 1-Awake.

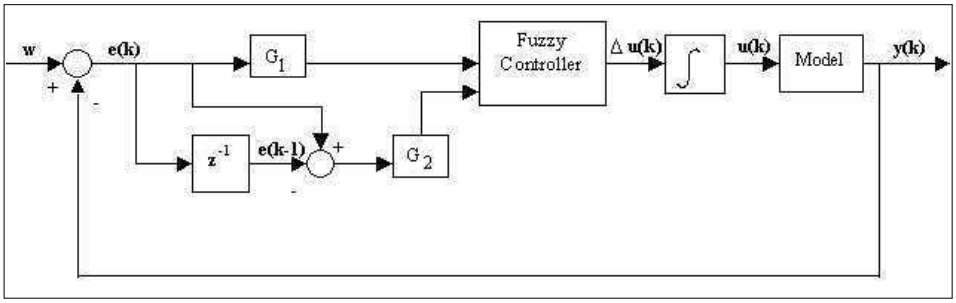

Figure 6-21: Structure of a fuzzy PI controller.

The fuzzy PI controller uses a set of 25 IF-THEN rules to control the change in infusion rate, with five output membership functions. The controller's rule-base is presented in Table 6-1.

Table 6-1: Rule-base of the fuzzy PI controller for DOA. The inputs are the error and the change of error, and the output is the change in propofol infusion rate.

	Change of error				
Error	**NB**	**NS**	**ZE**	**PS**	**PB**
NB	NB	NB	NB	NS	ZE
NS	NB	NS	NS	ZE	PS
ZE	NB	NS	ZE	PS	PB
PS	NS	ZE	PS	PS	PB
PB	ZE	PS	PB	PB	PB

The membership functions are labelled as: Negative Big (NB), Negative Small (NS), Zero (ZE), Positive Small (PS) and Positive Big (PB). Figures 6-22 and 6-23 show the

membership functions for the controller inputs, error and change of error, respectively. The input variables are normalized between [-1, 1].

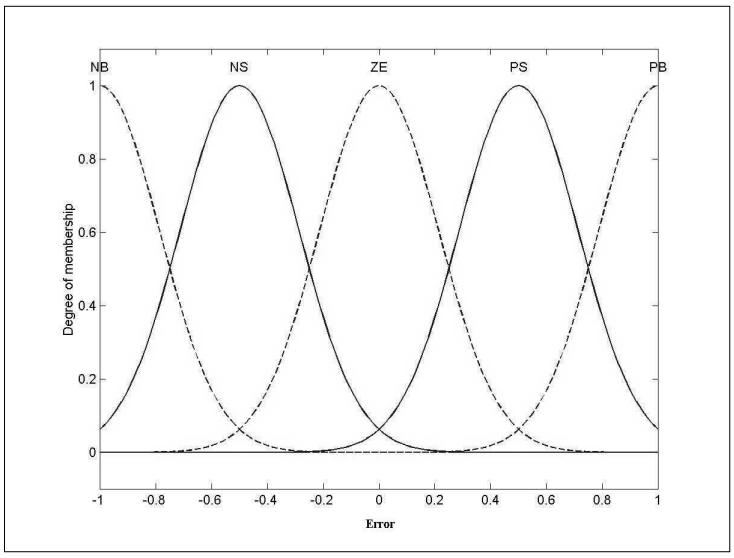

Figure 6-22: Input membership functions describing the error, in the fuzzy PI controller.

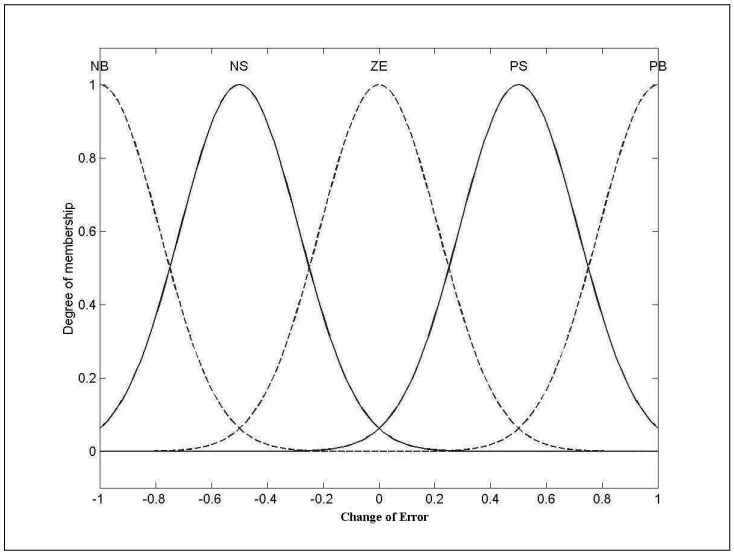

Figure 6-23: Input membership functions describing the change of error, in the fuzzy PI controller.

Figure 6-24 shows the output membership functions for the change in propofol infusion rate, which is normalized between [-1, 1]. The maximum level for the change in the infusion rate was set to 4000 mg/h considering the maximum conditions pre-set by the anaesthetist. The output control surface of this fuzzy PI controller is shown in Figure 6-25.

The next step in the controller's design is to obtain adequate values for the scaling factors G_1 and G_2. The performance of the fuzzy PI controller is affected by the choice of the input

scaling factors, hence, an optimization process is required.

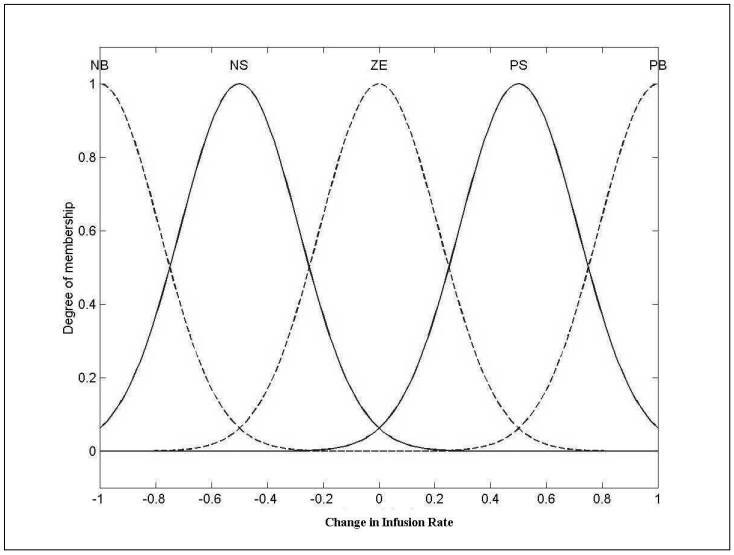

Figure 6-24: Output membership functions describing the change of propofol infusion rate, in the fuzzy PI controller.

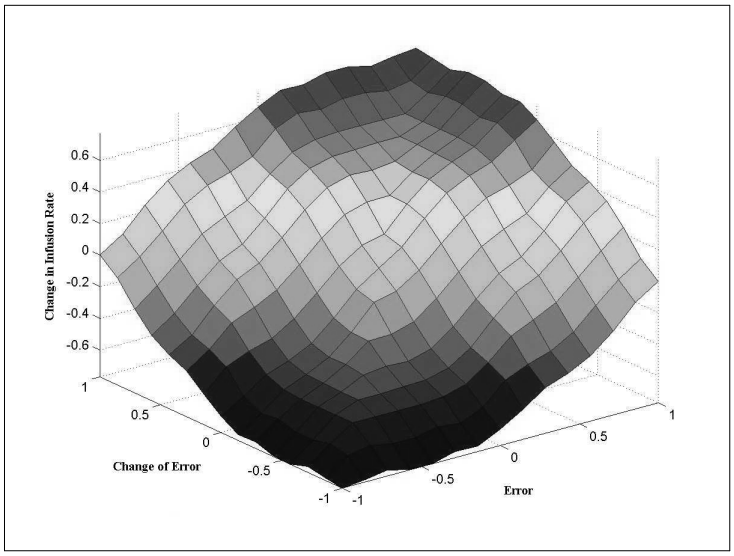

Figure 6-25: Output surface of the fuzzy PI controller.

6.4.2 Performance Index

The scaling factors G_1 and G_2 were optimized using a performance index and a genetic algorithm (GA).

A performance index is a quantitative measure of the performance of a system, and is chosen so that emphasis is given to the important system specifications. The integral of

time versus the absolute error index (ITAE) is shown in Equation 6-1. This index matches the intuitive expectations, by penalizing the error according to time.

$$ITAE = \sum_{k=0}^{N-1} k|e(k)| \qquad 6\text{-}1$$

The ITAE index was modified to include information about the control action, this new index is referred to as ITAE_M. The following formula was used:

$$ITAE_M = \lambda_1 \sum_{k=0}^{N-1} k|e(k)| + \lambda_2 \sum_{k=0}^{N-1} u(k) \qquad 6\text{-}2$$

where $e(k)$ is the error, $u(k)$ is the propofol infusion rate and N is the number of simulation samples. The weighting parameters λ_1 and λ_2 were chosen to place more emphasis on the error or on the infusion rate, so that an ideal balance between both can be reached (i.e. stable DOA and a smooth infusion rate). The ITAE_M was chosen as the performance index to evaluate the fuzzy PI controller's performance.

The objective is to obtain a set of values for G_1 and G_2 that minimize the performance index. Genetic algorithms (GAs) are search algorithms based on the mechanics of natural selection and natural genetics. They do not require a precise mathematical model of the system (which does not exist in this case) but instead use the objective function values associated with individual strings (Goldberg, 1989; Linkens and Nyongesa, 1995).

The GAs work with a coding of the parameter set (not the parameters themselves), search from a population of points, use payoff (i.e. objective function) information; derivations or other auxiliary knowledge are not required, and use probabilistic transition rules. These factors differentiate GAs from the other search methods. A simple GA has three operators: reproduction, crossover, and mutation. The general structure of a GA is presented in Figure 6-26.

A simple GA was used to minimize the ITAE_M index (fitness). The GA was implemented using MATLAB for a population size of 40 strings (representing a pair of values G_1 and G_2) each of length 20 (i.e. 20 bits), with a probability of crossover of 0.95 and a probability of mutation of 0.06. The implemented GA was allowed to run for 50 generations. Figure 6-27 shows the fitness curve relating to an experiment.

The optimization was run with the parameters $\lambda_1 = 0.4$ and $\lambda_2 = 0.6$, which were found to be representative of the specifications for the control system, giving a bigger weight to the infusion rate profile. The following intervals were used: $G_1 \in [0, 10]$ and $G_2 \in [-10, 10]$.

The GA based optimization led to the values of $G_1 = 0.3754$ and $G_2 = 7.7713$ with a minimum $ITAE_M$ index of 16.82.

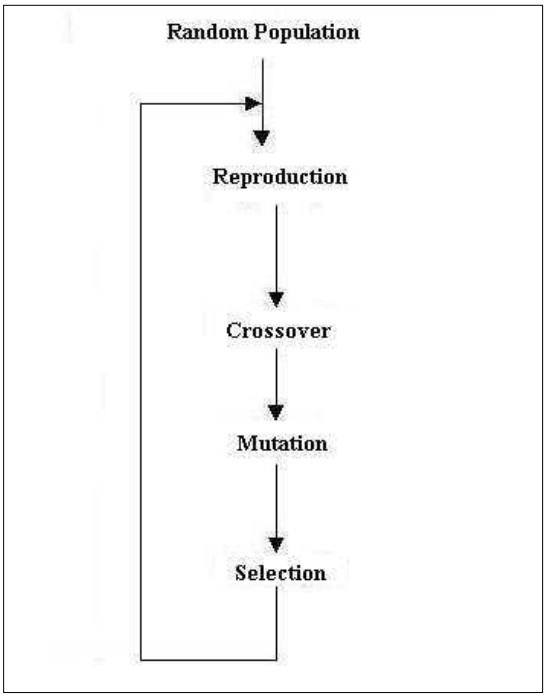

Figure 6-26: General structure of a genetic

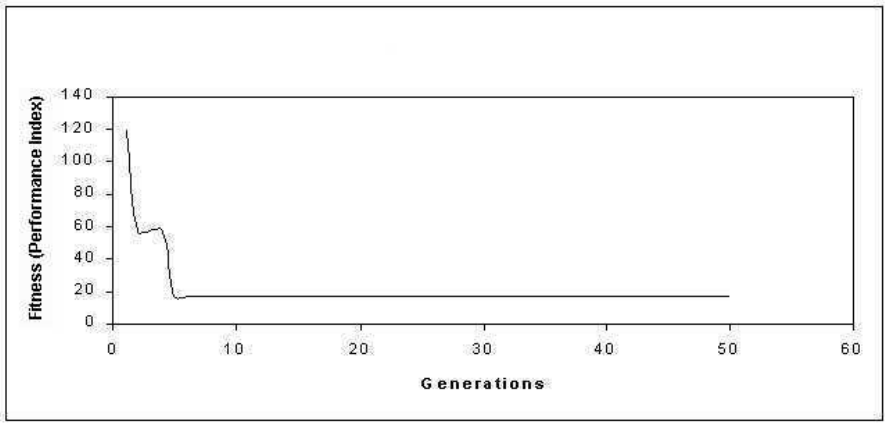

Figure 6-27: Fitness curve of the 50 generations of the GA. The performance index was calculated with λ_1=0.4 and λ_2=0.6.

6.4.3 Results

The results of the closed-loop simulation using the fuzzy PI controller with the GA optimized parameters ($G_1 = 0.3754$ and $G_2 = 7.7713$), are shown in Figures 6-28 to 6-31.

The propofol infusion rate profile used during the induction phase is the same as the one used with patient Pat1 (see Figure 5-1). The controller is activated at 1500 seconds, i.e. at the beginning of the maintenance phase.

Figure 6-28 shows the level of DOA for the closed-loop simulation. The OK DOA level is achieved at 1740 seconds and maintained constant thereafter.

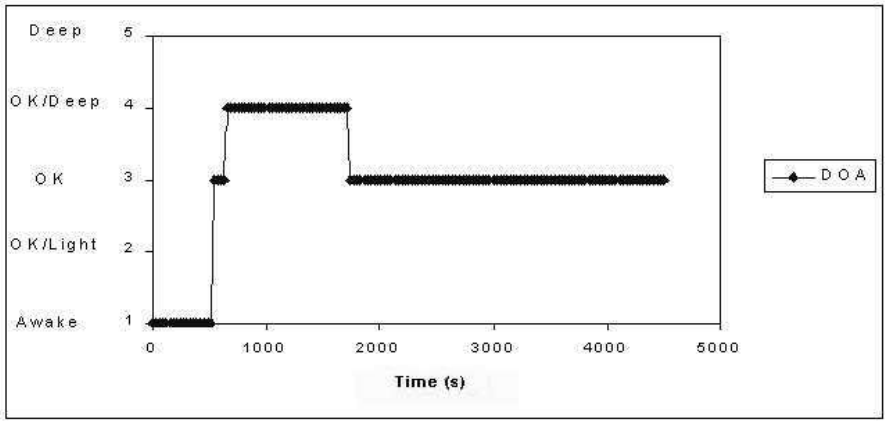

Figure 6-28: DOA level using the fuzzy PI controller with G_1=0.3754 and G_2=7.7713.

Figure 6-29 shows the propofol infusion rate for the simulation. The fuzzy PI controller kept a constant infusion rate of 0.1923 mg/s after 1740 seconds. The total amount of drug infused during the maintenance phase was of 536.5 mg. Figure 6-30 shows the propofol effect concentration during the simulation. The constant propofol infusion rate led to what can be described as a steady effect concentration.

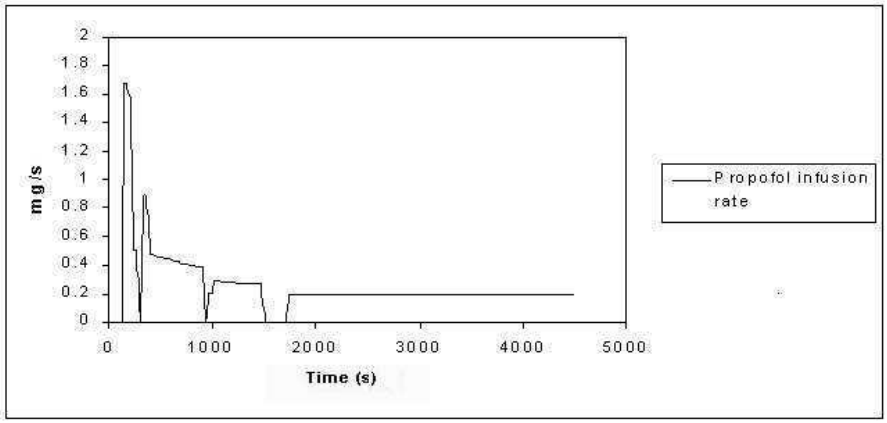

Figure 6-29: Propofol infusion rate for the fuzzy PI controller with G_1= 0.3754 and G_2=7.7713.

The cardiovascular parameters for this simulation are shown in Figure 6-31. The haemodynamic stability during the maintenance phase is the result of the steady effect

concentrations of the two drugs. The small peaks in the SAP and HR data are due to the surgical stimulus model.

This combination of propofol and remifentanil effect concentrations results in a stable DOA level, corresponding to a steady cardiovascular and CNS depression.

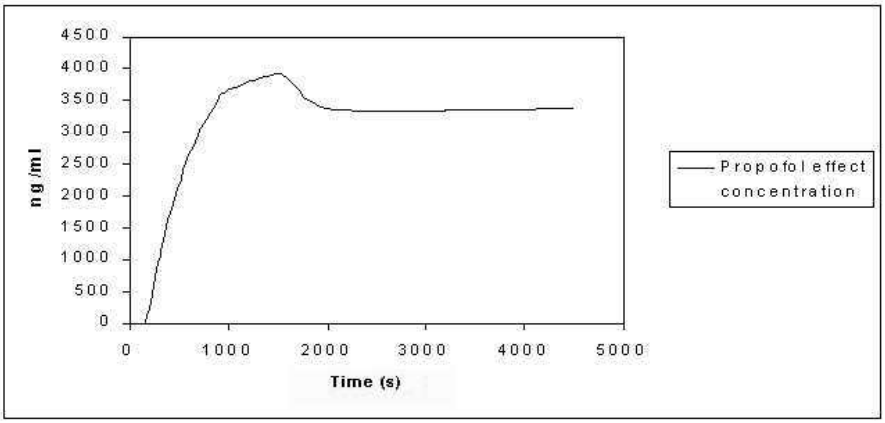

Figure 6-30: Propofol effect concentration for the infusion rate profile in Figure 6-29.

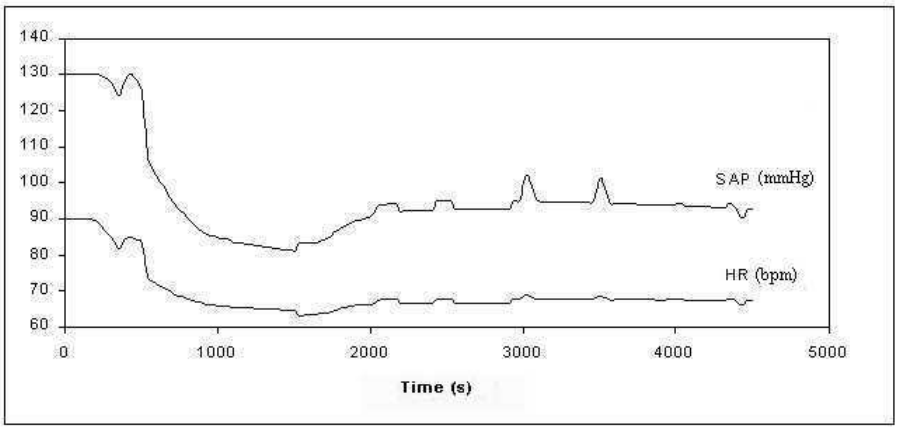

Figure 6-31: Systolic arterial pressure (SAP) and heart rate (HR) from the patient model using the propofol infusion profile in Figure 6-29.

6.4.4 Comparison with a Conventional Controller

The fuzzy PI controller performance will be compared with the performance of a conventional PI controller. The $ITAE_M$ index will be used to analyse the performance of both controllers. Some researchers use conventional PID controllers, however, in medical applications the derivative term can be a problem because of noise. The derivative term reacts to the noise in the measurement of the controlled variable, changing the controller output as a function of noise (Westenskow, 1997).

The next section presents the structure of the conventional PI controller and its results during a closed-loop simulation.

6.4.4.1 Conventional PI Controller

The output of a conventional PI controller can be written as follows:

$$u(t) = K_p e(t) + K_i \int e(t)dt \qquad 6\text{-}3$$

$$\frac{\mathrm{du(t)}}{\mathrm{dt}} = K_p \frac{\mathrm{de(t)}}{\mathrm{dt}} + K_i e(t) \qquad 6\text{-}4$$

where K_p and K_i are the proportional and integral terms relating to the controller, and e is the error. For a digital controller one can write:

$$\Delta u(k) = u(k) - u(k-1) = K_p \Delta e(k) + K_i e(k) \qquad 6\text{-}5$$

$$u(k) = u(k-1) + K_p \Delta e(k) + K_i e(k) \qquad 6\text{-}6$$

The conventional PI controller has the change in control action as the output, i.e. the change in the propofol infusion rate.

The GA was also used to optimized the parameters K_p and K_i for the conventional PI controller, using the ITAE_M index with $\lambda_1 = 0.4$ and $\lambda_2 = 0.6$ (Equation 6-2). The same specifications as for the fuzzy PI controller were used in the GA parameter optimization for the conventional PI controller.

The GA based optimization led to the values of $K_p = 0.7918$ and $K_i = 1.3763$ with a minimum ITAE_M index of 17.07.

The closed-loop simulation results for the conventional PI controller are presented in Figures 6-32 to 6-35. Figure 6-32 shows the DOA level for the closed-loop simulation. The OK DOA level is achieved at the same time as with the fuzzy PI controller (i.e. 1740 seconds). Figure 6-33 presents the propofol infusion rate, which is kept at a constant level of 0.1979 mg/s after 1740 seconds. The total amount of drug infused during the maintenance phase was of 552.1 mg.

Figure 6-34 shows the corresponding propofol effect concentration. The graph shows a continuous increase in the effect concentration after approximately 2000 seconds.

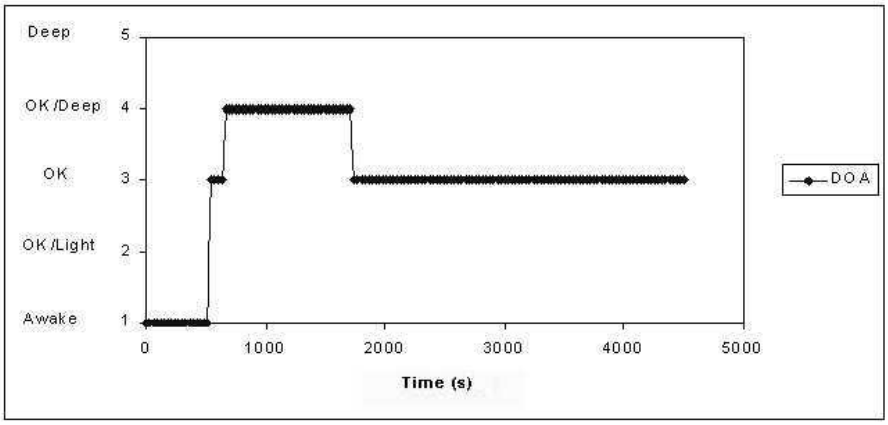

Figure 6-32: DOA level using the conventional PI controller with K_p= 0.7918 and K_i=1.3763.

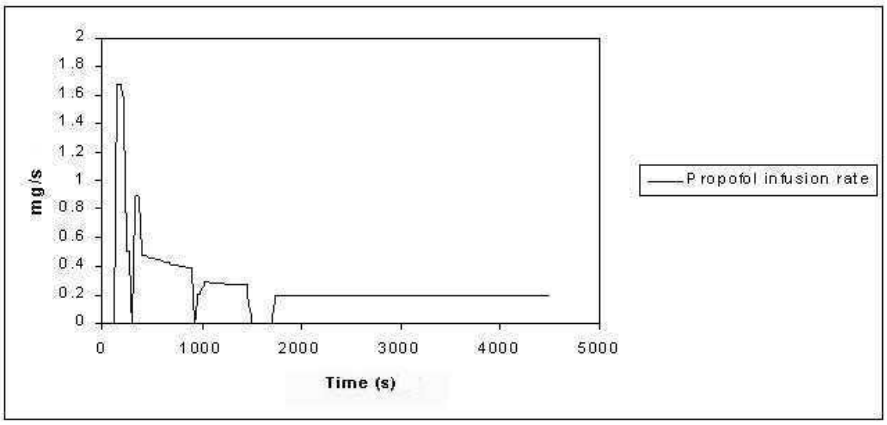

Figure 6-33: Propofol infusion rate for the conventional PI controller with K_p=0.7918 and K_i=1.3763.

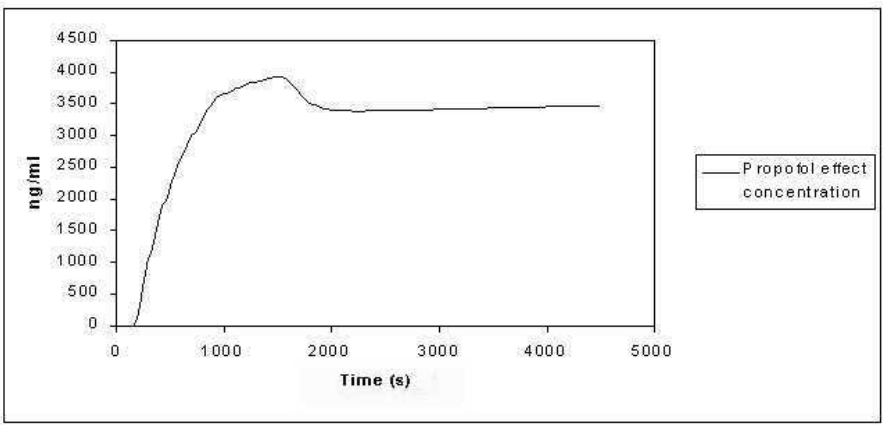

Figure 6-34: Propofol effect concentration for the infusion rate profile in Figure 6-33.

The cardiovascular parameters for this simulation are presented in Figure 6-35. There is a slight decrease in SAP corresponding to the increase in the propofol effect concentration.

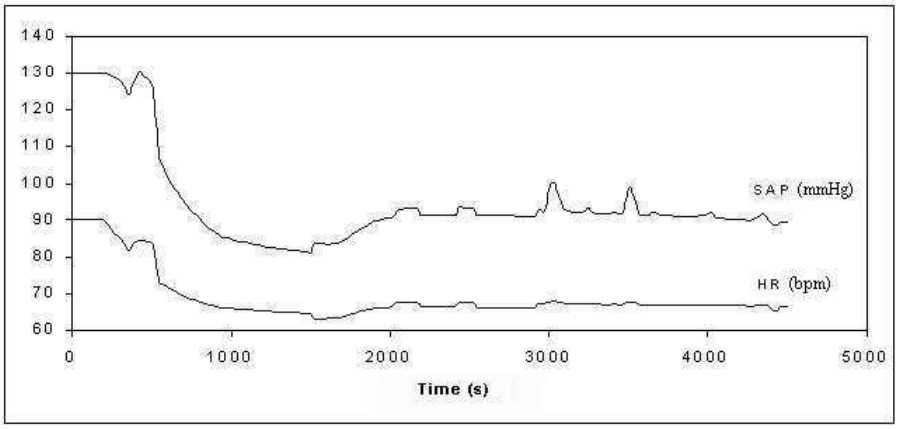

Figure 6-35: Systolic arterial pressure (SAP) and heart rate (HR) from the patient model using the propofol infusion profile in Figure 6-33.

The DOA level is the same using the conventional or the fuzzy PI controller. However, the performance index is smaller for the fuzzy PI controller due to the smaller amount of drug infused, 536 mg versus 552 mg of the conventional PI controller. In addition, the higher the infusion rate used by the conventional PI controller the greater the depression in the cardiovascular parameters will be. The mean value of SAP during the maintenance phase was of 92.7 mmHg using the fuzzy PI controller versus a mean value of 91 mmHg with the conventional PI controller. Therefore, the fuzzy PI controller can be considered to be a more effective option for the patient due to the smaller amount of drug infused.

The fuzzy PI controller has the ability to respond to unexpected disturbances, which can happen in the operating theatre and that are reflected in the DOA level. In the next section, the results of both controllers to set point changes (i.e. DOA target level) are compared.

6.4.4.2 General Results

The performance of the fuzzy PI controller is compared with the performance of the conventional PI controller, considering the response to a change in the DOA target level.

For test purposes, the DOA target level was changed to OK/Deep (i.e. 4) at 3000 seconds and changed back to the OK level (i.e. 3) at 3210 seconds. The responses of both controllers to this set point change are shown in Figures 6-36 and 6-37.

The DOA level (Figure 6-36) using the fuzzy PI controller achieves the OK/Deep level at 3120 seconds (i.e. 2 minutes after the set point change to OK/Deep) and returns to the OK level at 3720 seconds (i.e. 8.5 minutes after the set point change to OK), while the conventional PI controller reaches the OK/Deep level at 3090 seconds and returns to the

OK level at 4230 seconds. The conventional PI controller is faster in responding to the first set point change to OK/Deep, 1.5 minutes versus 2 minutes in the case of the fuzzy PI controller. Nevertheless, this is a small time difference of only 30 seconds. However, the conventional PI controller takes more 8.5 minutes to return to the OK level than the fuzzy PI controller. In total, the conventional PI controller needs 17 minutes to reach the OK level after the set point change at 3210 seconds; the DOA level is a reflection of the propofol infusion rate of both controllers (see Figure 6-37).

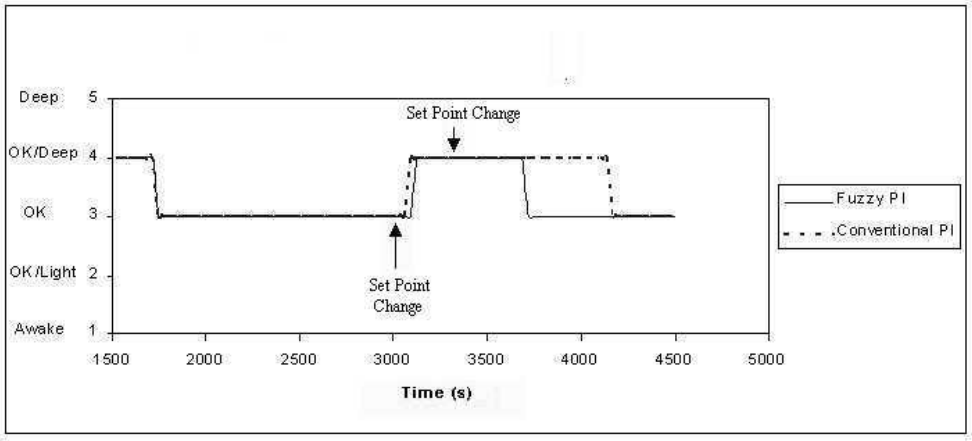

Figure 6-36: DOA level using the fuzzy PI controller (solid line) and the DOA level using the conventional PI controller (dashed line) during the maintenance phase. Set point change to OK/Deep at 3000 seconds and back to OK at 3210 seconds.

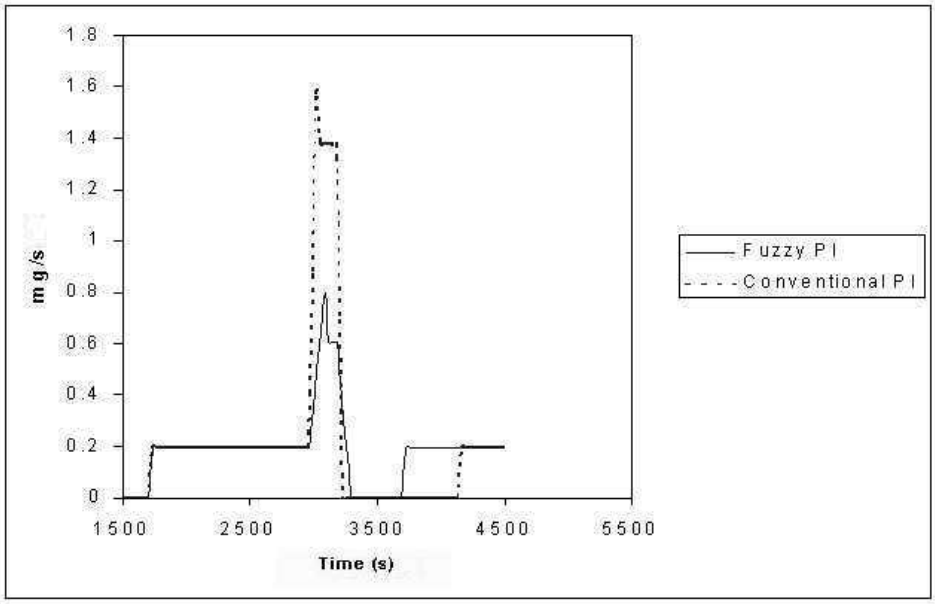

Figure 6-37: Propofol infusion rate of the fuzzy PI controller (solid line) and the propofol infusion rate of the conventional PI controller (dashed line) during the maintenance phase. Set point change to OK/Deep at 3000 seconds and back to OK at 3210 seconds.

The conventional PI controller responds to the set point change from OK to OK/Deep with a significantly higher propofol infusion rate than the fuzzy PI controller, which leads to a higher propofol effect concentration (see Figure 6-38). The fuzzy PI controller is able to maintain the OK/Deep level at a smaller effect concentration leading to a faster return to the OK level when required. The total amount of propofol infused during the maintenance phase was of 548.5 mg and 621.5 mg with the fuzzy and conventional PI controller, respectively.

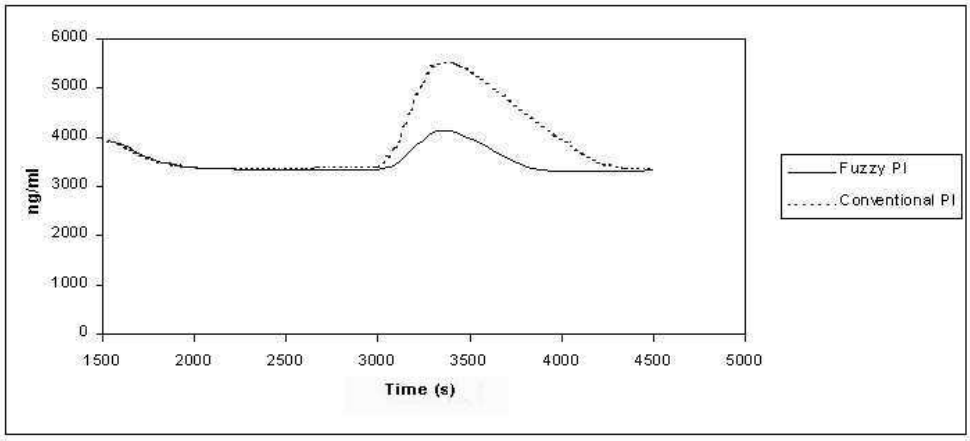

Figure 6-38: Propofol effect concentration using the fuzzy PI controller (solid line) and the propofol effect concentration using the conventional PI controller (dashed line) during the maintenance phase. Set point change to OK/Deep at 3000 seconds and back to OK at 3210 seconds.

The DOA level obtained using the conventional PI controller has a significant larger duration in the OK/Deep level, as a results of the high propofol infusion rate and corresponding effect concentration, this is considered to be unsafe. Overall, the fuzzy PI controller performs better than the conventional PI controller.

6.5 Multivariable Fuzzy Control

In general, propofol is used for maintenance of anaesthesia in combination with an opioid, hence, the anaesthetist is confronted with the dilemma of whether to vary propofol or the opioid. Zhang *et al.* (1998) reported on a closed-loop system for total intravenous anaesthesia by simultaneously administering propofol and fentanyl. They studied the interaction between propofol and fentanyl for loss of response to surgical stimuli using an unweighted least squares nonlinear regression analysis with human data. A look-up table of optimal and awakening combinations of concentrations was built, and used to determine

the fentanyl set point according to the propofol set point. To our knowledge, this is one of the only studies in simultaneous control of anaesthetic and analgesic drugs.

Multivariable controllers are not easy to design. There are several studies on the design of multivariable controllers, however, very few target biomedical systems. Yeh (1999) designed a multivariable fuzzy logic controller using a systematic method based on the negative gradient of a system performance index. This approach was applied to a two-inverted pendulum system.

King *et al.* (1994) described an integrated development system which permits the controller designer to test hypothesis, examine the effect of changes in the controller parameters and perform a complete off-line simulation of a proposed multivariable fuzzy controller. This system was applied to industrial processes and tested off-line with mathematical models. Another study on multivariable fuzzy control systems is the one by Jeon and Lee (1995). They developed a coordinator for the controller, which decides the dimension of the relational matrix using indices of applicability. A numerical example is presented showing that the coordinator could prevent a large amount of inference error.

Guan *et al.* (2001) designed a multivariable fuzzy controller for the laminal cooling process of hot rolled glab. This is a hybrid/statistical multivariable control system tested in simulation and practical experiments. The controller led to a robust performance.

Linkens and Nyongesa (1996) developed a hierarchical multivariable fuzzy controller for learning with GAs. This controller was applied to a simulation case study in anaesthesia, using mathematical models describing the action of atracurium and isoflurane (i.e. a muscle relaxant and an inhalational anaesthetic). This structure decomposes a complex multivariable fuzzy controller into several simple fuzzy controllers.

Fuzzy controllers are also used as gain scheduling approximators for multivariable controllers (Blanchett *et al.*, 2000; Chang and Fu, 1997; Chen and Chen, 1991; Palm and Rehfuess, 1997). Fuzzy rules and reasoning can be utilized on-line to determine the controller parameters based on the error signal and its first difference (Zhao *et al.*, 1993).

A review of conventional and fuzzy gain scheduling techniques is presented by Tan *et al.* (1997). They report on the improvement of the new neuro-fuzzy gain scheduling over other gain scheduling methods. Viljamaa (2000) did his PhD thesis on fuzzy gain scheduling and tuning of multivariable fuzzy control, with an overview of the methods of fuzzy computing in control systems. The examples presented by Viljamaa (2000) have well defined

mathematical models and information about the models is used in the tuning process.

Many of the researches mentioned above rely on mathematical models. The complexity of biomedical systems renders the task of control design more difficult. The highly nonlinear system behaviour and partly unknown dynamics are an area where fuzzy modelling and control methods can play an important role. The available qualitative operator and design knowledge can be implemented using fuzzy logic (Verbruggen and Bruijn, 1997).

The anaesthetist's knowledge and experience can be incorporated into the fuzzy control system as a set of linguistic rules. In addition, the interaction between remifentanil and propofol introduces information that could be used to determine the adequate combination of the two drugs.

A multivariable fuzzy controller was developed with the anaesthetist coordination. A simplified linguistic scheme of the controller can be described as follows:

- **If** DOA is OK **then** *no change*;
- **If** DOA is light and **if**:
  - stimulus **then** *increase remifentanil*;
  - no stimulus **then** *increase propofol*;
- **If** DOA is deep and **if**:
  - no stimulus and remifentanil high **then** *decrease remifentanil*;
  - no stimulus and remifentanil normal and propofol high **then** *decrease propofol*;
  - no stimulus and remifentanil normal and propofol normal **then** *decrease remifentanil*;
  - stimulus and propofol high **then** *decrease propofol* and *increase remifentanil*;
  - stimulus and propofol normal **then** *decrease remifentanil*.

It is important to note that a minimum effect concentration of propofol and remifentanil is required at all times, in order to ensure unconsciousness and prevent arousal.

The structure of the multivariable fuzzy controller for DOA, with simultaneous administration of propofol and remifentanil is presented in more details in the next sections.

6.5.1 Multivariable Fuzzy Controller Structure

The multivariable fuzzy controller for DOA comprises three different blocks, corresponding to the three possible values of DOA, i.e. the DOA level is the target level (i.e. OK), or the DOA is lighter than the desired (i.e. OK/Light or Awake level), or the

DOA is deeper than the desired (i.e. OK/Deep or Deep level). The controller will act differently according to these three stages.

Considering the three different possibilities for the level of DOA, the structure of the multivariable fuzzy controller is as follows:

- **If DOA is at the target level:**

  - $\Delta u_{propofol}$ is determined by the SISO fuzzy PI controller;

  - $\Delta u_{remifentanil} = 0$.

- **If DOA is light:**

  - **no stimulus present:** $\Delta u_{propofol}$ is determined by the SISO fuzzy PI controller, and $\Delta u_{remifentanil} = 0$;

  - **stimulus present:** $\Delta u_{propofol} = 0$, and $\Delta u_{remifentanil}$ is increased using the remifentanil rule-base 1.

- **If DOA is deep:**

  - **no stimulus present** and $Ce_{remifentanil}$ **is high:** $\Delta u_{propofol} = 0$, and $\Delta u_{remifentanil} = -0.025$ μg/kg/min;

  - **no stimulus present** and $Ce_{remifentanil}$ **is normal** and $Ce_{propofol}$ **is high:** $\Delta u_{propofol}$ is determined by the SISO fuzzy PI controller, and $\Delta u_{remifentanil} = 0$;

  - **no stimulus present** and $Ce_{remifentanil}$ **is normal** and $Ce_{propofol}$ **is normal:** $\Delta u_{propofol} = 0$, and $\Delta u_{remifentanil} = -0.001$ μg/kg/min;

  - **stimulus present** and $Ce_{remifentanil}$ **is high** and $Ce_{propofol}$ **is normal:** $\Delta u_{propofol} = 0$, and $\Delta u_{remifentanil} = -0.025$ μg/kg/min;

  - **stimulus present** and $Ce_{remifentanil}$ **is normal** and $Ce_{propofol}$ **is normal:** $\Delta u_{propofol} = 0$, and $\Delta u_{remifentanil} = -0.001$ μg/kg/min;

  - **stimulus present** and $Ce_{propofol}$ **is high:** $\Delta u_{propofol}$ is determined by the SISO fuzzy PI controller, and $\Delta u_{remifentanil}$ is increased using the remifentanil rule-base 2.

where $\Delta u_{propofol}$ is the change in propofol infusion rate, $\Delta u_{remifentanil}$ is the change in remifentanil infusion rate, $Ce_{remifentanil}$ is the remifentanil effect concentration, and $Ce_{propofol}$ is the propofol effect concentration. The SISO fuzzy PI controller is the controller developed in Section 6.4. The remifentanil rule-base 1 and rule-base 2 which determine the change in the remifentanil infusion rate according to the perceived stimulus intensity and the change in DOA error, are presented in the following sections.

The presence of stimulus is established according to the stimulus intensity. A value below 0.25 is considered as no stimulus, because a stimulus intensity below this value has very little, if any, influence in the cardiovascular parameters. The value of 0.25 is the peak of the VeryLow membership function in the perceived stimulus model (see Figure 5-59).

The ranges of the remifentanil effect concentration were established according to the perceived stimulus model and are the following:

- High: $Ce_{remifentanil} > 6$ ng/ml;
- Normal: $Ce_{remifentanil}$ between 4-6 ng/ml;
- Low: $Ce_{remifentanil} < 4$ ng/ml.

The propofol effect concentration was classified as follows:

- High: $Ce_{propofol} > 3520$ ng/ml;
- Normal: $Ce_{propofol}$ between 2500-3520 ng/ml;
- Low: $Ce_{propofol} < 2500$ ng/ml.

The decrements in the remifentanil infusion rate of 0.025 μg/kg/min were decided upon using literature results. The value of 0.001 μg/kg/min was considered adequate, so as to produce the desired effect without any detrimental effect on the level of analgesia.

Minimum propofol and remifentanil effect concentrations are required. The minimum values were established as 2250 ng/ml and 3.5 ng/ml for propofol and remifentanil, respectively. If the effect concentrations reach these minimum values, then the infusion rate of propofol and remifentanil will be increased by 0.2 mg/s and 0.025 μg/kg/min, respectively. The increment of 0.2 mg/s for propofol was chosen based on the infusion profiles analysed.

The next two sections describe the remifentanil rule-base 1 and rule-base 2 of the multivariable fuzzy controller structure.

6.5.2 Remifentanil Rule-Base 1

The remifentanil rule-base 1 determines the increment in the remifentanil infusion rate when the DOA level is light in the presence of stimulus. The rule-base is shown in Table 6-2, and uses the perceived stimulus and the change in DOA error to establish the increase in the remifentanil infusion rate.

The stimulus intensity is labelled Low, Medium and High, according to the membership functions in Figure 6-39. Figure 6-40 shows the membership functions for the change in DOA error labelled as: Negative (N), Zero (ZE), Positive Small (PS) and Positive Big (PB). These fuzzy partitions reflect the change in DOA error considering that the level of DOA is lighter than the set point. While a negative value is only the result of a change from the Awake to the OK/Light level, there are different possibilities for a positive change of DOA error. Therefore, one needs to differentiate between the positive values of the change of error.

Table 6-2: Rule-base 1 describing the change in remifentanil infusion rate using the stimulus level and the change of DOA error.

	Change of error			
Stimulus	**N**	**ZE**	**PS**	**PB**
Low	PS	PS	PM	PB
Medium	PS	PM	PM	PB
High	PM	PB	PB	PB

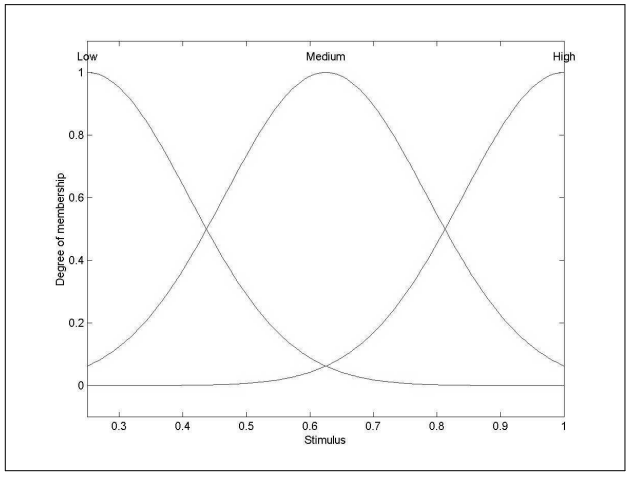

Figure 6-39: Input membership functions describing the stimulus level.

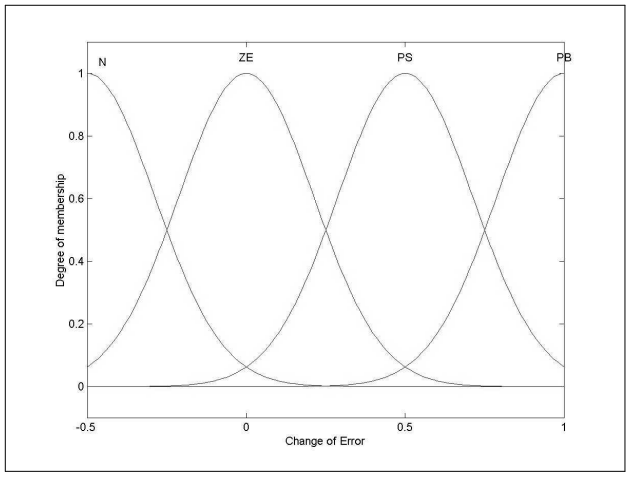

Figure 6-40: Input membership functions describing the change of DOA error, for rule-base 1.

The change in remifentanil infusion rate is described as: Positive Small (PS), Positive Medium (PM) and Positive Big (PB). The output membership functions for the change in remifentanil infusion rate are shown in Figure 6-41, followed by the output surface of rule-base 1 in Figure 6-42. The output surface shows how the remifentanil infusion rate changes according to the stimulus intensity and the change in DOA error. When DOA is light, higher changes in remifentanil infusion rate are required in order to respond to stimulus and increase the level of DOA.

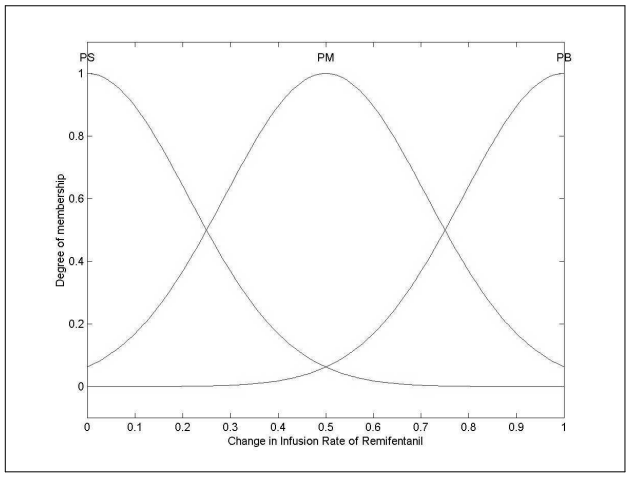

Figure 6-41: Output membership functions describing the change in remifentanil infusion rate.

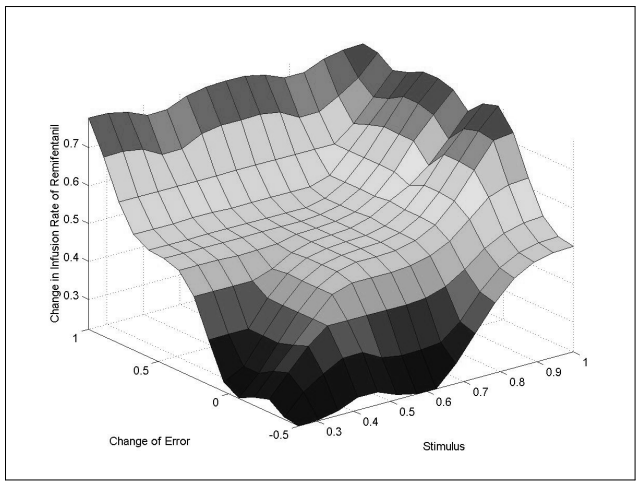

Figure 6-42: Output surface of rule-base 1, describing the change in remifentanil infusion rate.

The change in remifentanil infusion rate is normalized between [0,1], however, the maximum value of the variable was established as 0.03 μg/kg/min.

6.5.3 Remifentanil Rule-Base 2

The remifentanil rule-base 2 is used when the DOA is deep, however, there is stimulus present and an increment on the remifentanil infusion rate is necessary. Rule-base 2 is shown in Table 6-3. The perceived stimulus level and the change in DOA error are used to determine the change in remifentanil infusion rate, similarly to rule-base 1. The membership functions for the stimulus intensity are the same as for rule-base 1, and are shown in Figure 6-39.

Table 6-3: Rule-base 2 describing the change in remifentanil infusion rate using the stimulus level and the change of DOA error.

	Change of error			
Stimulus	**NB**	**NS**	**ZE**	**P**
Low	PS	PS	PS	PS
Medium	PS	PS	PM	PM
High	PS	PM	PM	PB

The change of error is labelled Negative Big (NS), Negative Small (NS), Zero (ZE) and Positive (P), according to the membership functions in Figure 6-43. The differences between rule-base 1 and rule-base 2, with respect to the ranges and membership functions of the change in DOA error, are due to the pre-defined fact that the DOA level is lighter or deeper than the target level.

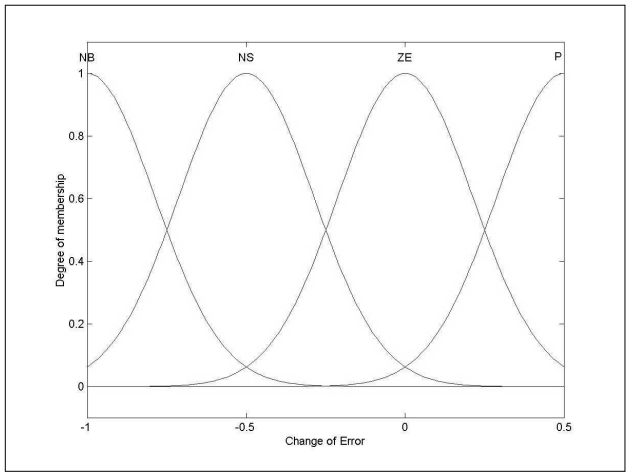

Figure 6-43: Input membership functions describing the change of DOA error, for rule-base 2.

The change in the remifentanil infusion rate is denoted in the same way as for rule-base 1, with the membership functions in Figure 6-41. In rule-base 2, the smaller increment in the

infusion rate is predominant, since the DOA is deep and the remifentanil is increased for its analgesic properties. In rule-base 1, the DOA is light, hence, remifentanil is increased as a response to stimulus and for its synergistic properties with propofol in order to increase the DOA level.

Figure 6-44 shows the output surface for rule-base 2, describing the change in remifentanil infusion rate. Analysing Figures 6-44 and 6-42 (output surface for rule-base 1), the difference in the value of the increment is significant. When DOA is light, higher changes in remifentanil infusion rates are used. If DOA is deep one needs to respond to stimulus, however, the DOA level should not increase.

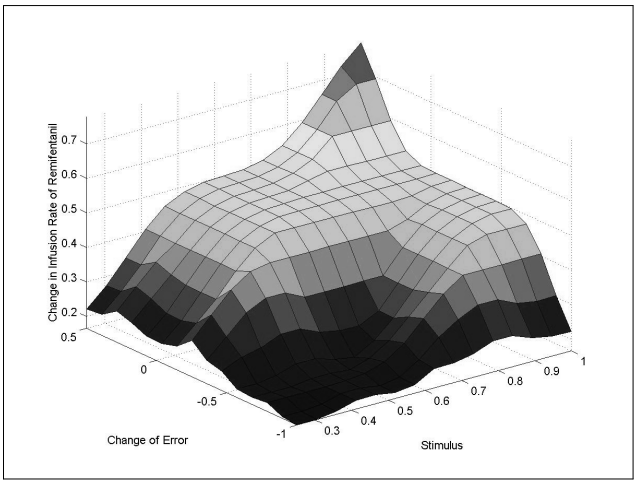

Figure 6-44: Output surface of rule-base 2, describing the change in remifentanil infusion rate.

The membership functions used in the multivariable controller, and even in the SISO fuzzy PI controller, are Gaussian. This is to obtain smoother control actions.

6.6. Simulation Results

The multivariable fuzzy controller was used in closed-loop simulations with the patient model. The results of three simulations are presented in the following sections, including the controller reactions to external disturbances. Note that the controller only starts acting at 1500 seconds (i.e. during the maintenance phase).

6.6.1 Simulation 1

In this simulation, the infusion profile for both drugs which was used during the induction phase was the same as the one used in the simulations with the SISO fuzzy PI controller. The DOA level for this simulation is shown in Figure 6-45. The OK DOA level is achieved at 1740 seconds.

Figure 6-46 shows the propofol and remifentanil infusion rates during this simulation. The corresponding effect concentrations are presented in Figures 6-47 and 6-48, respectively.

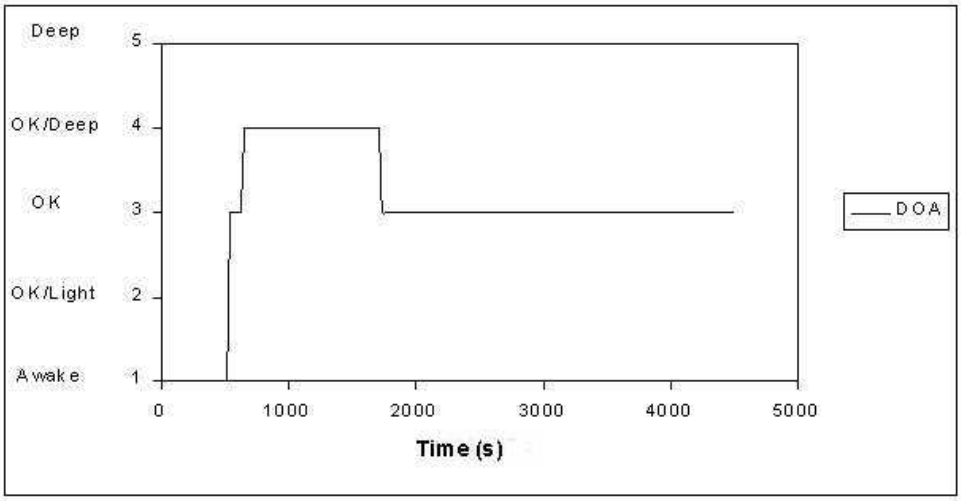

Figure 6-45: DOA level using the multivariable controller in simulation 1.

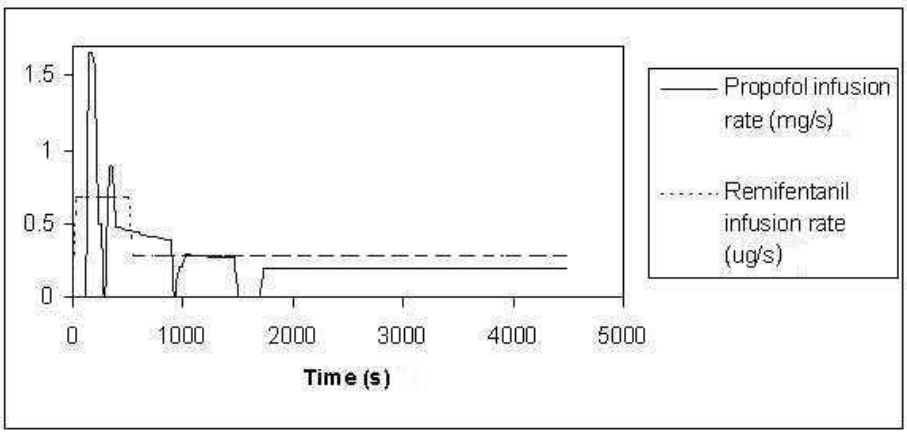

Figure 6-46: Propofol and remifentanil infusion rates as determined by the multivariable controller in simulation 1.

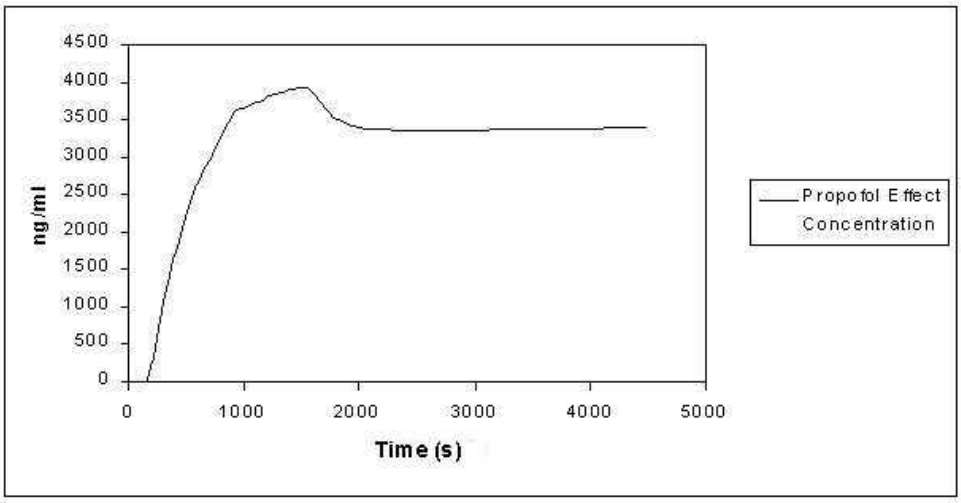

Figure 6-47: Propofol effect concentration for the infusion profile in Figure 6-46, simulation 1.

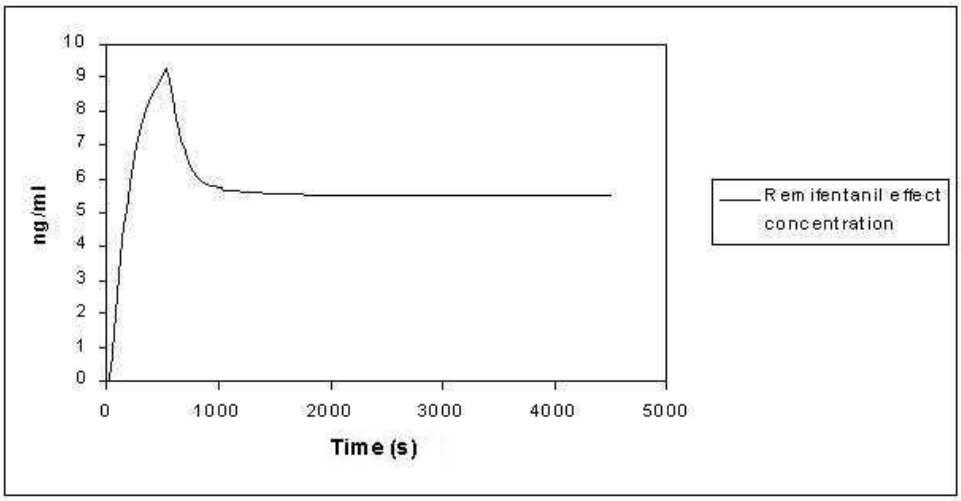

Figure 6-48: Remifentanil effect concentration for the infusion profile in Figure 6-46, simulation 1.

The multivariable fuzzy logic controller performed as well as the SISO fuzzy PI controller. In fact, the same infusion profiles were used. The OK DOA level was rapidly achieved, and the controller maintained efficiently a stable DOA level by keeping both infusion rates constant.

The cardiovascular parameters of simulation 1 are shown in Figure 6-49. The results of the patient model are the same as in Figure 6-31, corresponding to the same infusion profile as with the SISO fuzzy PI controller.

The multivariable controller reacts to changes in the system output, i.e. the DOA level, when the set point has been reached and the subsequent control action maintained a zero error, then it is not necessary to change the control output. In the next section, a change in

DOA target (set point) is introduced in order to assess the controller's performance.

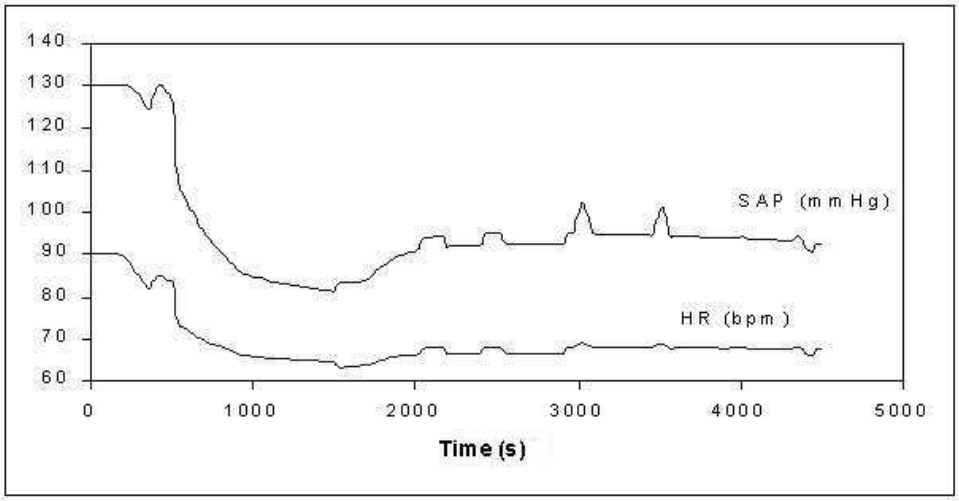

Figure 6-49: Systolic arterial pressure (SAP) and heart rate (HR) for simulation 1.

6.6.1.1 Change in DOA Target

The same conditions as in simulation 1 were considered, but with a set point change to the OK/Deep level at 3000 seconds. Figure 6-50 shows the infusion rates of propofol and remifentanil as determined by the multivariable controller during the maintenance phase. The DOA level is shown in Figure 6-51.

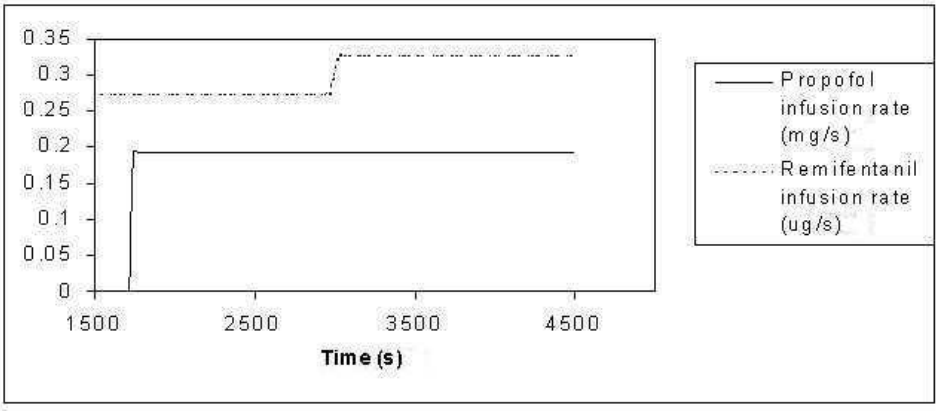

Figure 6-50: Propofol and remifentanil infusion rates as determined by the multivariable controller, during the maintenance phase. DOA target change to OK/Deep at 3000 seconds.

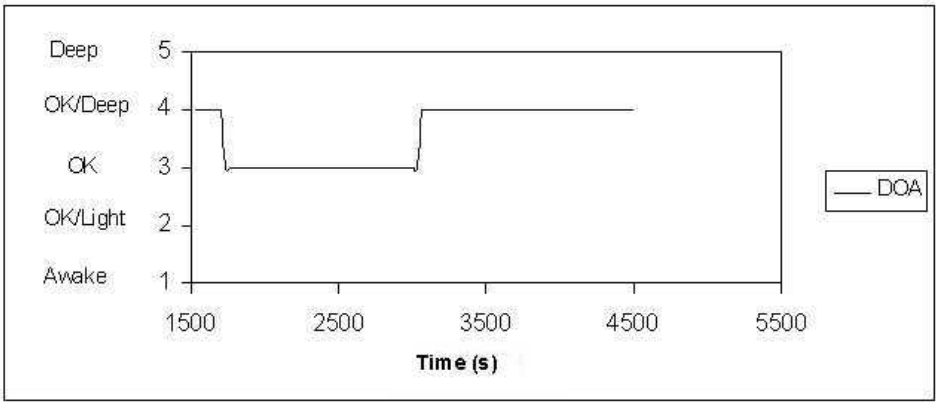

Figure 6-51: DOA level using the multivariable controller, during the maintenance phase. DOA target change to OK/Deep at 3000 seconds.

The OK/Deep DOA level is reached at 3060 seconds, i.e. only 60 seconds after the set point change. The multivariable controller reacts to the set point change by increasing the remifentanil infusion rate, due to the high stimulus level present in the system (see e.g. Figure 6-5). This increase in the remifentanil infusion rate, increases the level of analgesia and also potentiates the effect of propofol. This increases the DOA level faster than in the SISO fuzzy PI controller case. Figure 6-52 shows the SAP during the maintenance phase. The decrease in SAP following an increase in the remifentanil infusion rate shows how a deeper level of depression is achieved, leading to the OK/Deep DOA level. Therefore, the multivariable controller is taking advantage of the synergism between propofol and remifentanil for an efficient control of DOA.

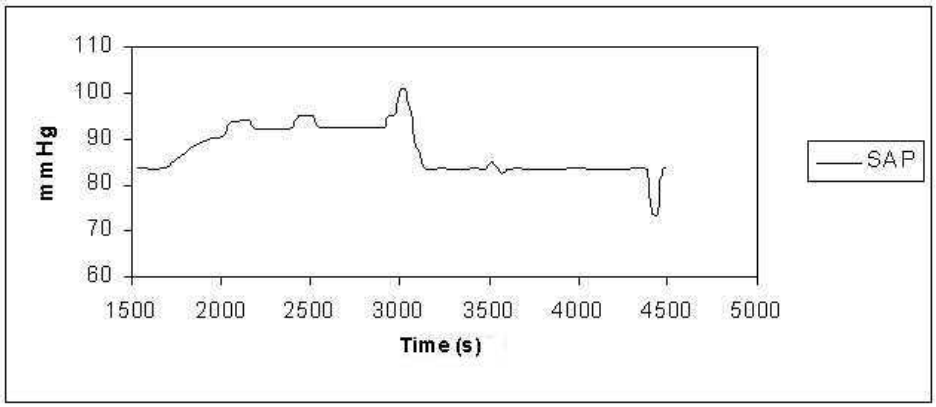

Figure 6-52: Systolic arterial pressure (SAP) during the maintenance phase. DOA target change to OK/Deep at 3000 seconds.

In order to analyse the response of the controller under different conditions, a set point change to the OK/Deep level at 3720 seconds was considered. Figure 6-53 shows the propofol and remifentanil infusion rates during this simulation. At the time of the change in

the set point (i.e. 3720 seconds) the perceived stimulus intensity is very low, therefore, the controller reacts by increasing the propofol infusion rate.

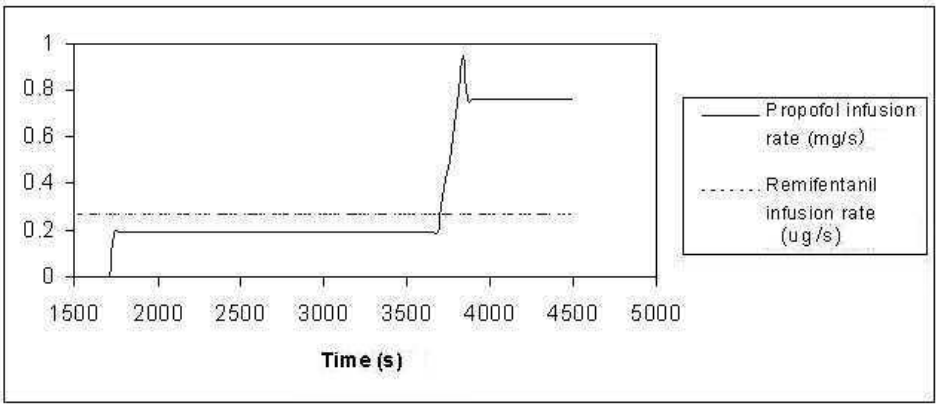

Figure 6-53: Propofol and remifentanil infusion rates as determined by the multivariable controller, during the maintenance phase. DOA target change to OK/Deep at 3720 seconds.

The DOA level for this simulation is shown in Figure 6-54. The OK/Deep DOA level is reached at 3870 seconds, i.e. 2.5 minutes after the set point change.

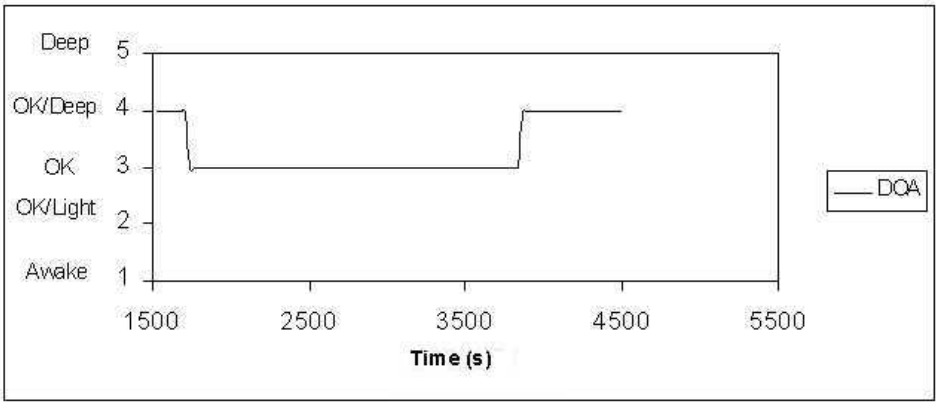

Figure 6-54: DOA level using the multivariable controller during the maintenance phase. DOA target change to OK/Deep at 3720 seconds.

The controller is able to achieve the OK/Deep DOA level in both situations in a relatively short time. In the first case, i.e. an increase of the remifentanil infusion rate, the OK/Deep level is reached faster due to the rapid onset of the action of remifentanil, a subsequent reduction in the perceived stimulus, and a synergism with propofol. In the second case, i.e. an increase of the propofol infusion rate, the OK/Deep level is the response to the increase in the propofol effect concentration.

6.6.2 Simulation 2

Simulation 2 considers a different propofol infusion profile during the induction phase, hence, different initial conditions for the multivariable fuzzy controller. The remifentanil infusion profile is the same as for simulation 1.

The DOA level for simulation 2 is shown in Figure 6-55, followed by the infusion profiles of propofol and remifentanil in Figure 6-56. The effect concentrations of propofol and remifentanil are presented in Figures 6-57 and 6-58, respectively.

At the beginning of the maintenance phase the DOA is at the OK level, i.e. the target level. The propofol and remifentanil infusion rates are kept constant by the controller. However, at approximately 1900 seconds the DOA level increases to OK/Deep. The multivariable controller responds with a decrease in the remifentanil infusion rate, since the propofol effect concentration is within the normal range.

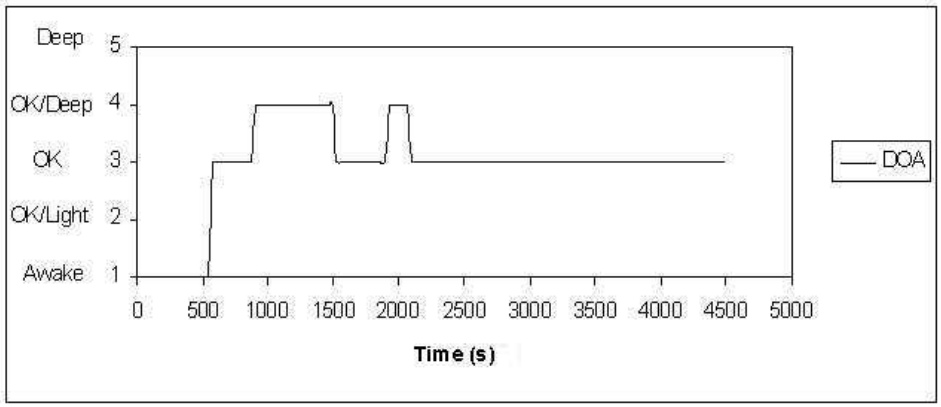

Figure 6-55: DOA level using the multivariable controller in simulation 2.

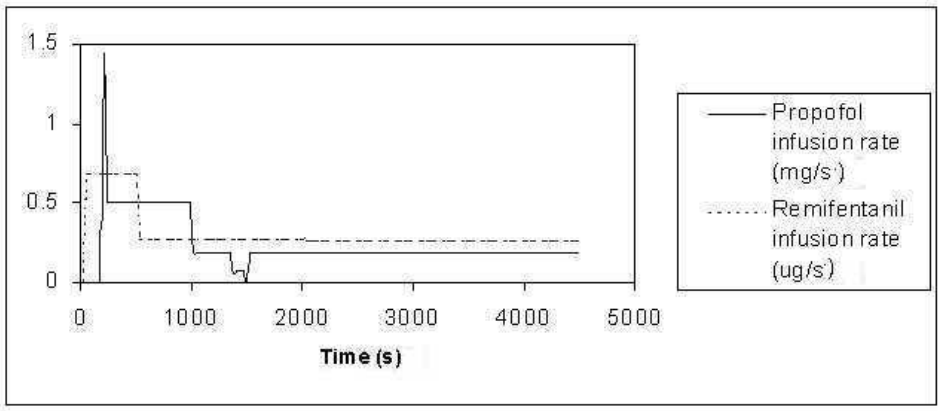

Figure 6-56: Propofol and remifentanil infusion rates as determined by the multivariable controller in simulation 2.

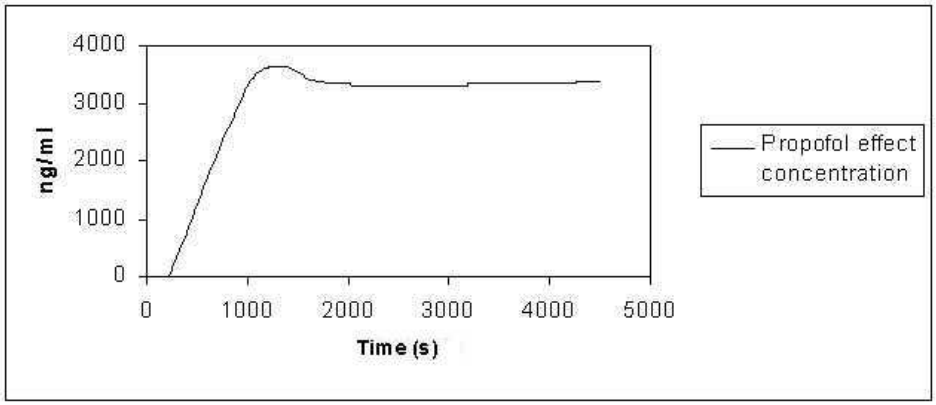

Figure 6-57: Propofol effect concentration for the propofol infusion profile in simulation 2 (Figure 6-56).

Figure 6-59 shows the decrease in the remifentanil infusion rate, which was not easily observed in Figure 6-56. The remifentanil effect concentration also decreases (see Figure 6-60), resulting in an effective return to the OK DOA level.

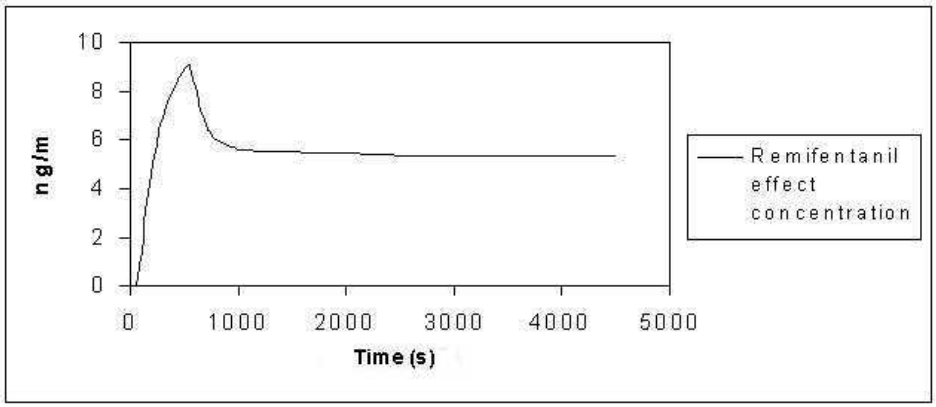

Figure 6-58: Remifentanil effect concentration for the remifentanil infusion profile in simulation 2 (Figure 6-56).

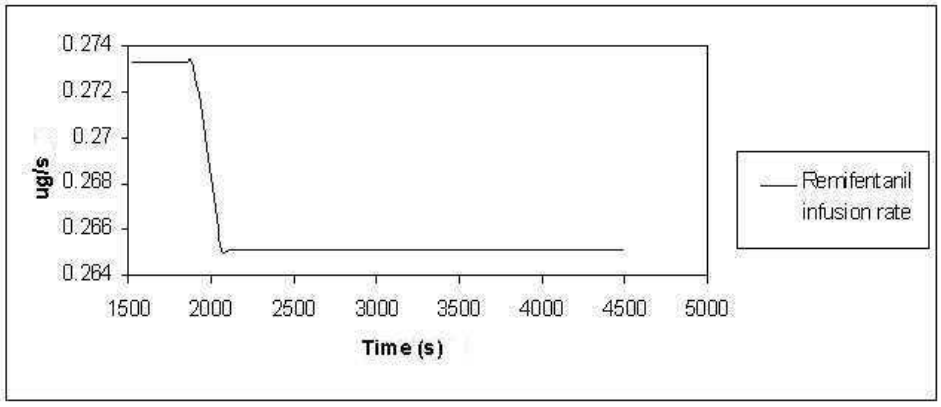

Figure 6-59: Remifentanil infusion rates as determined by the multivariable controller in simulation 2, during the maintenance phase (zoom on Figure 6-56).

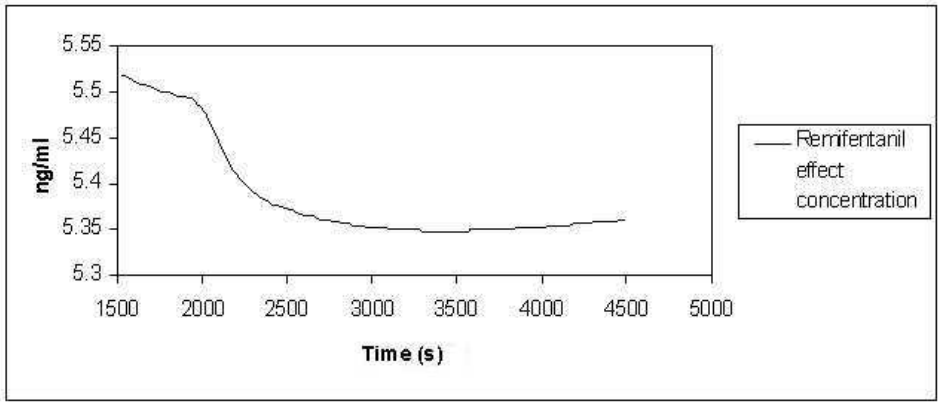

Figure 6-60: Remifentanil effect concentration during the maintenance phase in simulation 2 (zoom on Figure 6-58).

The decrease in the remifentanil infusion rate is very small, but it is proved sufficient in order to achieve the OK DOA level. The multivariable controller shows a smooth and gradual reaction to the change in DOA level, which has proved to be efficient in maintaining a stable level of DOA.

Figure 6-61 shows the stability of the cardiovascular parameters during this simulation.

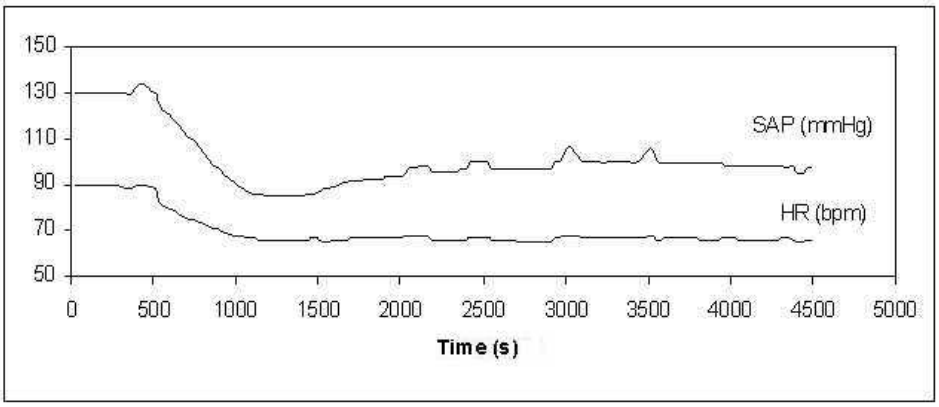

Figure 6-61: Systolic arterial pressure (SAP) and heart rate (HR) in simulation 2.

6.6.2.1 Disturbance Tests

Considering the same conditions as for simulation 2, a disturbance to the OK/Light DOA level was introduced at 3600 seconds. In a real situation, this could be due for instance to a high stimulus interference. Figure 6-62 shows the DOA level for this simulation, during the maintenance phase. The first OK/Deep DOA level (at approximately 1900 seconds) is the same as in the previous simulation.

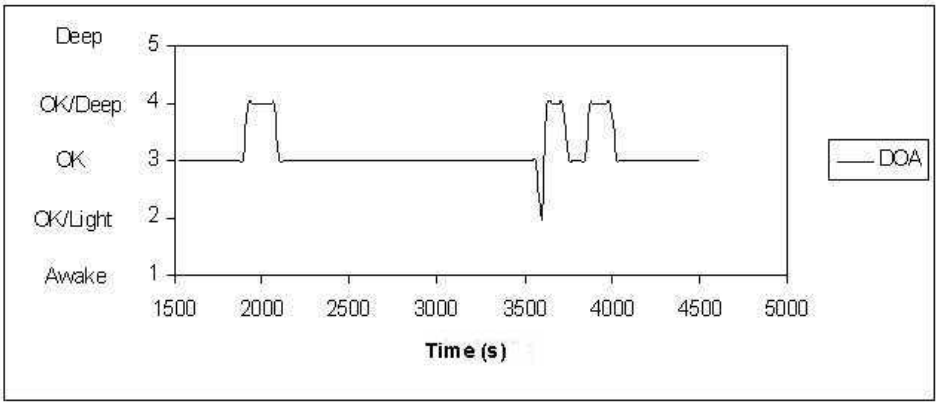

Figure 6-62: DOA level using the multivariable controller (maintenance phase only). Disturbance to the OK/Light DOA level at 3600 seconds.

Figure 6-63 shows the propofol and remifentanil infusion rates for this simulation. The propofol infusion rate is kept at a constant level from the start of the simulation. The remifentanil infusion rate is shown in Figure 6-64 in order to analyse the controller's behaviour. The first decrease in the remifentanil infusion rate is the same as in simulation 2.

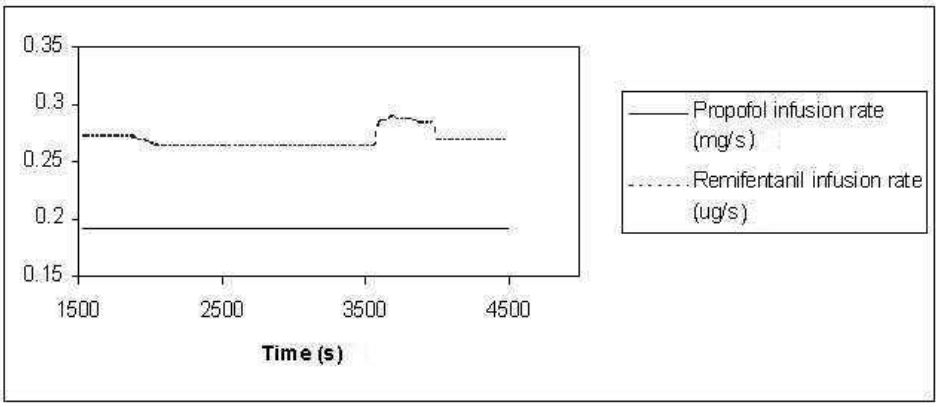

Figure 6-63: Propofol and remifentanil infusion rates using the multivariable controller (maintenance phase only). Disturbance to the OK/Light DOA level at 3600 seconds.

The controller responds to the OK/Light disturbance with an increase in the remifentanil infusion rate, which leads to an OK/Deep DOA level. Therefore, the controller subsequently decreases remifentanil in order to stabilize the effect concentration and lead to an OK DOA level. Figure 6-65 shows the remifentanil effect concentration for this simulation.

The fast onset of action of remifentanil allows the controller to manipulate the infusion rate in order to achieve rapidly the desired DOA level. Therefore, the controller is able to respond adequately to the external disturbance. Once again, only small changes in the

remifentanil infusion rate are used and proved to be efficient in achieving the OK DOA level.

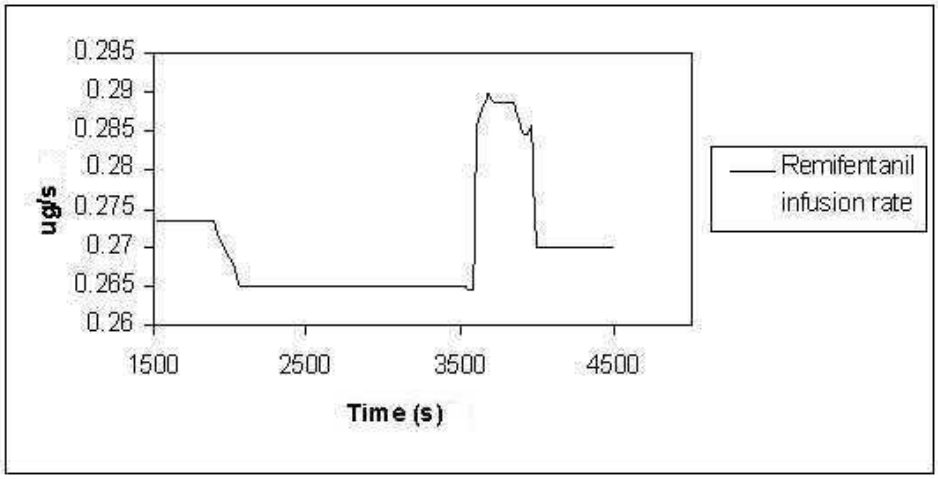

Figure 6-64: Remifentanil infusion rate using the multivariable controller (maintenance phase only). Disturbance to the OK/Light DOA level at 3600 seconds.

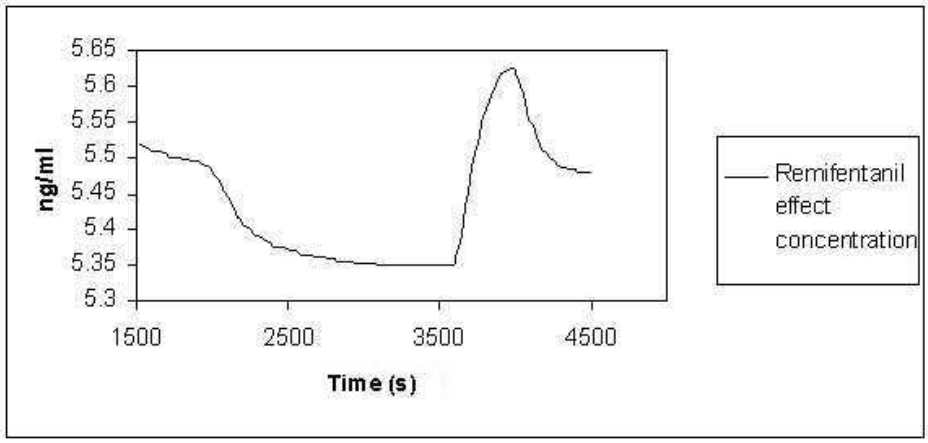

Figure 6-65: Remifentanil effect concentration for the infusion profile in Figure 6-64.

6.6.3 Simulation 3

Simulation 3 considers a different remifentanil infusion profile during the induction phase, while the propofol infusion profile is the same as the one used in simulation 1 (i.e. the one from patient Pat1). In other words, simulation 2 and 3 analyse the reaction of the controller to different initial conditions. The first changes the propofol infusion rate during induction, and the second changes the remifentanil profile.

Figure 6-66 shows the DOA level in simulation 3, while the propofol and remifentanil

infusion rates are shown in Figure 6-67. In contrast with the previous simulations, the multivariable controller changes both infusion rates in response to the OK/Deep DOA level at approximately 1700 seconds.

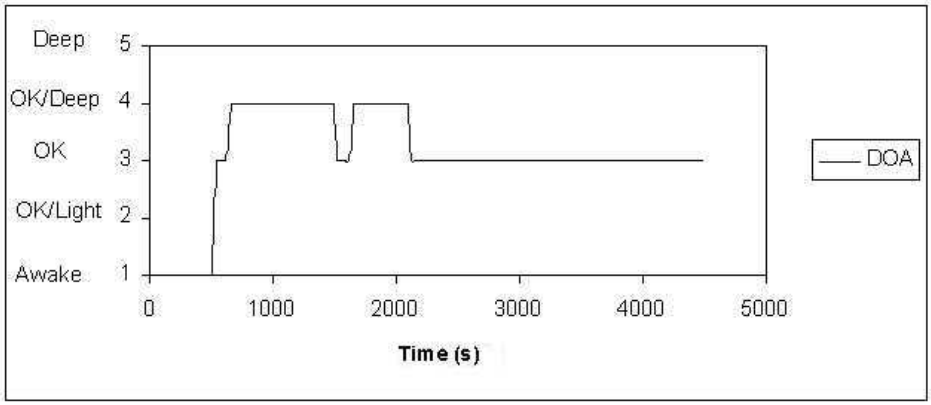

Figure 6-66: DOA level using the multivariable controller in simulation 3.

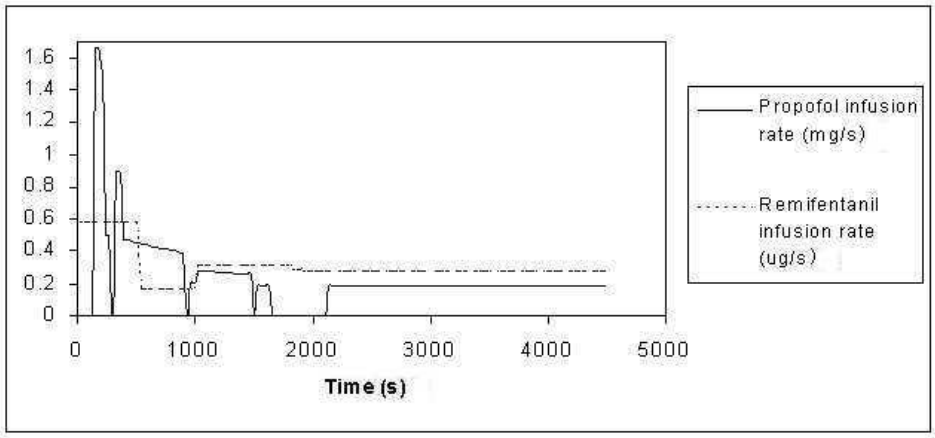

Figure 6-67: Propofol and remifentanil infusion rates as determined by the multivariable controller in simulation 3.

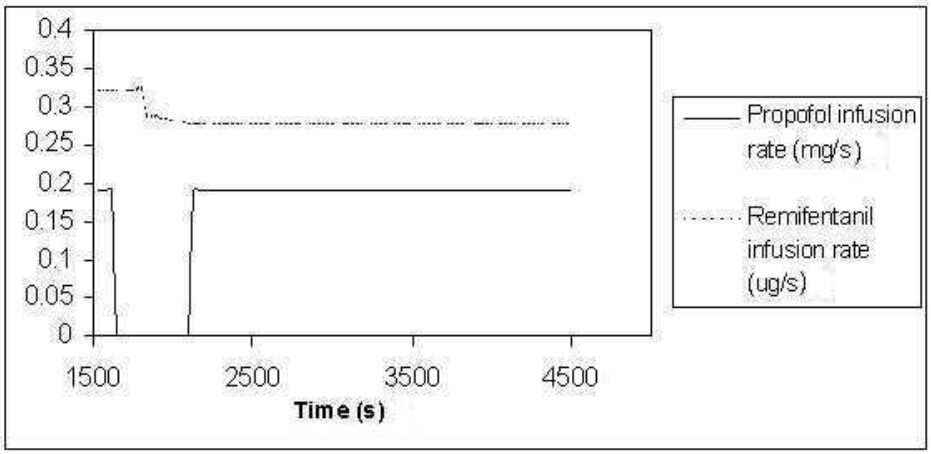

Figure 6-68: Propofol and remifentanil infusion rates as determined by the multivariable controller in simulation 3, during the maintenance phase (zoom on Figure 6-67).

Figure 6-68 shows the infusion rate of both drugs during the maintenance phase (zoom on Figure 6-67). The multivariable controller decreases the propofol infusion rate first and then gradually decreases the remifentanil infusion rate. The effect concentrations of propofol and remifentanil are presented in Figures 6-69 and 6-70, respectively.

The controller is able to determine the adequate combination of the two drugs, achieving and maintaining the OK DOA level.

The cardiovascular parameters for simulation 3 are presented in Figure 6-71. A stable haemodynamic profile is achieved throughout the maintenance phase. There is a small gradual decrease in SAP and HR due to the increase in the propofol effect concentration, however, the SAP and HR values were never below the pos-induction minimum values.

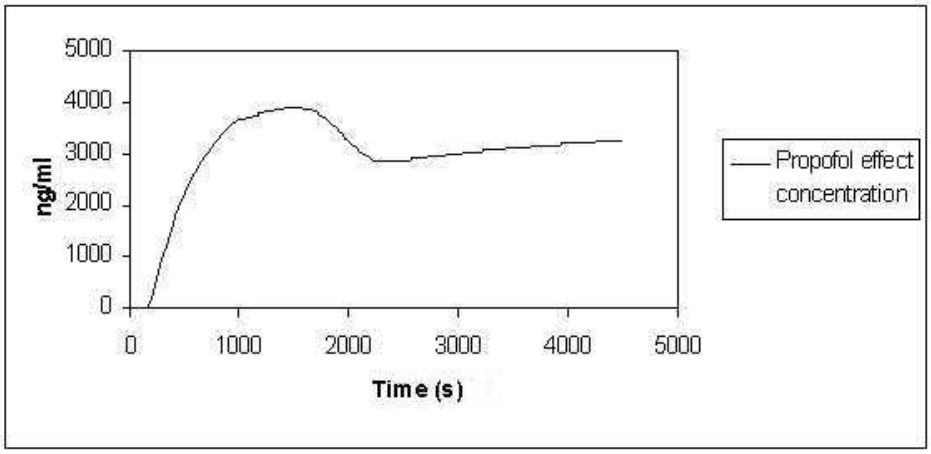

Figure 6-69: Propofol effect concentration for the propofol infusion rate in simulation 3 (Figure 6-67).

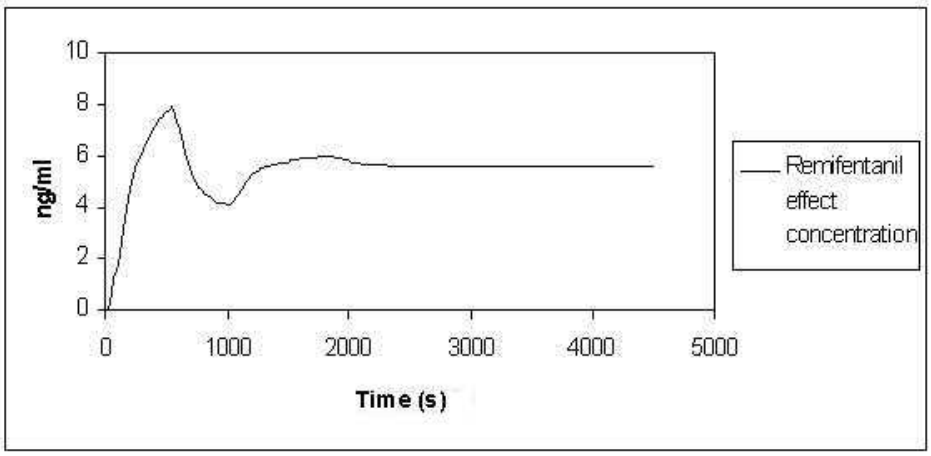

Figure 6-70: Remifentanil effect concentration for the remifentanil infusion rate in simulation 3 (Figure 6-67).

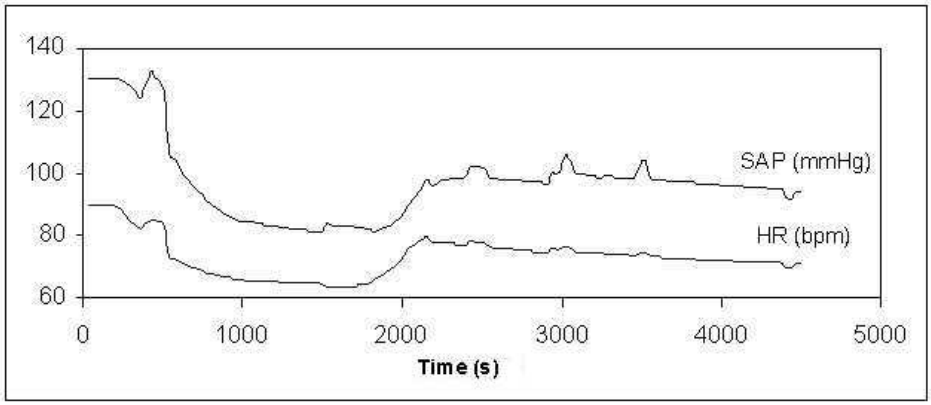

Figure 6-71: Systolic arterial pressure (SAP) and heart rate (HR) in simulation 3.

6.7 Summary

A closed-loop simulation structure for DOA was developed, linking the patient model, the FRC and a control system. This structure is an advisor system for the anaesthetist. In fact, the system should provide information about the adequate infusion rate of propofol and remifentanil simultaneously.

In a first stage, a SISO fuzzy PI controller was developed. This controller determines the change in propofol infusion rate according to the DOA error and based on the patient model. Remifentanil is considered as being manually controlled by the anaesthetist. The patient model uses the infusion rate of both drugs to determine the effect on the cardiovascular parameters and on the wavelet extracted AEP features.

The SISO fuzzy PI controller parameters were optimized using a GA. Overall, the controller had a good performance and was able to respond effectively to changes in the DOA set point. The fuzzy PI controller also proved to be better than a conventional PI controller under the same conditions.

The second stage of the study related to the development of a multivariable controller for the simultaneous administration of propofol and remifentanil. Fuzzy logic was used to construct the multivariable controller, which was based on the anaesthetist experience translated to linguistic rules.

The multivariable controller uses three rule-bases to establish the infusion rates of propofol and remifentanil, according to the DOA level. In the case of remifentanil, the perceived surgical stimulus intensity is also used to ensure an adequate level of analgesia. The

controller takes into account the synergistic interaction between the two drugs, and uses this to rapidly achieve the desired DOA level.

In order to test the reactions of the multivariable controller, several closed-loop simulations were performed using different induction profiles, and adding set point changes and disturbances to the system. The controller performed efficiently in all simulations, by adjusting the infusion rate of both drugs in response to DOA changes. These results can be used to determine ideal combinations of infusion profiles for future use in the operating theatre.

Chapter 7

Conclusions and Recommendations

7.1 Conclusions

Depth of anaesthesia (DOA) is defined as the degree of lack of response and recall to noxious stimuli. While clinical signs can be used to establish the lack of response to stimulus, they are not reliable indicators of possible recall. In addition, balanced anaesthesia comprises the use of a muscle relaxant, an analgesic and an anaesthetic, and such use of several different drugs may obscure the clinical signs. Unconsciousness is hard to define and measure accurately, however one should look for a DOA indicator within the central nervous system (CNS). Previous researchers investigated the auditory evoked potentials (AEP) as an indicator of DOA. The AEP are responses on the EEG to auditory stimuli, and have been proved to show similar graded changes with equipotent concentrations of different anaesthetics, and distinguish between the different DOA levels.

The introduction of balanced anaesthesia gave rise to another problem: how to determine the adequate infusion rate of the anaesthetic and analgesic drugs, considering that the two drugs interact and that there is no direct measure of analgesia (i.e. pain relief). The possibility of recall with implicit or explicit pain brings serious problems for the physician and for the patient.

The objective of this research project was to solve part of the problems that concern the anaesthetist in the operating theatre. The study was based on clinical data gathered during surgical procedures with the anaesthetic propofol and the analgesic remifentanil.

The first step was the classification of DOA. Multiresolution wavelet analysis was used to extract meaningful features from the AEP relating to the different DOA levels. A set of ten wavelet extracted AEP features was found to provide the necessary information to

distinguish between the DOA levels. A fuzzy relational classifier (FRC) was developed in order to process the AEP features and classify them into DOA levels. The FRC uses fuzzy clustering and fuzzy relational composition to establish the link between the natural data clusters and the DOA levels. An automatic system is required to process the AEP and translate the relevant information into a reference value, to which the anaesthetist can relate. Online AEP processing provides the anaesthetist with information about the CNS depression, hence, the degree of unconsciousness of the patient. The FRC classification was evaluated against the anaesthetist classification, which was taken as being the correct classification since there is no precise analysis to evaluate DOA. This is not an easy classification problem, and the overall trend of anaesthetic depth needs to be considered. The FRC was able to distinguish between the five different DOA levels, which were established by the anaesthetist. The results of the FRC were compared with the results of KSOM and ANFIS classifiers. Overall, the FRC achieved a better performance. Therefore, the FRC provided a reliable DOA indicator based on features extracted from the AEP, giving the anaesthetist the possibility of using brain signals as part of day-to-day surgical procedures. The cardiovascular parameters ΔSAP and ΔHR can also be used to reinforce the overall decision scheme.

Remifentanil is a potent analgesic with a strong interaction with propofol. Its rapid onset and offset of action make it ideal for general anaesthesia with a fast and efficient response to the effects of surgical stimuli. Remifentanil has a synergistic interaction with propofol, hence, the effects of propofol are potentiated by the use of remifentanil. From the family of synthetic opioids, remifentanil presents the strongest interaction with propofol. In fact, the optimal concentration of propofol is largely reduced in the presence of remifentanil. In addition, the use of this opioid can also reduce the recovery time. A patient model was developed to determine the effects of these two drugs on the cardiovascular parameters (i.e. SAP and HR) and on the AEP features. The objective was to establish the effects of the interaction between the two drugs and how this affects the adequate infusion rates to maintain a stable DOA level. It is worth noting that the two drugs interact only in the presence of stimuli.

A patient model was developed for the two phases of anaesthesia, i.e. induction and maintenance. In the induction phase, remifentanil acts by reducing the haemodynamic response to intubation which is the only strong stimulus during this phase. It was found that the cardiovascular parameters are largely affected by propofol. Therefore, Hill equation models were optimized and used to model the cardiovascular parameters, and linear quadratic models were developed to determine the effect of remifentanil on the response to

intubation. The AEP are not a reliable signal during the induction phase, due to the drastic changes in the drugs concentrations and tracheal intubation.

The maintenance phase is the longest and most important phase of general anaesthesia, since it is the period corresponding to the surgical procedure. In addition, surgical stimulus is almost a continuous event throughout the maintenance phase and the interaction between the two drugs is an important aspect. The anaesthetist is confronted with the dilemma of which drug to change in response to the DOA level. Surgical stimulus causes arousal, hence, the analgesic properties of remifentanil have to be titrated so as to block the stimulus effect.

The effect concentration governs the drug effect, since it is in the effect site that the drug exerts its action. Therefore, a fuzzy structure of models was built to relate the effect concentrations of both drugs with the patients vital signs. Only the pharmacodynamic interactions were considered, since they have a higher clinical importance than the pharmacokinetic interactions, which are obscured by the inter-patient variability.

The Adaptive Network-Based Fuzzy Inference System (ANFIS) was used to adapt Takagi-Sugeno-Kang (TSK) fuzzy models for ΔSAP, ΔHR and the AEP features, based on clinical data. The fuzzy models led to acceptable errors and reflected the drugs effect and synergistic interaction. Considering that during the maintenance phase the infusion rates follow a specific profile to maintain a stable DOA in the presence of stimulus, these fuzzy models are only valid within specified effect concentrations ranges and safety warnings have to be built in. Overall, this is a reasonable model that helps to understand the effects of the combination of propofol and remifentanil. The model has a good performance on the checking data sets and clearly shows how SAP and HR respond to the drug related synergism.

The patient model would not be complete if the effect of surgical stimulus was not included. The anaesthetist experience was used to construct a Mamdani type of fuzzy model describing the effect of surgical stimuli. The effect concentration of remifentanil was used to determine the level of analgesia and the level of stimulus perceived by the patient. This was used to establish the effect of the stimulus on SAP and HR. It was found that: **1.** the DOA level has some influence on the stimulus effect; **2.** the cardiovascular variables include a time-delay in response to surgical stimulus; **3.** the stimulus effect is proportional to its intensity.

The AEP features were also analysed according to the stimulus effect. The brain signals

respond immediately to stimulus indicating the degree of arousal. The low and high frequency AEP features respond differently to different stimuli. The effect of stimulus on the AEP was not modelled due to the lack of information and data. However, it is important to establish that there is a relation between these two signals and one needs to be aware of its influence on the state of the patient. In the future, SAP and HR may be considered safety indicators, while the AEP represent awareness.

Overall, the developed patient model has an adequate performance reflecting the effect of the drugs and of the surgical stimuli. This model represents a typical patient's behaviour during a surgical procedure, and should be recognized as such. A model describing the drugs effect and interactions is very important for the development of a closed-loop system in anaesthesia. The objective of a control system for DOA is to determine the infusion rates of the anaesthetic and analgesic drugs, helping the anaesthetist to decide which drug should be changed in response to different events.

The developed patient model was used to construct and test two different control structures. First, a SISO fuzzy PI controller was developed using GA optimization. The controller determines the change in propofol infusion rate according to the DOA level and its difference from the desired OK level. The remifentanil infusion rate is considered as manually controlled by the anaesthetist. This is the most common option for control systems in anaesthesia. However, the patient model considers the effects of both drugs and their interaction, hence, the propofol infusion rate will reflect this information. The SISO fuzzy PI controller performed better than a conventional PI controller, leading to a smaller amount of drug infused and being able to respond efficiently to set-point changes. This is one of the advantages of fuzzy logic controllers, which can prove to be robust against disturbances.

Second, the development of a multivariable controller for simultaneous administration of remifentanil and propofol during the maintenance phase was reviewed. Considering the complexity of the two components of anaesthesia (i.e. unconsciousness and analgesia), a multivariable fuzzy controller was developed with the anaesthetist's cooperation. The anaesthetist experience was incorporated into the control structure using linguistic rules. According to the different possibilities for the DOA level and for the surgical stimuli, the multivariable controller defines the required change in the infusion rates of the two drugs.

The controller is able to adjust the remifentanil infusion rate according to the stimulus intensity, and takes advantage of the synergistic interaction to change adequately the propofol infusion rate. Propofol is titrated to lower infusion rates, decreasing the amount of

drug infused, and speeding up recovery. In addition, the controller ensures adequate analgesia by titrating the remifentanil according to stimulus.

The multivariable fuzzy controller was tested under different simulations, and responded efficiently to different induction profiles, set point changes and disturbances. The infusion rates of both drugs were adequately changed to achieve and maintain a stable DOA level, taking advantage of the interaction between the two drugs. It was found that it is possible to model the interaction between propofol and remifentanil, and to use successfully this model to develop a closed-loop system in anaesthesia with simultaneous automatic control of both drugs.

Fuzzy logic techniques proved to be efficient in incorporating human knowledge for a better solution in biomedicine. The complexity of DOA, and the unavailability of large data sets, make this latter ideal for the application of fuzzy logic based concepts. The FRC, the TSK pharmacodynamic models and the multivariable fuzzy controller were combined successfully in a hybrid structure to provide a closed-loop simulation platform for anaesthesia. This system can act as an advisor to anaesthetists in the operating theatre.

In conclusion, the closed-loop system:

- decreases the amount of drug infused;
- reduces the anaesthetist workload;
- can be used as an alarm system;
- processes and provides information about the brain signals (i.e. AEP);
- models the interaction between propofol and remifentanil;
- administers both drugs simultaneously taking advantage of the existent synergism and adjusting to the presence of stimulus;
- leads to an overall increase in the patient's comfort and safety.

7.2 Further Work

The developed patient model represents a typical patient's response to a surgical procedure. Nevertheless, the gathering of more clinical data would be beneficial for improving generalization properties of the model. A balanced set of data from different patients could be used to develop Mamdani type of fuzzy models describing the drugs pharmacodynamics. This would lead to a better understanding of the drugs relations and the way they affect the patient physiological systems. Additional clinical data could be used in extended tests with

the developed patient model, and provide off-line testing of the multivariable controller.

Some aspects could improve the patient model and, hence, the closed-loop simulation system as a whole. Clinical data could be used to study the existence of the time-delay between the surgical stimulus and the haemodynamic responses, improving the quality of analgesia. Research on the effect of surgical stimuli in the presence of remifentanil on the AEP is a real challenge. If a model could be developed, relating the level of analgesia, the stimulus intensity and the effects on the brain signal, this would open a new area of biomedical studies.

Genetic programming could be used to decide on the nonlinear function relating the effects of each drug on the cardiovascular parameters to the final effect of the combination of the drugs. This could be used to compare the results of the patient model and provide new information.

A measure of patient sensitivity to the two drugs could be studied and included in the patient model. A gain could be introduced in the pharmacokinetic and the pharmacodynamic models. Therefore, the variability between patients could be accounted for and used in testing and generalization of the simulation system. In practice, the anaesthetist is faced with patients responding in different ways to the same drugs. If the patient's resistivity to the drug could be detected analysing the initial response during the induction phase, this information could be included in the control system. On-line Adaptive Fuzzy Controllers could also be used to deal with the interpatient variability. Therefore, the drugs would be titrated according to the DOA level, the surgical stimulus, the drugs interaction and also the patient's individual characteristics.

This is one of the first studies on the modelling of drug interactions and multivariable control in humans. The combination of propofol and remifentanil is becoming more popular in anaesthesia, due to specific and unique properties of remifentanil. Nevertheless, different drugs interact differently and this research could be extended to several combinations of anaesthetic and analgesic drugs.

A closed-loop simulation system helps to train the anaesthetist in the different aspects of DOA, and to develop and test different control structures. It also plays and important role in the study of drug interactions and possible side effects. However, the final objective is the implementation of the system in the operating theatre. The advantages of such an advisor system as a source of information and rapidly achieving optimal conditions, would improve the quality of general anaesthesia.

References and Bibliography

Abbod, M. F., and Linkens, D. A. (1998a). “Anaesthesia monitoring and control using fuzzy logic fusion.” Journal of Biomedical Engineering - Applications, Basis & Communications, 10(No 4 Special Issues on ”Control Methods in Anaesthesia”), 225-235.

Abbod, M. F., and Linkens, D. A. (1998b). “Anaesthesia simulator intelligent monitoring and control of depth of anaesthesia.” IEE Colloquium on ”Simulation in Medicine”, IEE, London, UK, 4, 1-5.

Abbod, M. F., Backory, J. K., and Linkens, D. A. (1998). “Monitoring and control of depth of anaesthesia using multi-anaesthetic depth measures with data fusion.” EUFIT’98, Aachen, Germany(September 7-10), 1793-1797.

Absalom, A. R., and Kenny, G. N. C. (1999). “Closed-loop control of anaesthesia using the bispectral index.” EuroSiva Amsterdam 2nd Annual Meeting, Amsterdam, Holand. *http://www.eurosiva.org/archive/Amsterdam/posters/Absalom.htm*

Absalom, A., and Kenny, G. N. C. (2000). “Closed loop control of general anaesthesia.” On the Study and Practice of Intravenous Anaesthesia, J. Vuyk, F. Engbers, and S. Groen-Mulder, eds., Kluwer Academic Publishers, 89-98.

Adlassing, K. F. (1986). “Fuzzy set theory in medical diagnosis.” IEEE Transactions on Systems, Man, and Cybernetics, SMC-16(2), 260-265.

Ahonen, J., Olkkola, K. T., Verkkala, K., Heikkinen, L., Jarvinen, A., and Salmenpera, M. (2000). “A comparison of remifentanil and alfentanil for use with propofol in patients undergoing minimally invasive coronary artery bypass surgery.” Anesthesia Analgesia, 90(6), 1269-1274.

Akay, M., Cohen, M., and Hudson, D. (1997). “Fuzzy sets in life sciences.” Fuzzy Sets and Systems, 90(2), 219-224.

Alexander, R. (2000a). “Remifentanil and propofol for tracheal intubation.” Anaesthesia, 55(5), 516.

Alexander, R. (2000b). “Remifentanil and intubating conditions.” Anaesthesia, 55(5), 517-518.

Alexander, R., Booth, J., Olufolabi, A. J., El-Moalem, H. E., and Glass, P. S. (1999a). “Comparison of remifentanil with alfentanil or suxamethonium following propofol

anaesthesia for tracheal intubation." Anaesthesia, 54(11), 1032-1036.

Alexander, R., Olufolabi, A. J., Booth, J., El-Moalem, H. E., and Glass, P. S. (1999b). "Dosing study of remifentanil and propofol for tracheal intubation without the use of muscle relaxants." Anaesthesia, 54(11), 1037-1040.

Allen, R., and Smith, D. (2001). "Neuro-fuzzy closed-loop control of depth of anaesthesia." Artificial Intelligence in Medicine, 21(1-3), 185-191.

Alvis, J. M., Reves, J. G., Spain, J. A., and Sheppard, L. C. (1985a). "Computer-assisted continuous infusion of the intravenous analgesic fentanyl during general anesthesia, an interactive system." IEEE Transactions on Biomedical Engineering, 32(5), 323-329.

Alvis, J., Reves, J., Govier, A., Menkhaus, P., Henling, C., Spain, J., and E, B. (1985b). "Computer-assisted continuous infusions of fentanyl during cardiac anesthesia: comparison with a manual method." Anesthesiology, 63(1), 41-49.

Asbury, A. J., and Linkens, D. A. (1986). "Clinical automatic control of neuromuscular blockade." Anaesthesia, 41(3), 316-320.

Asteroth, A., Moller, K., and Schwilden, H. (1997). "Adaptive control in anaesthesia." Neural Networks for Signal Processing VII. Proceedings of the 1997 IEEE Signal Processing Society Workshop, IEEE, New York, USA, 236-243.

Astrom, K. J., Anton, J. J., and Arzen, K. E. (1986). "Expert control." Automatica, 22(3), 277-286.

Aunon, J. I., McGillen, C. D., and Childers, D. G. (1981). "Signal processing in evoked potential research: averaging and modelling." CRC Critical Reviews in Bioengineering, 5(4), 323-367.

Babuska, R. (1998). Fuzzy Modelling for Control, Kluwer Academic Publishers, Aachen, Germany.

Backory, J. K. (1999). "Intelligent Monitoring, Modelling and Decision Support in Anaesthesia," PhD Thesis, University of Sheffield, Sheffield, UK.

Backory, J. K., Abbod, M. F., and Linkens, D. A. (1998). "Diagnosis and decision-making for awareness during general anaesthesia." UKACC International Conference on CONTROL'98, IEE, London, UK, 2, 73-78.

Bagshaw, O. (1999). "TIVA with propofol and remifentanil." Anaesthesia, 54(5), 501-502.

Bahoura, M., Hassani, M., and Hubin, M. (1997). "DSP implementation of wavelet transform for real time EEG wave forms detection and heart rate analysis." Computer Methods and Programs in Biomedicine, 52(1), 35-44.

Beale, R., and Jackson, T. (1994). Neural Computing an introduction, Institute of Physics Publishing, Bristol and Philadelphia.

Becker, K., Thull, B., Kasmacher-Leidinger, H., Stemmer, J., Rau, G., Kalff, G., and

Zimmermann, H. J. (1997). “Design and validation of an intelligent patient monitoring and alarm system based on fuzzy process model.” Artificial Intelligence in Medicine, 11(1), 33-53.

Bekker, A. Y., Berklayd, P., Osborn, I., Bloom, M., Yarmush, J., and Turndorf, H. (2000). “The recovery of cognitive function after remifentanil-nitrous oxide anesthesia is faster than after an isoflurane-nitrous oxide- fentanyl combination in elderly patients.” Anesthesia Analgesia, 91(1), 117-122.

Ben-Shlomo, I., Finger, J., Bar-Av, E., Perl, A. Z., Etchin, A., and Tverskoy, M. (1993). “Propofol and fentanyl act additively for induction of anaesthesia.” Anaesthesia, 48(2), 111-113.

Benson, M., Junger, A., Quinzio, L., Fuchs, C., Sciul, G., Michel, A., Marquardt, K., and Hempelmann, G. (2000). “Clinical and practical requirements of online software for anesthesia documentation - an experience report.” International Journal of Medical Informatics, 57(2-3), 155-164.

Berenbaum, M. (1989). “What is synergy?” Pharmacological Reviews, 41(2), 93-141.

Bezdek, J. C., and Pal, S. K. (1991). “Fuzzy Models for Pattern Recognition.” Fuzzy Models For Pattern Recognition, IEEE Press, New York, 1-25.

Bezerianos, A., Laskaris, N., Fotopoulos, S., and Papathanasopoulos, P. (1995). “Data dependent weighted averages for recording of evoked potential signals.” Evoked Potentials-Electroencephalography and Clinical Neurophysiology, 96(5), 468-471.

Blair, J. M., Hill, D. A., and Fee, J. P. (2001). “Patient-controlled analgesia for labour using remifentanil: a feasibility study.” British Journal of Anaesthesia, 87(3), 415-420.

Blanchett, T. P., Kember, G. C., and Dubay, R. (2000). “PID gain sheduling using fuzzy logic.” ISA Transactions, 39(3), 317-325.

Bojanic, S., Simpson, T., and Bolger, C. (2001). “Ocular microtremor: a tool for measuring depth of anaesthesia?” British Journal of Anaesthesia, 86(4), 519-522.

Bovill, J. G. (2000). “Targeting the effect site.” On the Study and Practice of Intravenous Anaesthesia, J. Vuyk, F. Engbers, and S. Groen-Mulder, eds., Kluwer Academic Publishers, Boston, USA, 17-26.

Brunner, M. D., Umo-Etuk, J., Sharpe, R. M., and Thornton, C. (1999). “Effect of a bolus dose of midazolam on the auditory evoked response in humans.” British Journal of Anaesthesia, 82(4), 633-634.

Cafiero, T., Mastronardi, P., Burrelli, R., and Santoro, R. (2000). “Gli effetti del remifentanil sulla risposta emodinamica all’intubazione. Studio comparativo con il fentanyl.” Minerva Anestesiologica, 66(11), 793-797.

Camu, F., and Royston, D. (1999). “Inpatient experience with remifentanil.” Anesthesia Analgesia, 89(4 Supplement), 15-21.

Carrie, L. E. S., Simpson, P. J., and Popat, M. T. (1996). Understanding Anaesthesia,

Butterworth-Heinemann, Oxford, UK.

Casati, A., Valentini, G., Zangrillo, A., Senatore, R., Mello, A., Airaghi, B., and Torri, G. (1999). "Anaesthesia for ultrasound guided oocyte retrieval: midazolam/remifentanil versus propofol/fentanyl regimens." European Journal of Anaesthesiology, 16(11), 773-778.

Casati, A., Fanelli, G., Albertin, A., Deni, F., Danelli, G., Grifoni, F., and Torri, G. (2001). "Small doses of remifentanil or sufentanil for blunting cardiovascular changes induced by tracheal intubation: a double-blind comparison." European Journal of Anaesthesiology, 18(2), 108-112.

Chang, C. S., and Fu, W. (1997). "Area load frequency control using fuzzy gain scheduling of PI controllers." Electric Power Systems Research, 42(2), 145-152.

Chassard, D., Joubaud, A., Colson, A., Guiraud, M., Dubreuil, C., and Banssillon, V. (1989). "Auditory evoked potentials during propofol anaesthesia in man." British Journal of Anaesthesia, 62(5), 522-526.

Chaudhri, S., White, M., and Kenny, G. N. C. (1992). "Induction of anaesthesia with propofol using a target-controlled infusion system." Anaesthesia, 47(7), 551-553.

Chen, C., and Chen, P. (1991). "Application of fuzzy logic controllers in single-loop tuning of multivariable system design." Computers in Industry, 17(1), 33-41.

Chilcoat, R. T., Lunn, J. N., and Mapleson, W. W. (1984). "Computer assistance on the control of depth of anaesthesia." British Journal of Anaesthesia, 56(12), 1417-1432.

Chollet-Rivier, M., and Chiolero, R. (2001). "Anaesthesia for procedures in the intensive care unit." Current Opinion in Anaesthesiology, 14(4), 447-451.

Chyka, P. A. (2000). "How many deaths occur annually from adverse drug reactions in the United States?" The American Journal of Medicine, 109(2), 122-130.

Cort, J. (2000). "Simple remifentanil infusions." Anaesthesia, 55(1), 90.

Crabb, I., Thornton, C., Konieczko, K. M., Chan, A., Aquilina, R., Frazer, N., Doré, C. J., and Newton, D. E. (1996). "Remifentanil reduces auditory and somatosensory evoked responses during isoflurane anaesthesia in a dose-dependent manner." British Journal of Anaesthesia, 76(6), 795-801.

Curatolo, M., Petersen-Felix, S., Gerber, A., and Arendt-Nielsen, L. (2000). "Remifentanil inhibits muscular more than cutaneous pain in humans." British Journal of Anaesthesia, 85(4), 529-532.

Davidson, J. A. H., Macleod, A. D., Howie, J. C., White, M., and Kennt, G. N. C. (1993). "Effective concentration 50 for propofol with and without 67% nitrous oxide." Acta Anaesthesiologica Scandinavica, 37(5), 458-464.

Davila, C. E., and Mobin, M. S. (1992). "Weighted averaging of evoked potentials." IEEE Transactions on Biomedical Engineering, 39(4), 338-345.

de Beer, N. A. M., van Hooff, J. C., Cluitmans, P. J. M., Korsten, H. H. M., and Grouls, R. J. E. (1996). "Haemodynamic responses to incision and sternotomy in relation to the auditory evoked potential and spontaneous EEG." British Journal of Anaesthesia, 76(5), 685-693.

Dershwitz, M., Randel, G. I., Rosow, C. E., Fragen, R. J., Connors, P. M., Librojo, E. S., Shaw, D. L., Peng, A. W., and Jamerson, B. D. (1995). "Initial clinical experience with remifentanil, a new opioid metabolized by esterases." Anesthesia Analgesia, 81(3), 619-623.

Doi, M., Gajraj, R. J., Mantzaridis, H., and Kenny, G. N. C. (1997). "Relationship between calculated blood concentration of propofol and electrophysiological variables, during emergence from anaesthesia: comparison of bispectral index, spectral edge frequency, median frequency and auditory evoked potential index." British Journal of Anaesthesia, 78(2), 180-184.

Domaingue, C. M. (2001). "Propofol/remifentanil in neurosurgery." Anaesthesia and Intensive Care, 29(2), 205-206.

Dorf, R. C., and Bishop, R. H. (1998). Modern Control Systems, Addison Wesley, Menlo Park, USA.

Doyle, J., and Tong, D. (1996). "Intraoperative awareness: a continuing clinical problem." Educational Synopses in Anesthesiology and Critical Care Medicine. The Online Journal of Anesthesiology, 3(6).

Doyle, P. W., Coles, J. P., Leary, T. M., Brazier, P., and Gupta, A. K. (2001). "A comparison of remifentanil and fentanyl in patients undergoing carotid endarterectomy." European Journal of Anaesthesiology, 18(1), 13-19.

Drover, D. R., and Lemmens, H. J. (1998). "Population pharmacodynamics and pharmacokinetics of remifentanil as a supplement to nitrous oxide anesthesia for elective abdominal surgery." Anesthesiology, 89(4), 869-877.

Duce, D., Glaisyer, H., and Sury, M. (2000). "An evaluation of propofol combined with remifentanil: a new intravenous anaesthetic technique for short painful procedures in children." Paediatric Anaesthesia, 10(6), 689-690.

Dunn, J. C. (1973). "A fuzzy relative of the ISODATA process and its use in detecting compact well-separated clusters." Journal of Cybernetics, 3(3), 32-57.

Dutton, K., Thompson, S., and Barraclough, B. (1997). The Art of Control Engineering, Addison Wesley, Reading, USA.

Egan, T. D., Lemmens, H. J. M., Fiset, P., Hermann, D. J., Muir, K. T., Stanski, D. R., and Shafer, S. L. (1993). "The pharmacokinetics of the new short-acting opioid remifentanil (GI87084B) in healthy adult male volunteers." Anesthesiology, 79(5), 881-892.

Egan, T. D., Minto, C. F., Hermann, D. J., Barr, J., Muir, K. T., and Shafer, S. L. (1996). "Remifentanil versus alfentanil." Anesthesiology, 84(4), 821-833.

Elkfafi, M. (1995). "Intelligent Signal Processing of Evoked Potentials for Control of Anaesthesia," PhD Thesis, University of Sheffield, Sheffield, UK.

Elkfafi, M., Shieh, J. S., Linkens, D. A., and Peacock, J. E. (1997). "Intelligent signal processing of evoked potentials for anaesthesia monitoring and control." IEE Proceedings - Control Theory and Applications, 144(4), 354-360.

Elkfafi, M., Shieh, J. S., Linkens, D. A., and Peacock, J. E. (1998). "Fuzzy logic for auditory evoked response monitoring and control of depth of anaesthesia." Fuzzy Sets and Systems, 100(1-3), 29-43.

Endoh, H., Honda, T., Komura, N., Shibue, C., Watanabe, I., and Shimoji, K. (1999). "Effects of nicardipine-, nitroglycerin-, and prostaglandin E1-induced hypotension on human cerebrovascular carbon dioxide reactivity during propofol-fentanyl anesthesia." Journal of Clinical Anesthesia, 11(7), 545-549.

Finianos, A., Hans, P., Coussaert, E., Brichant, J. F., Dewandre, P. Y., Cantraine, F., and Lamy, M. (1999a). "Remifentanil does not effect the bispectral index nor the relationship between propofol and the bispectral index at induction of anaesthesia." EuroSiva Amsterdam 2nd Annual Meeting, Amsterdam, Holand. *http://www.eurosiva.org/Archive/Amsterdam/posters/Finianos*2*.htm*

Finianos, A., Hans, P., Coussaert, E., Dewandre, P. Y., Brichant, J. F., Cantraine, F., and Lamy, M. (1999b). "Target-controlled anaesthesia with propofol and remifentanil: loss of eyelash reflex and evolution of the bispectral index at induction." EuroSiva Amsterdam 2nd Annual Meeting, Amsterdam, Holand. *http://www.eurosiva.org/Archive/Amsterdam/posters/Finianos.htm*

Fleisher, L. A., Hogue, S., Colopy, M., Twersky, R. S., Warner, D. S., Jamerson, B. D., Tuman, K. J., Glass, P. S., and Roizen, M. F. (2001). "Does functional ability in the postoperative period differ between remifentanil- and fentanyl-based anesthesia?" Journal of Clinical Anesthesia, 13(6), 401-406.

Fleming, P. J., and Purshouse, R. C. (2001). "Genetic algorithms in control systems engineering." Research Report 789, Department of Automatic Control & Systems Engineering, University of Sheffield, Sheffield, UK.

Fragen, R. J., and Fitzgerald, P. C. (2000). "Is an infusion pump necessary to safely administer remifentanil?" Anesthesia Analgesia, 90(3), 713-716.

Frei, C. W., Derighetti, M., Morari, M., Glattfelder, A. H., and Zbinden, A. M. (2000). "Improving regulation of mean arterial blood pressure during anaesthesia through estimates of surgery effects." IEEE Transactions on Biomedical Engineering, 47(11), 1456-1464.

Fu, P., Hope, A. D., and King, G. A. (1998). "A neurofuzzy pattern recognition algorithm and its application in tool condition monitoring process." ICSP '98, 1998 Fourth International Conference on Signal Processing, IEEE, Piscataway, NJ, USA, 2, 1193-6.

Gajraj, R. J., Doi, M., Mantzaridis, H., and Kenny, G. N. C. (1998). "Analysis of the EEG bispectrum, auditory evoked potentials and the EEG power spectrum during

repeated transitions from consciousness to unconsciousness." British Journal of Anaesthesia, 80(1), 46-52.

Gajraj, R. J., Doi, M., Mantzaridis, H., and Kenny, G. N. C. (1999). "Comparison of bispectral EEG analysis and auditory evoked potentials for monitoring depth of anaesthesia during propofol anaesthesia." British Journal of Anaesthesia, 82(5), 672-678.

Gentilini, A., Frei, C. W., Glattfedler, A. H., Morari, M., Sieber, T. W., Wymann, R., Schnider, T. W., and Zbinden, A. M. (2001a). "Multitasked closed-loop control in anaesthesia." IEEE Engineering in Medicine and Biology, 20(1), 39-53.

Gentilini, A., Rossoni-Gerosa, M., Frei, C., Wymann, R., Morari, M., Zbinden, A., and Schnider, T. (2001b). "Modeling and closed-loop control of hypnosis by means of bispectral index (BIS) with isoflurane." IEEE Transactions on Biomedical Engineering, 48(8), 874-889.

Gepts, E. (1998). "Pharmacokinetic concepts of TCI anaesthesia." Anaesthesia, 53(Supplement 1), 4-12.

Glass, P. S. A. (1998). "Anesthetic drug interactions." Anesthesiology, 88(1), 5-6.

Glass, P. S., Goodman, D. K., Ginsberg, B., Reves, J. G., and Jacobs, J. R. (1989). "Accuracy of pharmacokinetic model-driven infusion of propofol." Anesthesiology, 71(3A), A277.

Glass, P., Jacobs, J., Smith, L., Ginsberg, B., Quill, T., Bai, S., and Reves, J. (1990). "Pharmacokinetic model-driven infusion of fentanyl: assessment of accuracy." Anesthesiology, 73(6), 1082-1090.

Glass, P. S. A., Hardman, D., Kamiyama, Y., Quill, T. J., Marton, G., Donn, K. H., Grosse, C. M., and Hermann, D. (1993). "Preliminary pharmacokinetics and pharmacodynamics of an ultra-short-acting opioid: remifentanil (GI87084B)." Anesthesia Analgesia, 77(5), 1031-1040.

Glass, P. S. A., Iselin-Chaves, I. A., Goodman, D., Delong, E., and Hermann, D. J. (1999a). "Determination of the potency of remifentanil compared with alfentanil using ventilatory depression as the measure of opioid effect." Anesthesiology, 90(6), 1556-1563.

Glass, P. S. A., Gan, T. J., and Howell, S. (1999b). "A review of the pharmacokinetics and pharmacodynamics of remifentanil." Anesthesia Analgesia, 89(4 Supplement), 7-14.

Godfrey, K. (1983). Compartmental Models and Their Application, Academic Press, London, UK.

Goldberg, D. E. (1989). Genetic Algorithms in Search, Optimization, and Machine Learning, Addison-Wesley, Reading, USA.

Gourlay, G., Kowalski, S., Plummer, J., Cousins, M., and Armstrong, P. (1988). "Fentanyl blood concentration-analgesic response relationship in the treatment of

postoperative pain." Anesthesia Analgesia, 67(4), 329-337.

Graaf, P. M. A. de, Eijkel, G. C. van de, Vullings, H. J. L. M., and Mol, B. A. J. M. de (1997). "A decision-driven design of a decision support system is anaesthesia." Artificial Intelligence in Medicine, 11(2), 141-153.

Grant, S., Noble, S., Woods, A., Murdoch, J., and Davidson, A. (1998). "Assessment of intubating conditions in adults after induction with propofol and varying doses of remifentanil." British Journal of Anaesthesia, 81(4), 540-543.

Greenhow, S., Linkens, D., and Asbury, A. (1992). "Development of an expert system advisor for anaesthetic control." Computer Methods and Programs in Biomedicine, 37(3), 215-229.

Grewal, K., and Samsoon, G. (2001). "Facilitation of laryngeal mask airway insertion, effects of remifentanil administered before induction with target-controlled propofol infusion." Anaesthesia, 56(9), 897-901.

Grundmann, U., Uth, M., Eichner, A., Wilhelm, W., and Larsen, R. (1998). "Total intravenous anaesthesia with propofol and remifentanil in paediatric patients: a comparison with a desflurane-nitrous oxide inhalation anaesthesia." Acta Anaesthesiologica Scandinavica, 42(7), 845-850.

Grundmann, U., Silomon, M., Bach, F., Becker, S., Bauer, M., Larsen, B., and Kleinschmidt, S. (2001). "Recovery profile and side effects of remifentanil-based anaesthesia with desflurane or propofol for laparoscopic cholecystectomy." Acta Anaesthesiologica Scandinavica, 45(3), 320-326.

Guan, S., Li, H. X., and Tso, S. K. (2001). "Multivariable fuzzy supervisory control for the laminar cooling process of hot rolled slab." IEEE Transactions on Control Systems Technology, 9(2), 348-356.

Guez, A., and Nevo, I. (1996). "Neural networks and fuzzy logic in clinical laboratory computing with application to integrated monitoring." Clinica Chimica Acta, 248(1), 73-90.

Guignard, B., Menigaux, C., Dupont, X., Fletcher, D., and Chauvin, M. (2000). "The effect of remifentanil on the bispectral index change and hemodynamic responses after orotracheal intubation." Anesthesia Analgesia, 90(1), 161-167.

Gustafson, D. E., and Kessel, W. C. (1979). "Fuzzy clustering with a fuzzy covariance matrix." IEEE Conference on Decision and Control San Diego, CA, USA, 761-766.

Gustorff, B., Felleiter, P., Nahlik, G., Brannath, W., Hoerauf, K., Spacek, A., and Kress, H. (2001). "The effect of remifentanil on the heat pain threshold in volunteers." Anesthesia Analgesia, 92(2), 369-374.

Hall, A. P., Thompson, J. P., Leslie, N. A. P., Kumar, N., and Rowbotham, D. J. (2000). "Comparison of different doses of remifentanil on the cardiovascular response to laryngoscopy and tracheal intubation." British Journal of Anaesthesia, 84(1), 100-102.

Hans, P., Bonhomme, V., Born, J. D., Maerstens de Noordhoudt, A., Brichant, J. F., and Dewandre, P. Y. (2000). "Target-controlled infusion of propofol and remifentanil combined with bispectral index monitoring for awake craniotomy." Anaesthesia, 55(3), 255-259.

Hathaway, R. J., Overstreet, D. D., Yingkang, H., and Davenport, J. W. (1999). "Generalized fuzzy c-means clustering in the presence of outlying data." Proceedings of the SPIE, The International Society for Optical Engineering, 3722, 509-17.

Haughton, A., Turley, A., and Pollock, N. (1999). "Remifentanil for rapid sequence induction." Anaesthesia and Intensive Care, 27(3), 319-320.

Heidvall, M., Hein, A., Davidson, S., and Jakobsson, J. (2000). "Cost comparison between three different general anaesthetic techniques for elective arthroscopy of the knee." Acta Anaesthesiologica Scandinavica, 44(2), 157-162.

Hermann, D. J., Egan, T. D., and Muir, K. T. (1999). "Influence of arteriovenous sampling on remifentanil pharmacokinetics and pharmacodynamics." Clinical Pharmacology and Therapeutics, 65(5), 511-518.

Hess-Nielsen, N., and Wickerhauser, M. V. (1996). "Wavelets and time-frequency analysis." Proceedings of the IEEE, 84(4), 523-540.

Hirota, K., Ebina, T., Sato, T., Ishihara, H., and Matsuki, A. (1999). "Is total body weight an appropriate predictor for propofol maintenance dose?" Acta Anaesthesiologica Scandinavica, 43(8), 842-844.

Hogue, C. W. J., Bowdle, T. A., OLeary, C., Duncalf, D., Miguel, R., Pitts, M., Streisand, J., Kirvassilis, G., Jamerson, B., McNeal, S., and Batenhorst, R. (1996). "A multicenter evaluation of total intravenous anesthesia with remifentanil and propofol for elective inpatient surgery." Anesthesia Analgesia, 83(2), 279-285.

Hoke, J. F., Shlugman, D., Dershwitz, M., Michalowski, P., Malthouse, D. S., Connors, P. M., Martel, D., Rosow, C. E., Muir, K. T., Rubin, N., and Glass, P. S. (1997). "Pharmacokinetics and pharmacodynamics of remifentanil in persons with renal failure compared with healthy volunteers." Anesthesiology, 87(3), 533-541.

Holas, A., Krafft, P., Marcovic, M., and Quehenberger, F. (1999). "Remifentanil, propofol or both for conscious sedation during eye surgery undergoing regional anaesthesia." European Journal of Anaesthesiology, 16(11), 741.

Howie, M., Cheng, D., Newman, M., Pierce, E. T., Hogue, C., Hillel, Z., Bowdle, A., and Bukenya, D. (2001). "A randomized double-blinded multicenter comparison of remifentanil versus fentanyl when combined with isoflurane/propofol for early extubation in coronary artery bypass graft surgery." Anesthesia Analgesia, 92(5), 1084-1093.

Hoymork, S. C., Grismo, B., and Raeder, J. (1999). "Bispectral index and serum drugs levels during TCI of remifentanil and propofol for cholecystectomy." EuroSiva Amsterdam 2nd Annual Meeting, Amsterdam, Holand.

http://www.eurosiva.org/Archive/Amsterdam/posters/Hoymork.htm

Hoymork, S., Raeder, J., Grimsmo, B., and Steen, P. (2000). "Bispectral index, predicted and measured drug levels of target-controlled infusions of remifentanil and propofol during laparoscopic cholecystectomy and emergence." Acta Anaesthesiologica Scandinavica, 44(9), 1138-1144.

Hu, J. Q., and Rose, E. (1999). "Generalized predictive control using a neuro-fuzzy model." International Journal of Systems Science, 30(1), 117-122.

Huang, J. W., Lu, Y. Y., Nayak, A., and Roy, R. J. (1999). "Depth of anaesthesia estimation and control." IEEE Transactions on Biomedical Engineering, 46(1), 71-81.

Iselin-Chaves, I. A., Flaishon, R., Sebel, P. S., Howell, S., Gan, T. J., Sigl, J., Ginsberg, B., and Glass, P. S. A. (1998). "The effect of the interaction of propofol and alfentanil on recall, loss of consciousness, and the bispectral index." Anesthesia Analgesia, 87(4), 949-955.

Jacobs, J. R. (1990). "Algorithm for optimal linear model-based control with application to pharmacokinetic model-driven drug delivery." IEEE Transactions on Biomedical Engineering, 37(1), 107-109.

Jacobs, J. R., and Williams, E. A. (1993). "Algorithm control "effect compartment" drug concentration in pharmacokinetics model-driven delivery." IEEE Transactions on Biomedical Engineering, 40(10), 993-999.

Jang, J. S. R. (1993). "ANFIS: adaptive-network-based fuzzy inference system." IEEE Transactions on Systems, Man and Cybernetics, 23(3), 665-685.

Jang, J. S. R., and Sun, C. T. (1995). "Neuro-fuzzy modeling and control." Proceedings of the IEEE, 83(3), 378-406.

Jeon, G. J., and Lee, P. G. (1995). "Structure of multivariable fuzzy control systems with a coordinator." Fuzzy Sets and Systems, 71(1), 85-94.

Jessop, J., Griffiths, D., Furness, P., Jones, J., Sapsford, D., and Breckon, D. (1991). "Changes in amplitude and latency of the P300 component of the auditory evoked potential with sedative and anaesthetic concentrations of nitrous oxide." British Journal of Anaesthesia, 67(5), 524-531.

Jones, P. G. (1994). "Perception and memory during general anaesthesia." British Journal of Anaesthesia, 73(1), 31-37.

Jones, J. G. (1996). "Depth of anaesthesia." Current Opinion in Anaesthesiology, 9(6), 452-456.

Jones, R. W., Harrison, M. J., and Lowe, A. (2001). "Computerised anaesthesia monitoring using fuzzy trend templates." Artificial Intelligence in Medicine, 21(1-3), 247-251.

Joo, H. S., Perks, W. J., and Belo, S. E. (2001). "Sevoflurane with remifentanil allows rapid tracheal intubation without neuromuscular blocking agents." Canadian Journal of

Anaesthesia, 48(7), 646-650.

Jordan, C., Weller, C., Thornton, C., and Newton, D. (1995). "Monitoring evoked potentials during surgery to assess the level of anaesthesia." Journal of Medical Engineering & Technology, 19(2-3), 77-79.

Kallar, S. K., Hurt, T. W., Wetchler, B. V., Shaw, D. L., and Jamerson, B. (1994). "A single blind, comparative study of the safety and efficacy of remifentanil and alfentanil for outpatient anesthesia." Anesthesiology, 81(3A), A32.

Karayiannis, N. B. (1996). "Fuzzy and possibilistic clustering algorithms based on generalized reformulation." Proceedings of the Fifth IEEE International Conference on Fuzzy Systems, FUZZ-IEEE '96, IEEE, New York, USA, 2, 1393-1399.

Kazama, T., Ikeda, K., and Morita, K. (1997). "Reduction by fentanyl of the Cp50 values of propofol and hemodynamic responses to various noxious stimuli." Anesthesiology, 87(2), 213-227.

Kazama, T., Ikeda, K., Morita, K., Katoh, T., and Kikura, M. (1998a). "Propofol concentration required for endotracheal intubation with a laryngoscope or fiberscope and its interaction with fentanyl." Anesthesia Analgesia, 86(4), 872-879.

Kazama, T., Ikeda, K., and Morita, K. (1998b). "The pharmacodynamic interaction between propofol and fentanyl with respect to the suppression of somatic or hemodynamic responses to skin incision, peritoneum incision, and abdominal wall retraction." Anesthesiology, 89(4), 894-906.

Kazmaier, S., Hanekop, G. G., Buhre, W., Weyland, A., Busch, T., Radke, O. C., Zoelffel, R., and Sonntag, H. (2000). "Myocardial consequences of remifentanil in patients with coronary artery disease." British Journal of Anaesthesia, 84(5), 578-583.

Keidan, I., Berkenstadt, H., Sidi, A., and Perel, A. (2001). "Propofol/remifentanil versus propofol alone for bone marrow aspiration in paediatric haemato-oncological patients." Paediatric Anaesthesia, 11(3), 297-301.

Kenny, G. N. C. (2000). "Closed loop control of intravenous agents." EuroSiva Vienna 3th annual meeting 2000, Vienna, Austria. *http://www.eurosiva.org/Archive/Vienna/abstracts/Speakers/Kenny.htm*

Kenny, G. N. C., and Mantzaridis, H. (1999). "Closed-loop control of propofol anaesthesia." British Journal of Anaesthesia, 83(2), 223-228.

Kenny, G. N. C., McFadzcan, W., Mantzaridis, H., and Fisher, A. C. (1993). "Propofol requirements during closed-loop anesthesia." Anesthesiology, 79(3A), A329.

King, R. E., Magoulas, G. D., and Stathaki, A. A. (1994). "Multivariable fuzzy controller design." Control Engineering Practice, 2(3), 431-437.

Kissin, I. (2000). "Depth of anesthesia and bispectral index monitoring." Anesthesia Analgesia, 90(5), 1114-1117.

Ko, C.-W., Lin, Y.-D., Chung, H.-W., and Jan, G.-J. (1998). "An EEG detection algorithm

using artificial neural network with multi-channel correlation." 20th Annual International Conference of the IEEE Engineering in Medicine and Biology - Proceedings, IEEE, Piscataway, USA, 4, 2070-2073.

Kochs, E., Kalkman, C., Thornton, C., Newton, D., Bischoff, P., Kuppe , H., Abke, J., Konecny, E., Nahm, W., and Stockmanns, G. (1999). "Middle latency auditory evoked responses and electroencephalographic derived variables do not predict movement to noxious stimulation during 1 minimum alveolar anesthetic concentration isoflurane/nitrous oxide anesthesia." Anesthesia Analgesia, 88(6), 1412-1417.

Kochs, E., Cote, D., Deruyck, L., Rauhala, V., Puig, M., Polati, E., Verbist, J., Upadhyaya, B., and C., H. (2000). "Postoperative pain management and recovery after remifentanil based anaesthesia with isoflurane and propofol for major abdominal surgery." British Journal of Anaesthesia, 84(2), 169-173.

Kong, X., and Qiu, T. (1998). "New adaptive time delay estimation algorithm with local variable gain for evoked potential latency change estimation." Annual International Conference of the IEEE Engineering in Medicine and Biology - Proceedings, 4, 2050-2053.

Kuizenga, K., Kalkman, C. J., and Hennin, P. J. (1998). "Quantitative electroencephalographic analysis of the biphasic concentration-effect relationship of propofol in surgical patients during extradural analgesia." British Journal of Anaesthesia, 80(6), 725-732.

Kulkarni, A. (2000). "Remifentanil and propofol for tracheal intubation." Anaesthesia, 55(5), 516.

Kumar, A., Bhattacharya, A., and Makhija, N. (2000). "Evoked potential monitoring in anaesthesia and analgesia." Anaesthesia, 55(3), 225-241.

Larsen, B., Seitz, A., and R., L. (2000). "Recovery of cognitive function after remifentanil-propofol anesthesia: a comparison with desflurane and sevoflurane anesthesia." Anesthesia Analgesia, 90(1), 168-174.

Lee, C. C. (1990a). "Fuzzy logic in control systems: fuzzy logic controller - part I." IEEE Transactions on Systems, Man, and Cybernetics, 20(2), 404-418.

Lee, C. C. (1990b). "Fuzzy logic in control systems: fuzzy logic controller - part II." IEEE Transactions on Systems, Man, and Cybernetics, 20(2), 419-435.

Lee, Y. H., Kim, S. I., and Lee, D. S. (1997). "Estimation of evoked potentials based on the wavelet analysis." Annual International Conference of the IEEE Engineering in Medicine and Biology - Proceedings, 4, 1464-1467.

Lee, Y. H., Lee, D. H., Kim, Y. S., Lee, D. S., and Kim, S. I. (1998). "Estimation of evoked potentials using segment latency corrected average." Annual International Conference of the IEEE Engineering in Medicine and Biology - Proceedings, 4, 2000-2003.

Lee, M. P., Kua, J. S., and Chiu, W. K. (2001). "The use of remifentanil to facilitate the

insertion of the laryngeal mask airway." Anesthesia Analgesia, 93(2), 359-362.

Lehmann, A., Zeitler, C., Thaler, E., Werling, C., and Boldt, J. (1999). "Total intravenous anaesthesia with remifentanil and propofol for implantation of cardioverter defibrillators in patients with severely reduced left ventricular function." EuroSiva Amsterdam 2nd Annual Meeting, Amsterdam, Holand. *http://www.eurosiva.org/Archive/Amsterdam/posters/Lehman.htm*

Leith, D., and Leithead, W. (1998). "Appropriate realisation of MIMO gain-sheduled controllers." International Journal of Control, 70(1), 13-50.

Leslie, K., Sessler, D. I., Bjorksten, A. R., and Moayeri, A. (1993). "Propofol pharmacokinetics, hepatic blood flow and EEG responses during mild hypothermia." Anesthesiology, 79(3A), A335.

Levy, G. (1998). "Impact of pharmacodynamic variability on drug delivery." Advanced Drug Delivery Reviews, 33(3), 201-206.

Li, C., Zheng, C., and Tai, C. (1995). "Detection of the EEG characteristic points using wavelet transforms." IEEE Transactions on Biomedical Engineering, 42(1), 21-28.

Li, S., and Elbestawi, M. (1996). "Fuzzy clustering for automated tool condition monitoring in machining." Mechanical Systems and Signal Processing, 10(5), 533-550.

Linkens, D. A., and Abbod, M. F. (1991). "On-line self-organising fuzzy logic control with patient simulators." IEE Colloquium on "Knowledge-based control: principles and applications"(April 30), 4/1-5.

Linkens, D. A., and Abbod, M. F. (1992a). "Self-organising fuzzy logic control and the selection of its scaling factors." Transactions of the Institute of Measurement and Control, 14(3), 114-125.

Linkens, D. A., and Abbod, M. F. (1992b). "Supervisory hierarchical intelligent control for medical and industrial systems." ISA Conference and Exhibition on Industrial Automation(June 1-3), 1.21-1.24.

Linkens, D. A., and Abbod, M. F. (1993a). "Supervisory intelligent control using a fuzzy logic hierarchy." Transactions of the Institute of Measurement and Control, 15(3), 112-132.

Linkens, D. A., and Abbod, M. F. (1993b). "Anaesthesia simulators for the design of supervisory rule-based control in operating theatre." IEE Computing and Control Engineering Journal, 4(2), 55-62.

Linkens, D. A., and Abbod, M. F. (1994). "Generic system architecture for supervisory fuzzy control." IEE Intelligent Systems Engineering, 3(4), 181-193.

Linkens, D. A., and Abbod, M. F. (1998). "Intelligent control in anaesthesia." TOOLMET'98 Symposium (Tool Environments and Developments Methods for Intelligent Systems), University of Oulu, Oulu, Finland(16-17 April), 1-8.

Linkens, D. A., and Mahfouf, M. (1994). "Supervisory generalised predictive control and

fault detection for multivariable anaesthesia." IEE Proceedings : Control Theory Applications, 141(2), 70-82.

Linkens, D. A., and Mahfouf, M. (2001). "The Intelligent Systems in Biomedicine laboratory in the Department of Automatic Control and Systems Engineering at the University of Sheffield, UK." Artificial Intelligence in Medicine, 21(1-3), 171-176.

Linkens, D. A., and Nyongesa, H. O. (1995). "Genetic algorithms for fuzzy control. Part 1: Online system development and application." IEE Proceedings Control Theory and Applications, 142(3), 161-176.

Linkens, D. A., and Nyongesa, H. O. (1996). "A hierarchical multivariable fuzzy controller for learning with genetic algorithms." International Journal of Control, 63(5), 865-883.

Linkens, D. A., and Rehman, H. U. (1992). "Non-linear control for anaesthetic depth using neural networks and regression." Proceedings of the 1992 IEEE International Symposium on Intelligent Control, IEEE, New York, USA, 410-415.

Linkens, D. A., and Shieh, J. S. (1992). "Self-organising fuzzy modelling for nonlinear system control." Proceedings of the 1992 IEEE International Symposium on Intelligent Control, IEEE, New York, USA, 210-215.

Linkens, D. A., Mahfouf, M., and Abbod, M. F. (1992). "Self-adaptive and self-organising control applied to non-linear multi-variable anaesthesia: a model based comparative study." IEE Proceedings D (Control Theory and Applications), 139(4), 381-394.

Linkens, D. A., Mahfouf, M., and Peacock, J. E. (1993). "Propofol induced anaesthesia: a comparative study using a derived pharmacokinetic-pharmacodynamic model." Internal Report, Department of Automatic Control and Systems Engineering, University of Sheffield, Sheffield, UK.

Linkens, D. A., Abbod, M. F., and Backory, J. K. (1996a). "Fuzzy logic control of depth of anaesthesia using auditory evoked responses." IEE Colloquium on Fuzzy Logic Controller in Practice, IEE Savoy Place, London, UK (15 November), 4/(1-6).

Linkens, D. A., Shieh, J. S., and Peacock, J. E. (1996b). "Hierarchical fuzzy modelling for monitoring depth of anaesthesia." Fuzzy Sets and Systems, 79(1), 43-57.

Linkens, D. A., Shieh, J. S., Elkfafi, M., and Peacock, J. E. (1996c). "Hierarchical fuzzy-based support system for anaesthesia monitoring and control." IEEE International Conference on Fuzzy Systems, FUZZ-IEEE'96, New York, USA, 3, 1989-1993.

Linkens, D. A., Abbod, M. F., and Backory, J. K. (1997a). "Auditory evoked responses for measuring depth of anaesthesia using a wavelet-fuzzy logic system." IFAC'97, IFAC Symposium on Modelling and Control in Biomedical Systems, Pergamon, Oxford, UK, 193-198.

Linkens, D. A., Abbod, M. F., and Backory, J. K. (1997b). "Closed-loop control of anaesthesia using a wavelet-based fuzzy logic system." EUFIT'97, Aachen,

Germany(September 8-12), 2298-2303.

Linkens, D. A., Abbod, M. F., and Backory, J. K. (1997c). "Closed-loop control of depth of anaesthesia: a simulation study using auditory evoked responses." Control Engineering Practice, 5(2), 1717-1725.

Linkens, D. A., Abbod, M. F., Backory, J. K., and Shieh, J. S. (1998). "Closed-loop control of anaesthesia using fuzzy logic." Fuzzy Systems in Medicine, P. S. Szczepaniak, P. J. G. Lisboa, and S. Tsumoto, eds., Springler-Verlag, New York, USA.

Litman, R. S. (2000). "Conscious sedation with remifentanil during painful medical procedures." Journal of Pain and Symptom Management, 19(6), 468-471.

Loop, T., and Priebe, H. J. (2000). "Recovery after anesthesia with remifentanil combined with propofol, desflurane, or sevoflurane for otorhinolaryngeal surgery." Anesthesia Analgesia, 91(1), 123-129.

Lorenz, I. H., Kolbitsch, C., Schocke, M., Kremser, C., Zschiegner, F., Hinteregger, M., Felber, S., Hormann, C., and Benzer, A. (2000). "Low-dose remifentanil increases regional cerebral blood flow and regional cerebral blood volume, but decreases regional mean transit time and regional cerebrovascular resistance in volunteers." British Journal of Anaesthesia, 85(2), 199-204.

Lowe, A., Harrison, M. J., and Jones, R. W. (1999a). "Diagnostic monitoring in anaesthesia using fuzzy trend templates for matching temporal patterns." Artificial Intelligent in Medicine, 16(2), 183-199.

Lowe, A., Jones, R. W., and Harrison, M. J. (1999b). "Temporal pattern matching using fuzzy templates." Journal of Intelligent Information Systems, 13(1-2), 27-45.

Lowe, A., Jones, R. W., and Harrison, M. J. (2001). "The graphical presentation of decision support information in an intelligent anaesthesia monitor." Artificial Intelligence in Medicine, 22(2), 173-191.

Luginbuhl, M., and Schnider, T. (2002). "Detection of awareness with the bispectral index: two case reports." Anesthesiology, 96(1), 241-243.

Lysakowski, C., Dumont, L., Pellégrini, M., Clergue, F., and Tassonyi, E. (2001). "Effects of fentanyl, alfentanil, remifentanil and sufentanil on loss of consciousness and bispectral index during propofol induction of anaesthesia." British Journal of Anaesthesia, 86(4), 523-527.

Maguire, A. M., Kumar, N., Parker, J. L., Rowbotham, D. J., and Thompson, J. P. (2001). "Comparison of effects of remifentanil and alfentanil on cardiovascular response to tracheal intubation in hypertensive patients." British Journal of Anaesthesia, 86(1), 90-93.

Mahfouf, M. (1994). "Generalized predictive control (GPC) in the operating theatre." Intelligent Control in Biomedicine, D. A. Linkens, ed., Taylor Francis, Bristol, UK, 37-77.

Mahfouf, M., and Linkens, D. A. (1994). "The opioids revisited." Research Report,

Department of Automatic Control and Systems Engineering, University of Sheffield, Sheffield, UK.

Mahfouf, M., and Linkens, D. A. (1997). "Constrained multivariable generalized predictive control (GPC) for anaesthesia: the quadratic-programming approach (QP)." International Journal of Control, 67(4), 507-527.

Mahfouf, M., Linkens, D. A., and Asbury, A. J. (1997). "Generalized predictive control (GPC): a powerful control tool in medicine." IEE Proceedings: Control Theory and Applications, 144(1), 8-14.

Mahfouf, M., Abbod, M. F., and Linkens, D. A. (2001). "A survey of fuzzy logic in monitoring and control utilisation in medicine." Artificial Intelligence in Medicine, 21(1-3), 27-42.

Mallat, S. (1999). A Wavelet Tour of Signal Processing, Academic Press, San Diego, USA.

Marsh, B., White, M. N. M., and Kenny, G. N. C. (1991). "Pharmacokinetic model driven infusion of propofol in children." British Journal of Anaesthesia, 67(1), 41-48.

Matot, I., Neely, C. F., and Marshall, B. E. (1993). "Fentanyl and pulmonary uptake of propofol: effect of time between injections." Anesthesiology, 79(3A), A334.

McAtamney, D., O'Hare, R., Hughes, D., Carabine, U., and Mirakhur, R. (1998). "Evaluation of remifentanil for control of haemodynamic response to tracheal intubation." Anaesthesia, 53(12), 1223-1227.

McFarlan, C., Anderson, B., and Short, T. (1999). "The use of propofol infusions in paediatric anaesthesia: a practical guide." Paediatric Anaesthesia, 9(3), 209-216.

McGregor, R. R., Allan, L. G., Sharpe, R. M., Thornton, C., and Newton, D. E. (1998). "Effect of remifentanil on the auditory evoked response and haemodynamic changes after intubation and surgical incision." British Journal of Anaesthesia, 81(5), 785-786.

McLeod, S., and Ball, D. R. (2000). "Remifentanil and seizures." Anaesthesia, 55(10), 1038-1039.

Mertens, M. J., Vuyk, J., Burn, A. G. L., and Bovill. (1999). "The predictive performance of a remifentanil pharmacokinetic data set during target controlled infusion." EuroSiva Amsterdam 2nd Annual Meeting, Amsterdam, Holand. *http://www.eurosiva.org/Archive/Amsterdam/posters/mertens*2.*htm*

Mertens, M., Vuyk, J., Olofsen, E., Engbers, F., and Burm, A. (2001). "The pharmacodynamic interaction between remifentanil and propofol." EuroSiva Göteborg 4th Annual Meeting, Göteborg, Sweden. *http://www.eurosiva.org/Archive/Goteborg/Posters/Mertens.htm*

Michelsen, L. G. (2000). "Hemodynamic effects of remifentanil in patients undergoing cardiac surgery." Anesthesia Analgesia, 91(6), 1563.

Miller, M. J., Freudinger, L. C., and Brenner, M. J. (1998). "Real-time interactive wavelet

analysis." Proceedings of the International Modal Analysis Conference - IMAC, 2, 1581-1586.

Milne, S. E., and Kenny, G. N. C. (1998). "Future applications for TCI systems." Anaesthesia, 53(Supplement 1), 56-60.

Milne, S. E., and Kenny, G. N. C. (1999). "Increasing the blood target concentration of remifentanil does not improve the accuracy of closed loop propofol anaesthesia." EuroSiva Amsterdam 2nd Annual Meeting, Amsterdam, Holand. *http://www.eurosiva.org/Archive/Amsterdam/posters/Milne.htm*

Minto, C. F., Schnider, T. W., Egan, T. D., Youngs, E., Lemmens, H. J., Gambus, P. L., Billard, V., Hoke, J. F., Moore, K. H., Hermann, D. J., Muir, K. T., W., M. J., and Shafer, S. L. (1997a). "Influence of age and gender on the pharmacokinetics and pharmacodynamics of remifentanil. I. Model development." Anesthesiology, 86(1), 10-23.

Minto, C. F., Schnider, T. W., and Shafer, S. L. (1997b). "Pharmacokinetics and pharmacodynamics of remifentanil. II. Model application." Anesthesiology, 86(1), 24-33.

Minto, C. F., Schnider, T. W., Short, T. G., Gregg, K. M., Gentilini, A., and Shafer, S. L. (2000). "Response surface model for anesthetic drug interactions." Anesthesiology, 92(6), 1603-1616.

Moiny, C., Coussaert, E., Schmartz, D., and Barvais, L. (2000). "Influence of the gradient between plasma and effect-site concentration: remifentanil as an example." EuroSiva Vienna 3th annual meeting 2000, Vienna, Austria. *http://www.eurosiva.org/Archive/Vienna/abstracts/posters/Moiny.htm*

Monk, T. G., Batenhorst, R. L., Folger, W. H., Kirkham, A. J. T., Lemon, D. J., Martin, K. J., and Venker, D. C. (1994). "A comparison of remifentanil and alfentanil during nitrous-narcotic anaesthesia." Anesthesia Analgesia, 78(Supplement), S293.

Morgan, M. (1983). "Total intravenous anaesthesia." Anaesthesia, 38(Supplement), 1-9.

Morita, K., Kazama, T., Sato, S., and Ikeda, K. (2000). "Effect sites of intravenous anaesthetic agents." On the Study and Practice of Intravenous Anaesthesia, J. Vuyk, F. Engbers, and S. Groen-Mulder, eds., Kluwer Academic Publishers, 27-20.

Morley, A., Derrick, J., Mainland, P., Lee, B., and Short, T. (2000). "Closed loop control of anaesthesia: an assessment of the bispectral index as the target of control." Anaesthesia, 55(10), 953-959.

Mortier, E., and Struys, M. (2000). "Effect site modelling and its application in TCI." EuroSiva Vienna 3th annual meeting 2000, Vienna, Austria. *http://www.eurosiva.org/Archive/Vienna/abstracts/Speakers/MORTIER.htm*

Mortier, E., Struys, M., DeSmet, T., Versichelen, L., and Rolly, G. (1998). "Closed loop controlled administration of propofol using bispectral analysis." Anaesthesia, 53(8), 749-754.

Munglani, R. (1994). “Depth of anaesthesia.” Anaesthesia, 49(1), 78-79.

Munglani, R., Andrade, J., Sapsford, D., Baddeley, A., and Jones, J. (1993). “A measure of consciousness and memory during isoflurane administration: the coherent frequency.” British Journal of Anaesthesia, 71(5), 633-641.

Muthuswamy, J., and Roy, R. J. (1999). “The use of fuzzy integrals and bispectral analysis of the electroencephalogram to predict movement under anesthesia.” IEEE Transactions on Biomedical Engineering, 46(3), 291-299.

Nagels, W., and Absalom, A. (2001). “Use of remifentanil for major abdominal surgery.” European Journal of Anaesthesiology, 18(1), 64-65.

Natalini, G., Fassini, P., Seramondi, V., Amicucci, G., Toninelli, C., Cavaliere, S., and Candiani, A. (1999). “Remifentanil vs. fentanyl during interventional rigid bronchoscopy under general anaesthesia and spontaneous assisted ventilation.” European Journal of Anaesthesiology, 16(9), 605-609.

Nayak, A., and Roy, R. J. (1995). “Neural networks for predicting depth of anesthesia from auditory evoked potentials: a comparison of the wavelet transform with autoregressive modeling and power spectrum feature extraction methods.” Annual International Conference of the IEEE Engineering in Medicine and Biology - Proceedings, IEEE, Piscataway, USA, 17(1), 797-798.

Nayak, A., and Roy, R. J. (1998). “Anaesthesia control using midlatency auditory evoked potentials.” IEEE Transactions on Biomedical Engineering, 45(4), 409-421.

Newton, D. E. F. (1993). “Editorial - depth of anaesthesia.” Anaesthesia, 48(5), 367-368.

Newton, D. E., Thornton, C., Creagh Barry, P., and Doré, C. J. (1989). “Early cortical auditory evoked response in anaesthesia: comparison of the effects of nitrous oxide and isoflurane.” British Journal of Anaesthesia, 62(1), 61-65.

Ng, H. P., Chen, F. G., Yeong, S. M., Wong, E., and Chew, P. (2000). “Effect of remifentanil compared with fentanyl on intraocular pressure after succinylcholine and tracheal intubation.” British Journal of Anaesthesia, 85(5), 785-787.

Norgaard, M., Rawn, O., and Poulsen, N. K. (2001). “NNSYSID and NNCTRL tools for system identification and control with neural networks.” Computing & Control Engineering Journal, 12(1), 29-36.

Nuwer, M. R. (1998). “Fundamentals of evoked potentials and common clinical applications today.” Electroencephalography and Clinical Neurophysiology, 106(2), 142-148.

O’Hare, R., McAtamney, D., Mirakhur, R. K., Hughes, D., and Carabine, U. (1999). “Bolus dose remifentanil for control of haemodynamic response to tracheal intubation during rapid sequence induction of anaesthesia.” British Journal of Anaesthesia, 82(2), 283-285.

O’Hare, R. A., Mirakhur, R. K., Reid, J. E., Breslin, D. S., and Hayes, A. (2001). “Recovery from propofol anaesthesia supplemented with remifentanil.” British

Journal of Anaesthesia, 86(3), 361-365.

Olivier, P., Sirieix, D., Dassier, P., D'Attelis, N., and Baron, J. (2000). "Continuous infusion of remifentanil and target-controlled infusion of propofol for patients undergoing cardiac surgery: a new approach for scheduler early extubation." Journal of Cardiothoracic and Vascular Anesthesia, 14(1), 29-35.

Olkkola, K., and Ahonen, J. (2001). "Drug interactions." Current Opinion in Anaesthesiology, 14(4), 411-416.

Pal, K., Pal, N. R., Runkler, T. A., and Bezdek, J. C. (2000). "Fuzzy rule extraction by clustering: the role of tendency assessment." Proceedings of COLL 2000, Symposium on Computational Intelligence and Learning, ERUDIT (ed.), June 22-23, Chios, Greece, 3-16.

Palm, R., and Rehfuess, U. (1997). "Fuzzy controllers as gain scheduling approximators." Fuzzy Sets and Systems, 85(2), 233-246.

Palm, R., Driankov, D., and Hellendoorn, H. (1997). Model Based Fuzzy Control :Fuzzy Gain Scheduling and Sliding Mode Fuzzy Control, Springer, New York, USA.

Palm, S., Linstedt, U., Petry, A., and Wulf, H. (2001). "Dose-response relationship of propofol on mid-latency auditory evoked potentials (MLAEP) in cardiac surgery." Acta Anaesthesiologica Scandinavica, 45(8), 1006-1010.

Pan, Z., and Wang, X. (1996). "Wavelets and dynamic pattern recognition." International Conference on Signal Processing Proceedings, ICSP, 2, 1304-1307.

Papilas, K., Mitselou, M., Papaspyrou, L., Bairaktari, A., and Vafiadou, M. (1999). "Remifentanil infusion in combined general and epidural anaesthesia." EuroSiva Amsterdam 2nd Annual Meeting, Amsterdam, Holand. *http://www.eurosiva.org/Archive/Amsterdam/posters/Papilas.htm*

Passino, K. M., and Yurkovich, S. (1998). Fuzzy Control, Addison Wesley Longman, Menlo Park, USA.

Peacock, J. E., and Philip, B. K. (1999). "Ambulatory anesthesia experience with remifentanil." Anesthesia Analgesia, 89(4 Supplement), 22-27.

Peacock, J. E., Lewis, R. P., Reilly, C. S., and Nimmo, W. S. (1990). "Effect of different rates of infusion of propofol for induction of anaesthesia in elderly patients." British Journal of Anaesthesia, 65(3), 346-352.

Peacock, J. E., Luntley, J. B., O'Connor, B., Reilly, C. S., Ogg, T. W., Watson, B. J., and Shaikh, S. (1998). "Remifentanil in combination with propofol for spontaneous ventilation anaesthesia." British Journal of Anaesthesia, 70(4), 509-511.

Pechstein, U., Nadstawek, J., Zentner, J., and Schramm, J. (1998). "Isoflurane plus nitrous oxide versus propofol for recording of motor evoked potentials after high frequency repetitive electrical stimulation." Electroencephalography and Clinical Neurophysiology/Evoked Potentials Section, 108(2), 175-181.

Pedrycz, W. (1994). “Reasoning by analogy in fuzzy controllers.” Fuzzy Control Systems, A. Kandel and G. Langholz, eds., CRC Press, Boca Raton, Florida, 55-74.

Pelosi, G., Gratarola, A., Pissaia, C., Mendola, C., and Bellomo, G. (1999). “Total intravenous anesthesia with propofol and remifentanil for elective non-cardiac surgery.” Minerva Anestesiologica, 65(11), 791-798.

Petersen-Felix, S., Arendt-Nielsen, L., Bak, P., Fischer, M., and Zbinden, A. M. (1996). “Psychophysical and electrophysiological responses to experimental pain may be influenced by sedation: comparison of the effects of a hypnotic (propofol) and an analgesic (alfentanil).” British Journal of Anaesthesia, 77(2), 165-171.

Petrie, J., and Glass, P. (2001). “Intranevous anesthetics.” Current Opinion in Anaesthesiology, 14(4), 393-397.

Philip, B. K., Scuderi, P. E., Chung, F., Conahan, T. J., Maurer, W., Angel, J. J., Kallar, S. K., Skinner, E. P., and Jamerson, B. D. (1997). “Remifentanil compared with alfentanil for ambulatory surgery using total intravenous anesthesia.” Anesthesia Analgesia, 84(3), 515-521.

Pinerua-Shuhaibar, L., Prieto-Rincon, D., Ferrer, A., Bonilla, E., Maixner, W., and Suarez-Roca, H. (1999). “Reduced tolerance and cardiovascular response to ischemic pain in minor depression.” Journal of Affective Disorders, 56(2-3), 119-126.

Prakash, N., McLeod, T., and Gao Smith, F. (2001). “The effects of remifentanil on haemodynamic stability during rigid bronchoscopy.” Anaesthesia, 56(6), 576-580.

Preston, R. A., Csontos, E. R., East, K. A., Kessler, K. F., Fisk, S. P., and Streisand, J. B. (1993). “Plasma fentanyl concentrations after oral transmucosal fentanyl citrate: children versus adults.” Anesthesiology, 79(3A), A370.

Procyk, T. J., and Mamdani, E. H. (1979). “A linguistic self-organising process controller.” Automatica, 15(1), 15-30.

Qin, S., Chen, Z., Xu, M., and Tang, B. (1998). “Sampling principle and technology in wavelet analysis for signals.” Chinese Journal of Mechanical Engineering (English Edition), 11(4), 257-263.

Rao, R. R., Bequette, B. W., and Roy, R. J. (2000). “Simultaneous regulation of hemodynamic and anesthetic states: a simulation study.” Annals of Biomedical Engineering, 28(1), 71-84.

Reves, J. G. (1999). “Educational considerations for the clinical introduction and use of remifentanil.” Anesthesia Analgesia, 89(4 Supplement), 4-6.

Reves, J. G., Spain, J. A., Alvis, J. M., and Ritchie, R. G. (1984). “Continuous infusion of fentanyl during cardiac anesthesia: an automated system.” Anesthesia Analgesia, 63(1), 266.

Rioul, O. (1993). “A discrete-time multiresolution theory.” IEEE Transactions on Signal

Processing, 41(8), 2591-2606.

Robb, H., Asbury, A., Gray, W., and Linkens, D. (1993). "Towards a standardized anaesthetic state using isoflurane and morphine." British Journal of Anaesthesia, 71(3), 366-369.

Roberts, F. L., Dixon, J., Lewis, G. T. R., Tackley, R. M., and Prys-Roberts, C. (1988). "Induction and maintenance of propofol anaesthesia." Anaesthesia, 43(Supplement), 14-17.

Ropcke, H., Konen-Bergmann, M., Cuhls, M., Bouillon, T., and Hoeft, A. (2001). "Propofol and remifentanil pharmacodynamic interaction during orthopedic surgical procedures as measured by effects on bispectral index." Journal of Clinical Anesthesia, 12(3), 198-207.

Rosow, C. (1993). "Remifentanil: a unique opioid analgesic." Anesthesiology, 79(5), 875-876.

Rosow, C. E. (1999). "An overview of remifentanil." Anesthesia Analgesia, 89(4 Supplement), 1-3.

Roubos, J. A., Mollov, S., Babuska, R., and Verbruggen, H. B. (1999). "Fuzzy model-based predictive control using Takagi-Sugeno models." International Journal of Approximate Reasoning, 22(1), 3-30.

Rowbotham, D. J., Peacock, J. E., Jones, R. M., Speedy, H. M., Sneyd, J. R., Morris, R. W., Nolan, J. P., Jolliffe, D., and Lang, G. (1998). "Comparison of remifentanil in combination with isoflurane of propofol for short-stay surgical procedures." British Journal of Anaesthesia, 80(6), 752-755.

Ruspini, E. H. (1969). "A new approach to clustering." Information and Control, 15(1), 22-32.

Russell, D., Wilkes, M. P., Hunter, S. C., Glen, J. B., Hutton, P., and Kenny, G. N. C. (1995). "Manual compared with target-controlled infusion of propofol." British Journal of Anaesthesia, 75(5), 562-566.

Samra, S. K., Dy, E. A., Welch, K. B., Lovely, L. K., and Graziano, G. P. (2001). "Remifentanil- and fentanyl-based anesthesia for intraoperative monitoring of somatosensory evoked potentials." Anesthesia Analgesia, 92(6), 1510-1515.

Sasada, M., and Smith, S. (2000). Drugs in Anaesthesia & Intensive Care, Oxford University Press, Oxford, UK.

Sato, M., Sato, Y., and Jain, L. C. (1997). Fuzzy Clustering Models and Applications, Physica-Vergag (A Spinger-Verlag Company), New-York.

Savoia, G., Esposito, C., Belfiore, F., Amantea, B., and Cuocolo, R. (1988). "Propofol infusion and auditory evoked potentials." Anaesthesia, 43(Supplement), 46-49.

Schnider, T. W. (2000). "Propofol pharmacokinetic/dynamic changes with age." EuroSiva Vienna 3th annual meeting 2000, Vienna, Austria.

http://www.eurosiva.org/Archive/Vienna/abstracts/Speakers/SCHNIDER.htm

Schnider, T. W., Minto, C. F., Shafer, S. L., Gambus, P. L., Andresen, C., Goodale, D. B., and Youngs, E. J. (1999). "The influence of age on propofol pharmacodynamics." Anesthesiology, 90(6), 1502-1516.

Schraag, S., Kenny, G. N., Mohl, U., and Georgieff, M. (1998). "Patient-maintained remifentanil target-controlled infusion for the transition to early postoperative analgesia." British Journal of Anaesthesia, 81(3), 365-368.

Schraag, S., Mohl, U., Bothner, U., and Georgieff, M. (1999a). "Interaction modeling of propofol and sufentanil on loss of consciousness." Journal of Clinical Anesthesia, 11(5), 391-396.

Schraag, S., Bothner, U., Gajraj, R., Kenny, G., and Georgieff, M. (1999b). "The performance of electroencephalogram bispectral index and auditory evoked potential index to predict loss of consciousness during propofol infusion." Anesthesia Analgesia, 89(5), 1311-1315.

Schulze, H.-J., Wendel, H. P., Kleinhams, M., Oehmichen, S., Heller, W., and Elert, O. (1999). "Effects of the propofol combination anesthesia on the intrinsic blood-clotting system." Immunopharmacology, 43(2-3), 141-144.

Schuttler, J., and Ihmsen, H. (1993). "Population pharmacokinetics of propofol." Anesthesiology, 79(3A), A331.

Schuttler, J., and Schwilden, H. (1996). "Closed-loop systems in clinical anaesthesia." Current Opinion in Anaesthesiology, 9(2), 457-461.

Schwender, D., Rimkus, T., Haessler, R., Klasing, S., Poppel, E., and Peter, K. (1993). "Effects of increasing doses of alfentanil, fentanyl and morphine on mid-latency auditory evoked potentials." British Journal of Anaesthesia, 71(5), 622-628.

Schwender, D., Golling, W., Klasing, S., Faber-Zullig, E., Poppler, E., and Peter, K. (1994). "Effects of surgical stimulation on midlatency auditory evoked potentials during general anaesthesia with propofol/fentanyl, isoflurane/fentanyl and flunitrazepam/fentanyl." Anaesthesia, 49(7), 572-578.

Schwender, D., Daunderer, M., Mulzer, S., Klasing, S., Finsterer, U., and Peter, K. (1997). "Midlatency auditory evoked potentials predict movements during anesthesia with isoflurane or propofol." Anesthesia Analgesia, 85(1), 164-173.

Schwender, D., Daunderer, M., Klasing, S., Finsterer, U., and Peter, K. (1998). "Power spectral analysis of the electroencephalogram during increasing end-expiratory concentrations of isoflurane, desflurane and sevoflurane." Anaesthesia, 53(4), 335-342.

Scott, J. C., and Stanski, D. R. (1987). "Decreased fentanyl and alfentanil dose requirements with age. A simultaneous pharmacokinetic and pharmacodynamic evaluation." Journal of Pharmacology and Experimental Therapeutics, 240(1), 159-166.

Scott, J. C., Ponganis, K. V., and Stanski, D. R. (1985). "EEG quantitation of narcotic effect: the comparative pharmacodynamics of fentanyl and alfentanil." Anesthesiology, 62(3), 234-241.

Seng, T. L., Khalid, M., Yusof, R., and Omatu, S. (1998). "Adaptive neuro-fuzzy control system by RBF and GRNN neural networks." Journal of Intelligent and Robotic Systems: Theory & Applications, 23(2-4), 267-289.

Setnes, M., and Babuska, R. (1999). "Fuzzy relational classifier trained by fuzzy clustering." IEEE Transactions on Systems, Man and Cybernetics, Part B (Cybernetics), 29(5), 619-625.

Shafer, S. L., and Varvel, J. R. (1991). "Pharmacokinetics, pharmacodynamics, and rational opioid selection." Anesthesiology, 74(1), 53-63.

Shafer, S., Varvel, J., Aziz, N., and Scott, J. (1990). "Pharmacokinetics of fentanyl administered by computer-controlled infusion pump." Anesthesiology, 73(6), 1091-1102.

Sheiner, L. B., Stanski, D. R., Vozeh, S., Miller, R. D., and Ham, J. (1979). "Simultaneous modeling of pharmacokinetics and pharmacodynamics: application to d-tubocurarine." Clinical Pharmacology and Therapeutics, 25(3), 358-371.

Shieh, J. S. (1994). "Hierarchical Fuzzy Logic Monitoring and Control in Anaesthesia," PhD Thesis, University of Sheffield, Sheffield, UK.

Shinner, G., Sharpe, R. M., Thornton, C., Dore, C. J., and Brunner, M. D. (1999). "Effect of bolus doses of alfentanil on the arousal response to intubation, as assessed by the auditory evoked response." British Journal of Anaesthesia, 82(6), 925-928.

Simanski, O., Kahler, R., Pohl, B., Hofmockel, R., and Lampe, B. (2001). "Control in general anaesthesia - a contribution." Intelligent Systems in Patient Care. Proc. of the EUNITE-Workshop, Austria(October 5), 169-175.

Singh, H. (1999). "Bispectral index (BIS) monitoring during propofol-induced sedation and anaesthesia." European Journal of Anaesthesiology, 16(1), 31-36.

Smith, C., Jhaveri, R., Wilkinson, M., and Goodman, D. (1992). "Reduction of propofol Cp50 by fentanyl." Anesthesiology, 77(3A), A340.

Smith, C., McEwan, A., Jhaveri, R., Wilkinson, M., Goodman, D., Smith, L., Canada, A., and Glass, P. (1994). "The interaction of fentanyl on the Cp50 of propofol for loss of consciousness and skin incision." Anesthesiology, 81(4), 820-828.

Smith, W. D., Dutton, R. C., and Smith, N. T. (1996). "Measuring the performance of anaesthetic depth indicators." Anesthesiology, 84(1), 38-51.

Smith, I., Avramov, M. N., and White, P. F. (1997). "A comparison of propofol and remifentanil during monitored anesthesia care." Journal of Clinical Anesthesia, 9(2), 148-154.

Sneyd, J. R. (1999). "Monitored anaesthesia care and sedation with remifentanil." EuroSiva

Amsterdam 2nd Annual Meeting, Amsterdam, Holand.

Sneyd, J. R., Whaley, A., Dimpel, H. L., and Andrews, C. J. (1998). "An open, randomized comparison of alfentanil, remifentanil and alfentanil followed by remifentanil in anaesthesia for craniotomy." British Journal of Anaesthesia, 81(3), 361-364.

Sneyd, J. R., Camu, F., Doenicke, A., Mann, C., Holgersen, O., Helmers, J. H., Appelgren, L., Noronha, D., and Upadhyaya, B. K. (2001). "Remifentanil and fentanyl during anaesthesia for major abdominal and gynaecological surgery. An open, comparative study of safety and efficacy." European Journal of Anaesthesiology, 18(9), 605-614.

Song, X., and Qi, F. (1996). "Fast convergence algorithm for wavelet neural network used for signal or function approximation." ICSP'96, 3rd International Conference on Signal Processing Proceedings, IEEE, New York, USA, 2, 1401-1404.

Song, D., Whitten, C. W., and White, P. F. (1999). "Use of remifentanil during anesthetic induction: a comparison with fentanyl in the ambulatory setting." Anesthesia Analgesia, 88(4), 734-736.

Song, D., Whitten, C. W., and White, P. F. (2000). "Remifentanil infusion facilitates early recovery for obese outpatients undergoing laparoscopic cholecystectomy." Anesthesia Analgesia, 90(5), 1111-1113.

Sousa, J. M., Setnes, M., and Kaymak, U. (1998). "Adaptive decision alternatives in fuzzy predictive control." IEEE International Conference on Fuzzy Systems Proceedings, New York, USA, 1, 698-703.

Stanski, D. R. (1994). "Monitoring depth of anaesthesia." Anaesthesia, R. D. Miller, ed., Churchill-Levingstone, New York, 1127-1159.

Steimann, F. (1997). "Fuzzy set theory in medicine." Artificial Intelligence in Medicine, 11(1), 1-7.

Stockmanns, G., Nahm, W., Thornton, C., Shannon, C., Konecny, E., and Kochs, E. (1997). "Wavelet-analysis of middle latency auditory evoked potentials during repetitive propofol sedation." Anesthesiology, 87(3S), 465A.

Strachan, A. N., and Edwards, N. D. (2000). "Randomized placebo-controlled trial to assess the effect of remifentanil and propofol on bispectral index and sedation." British Journal of Anaesthesia, 84(4), 489-490.

Strackeljan, J., and Schubert, A. "Using an evolutionary strategy to select input features for a neural network classifier." COLL 2000, Symposium on Computational Intelligence and Learning, Chios, Greece, 77-85.

Takagi, T., and Sugeno, M. (1985). "Fuzzy identification of systems and its applications to modeling and control." IEEE Transactions on Systems, Man and Cybernetics, SMC-15(2), 116-132.

Tamura, S., Higuchi, S., and Tanaka, K. (1971). "Pattern classification based on fuzzy relations." IEEE Transactions on Systems, Man and Cybernetics, SMC-1(1), 61-66.

Tan, S., Hang, C., and Chai, J. (1997). "Gain scheduling: from conventional to neuro-fuzzy." Automatica, 33(3), 411-419.

Tassorelli, C., Micieli, G., Osipova, V., Rossi, F., and Nappi, G. (1995). "Pupillary and cardiovascular responses to the cold-pressor test." Journal of Autonomic Nervous System, 55(1-2), 45-49.

Thakor, N. V., Xin-rong, G., Yi-Chun, S., and Hanley, D. (1993). "Multiresolution wavelet analysis of evoked potentials." IEEE Transactions on Biomedical Engineering, 40(11), 1085-1094.

Thomas, R., McEwen, J., and Asbury, A. (1996). "The Glasgow pain questionnaire: a new generic measure of pain; development and testing." International Journal of Epidemiology, 25(5), 1060-1067.

Thompson, J. P., and Rowbotham, D. J. (1996). "Remifentanil–an opioid for the 21st century." British Journal of Anaesthesia, 76(3), 341-343.

Thompson, J. P., Hall, A. P., Russell, J., Cagney, B., and Rowbotham, D. J. (1998). "Effect of remifentanil on the haemodynamic response to orotracheal intubation." British Journal of Anaesthesia, 80(4), 467-469.

Thornton, C., and Jones, J. (1993). "Evaluating depth of anesthesia: review of methods." International Anesthesiology Clinics, 31(4), 67-88.

Thornton, C., and Sharpe, R. M. (1998). "Evoked responses in anaesthesia." British Journal of Anaesthesia, 81(5), 771-781.

Thornton, C., Konieczko, K., Jones, J., Jordan, C., Doré, C., and Heneghan, C. (1988). "Effect of surgical stimulation on the auditory evoked response." British Journal of Anaesthesia, 60(4), 372-378.

Thornton, C., Barrowcliffe, M. P., Konieczko, K. M., Ventham, P., Doré, C. J., Newton, D. E. F., and Jones, J. G. (1989a). "The auditory evoked response as an indicator of awareness." British Journal of Anaesthesia, 63(1), 113-115.

Thornton, C., Konieczko, K. M., Knight, A. B., Kaul, B., Jones, J. G., Doré, C. J., and White, D. C. (1989b). "Effect of propofol on the auditory evoked response and oesophageal contractility." British Journal of Anaesthesia, 63(4), 411-417.

Twersky, R. S., Jamerson, B., Warner, D. S., Fleisher, L. A., and Hogue, S. (2001). "Hemodynamics and emergence profile of remifentanil versus fentanyl prospectively compared in a large population of surgical patients." Journal of Clinical Anesthesia, 13(6), 407-415.

Umayahara, K., and Nakamori, Y. (1998). "Linear varieties clustering and elliptic type fuzzy models." Japanese Journal of Fuzzy Theory and Systems, 10(1), 89-101.

van den Nieuwenhuyzen, M. C. O., Engbers, F. H. M., Vuyk, J., and Burn, A. G. L. (2000). "Target-controlled infusion systems: role in anaesthesia and analgesia." Clinical Pharmacokinetics, 38(2), 181-190.

van Dongen, E. P., Beek, H. T. t., Schepens, M. A., Morshuis, W. J., Boer, A. d., Aarts, L. P., and Boezeman, E. H. (1999). "Within patient variability of lower extremity muscle responses to transcranial electrical stimulation with pulse trains in aortic surgery." Clinical Neurophysiology, 110(6), 1144-1148.

Vefghi, L., and Linkens, D. A. (1999). "Internal representation in neural networks used for classification of patient anaesthetic states and dosage." Computer Methods and Programs in Biomedicine, 59(2), 75-89.

Verbruggen, H. B., and Bruijn, P. M. (1997). "Fuzzy control and conventional control: what is (and can be) the real contribution of fuzzy systems?" Fuzzy Sets and Systems, 90(2), 151-160.

Viljamaa, P. (2000). "Fuzzy Gain Scheduling and Tuning of Multivariable Fuzzy Control - Methods of Fuzzy Computing in Control Systems," PhD Thesis, Tampere University of Technology, Tampere, Finland.

Vuyk, J. (1997). "Pharmacokinetic and pharmacodynamic interactions between opioids and propofol." Journal of Clinical Anesthesia, 9(Supplement 6), 23S-26S.

Vuyk, J. (1998). "TCI: supplementation and drug interactions." Anaesthesia, 53(Supplement 1), 35-41.

Vuyk, J. (1999). "Drug interactions in anaesthesia." Minerva Anestesiologica, 65(5), 215-218.

Vuyk, J. (2000). "The effect of opioids on the pharmacokinetics and pharmacodynamics of propofol." On the Study and Practice of Intravenous Anaesthesia, J. Vuyk, F. Engbers, and S. Groen-Mulder, eds., Kluwer Academic Publishers, Boston, USA, 99-111.

Vuyk, J., Lim, T., Engbers, F. H. M., Burm, A. G. L., Vletter, A. A., and Bovill, J. G. (1993). "The pharmacodynamic interaction of propofol and alfentanil during lower abdominal surgery in female patients." Anesthesiology, 79(3A), A332.

Vuyk, J., Lim, T., Engbers, F., Burm, A., Vletter, A., and Bovill, J. (1995). "The pharmacodynamic interaction of propofol and alfentanil during lower abdominal surgery in women." Anesthesiology, 83(1), 8-22.

Vuyk, J., Engbers, F., Burm, A., Vletter, A., Griever, G., Olofsen, E., and Bovill, J. (1996). "Pharmacodynamic interaction between propofol and alfentanil when given for induction of anesthesia." Anesthesiology, 84(2), 288-299.

Vuyk, J., Mertens, M., Olofsen, E., Burm, A., and Bovill, J. (1997). "Propofol anesthesia and rational opioid selection: determination of optimal EC50-EC95 propofol-opioid concentrations that assure adequate anesthesia and a rapid return of consciousness." Anesthesiology, 87(6), 1549-1562.

Vuyk, J., Oostwouder, C., Vletter, A., Burm, A., and Bovill, J. (2001). "Gender differences in the pharmacokinetics of propofol in elderly patients during and after continuous infusion." British Journal of Anaesthesia, 86(2), 183-188.

Wakeling, H., Zimmerman, J., Howell, S., and Glass, P. (1999). "Targeting the effect compartment or central compartment concentration of propofol: what predicts loss of consciousness?" Anesthesiology, 90(1), 92-97.

Wang, L.-X. (1994). Adaptive Fuzzy Systems and Control, PTR Prentice Hall, Englewood Cliffs, USA.

Wang, L.-X. (1997). A Course in Fuzzy Systems and Control, PTR Prentice-Hall, Upper Saddle River, USA.

Webb, A., Allen, R., and Smith, D. (1996). "Closed-loop control of depth of anaesthesia." Measurement and Control, 29(7), 211-215.

Weiss, M. (2000). "Physiological modelling and the effect site." On the Study and Practice of Intravenous Anaesthesia, J. Vuyk, F. Engbers, and S. Groen-Mulder, eds., Kluwer Academic Publishers, Boston, USA, 3-16.

Wessén, A., Persson, P. M., Nilsson, A., and Hartvig, P. (1993). "Concentration-effect relationships of propofol after total intravenous anesthesia." Anesthesia Analgesia, 77(5), 1000-1007.

Westenskow, D. R. (1997). "Fundamentals of feedback control: PID, fuzzy logic, and neural networks." Journal of Clinical Anesthesia, 9(6), 33S-35S.

Westmoreland, C. L., Hoke, J. F., Sebel, P. S., Hug, C. C., and Muir, K. T. (1993). "Pharmacokinetics of remifentanil (GI87084B) and its major metabolite (GI90291) in patients undergoing elective inpatient surgery." Anesthesiology, 79(5), 893-903.

White, M., and Kenny, G. N. C. (1989). "Evaluation of a computerised propofol infusion system." Anesthesiology, 71(3A), A278.

White, M., Sckenkels, M. J., Engbers, F. H. M., Vletter, A., Burm, A. G. L., Bovill, J. G., and Kenny, G. N. C. (1999). "Effect-side modelling of propofol using auditory evoked potentials." British Journal of Anaesthesia, 82(3), 333-339.

Williams, M. (2000). "Remifentanil infusions for cardiac and vascular anaesthesia." Anaesthesia, 55(4), 408-409.

Woods, A. W., and Grant, S. (2000). "Remifentanil and intubating conditions." Anaesthesia, 55(5), 516-517.

Woods, A., Grant, S., and Davidson, A. (1999). "Duration of apnoea with two different intubating doses of remifentanil." European Journal of Anaesthesiology, 16(9), 634-637.

Wuesten, R., Van Aken, H., Glass, P. S. A., and Buerkle, H. (2001). "Assessment of depth of anesthesia and postoperative respiratory recovery after remifentanil-versus alfentanil-based total intravenous anesthesia in patients undergoing ear-nose-throat surgery." Anesthesiology, 94(2), 211-217.

Xie, X. L., and Beni, G. (1991). "A validity measure for fuzzy clustering." IEEE

Transactions on Pattern Analysis and Machine Intelligence, 13(8), 841-847.

Yeh, Z. M. (1999). "A systematic method for design of multivariable fuzzy logic control systems." IEEE Transactions on Fuzzy Systems, 7(6), 741-752.

Zadeh, L. A. (1965). "Fuzzy sets." Information and Control, 8(3), 338-353.

Zadeh, L. A. (1994a). "The role of fuzzy logic in modelling, identification and control." Modelling, Identification and Control, 15(3), 191-203.

Zadeh, L. A. (1994b). "Soft computing and fuzzy logic." IEEE Software, 11(6), 48-58.

Zadeh, L. A. (1997). "Toward a theory of fuzzy information granulation and its centrality in human reasoning and fuzzy logic." Fuzzy Sets and Systems, 90(2), 111-127.

Zahid, N., Abouelala, O., Limouri, M., and Essaid, A. (1999). "Unsupervised fuzzy clustering." Pattern Recognition Letters, 20(2), 123-129.

Zbinden, A. M., and Luginbuhl, M. (1996). "Inhalational versus intravenous anaesthetic in day-care surgery." Current Opinion in Anaesthesiology, 9(2), 462-470.

Zhang, X. S., and Roy, R. J. (1999). "Depth of anesthesia estimation by adaptive-network-based fuzzy inference system." Proceedings of the First Joint BMES/EMBS Conference, 1999 IEEE Engineering in Medicine and Biology 21st Annual Conference and the 1999 Annual Fall Meeting of the Biomedical Engineering Society Piscataway, NJ, USA, 1, 391.

Zhang, X. S., and Roy, R. J. (2001). "Derived fuzzy knowledge model for estimating the depth of anesthesia." IEEE Transactions on Biomedical Engineering, 48(3), 312-323.

Zhang, X. S., Roy, R. J., and Huang, J. W. (1998). "Closed-loop system for total intravenous anesthesia by simultaneously administering two anesthetic drugs." Proceedings of the 20th Annual International Conference of the IEEE Engineering in Medicine and Biology Society, Vol.20 Biomedical Engineering Towards the Year 2000 and Beyond Piscataway, NJ, USA, 6, 3052-3055.

Zhang, X., Roy, R., Schwender, D., and Daunderer, M. (2001). "Discrimination of anesthetic states using mid-latency auditory evoked potential and artificial neural networks." Annals of Biomedical Engineering, 29(5), 446-453.

Zhang, Y., Wen, C., and Soh, Y. C. (1999). "Robust adaptive control of uncertain discrete-time systems." Automatica, 35(2), 321-329.

Zhao, Z.-Y., Tomizuka, M., and Isaka, S. (1993). "Fuzzy gain scheduling of PID controllers." IEEE Transactions on Systems, Man, and Cybernetics, 23(5), 1392-1398.

Appendix A

Glossary

AEP - Auditory Evoked Potentials

ANFIS - Adaptive Network-Based Fuzzy Inference System

ANN - Artificial Neural Network

BIS - Bispectral Index of the EEG

CNS - Central Nervous System

CWT - Continuous-Time Wavelet Transform

DAP - Diastolic Arterial Pressure

DOA - Depth of Anaesthesia

DSP - Digital Signal Processing

DTWT - Discrete Time Wavelet Transform

ECG - Electrocardiogram

EEG - Electroencephalogram

EP - Evoked Potentials

FIS - Fuzzy Inference System

FRC - Fuzzy Relational Classifier

GA - Genetic Algorithm

HR - Heart Rate

ICU - Intensive Care Unit

KSOM - Kohonen Self-Organizing Map

MAC - Minimum Alveolar Concentration

MAP - Mean Arterial Pressure

MLAEP - Middle Latency Auditory Evoked Potentials

MEP - Motor Evoked Potentials

MF - Median Frequency of the EEG

MRA - Multiresolution Analysis

NCD - Nonlinear Control Design

OMT - Ocular Microtremor

PC - Personal Computer

PD - Proportional-Derivative

PI - Proportional-Integral

PID - Proportional-Integral-Derivative

SAP - Systolic Arterial Pressure

SEF - Spectral Edge Frequency of the EEG

SEP - Somatosensory Evoked Potentials

SISO - Single Input Single Output

STFT - Short-Time Fourier Transform

TCI - Target Controlled Infusion

TIVA - Total Intravenous Anaesthesia

TSK - Takagi-Sugeno-Kang

VEP - Visual Evoked Potentials

WT - Wavelet Transform

ΔSAP - Change in Systolic Arterial Pressure from Baseline

ΔHR - Change in Heart Rate from Baseline

Appendix B

Fuzzy Logic

B.1 Fuzzy Sets and Systems

Classical sets are crisply defined collections of distinct elements (numbers, symbols, objects), and for this reason are also called crisp sets. The elements of all the sets under consideration in a given situation belong to an invariable, constant set, called the universe of discourse. The fact that elements of a set *A* either belong or do not belong to a crisp set *A* can be formally indicated by the characteristic function of *A* defined as:

$$\chi_A(x) = \begin{cases} 1 \text{ if and only if } x \in A \\ 0 \text{ if and only if } x \notin A \end{cases} \qquad \text{B-1}$$

where the symbols $\in$ and $\notin$ denote that *x* is and is not a member of *A*, respectively. The pair of numbers $\{0, 1\}$ is called the valuation set. Another way of writing Equation B-1 is:

$$\chi_A(x) : X \rightarrow \{0, 1\} \qquad \text{B-2}$$

There is a restrict sense of membership to a set in classical set theory, i.e. an element either belongs or does not belong to the set.

In 1965, Zadeh launched the foundation of fuzzy set theory, where a more flexible sense of membership is possible. In fuzzy sets many degrees of membership are allowed. The degree of membership to a set is indicated by a number between 0 and 1, i.e. a number in the interval $[0, 1]$. Fuzzy sets generalize the valuation set from the pair of numbers $\{0, 1\}$ to all numbers found in $[0, 1]$. By expanding the valuation set the nature of the characteristic function is altered, and called membership function and denoted by $\mu_A(x)$. Therefore, an infinite number of membership degrees are possible, since there is an infinity of numbers in

the interval $[0,1]$. The membership function maps every element of the universe of discourse X to the interval $[0,1]$, and this is written as:

$$\mu_A(x) : X \rightarrow [0,1] \qquad \text{B-3}$$

Membership functions are a mathematical tool for indicating flexible membership to a set, and for modelling and quantifying the meaning of symbols. Membership functions may represent an individual's subjective notion of a value class.

Definition B.1. A fuzzy set in an universe of discourse X is characterized by a membership function $\mu_A(x)$ that takes values in the interval $[0,1]$.

Fuzzy systems are knowledge-based or rule-based systems. In the centre of a fuzzy system is a knowledge base consisting of the so-called IF-THEN rules. A fuzzy IF-THEN rule is an IF-THEN statement in which some words are characterized by continuous membership functions For example, the following is a fuzzy IF-THEN rule:

IF the speed of a car is low, THEN apply less force to the accelerator B-4

where the words "high" and "less" are characterized by membership functions. A fuzzy set is constructed from a collection of fuzzy IF-THEN rules. Formally:

IF premise (antecedent), THEN conclusion (consequent) B-5

In the linguistic fuzzy system (also called the Mamdani model), both the antecedent and the consequent are fuzzy propositions. A general form of the linguistic fuzzy rules is:

$$R_i : \text{If } x \text{ is } A_i \text{ then } y \text{ is } B_i,\ i = 1,2,\ldots,K \qquad \text{B-6}$$

where x is the antecedent variable, which represents the input to the fuzzy system, and y is the consequent variable representing the output of the fuzzy system. In most cases, real-valued vector inputs and outputs are used: $x \in X \subset \Re^p$ and $y \in Y \subset \Re^q$. A_i and B_i are linguistic terms (fuzzy sets) defined by multivariable membership functions $\mu_{A_i}(x) : X \rightarrow [0,1]$ and $\mu_{B_i}(y) : Y \rightarrow [0,1]$, respectively. Finally, K denotes the number of rules in the system.

Instead of considering the fuzzy IF-THEN rules in the form of Equation B-6, in the Takagi-Sugeno-Kang (TSK) system, the rules consequent are crisp functions of the model inputs:

$$R_i : \text{If } x \text{ is } A_i \text{ then } y_i = f_i(x),\ i = 1, 2, \ldots, K \qquad \text{B-7}$$

where $x \in \Re^p$ is the input (antecedent) variable and $y_i \in \Re$ is the output (consequent) variable. R_i denotes the ith rules, and K is the number of rules in the rule base. A_i is the antecedent fuzzy set of the ith rule. As in the linguistic model, the antecedent proposition "x is A_i" is usually expressed as a logical combination of simple propositions with invariant fuzzy set defined for the individual components of x, often in the conjunctive form:

$$R_i : \text{If } x_1 \text{ is } A_{i1} \text{ and } x_2 \text{ is } A_{i2} \text{ and ... and } x_p \text{ is } A_{ip} \text{ then } y_i = f_i(x),\ i = 1, 2, \ldots, K \qquad \text{B-8}$$

The consequent functions f_i are typically chosen as instances of a suitable parameterised function, whose structure remains equal in all the rules and only in the parameters vary. A special case of the TSK fuzzy systems is the system that uses rules in the form of Equation B-8 but $f_i(x)$ is a linear function of x: $f_i(x) = c_i x + b_i$ where c_i and b_i are constants.

B.2 Fuzzy Sets Operations and Properties

Assume that A and B are fuzzy sets defined in the same universe of discourse U.

1. A and B are equal if an only if $\mu_A(x) = \mu_B(x)$ for all $x \in U$.

2. B contains A, denoted by $A \subset B$, if and only if $\mu_A(x) \leq \mu_B(x)$ for all $x \in U$.

3. The complement of A is a fuzzy set $\overline{A}$ in U whose membership function is defined as:

$$\mu_{\overline{A}}(x) = 1 - \mu_A(x) \qquad \text{B-9}$$

4. The union of A and B is a fuzzy set in U, denoted by $A \cup B$, with the membership function defined as (Figure B-1):

$$\mu_{A \cup B} = \max[\mu_A(x), \mu_B(x)] \qquad \text{B-10}$$

5. The intersection of A and B is a fuzzy set $A \cap B$ with membership function (Figure B-2):

$$\mu_{A \cap B} = \min[\mu_A(x), \mu_B(x)] \qquad \text{B-11}$$

6. Morgan's Laws are true for fuzzy sets:

$$\overline{A \cup B} = \overline{A} \cap \overline{B} \qquad \text{B-12}$$

$$\overline{A \cap B} = \overline{A} \cup \overline{B} \qquad \text{B-13}$$

7. Extension Principle 1: If A is a fuzzy set in the universe U and f is a mapping from U to the universe of discourse V such that $y = f(x)$, then the extension principle allows to define a fuzzy set B in V such that:

$$B = f(A) = \{(y, \mu_B(y)) \; y = f(x), \; x \in U\} \qquad \text{B-14}$$

where,

$$\mu_B(y) = \left\{ \begin{array}{cc} \sup \mu_A(x) & \text{if } f^{-1}(y) \neq 0 \\ 0 & \text{if } f^{-1}(y) = 0 \end{array} \right\} \qquad \text{B-15}$$

8. Zadeh's Principle: Let X be a cartesian product of the universes $U_1, U_2, \ldots, U_n$ such that $X = U_1 * U_2 * \ldots * U_n$ and $A_1, A_2, \ldots, A_n$ are fuzzy sets in these universes. f is a mapping from X to the universe of discourse V, where $y = f(x_1, x_2, \ldots, x_n)$. The fuzzy set B in V is defined as:

$$B\{(y, \mu_B(y)) \; y = f(x_1, x_2, \ldots, x_n), \; (x_1, x_2, \ldots, x_n) \in X\} \qquad \text{B-16}$$

where

$$\mu_B(y) = \left\{ \begin{array}{cc} \sup \min\{\mu_{A_1}(x_1), \ldots, \mu_{A_n}(x_n)\} & \text{if } f^{-1}(y) \neq 0, (x_1, x_2, \ldots, x_n) \in f^{-1}(y) \\ 0 & \text{if } f^{-1}(y) = 0 \end{array} \right\} \text{B-17}$$

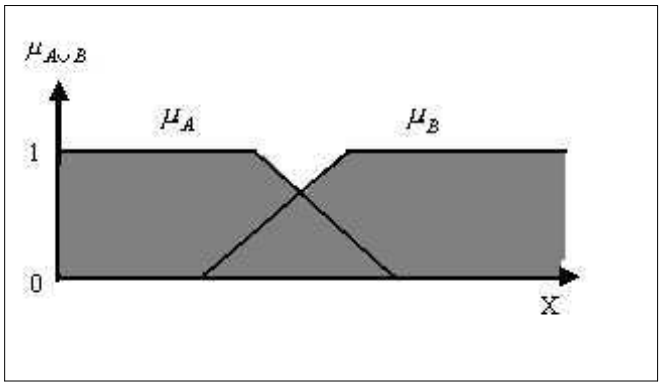

Figure B-1: Union of fuzzy sets A and B.

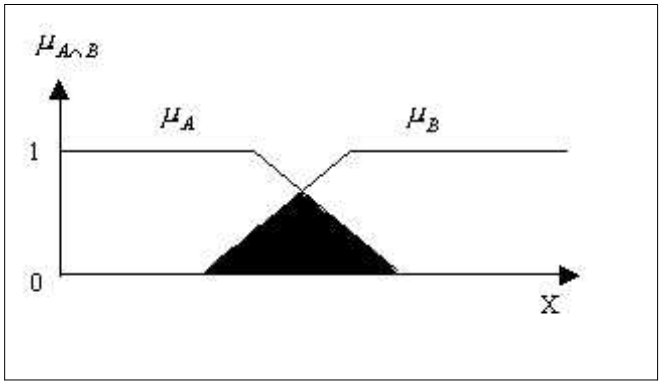

Figure B-2: Intersection of fuzzy sets A and B.

B.3 Properties of a Fuzzy System (Set of Rules)

1. A set of fuzzy IF-THEN rules is complete if for any $x \in U$, there exists at least one rule-base, say rule R_l (in the form of Equations B-6 or B-7), such that

$$\mu_{A_i^l}(x_i) \neq 0 \qquad \text{B-18}$$

for all $i = 1, 2, \ldots, K$.

2. A set of fuzzy IF-THEN rules is consistent if there are no rules with the same IF parts but different THEN parts.

3. A set of fuzzy IF-THEN rules is continuous if it does not exist such neighbouring rules whose THEN part fuzzy sets have empty intersection.

B.4 Fuzzy Relations

In a fuzzy inference engine, fuzzy logic principles are used to combine the fuzzy IF-THEN rules in the fuzzy rule base into a mapping from a fuzzy set A in U to a fuzzy set B in V. A fuzzy relation of the form:

$$\text{If } A \text{ then } B \text{ or } A \rightarrow B \qquad \text{B-19}$$

is denoted as R (relational matrix) and is defined as a relationship of two fuzzy sets $A \in U$, $B \in V$, and it is a subset on the Cartesian product $U * V$. R is characterized by the

membership function $\mu_R(x,y)$, $x \in U, y \in V$ such that:

$$R = A * B = \sum \mu_R(x,y)/(x,y) = \left\{ \begin{array}{c} \sum \min(\mu_A(x), \mu_B(y)) \\ \sum \mu_A(x)\mu_B(y) \end{array} \right\} \qquad \text{B-20}$$

the $\sum$ represents all possible combinations of all elements of both universes of discourse and not the mathematical operation sum.

If R is a fuzzy relation in $U * V$ and A is a fuzzy set in U then the fuzzy set B in V is given by:

$$B = A \circ R \qquad \text{B-21}$$

B is inferred from A using the relational matrix R which defines the mapping between U and V, and the operation $\circ$ is defined as the "max-min" operation.

B.5 Fuzzifiers and Defuzzifiers

The fuzzy inference engine combines the rules in the fuzzy rule-base into a mapping from fuzzy set A in U to fuzzy set B in V. Because in most applications the input and output of the fuzzy system are real valued numbers, interfaces must be constructed between the fuzzy inference system and the environments. The interfaces are the fuzzifier and the defuzzifier (Figure B-3).

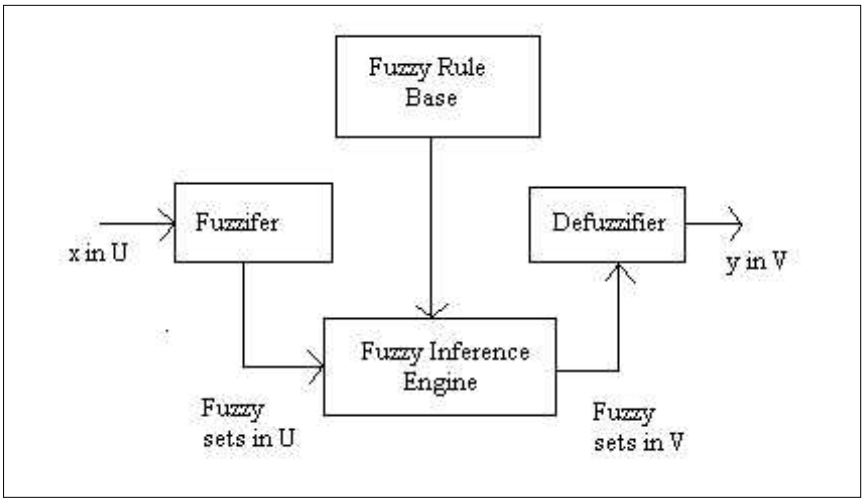

Figure B-3: Basic configuration of fuzzy systems with fuzzifier and defuzzifier.

Fuzzy systems can be used either as open-loop controllers or closed-loop controllers. When used as an open-loop controller, the fuzzy system usually sets up some controller parameters and then the system operates according to these parameters. When used as a closed-loop controller, the fuzzy system measures the outputs of the process and takes control actions on the process continuously. However, fuzzy systems have been applied to a wide variety of fields ranging from control, signal processing, communications and expert systems (modelling).

B.5.1 Fuzzifiers

Fuzzification is the process which allows to convert a numeric input into a fuzzy input. There are two types of fuzzifiers.

Fuzzification maps a crisp input $x_i \in U$ into a fuzzy set A_{x_i} in U such that:

1. A_{x_i} is a fuzzy singleton:

$$\mu_{A_{x_i}}(x) = \left\{ \begin{array}{ll} 1 & \text{if } x = x_i \\ 0 & \text{otherwise} \end{array} \right\} \qquad \text{B-22}$$

2. A_{x_i} is a fuzzy set (triangular, trapezoidal, Gaussian):

$$\mu_{A_{x_i}}(x) = \left\{ \begin{array}{ll} 1 & \text{if } x = x_i \\ \text{decreases} & \text{from 1 as } x \text{ moves from } x_i \end{array} \right\} \qquad \text{B-23}$$

B.5.2 Defuzzifiers

Defuzzification is the conversion of a fuzzy quantity into a crisp one. Formally, a defuzzifier is defined as a mapping from fuzzy set B in $V \subset \Re$ (which is the output of the fuzzy inference engine) to a crisp point $y^* \in V$. The defuzzifier specifies a point in V that best represents the fuzzy set B. The following three criteria should be considered in choosing a defuzzification scheme:

- Plausibility: the point y^* should represent B from an intuitive point of view;
- Computational simplicity;

- Continuity: a small change in B should not result in a large change in y^*.

The defuzzifier is only necessary for the Mamdani system type. Three different defuzzifiers are presented next.

B.5.2.1 Centre of Gravity Defuzzifier

The centre of gravity defuzzifier specifies y^* as the centre of the area covered by the membership function of B, that is:

$$y^* = \frac{\int_V y\mu_B(y)dy}{\int_V \mu_B(y)dy} \qquad \text{B-24}$$

where $\int_V$ is the conventional integral.

B.5.2.2 Centre Average Defuzzifier

The fuzzy set B is the union or intersection of M fuzzy sets, a good approximation of Equation B-24 is the weighted average of the centers of the M fuzzy sets, with the weights equal to heights of the corresponding fuzzy sets. Let $\overline{y}^l$ be the centre of the l'th fuzzy set and w_l be its height, the centre average defuzzifier determines y^* as:

$$y^* = \frac{\sum_{l=1}^{M} \overline{y}^l w_l}{\sum_{l=1}^{M} w_l} \qquad \text{B-25}$$

B.5.2.3 Maximum Defuzzifier

The maximum defuzzifier chooses y^* as the point in V at which $\mu_B(y)$ achieves its maximum value. Define the set:

$$hgt(B) = \left\{ y \in V | \mu_B(y) = \sup_{y \in V} \mu_B(y) \right\} \qquad \text{B-26}$$

$hgt(B)$ is the set of all points in V at which $\mu_B(y)$ achieves its maximum value. The maximum defuzzifier defines y^* as an arbitrary element in $hgt(B)$.

$$y^* = \text{any point in } hgt(B) \qquad \text{B-27}$$

B.6 Fuzzy Control

A simple fuzzy logic controller can generally be depicted by a block diagram such as that shown in Figure B-4. A number of assumptions are implicit in a fuzzy control system design:

1. The plant is observable and controllable: state, input, and output variables are usually available for observation and measurement or computation;

2. There exists a body of knowledge comprised of a set of expert production linguistic rules;

3. A solution exists;

4. The control engineer is looking for a "good enough" solution, not necessarily the optimum one;

5. A controller will be designed to the best of the available knowledge and within an acceptable range of precision;

6. The problems of stability and optimality are still open problems in fuzzy controller design.

The knowledge-base module in Figure B-4 contains knowledge about all the input and output fuzzy partitions. It includes the term set and the corresponding membership functions defining the input variables to the fuzzy rule-base system and the output variables, or control actions, to the plant under control.

The steps in designing a simple fuzzy logic control system are as follows:

1. Identify the variables (input, states, and outputs) of the plant;

2. Partition the universe of discourse or the interval spanned by each variable into a number of fuzzy subsets, assigning each a linguistic label (subsets include all the elements in the universe);

3. Assign or determine a membership function for each fuzzy subset;

4. Assign the fuzzy relationships between the inputs (or states) fuzzy subsets on the one

hand and the outputs fuzzy subsets on the other hand, thus forming the rule-base;

5. Choose appropriate scaling factors for the input and output variables in order to normalize the variables to the $[0, 1]$ or the $[-1, 1]$ interval;

6. Fuzzify the inputs to the controller;

7. Use fuzzy appropriate reasoning to infer the output contributed from each rule;

8. Aggregate the fuzzy outputs recommended by each rule;

9. Apply defuzzification to form a crisp output.

The results of the nine steps mentioned above are fixed in a nonadaptive simple fuzzy logic controller. In an adaptive fuzzy logic controller, they are adaptively modified based on some adaptation law in order to optimize the controller.

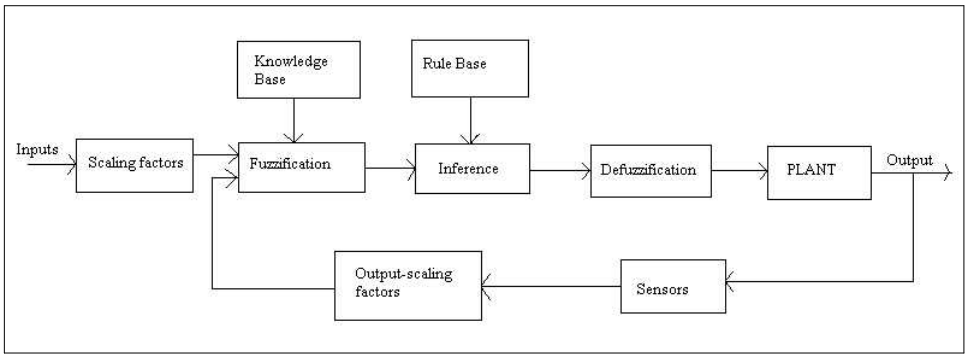

Figure B-4: A simple fuzzy logic control system block diagram.

B.6.1 Fuzzy Linguistic Controllers

The core of a fuzzy controller is a linguistic description prescribing appropriate action for a given state. Fuzzy linguistic descriptions involve associations of fuzzy variables and procedures for inferring. In order to design a proportional-integral-derivative (PID) like fuzzy controller, it is necessary to choose the input and output variables and the rules of the controller.

B.6.1.1 Input Variables

The most common input variable in fuzzy control is the *error*, or *e*. It is defined on the

universe of discourse of crisp error *e*, which is the deviation of some measured variable *y* from a setpoint or reference *r*. At anytime time $t = k$ crisp error is defined as:

$$e(k) = r - y(k) \qquad \text{B-28}$$

The change in error, Δe, between two successive time steps is also commonly used as an input variable. It is defined on the universe of discourse of crisp changes in error. At time $t = k$ the crisp change in error is the difference between the present error and the error in the previous time step $t = k - 1$

$$\Delta e = e(k) - e(k-1) \qquad \text{B-29}$$

The sum of errors $\overline{e}(k)$ may be used as an input fuzzy variable also. It takes into account the integrated effect of all past errors and is defined as:

$$\overline{e}(k) = \sum_{i=1}^{k} e(i) \qquad \text{B-30}$$

B.6.1.2 Output Variables

Output variables may be any directly manipulated variable. An output fuzzy variable *u* can be defined on the universe of discourse of a crisp manipulated variable. The change in output Δu is more often used as the output variable. Δu indicates the extent of change of the control variable *u* at time $t = k$, i.e. the change in action. Therefore, if the defuzzified output at time *k* is $\Delta u^*(k)$, the overall crisp output of the controller will be:

$$u(k) = u(k-1) + \Delta u^*(k) \qquad \text{B-31}$$

B.6.1.3 IF-THEN Rules and Inference

For the proportional fuzzy controller, as a SISO fuzzy controller, the rule-base can be constructed in a symmetric fashion with rules of the following form:

1. If *e* is NB then *u* is NB
2. If *e* is NM then *u* is NM
3. If *e* is NS then *u* is NS
4. If *e* is ZE then *u* is ZE
5. If *e* is PS then *u* is PS
6. If *e* is PM then *u* is PM

7. If e is PB then u is PB

where NB, NM, NS, ZE, PS, PM, and PB are linguistic values representing “negative big”, “negative medium”, “negative small”, “zero”, “positive small”, and so on.

A fuzzy controller emulating a conventional proportional-derivative (PD) model of controller would consist of rules of the form:

$$\text{If } e \text{ is } A \text{ and } \Delta e \text{ is } B \text{ then } u \text{ is } C \qquad \text{B-32}$$

The complete set of rules is shown in tabulated form in Table B-1.

Table B-1: Rule table for a PD fuzzy controller.

Output u		change of error $\Delta e(k)$						
		NB	NM	NS	ZE	PS	PM	PB
error e	NB	NB	NB	NB	NB	NM	NS	ZE
	NM	NB	NB	NB	NM	NS	ZE	PS
	NS	NB	NB	NM	NS	ZE	PS	PM
	ZE	NB	NM	NS	ZE	PS	PM	PB
	PS	NM	NS	ZE	PS	PM	PB	PB
	PM	NS	ZE	PS	PM	PB	PB	PB
	PB	ZE	PS	PM	PB	PB	PB	PB

A proportional-integral (PI) controller would have rules of the form:

$$\text{If } e \text{ is } A \text{ and } \Delta e \text{ is } B \text{ then } \Delta u \text{ is } C \qquad \text{B-33}$$

The complete set of rules is shown in tabulated form in Table B-2.

Table B-2: Rule table for a PI fuzzy controller.

Output Δu		change of error $\Delta e(k)$						
		NB	NM	NS	ZE	PS	PM	PB
error e	NB	NB	NB	NB	NB	NM	NS	ZE
	NM	NB	NB	NB	NM	NS	ZE	PS
	NS	NB	NB	NM	NS	ZE	PS	PM
	ZE	NB	NM	NS	ZE	PS	PM	PB
	PS	NM	NS	ZE	PS	PM	PB	PB
	PM	NS	ZE	PS	PM	PB	PB	PB
	PB	ZE	PS	PM	PB	PB	PB	PB

Tables B-1 and B-2 are examples of PD and PI configurations, not all controllers have the same configuration, this depends on the specific problem at hand.

The rule form of a PID like fuzzy controller is:

$$\text{If } e \text{ is } A \text{ and } \Delta e \text{ is } B \text{ and } \overline{e} \text{ is C then } u \text{ is } D \qquad \text{B-34}$$

The previous fuzzy algorithms are presented in terms of rules involving fuzzy values as the output variable, such rules are the Mamdani rules. However several fuzzy controllers use rules where the output variable is given in terms of a functional relation of the inputs (TSK systems, Equation B-7).

B.7 References

Akay, M. (2000). Nonlinear Biomedical Signal Processing Vol I : Fuzzy Logic, Neural Networks and New Algorithms, IEEE Press Series on Biomedical Engineering, M. Akay, ed., IEEE Press.

Babuska, R. (1998). Fuzzy Modeling for Control, Kluwer Academic Publishers, Aschen, Germany.

Ross, T. (1995). Fuzzy Logic with Engineering Applications, McGraw-Hill, Inc., United States of America.

Tsoukalas, L. H., and Uhrig, R. E. (1996). Fuzzy and Neural Approaches in Engineering, John Wiley.

Wang, L.-X. (1997). A Course in Fuzzy Systems and Control, Prentice-Hall , Inc., United States of America.

Zadeh, L. A. (1965). “Fuzzy sets.” Information and Control, 8(3), 338-353.

Appendix C

Multiresolution Wavelet Analysis

The objective of signal analysis is to devise a transformation that represents the signal features simultaneously in time and frequency. Standard Fourier analysis decomposes the signal into frequency components and determines the relative strength of each component. It does not tell when a signal exhibited the particular frequency characteristic. In transforming to the frequency domain, time information is lost. Looking at a Fourier transform of a signal, it is impossible to tell when a particular event took place. The short-time Fourier Transform (STFT) analyses a small section of the signal at a time, it maps a signal into a two-dimensional function of time and frequency. The STFT drawback is that once a particular size for the time window in chosen, that window is the same for all frequencies. Wavelet analysis is a windowing technique with variable-sized regions. It allows the use of long time intervals when more precise low frequency information is required, and shorter regions for high frequency information. Wavelet analysis has the ability to perform local analysis.

C.1 Fourier Transform

The Fourier transform rules over linear time-invariant signal processing because sinusoidal waves $e^{i\omega t}$ are eigenvectors of linear time-invariant operators. A linear time-invariant operator L is entirely specified by the eigenvalues $\widehat{h}(\omega)$:

$$\forall \omega \in \Re,\ Le^{i\omega t} = \widehat{h}(\omega)e^{i\omega t} \qquad \text{C-1}$$

To compute Lf, a signal f is decomposed as a sum of sinusoidal eigenvectors $\{e^{i\omega t}\}_{\omega\in\Re}$:

$$f(t) = \frac{1}{2\pi}\int_{-\infty}^{+\infty} F(\omega)e^{i\omega t}d\omega \qquad \text{C-2}$$

If f has a finite energy, the theory of Fourier integrals proves that the amplitude $F(\omega)$ of each sinusoidal wave $e^{i\omega t}$ is the Fourier transform of f:

$$F(\omega) = \int_{-\infty}^{+\infty} f(t)e^{-i\omega t}dt \qquad \text{C-3}$$

Applying the operator L to f in Equation C-2 and inserting the eigenvector expression of Equation C-1 gives:

$$Lf(t) = \frac{1}{2\pi}\int_{-\infty}^{+\infty} F(\omega)\hat{h}(\omega)e^{i\omega t}d\omega \qquad \text{C-4}$$

The operator L amplifies or attenuates each sinusoidal component $e^{i\omega t}$ of f by $\hat{h}(\omega)$. It is a frequency filtering of f.

If the frequency content of a signal were to vary drastically from interval to interval as in a musical scale, the standard Fourier transform would sweep over the entire time axis and wash out any local anormalities in the signal. It is not adequate for such nonstationary signals.

C.1.1 Short-Time Fourier Transform

The windowed short-time Fourier transform (STFT), moves a fixed-duration window over the time function and extracts the frequency content in that interval. This would be suitable for signals that are locally stationary, but globally nonstationary.

The STFT positions a window $g(t)$ at some point τ on the time axis, and calculates the Fourier transform of the signal within the extent or spread of that window:

$$F(\omega,\tau) = \int_{-\infty}^{+\infty} f(t)g^*(t-\tau)e^{-i\omega t}dt \qquad \text{C-5}$$

The inner product between two functions is denoted by:

$$\langle f,g\rangle = \int_{-\infty}^{+\infty} f(t)g^*(t)dt \qquad \text{C-6}$$

When the window $g(t)$ is Gaussian, the STFT is called a Gabor transform. The basis of this transform is generated by modulation and translation of the window function $g(t)$, where ω and τ are modulation and translation parameters, respectively. The difficulty with the STFT is that the fixed-duration window $g(t)$ is accompanied by a fixed frequency resolution and thus allows only a fixed time-frequency resolution. The STFT maps a function of one

variable into a function of two variables, corresponding to the time and frequency. These transforms are highly redundant in the parameters (ω, τ).

C.1.1.1 Discrete Short-Time Fourier Transform

An appreciation of the time-frequency properties of the STFT can be developed by discretising (ω, τ), sampling the continuous STFT, Equation C-5, on a uniform grid to obtain the discrete STFT. With:

$$\omega = m\omega_0 \qquad \tau = n\tau_0 \tag{C-7}$$

$$F(m,n) = \int_{-\infty}^{+\infty} f(t)g^*(t - n\tau_0)e^{-im\omega_0 t}dt = \langle f(t), e^{im\omega_0 t}g^*(t - n\tau_0)\rangle \tag{C-8}$$

This is also the inner product between $f(t)$ and the windowed sinusoid $e^{im\omega_0 t}$ over the spread of $g(t - n\tau_0)$.

The STFT can be interpreted as the convolution of $\tilde{g}(\tau) \triangleq g^*(-\tau)$ with the modulated signal $e^{-i\omega t}f(t)$

$$F(\omega, t) = \tilde{g}(t) * e^{-i\omega t}f(t) \tag{C-9}$$

The discretisation can be carry even further so that the time function itself is sampled, $f(n)$. The discrete version of the STFT is then:

$$F(k,n) = \sum_{m=-\infty}^{\infty} g(m - n)f(m)e^{-i\frac{2\pi}{M}km}, \quad k = 0, 1, \ldots, M - 1 \tag{C-10}$$

where $g(m)$ is a sampled window function of finite extent (or compact support M).

C.1.1.2 Continuous Short-Time Fourier Transform

The continuous STFT (Equation C-5) is a function of the continuous variables ω and τ. The STFT can be conceptualized as the limit of the discrete STFT of Equation C-8 as $m\omega_0 \to \omega$ and $n\tau_0 \to \tau$. The discrete function defined on the grid points involves into a continuous function over the ω, τ plane. The interpretation of constant resolution cells is still applicable, with $m\omega_0 = \omega$, and $n\tau_0 = \tau$.

To summarize these properties, for $g(t) \in L^2(\Re)$ let

$$F(\omega, \tau) = f(t)e^{-i\omega t} * \tilde{g}(\tau) = \int_{-\infty}^{+\infty} f(t)g^*(t - \tau)e^{-i\omega t}dt \tag{C-11}$$

That is, the transform is a highly redundant mapping $L^2(\Re) \rightarrow L^2(\Re^2)$. It can be shown that the reconstruction formula is:

$$f(t) = \frac{1}{2\pi}\int_{-\infty}^{+\infty}\int_{-\infty}^{+\infty} F(\omega,\tau)g(t-\tau)e^{i\omega t}d\omega d\tau \qquad \text{C-12}$$

C.2 Wavelet Transform

Certain signals can be modelled suitably by combining translations and dilations of a simple, oscillatory function of finite duration called a wavelet. A wavelet is a waveform of effective limited duration that has an average value of zero. Wavelet analysis is the breaking up of a signal into shifted and scaled versions of the original (or mother) wavelet.

Consider a real or complex-value continuous-time function $\psi(t)$ with the following properties:

1. The function integrates to zero:

$$\int_{-\infty}^{+\infty}\psi(t)dt = 0 \qquad \text{C-13}$$

2. It is square integrable or, equivalently, has finite energy:

$$\int_{-\infty}^{+\infty}|\psi(t)|^2 dt < \infty \qquad \text{C-14}$$

The function $\psi(t)$ is a mother wavelet or wavelet if it satisfies these two properties as well as the admissibility condition (Equation C-29).

C.2.1 Continuous-Time Wavelet Transform

Let $f(t)$ be any square integrable function. The Continuous-Time Wavelet Transform (CWT) or continuous-time wavelet transform of $f(t)$ with respect to a wavelet $\psi(t)$ is defined as:

$$W(a,b) = \int_{-\infty}^{+\infty} f(t)\frac{1}{\sqrt{|a|}}\psi^*\left(\frac{t-b}{a}\right)dt \qquad \text{C-15}$$

where a and b are real and $*$ denotes complex conjugation. Thus, the wavelet transform is a function of two variables. Both $f(t)$ and $\psi(t)$ belong to $L^2(\Re)$, the set of square integrable

functions, also called the set of energy signals. Equation C-15 can be written in a more compact form by defining $\psi_{a,b}(t)$ as:

$$\psi_{a,b}(t) = \frac{1}{\sqrt{|a|}}\psi\left(\frac{t-b}{a}\right) \quad \text{C-16}$$

Then, combining Equations C-15 and C-16,

$$W(a,b) = \int_{-\infty}^{+\infty} f(t)\psi^*_{a,b}(t)dt \quad \text{C-17}$$

Notice that

$$\psi_{1,0}(t) = \psi(t) \quad \text{C-18}$$

The normalizing factor of $\frac{1}{\sqrt{|a|}}$ ensures that the energy stays the same for all a and b:

$$\int_{-\infty}^{+\infty}|\psi_{a,b}(t)|^2 dt = \int_{-\infty}^{+\infty}|\psi(t)|^2 dt \quad \text{C-19}$$

For any given value of a, the function $\psi_{a,b}(t)$ is a shift of $\psi_{a,0}(t)$ by an amount b along the time axis. The variable b represents time shift or translation. From:

$$\psi_{a,0}(t) = \frac{1}{\sqrt{|a|}}\psi\left(\frac{t}{a}\right) \quad \text{C-20}$$

it follows that $\psi_{a,0}(t)$ is a time-scaled and amplitude-scaled version of $\psi(t)$. Since a determines the amount of time scaling or dilation, it is referred to as the scale or dilation variable. If $a > 1$, there is a stretching of $\psi(t)$ along the time axis, whereas if $0 < a < 1$, there is a contraction of $\psi(t)$. Negative values of a result in a time reversal in combination with dilation. As a increases, wavelets are stretched and analyse low frequencies, while for small a, contracted wavelets analyse high frequencies. Since the CWT is generated using dilates and translates of the single function $\psi(t)$, the wavelet for the transform is referred to as the mother wavelet.

The CWT is essentially a collection of innerproducts of a signal $f(t)$ and the translated and dilated wavelet $\psi_{a,b}(t)$ for all a and b:

$$W(a,b) = \langle f(t), \psi_{a,b}(t)\rangle \quad \text{C-21}$$

C.2.1.1 The Continuous-Time Wavelet Transform as an Operator

The CWT takes a member in the set of square integrable functions of one real variable in

$L^2(\Re)$ and transforms it into a member of the set of functions of two real variables. It can be seen as a mapping operator from $L^2(\Re)$ to the latter set.

$$W_\psi[f(t)] = W(a,b) \qquad \text{C-22}$$

Then $W_\psi[]$ is to be read "CWT with respect to $\psi(t)$ of". The transform depends not only on the function $f(t)$ but also on the mother wavelet. These are some properties of the CWT using the operator notation:

1. Linearity

$$W_\psi[\alpha f(t) + \beta g(t)] = \alpha W_\psi[f(t)] + \beta W_\psi[g(t)] \qquad \text{C-23}$$

for scalars α and β and functions $f(t)$, $g(t) \in L^2(\Re)$.

2. Translation

$$W_\psi[f(t-\tau)] = W(a, b-\tau) \qquad \text{C-24}$$

3. Scaling

$$W_\psi\left[\frac{1}{\sqrt{\alpha}} f\left(\frac{1}{\alpha}\right)\right] = W\left(\frac{a}{\alpha}, \frac{b}{\alpha}\right) \qquad \text{C-25}$$

for $\alpha > 0$.

4. Wavelet shifting: Let $\widehat{\psi}(t) = \psi(t-\tau)$. Then

$$W_{\widehat{\psi}}[f(t)] = W(a, b+a\tau) \qquad \text{C-26}$$

The CWT obtained by shifting the wavelet is different from the one obtained by shifting the signal.

5. Wavelet scaling: Let $\widehat{\psi}(t) = \frac{\psi(t/\alpha)}{\sqrt{|\alpha|}}$. Then

$$W_{\widehat{\psi}}[f(t)] = W(a\alpha, b) \qquad \text{C-27}$$

CWT is a scaled version of the original in the a variable.

6. Linear combination of wavelets: Given two wavelets $\psi_1(t)$ and $\psi_2(t)$, their linear combination $\alpha\psi_1(t) + \beta\psi_2(t)$ for scalars α and β is also a wavelet.

$$W_{\alpha\psi_1+\beta\psi_2}[f(t)] = \alpha W_{\psi_1}[f(t)] + \beta W_{\psi_2}[f(t)] \quad \text{C-28}$$

C.2.1.2 Inverse Continuous-Time Wavelet Transform

If the mother wavelet satisfies the (sufficient) condition:

$$C = \int_{-\infty}^{+\infty} \frac{|\Psi(\omega)|^2}{|\omega|} d\omega \quad \text{C-29}$$

where $\Psi(\varpi)$ is the Fourier transform of $\psi(t)$, and is such that $0 < C < \infty$, then

$$f(t) = \frac{1}{C} \int_{a=-\infty}^{+\infty} \int_{b=-\infty}^{+\infty} \frac{1}{|a|^2} W(a,b)\psi_{a,b}(t)\, da\, db \quad \text{C-30}$$

The condition in Equation C-29 is known as the admissibility condition on $\psi(t)$.

Equation C-30 expresses $W(a,b)$ as the convolution of $f(t)$ and $\psi_{a,0}(-b)$. In the frequency domain this becomes

$$\int_{b=-\infty}^{+\infty} W(a,b)e^{-jwb}db = \sqrt{|a|}\, F(\omega)\Psi^*(a\omega) \quad \text{C-31}$$

where $F(\omega)$ and $\Psi(\omega)$ are the Fourier transforms of $f(t)$ and $\psi(t)$ respectively. Multiplying both sides of Equation C-31 by $\Psi(a\omega)/|a|^{3/2}$ and integrating with respect to a yields

$$\int_{a=-\infty}^{+\infty} \int_{b=-\infty}^{+\infty} \frac{1}{|a|^{3/2}} W(a,b)\Psi(a\omega)e^{-j\omega b} da\, db = F(\omega) \int_{a=-\infty}^{+\infty} \frac{|\Psi(a\omega)|^2}{|a|} da \quad \text{C-32}$$

and

$$\int_{a=-\infty}^{+\infty} \frac{|\Psi(a\omega)|^2}{|a|} da = \int_{\omega=-\infty}^{+\infty} \frac{|\Psi(\omega)|^2}{|w|} d\omega = C \quad \text{C-33}$$

where C is the constant from the admissibility condition. Therefore,

$$F(\omega) = \frac{1}{C} \int_{a=-\infty}^{+\infty} \int_{b=-\infty}^{+\infty} \frac{1}{|a|^{3/2}} W(a,b)\Psi(a\omega)e^{-j\omega b} da\, db \quad \text{C-34}$$

The expression of the inverse CWT in Equation C-30 is obtained by taking the inverse Fourier transform on both sides of Equation C-34.

C.2.2 Discrete-Time Wavelet Transform

The discrete-time wavelet transform (DTWT) is generated by sampling the wavelet

parameters (a, b) on a grid or lattice.

Let the sampling lattice be

$$a = a_0^m \qquad b = nb_0a_0^m \tag{C-35}$$

so that

$$\psi_{mn}(t) = a_0^{-m/2}\psi(a_0^{-m}t - nb_0) \tag{C-36}$$

where $m, n \in Z$. If this set is complete in $L^2(\Re)$ for some choice of $\psi(t)$, a, b, then the $\{\psi_{mn}\}$ are called affine wavelets. Then we can express any $f(t) \in L^2(\Re)$ as the superposition:

$$f(t) = \sum_m \sum_n d_{m,n}\psi_{mn}(t) \tag{C-37}$$

where the wavelet coefficient $d_{m,n}$ is the inner product:

$$d_{m,n} = \langle f(t), \psi_{mn}(t) \rangle = \frac{1}{a_0^{m/2}} \int f(t)\psi(a_0^{-m}t - nb_0)dt \tag{C-38}$$

The two-dimensional sequence $d_{m,n}$ is commonly referred to as the DTWT of $f(t)$. DTWT is still the transform of a continuous-time signal. The discretisation is only in the a and b variables.

The orthonormal wavelets $\{\psi_{mn}\}$ satisfy:

$$\int \psi_{mn}(t)\psi_{m'n'}(t)dt = \left\{ \begin{array}{ll} 1 & m = m', n = n' \\ 0 & otherwise \end{array} \right\} \tag{C-39}$$

and are orthonormal in both indices. This means, that for the same scale m they are orthonormal in time, and they are also orthonormal across the scales.

C.2.3 Examples of Wavelets

C.2.3.1 Daubechies Wavelets

Daubechies wavelets have a support of a minimum size for any given number p of vanishing moments. They are wavelets of compact support and can be computed with finite

impulse response conjugate mirror filters h. Consider the real causal filters $h[n]$, which implies that $\widehat{h}$ is a trigonometric polynomial:

$$\widehat{h}(\omega) = \sum_{n=0}^{N-1} h[n]e^{-in\omega} \qquad \text{C-40}$$

To ensure that ψ has p vanishing moments, $\widehat{h}$ must have a zero of order p at $\omega = \pi$. A minimum size polynomial having p zeros at $\omega = \pi$, is:

$$\widehat{h}(\omega) = \sqrt{2}\left(\frac{1+e^{-i\omega}}{2}\right)^{p} R(e^{-i\omega}) \qquad \text{C-41}$$

The difficulty is to design a polynomial $R(e^{-i\omega})$ of minimum degree m such that $\widehat{h}$ satisfies:

$$\left|\widehat{h}(\omega)\right|^2 + \left|\widehat{h}(\omega+\pi)\right|^2 = 2 \qquad \text{C-42}$$

As a result, h has $N = m + p + 1$ non-zero coefficients. The minimum degree of R is $m = p - 1$.

The minimum degree polynomial

$$R(e^{-i\omega}) = r_0 \prod_{k=0}^{m} (1 - a_k e^{-iw}) \qquad \text{C-43}$$

Let $z = e^{-i\omega}$:

$$R(z)R(z^{-1}) = r_0^2 \prod_{k=0}^{m} (1 - a_k z)(1 - a_k z^{-1}) \qquad \text{C-44}$$

To design $R(z)$ that satisfies Equation C-44, lets choose each root a_k of R among a pair $(c_k, 1/c_k)$ and include a_k^* as a root to obtain real coefficients. This procedures yields a polynomial of minimum degree $m = p - 1$, with $r_0^2 = 2^{p-1}$. The resulting filter h of minimum size has $N = p + m + 1 = 2p$ non zero coefficients.

If ψ is a wavelet with p vanishing moments that generates an orthonormal basis of $L^2(\Re)$, then it has a support of size larger than or equal to $2p - 1$. A daubechies wavelet has a minimum size support equal to $[-p + 1, p]$. The support of the corresponding scaling function ϕ is $[0, 2p - 1]$. Figure C-1 displays the graphs of ψ for $p = 2, 3, \ldots, 10$.

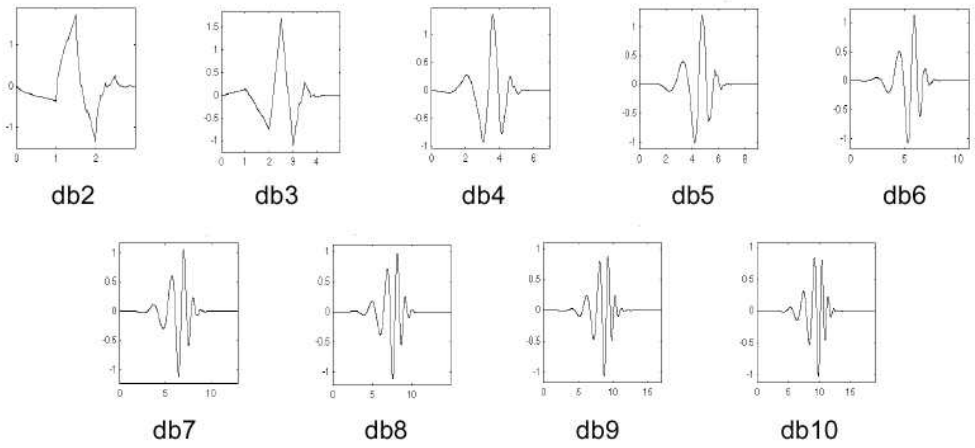

Figure C-1: Daubechies wavelet ψ with p $= 2, 3, 4, 5, 6, 7, 8, 9, 10$ vanishing moments.

C.2.3.2 Coiflet Wavelets

The family of coiflet wavelets ψ has p vanishing moments and a minimum size support, and the scaling functions satisfy:

$$\int \phi(t)dt = 1 \text{ and } \int t^k \phi(t)dt = 0 \text{ for } 1 \leq k \leq p \qquad \text{C-45}$$

Such scaling functions are useful in establishing precise quadrature formulas. The coiflets wavelets ψ are shows in Figure C-2.

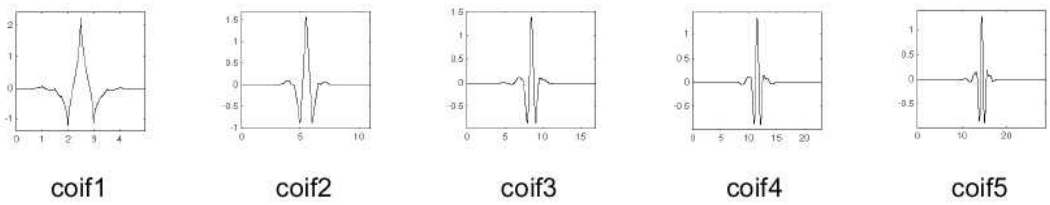

Figure C-2: Coiflets wavelets with p $= 1, 2, 3, 4, 5$.

C.2.3.3. Mexican Hat Wavelets

The mexican hat wavelet is equal to the second derivative of a Gaussian. The normalised mexican hat wavelet is:

$$\psi(t) = \frac{2}{\pi^{1/4}\sqrt{3\sigma}} \left(\frac{t^2}{\sigma^2} - 1 \right) \exp\left(\frac{-t^2}{2\sigma^2} \right) \qquad \text{C-46}$$

For $\sigma = 1$, Figure C-3 plots $-\psi$.

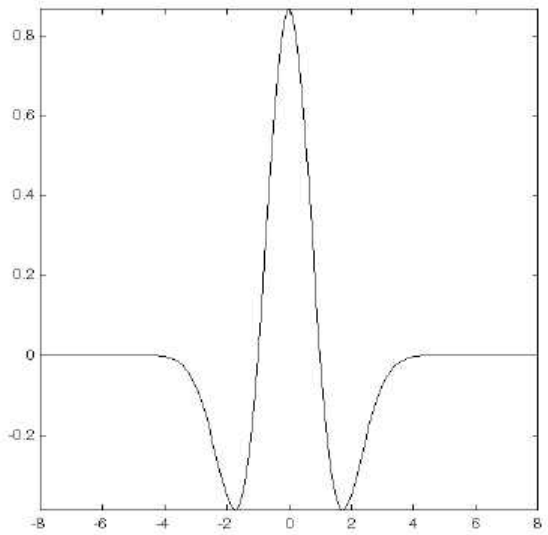

Figure C-3: Mexican hat wavelet for $\sigma = 1$.

C.2.3.4 Meyer Wavelets

A meyer wavelet is a frequency band-limited function whose Fourier transform is smooth. This smoothness provides a much faster asymptotic decay in time. These wavelets are constructed with conjugate mirror filters $\hat{h}(\omega)$ that are C^n and satisfy:

$$\hat{h}(\omega) = \left\{ \begin{array}{cc} \sqrt{2} & \text{if } \omega \in [-\pi/3, \pi/3] \\ 0 & \text{if } \omega \in [-\pi, -2\pi/3] \cup [2\pi/3, \pi] \end{array} \right\} \qquad \text{C-47}$$

The only degree of freedom is the behaviour of $\hat{h}(\omega)$ in the transition bands $[-2\pi/3, -\pi/3] \cup [\pi/3, 2\pi/3]$. It must satisfy the quadrature condition:

$$\left|\hat{h}(\omega)\right|^2 + \left|\hat{h}(\omega + \pi)\right|^2 = 2 \qquad \text{C-48}$$

and to obtain C^n junctions at $|\omega| = \pi/3$ and $|\omega| = 2\pi/3$, then n first derivatives must vanish at these abscissa. The scaling function $\hat{\phi}(\omega) = \prod_{p=1}^{+\infty} 2^{-1/2} \hat{h}(2^{-p}\omega)$ has a compact support and

$$\hat{\phi}(\omega) = \left\{ \begin{array}{cc} 2^{-1/2}\hat{h}(\omega/2) & \text{if } |\omega| \leq 4\pi/3 \\ 0 & \text{if } |\omega| > 4\pi/3 \end{array} \right\} \qquad \text{C-49}$$

The resulting wavelet is

$$\hat{\psi}(\omega) = \left\{ \begin{array}{cc} 0 & \text{if } |\omega| \leq 2\pi/3 \\ 2^{-1/2} e^{-i\omega/2} \hat{h}^* \left(\frac{\omega}{2} + \pi\right) & \text{if } 2\pi/3 \leq |\omega| \leq 4\pi/3 \\ 2^{-1/2} e^{-i\omega/2} \hat{h}^* \left(\frac{\omega}{4}\right) & \text{if } 4\pi/3 \leq |\omega| \leq 8\pi/3 \\ 0 & \text{if } |\omega| > 8\pi/3 \end{array} \right\} \qquad \text{C-50}$$

Since $\hat{\psi}(\omega)$ in the neighbourhood of $\omega = 0$, all its derivatives are zero at $\omega = 0$, which proves that ψ has an infinite number of vanishing moments. Figure C-4 shows the meyer wavelet ψ.

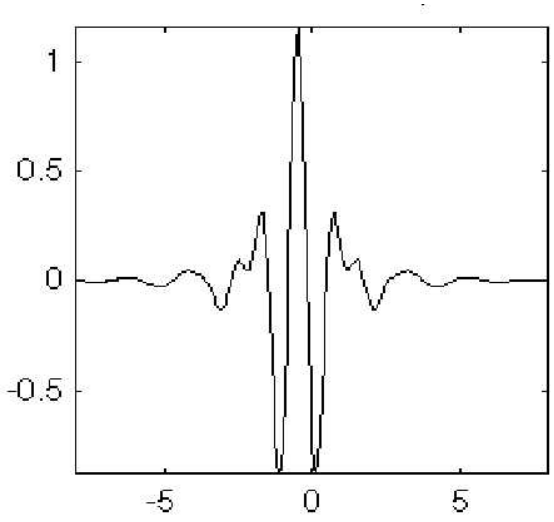

Figure C-4: The meyer wavelet ψ.

C.3 Multiresolution Signal Decomposition

Multiresolution signal analysis (MRA) provides the links between orthonormal wavelet families of compact support, and the pyramid-dyadic tree expansions of a signal. In this representation, a function $f \in L^2$ is expressed as a limit of successive approximations, each of which is a smoothed version of $f(t)$. These successive approximations correspond to different resolutions. This smoothing is accomplished by convolution with a low-pass

kernel called the scaling function $\phi(t)$.

C.3.1 Multiresolution Analysis Spaces

A multiresolution analysis consists of a sequence of closed subspaces $\{V_m | m \in Z\}$ of $L^2(\Re)\}$ which have the following properties:

- Containment:

$$\ldots V_2 \subset \underset{\leftarrow Coarser}{V_1} \subset V_0 \subset \underset{Finer\rightarrow}{V_{-1}} \subset V_{-2} \ldots \qquad \text{C-51}$$

- Completeness:

$$\bigcap_{m \in Z} V_m = \{0\} \qquad \bigcup_{m \in Z} V_m = L^2(\Re) \qquad \text{C-52}$$

- Scaling property:

$$f(x) \in V_m \Leftrightarrow f(2x) \in V_{m-1} \qquad \text{C-53}$$

for any function $f \in L^2(\Re)$.

- The Basis/Frame property: There exists a scaling function $\phi(t) \in V_0$ such that $\forall m \in Z$, the set

$$\{\phi_{mn}(t) = 2^{-m/2}\phi(2^{-m}t - n)\} \qquad \text{C-54}$$

is an orthonormal basis for V_m, i.e.

$$\int \phi_{mn}(t)\phi_{mn'}(t)dt = \delta_{n-n'} \qquad \text{C-55}$$

Let W_m be the orthogonal component of V_m in V_{m-1}, i.e.

$$V_{m-1} = V_m \oplus W_m \qquad \text{C-56}$$

$$V_m \perp W_m \qquad \text{C-57}$$

Furthermore, let the direct sum of the possibly infinite spaces W_m span $L^2(\Re)$:

$$\ldots \oplus W_j \oplus W_{j-1} \ldots \oplus W_0 \ldots \oplus W_{-j+1} \oplus W_{-j+2} \ldots = L^2(\Re) \qquad \text{C-58}$$

Associate the scaling function $\phi(t)$ with the space V_0, and the wavelet function with W_0. The projection operators P_m, Q_m from $L^2(\Re)$ onto V_m and W_m respectively. The completeness property ensures that $\lim_{m\to-\infty} P_m f = f$, for any $f \in L^2(\Re)$. The containment property implies that as m decreases $P_m f$ leads to successively better approximations of f.

Any function f can be approximated by $P_{m-1}f$, its projection onto V_{m-1}. From Equation C-56 this can be expressed as a sum of projections onto V_m, and W_m

$$P_{m-1}f = P_m f + Q_m f \qquad \text{C-59}$$

$P_m f$ is the low pass part of f in V_m and $Q_m f$ is the high frequency detail or difference, i.e. the increment in information in going from V_m to V_{m-1}.

Equation C-59 can be expressed as $Q_m f = P_{m-1}f - P_m f$, where $Q_m f \in W_m$. Hence, it can be said that the orthogonal or complementary space W_m is given by the difference $V_{m-1} \ominus V_m$. Now $\phi(t-n) \in V_0$ and $\phi(2t-n) \in V_{-1}$. Since $V_0 = span\{\phi(t-n)\}$ and $V_{-1} = span\{\phi(2t-n\}$, it is reasonable to expect the existence of a function $\psi(t) \in W_0$, such that $W_0 = span\{\psi(t-n)\}$. This function $\psi(t)$ is the wavelet function associated with the multiscale analysis.

By the scaling property, $W_m = span\{\psi(2^{-m}t-n)\}$. The term W_m is also generated by the translates and dilations $\{\psi_{mn}(t)\}$ of a single wavelet $\psi(t)$. The containment and completeness properties together with $W_m \perp V_m$, and $V_{m-1} = V_m \oplus W_m$ imply that the spaces W_m are mutually orthogonal and that their direct sum is $L^2(\Re)$. Since for each m, the set $\{\psi_{mn}(t); n \in Z\}$ constitutes an orthonormal basis of W_m, it follows that the whole collection $\{\psi_{mn}(t); m,n \in Z\}$ is an orthonormal wavelet basis for $L^2(\Re)$. The set $\{\psi_{mn}(t) = 2^{-m/2}\psi(2^{-m}t-n)\}$ is the wavelet basis associated with the multiscale analysis, with property

$$\int \psi_{mn}(t)\psi_{m'n'}(t)dt = \delta_{m-m'}\delta_{n-n'} \qquad \text{C-60}$$

Since

$$V_{i-1} = W_i \oplus V_i = W_i \oplus W_{i+1} \oplus W_{i+2} \oplus \ldots \qquad \text{C-61}$$

the function $P_{m-1}f$ at a given resolution can be represented as a sum of added details at different scales.

C.3.2 Multiresolution Pyramid Decomposition

The MRA is used to decompose the signal into successive layers at coarser resolutions plus detail signals, also at coarser decomposition.

Let $f \in V_0$. Then, since $\{\phi(t-n)\}$ spans V_0, f can be represented as a superposition of translated scaling functions:

$$f(t) = \sum_n c_{0,n}\phi(t-n) = \sum_n c_{0,n}\phi_{0n}(t) \qquad \text{C-62}$$

where

$$c_{0,n} = \langle f, \phi_{on} \rangle = \int f(t)\phi(t-n)dt \qquad \text{C-63}$$

Since, $V_0 = V_1 \oplus W_1$, f can be expressed as the sum of two functions, one lying entirely in V_1 and the other in the orthogonal complement W_1:

$$f(t) = P_1 f + Q_1 f = \underbrace{\sum_n c_{1,n}\phi_{1n}(t)}_{f_v^1(t)} + \underbrace{\sum_n d_{1,n}\psi_{1n}(t)}_{f_\omega^1(t)} \qquad \text{C-64}$$

where the scaling coefficients $c_{1,n}$, and the wavelet coefficients $d_{1,n}$ are given by:

$$c_{1,n} = \langle f_v^1, \phi_{1n} \rangle = \frac{1}{\sqrt{2}} \int f_v^1(t)\phi\left(\frac{t}{2} - n\right)dt \qquad \text{C-65}$$

$$d_{1,n} = \langle f_\omega^1, \psi_{1n} \rangle = \frac{1}{\sqrt{2}} \int f_\omega^1(t)\phi\left(\frac{t}{2} - n\right)dt \qquad \text{C-66}$$

The discrete signal $d_{1,n}$ is just the discrete wavelet transform coefficient at resolution 1/2. It represents the detail or difference information between the original signal $c_{0,n}$ and its smoothed down-sampled approximation $c_{1,n}$. These signals $c_{1,n}$ and $d_{1,n}$ are said to have a resolution of 1/2, if $c_{0,n}$ has unity resolution. Every down-sampling by 2 reduces the resolution by that factor.

The next stage of decomposition is now easily obtained. Take $f_v^1 \in V_1 = V_2 \oplus W_2$ and represent it by a component in V_2 and another in W_2

$$f_v^1(t) = f_v^2(t) + f_\omega^2(t) \qquad \text{C-67}$$

$$f_v^2(t) = \sum c_{2,n}\phi_{2n}(t) \qquad \text{C-68}$$

$$f_\omega^2(t) = \sum d_{2,n}\psi_{2n}(t) \qquad \text{C-69}$$

The decomposition into coarser, smoother approximation and detail can be continued as far as necessary.

C.3.3 Finite Resolution Wavelet Decomposition

The function $f \in V_0$ can be represented as Equation C-62, and decomposed into the sum of a lower-resolution signal (approximation) plus detail (approximation error):

$$f(t) = f_v^1(t) + f_\omega^1(t) = \sum c_{1,n}2^{-1/2}\phi(t/2 - n) + \sum d_{1,n}2^{-1/2}\psi(t/2 - n) \qquad \text{C-70}$$

The coarse approximation $f_v^1(t)$ can be decomposed as Equation C-67, so that:

$$f(t) = f_v^2(t) + f_\omega^2(t) + f_\omega^1(t) \qquad \text{C-71}$$

Continuing up to $f_v^L(t)$, we have

$$f(t) = f_v^L(t) + f_\omega^L(t) + f_\omega^{L-1}(t) + \ldots + f_\omega^1(t) \qquad \text{C-72}$$

or

$$f(t) = \sum_{n=-\infty}^{\infty} c(L,n)2^{-L/2}\phi\left(\frac{1}{2^L} - n\right) + \sum_{m=1}^{L}\sum_{n=-\infty}^{\infty} d(m,n)2^{-m/2}\psi\left(\frac{t}{2^m} - n\right) \qquad \text{C-73}$$

The purely wavelet expansion of Equation C-37 requires infinite number of resolutions for the complete representation of the signal. Equation C-73 shows that $f(t)$ can be represented as a low-pass approximation at scale L plus the sum of L detail (wavelet) components at different resolutions.

C.4 References

Akansu, A., and Haddad, R. (1992). Multiresolution Signal Decomposition, Academic Press.

Coca, D., and Billings, S. A. (2001). "System Identification Using Wavelets." Research Report 785, Department of Automatic Control and Systems Engineering, University

of Sheffield, Sheffield, UK.

Cohen, A., and Kovacevic, J. (1996). "Wavelets: the mathematical background." Proceedings of the IEEE, 84(4), 514-522.

Hess-Nielsen, N., and Wickerhauser, M. V. (1996). "Wavelets and time-frequency analysis." Proceedings of the IEEE, 84(4), 523-540.

Mallat, S. (1999). A Wavelet Tour of Signal Processing, Academic Press.

Press, W. H., Teukolsky, S. A., Vetterling, W. T., and Flannery, B. P. (1992). Numerical Recipes in C, Cambridge University Press.

Rao, R., Bopardikar, A. (1998). Wavelet Transformns: Introduction to Theory and Applications, Addison-Wesley.

Rioul, O. (1993). "A discrete-time multiresolution theory." IEEE Transactions on Signal Processing, 41(8), 2591-2606.

Thuillard, M. (2000). "Multiresolution learning: from GA to fuzzy-wavenets." COLL 2000, Symposium on Computational Intelligence and Learning, Chios, Greece, 67-76.

Appendix D

Wavelet Extracted AEP Features Fuzzy Models

In this appendix, the fuzzy TSK models for the six wavelet extracted AEP features, not presented in Chapter 5, are detailed (i.e. D_2, D_{31}, D_{32}, D_{33}, D_4 and D_{52}). The inputs of the fuzzy TSK models are the propofol effect concentration (PC_e) and the remifentanil effect concentration (RC_e). The TSK models were obtained using the ANFIS MATLAB Toolbox for each of the AEP features, considering the training and checking data sets. For each of the AEP features, the models are presented in the following order:

- Input membership functions;
- Rule-base table;
- Output membership functions;
- Output surface;
- Results on the training and checking data sets.

D.1 AEP Feature D_2

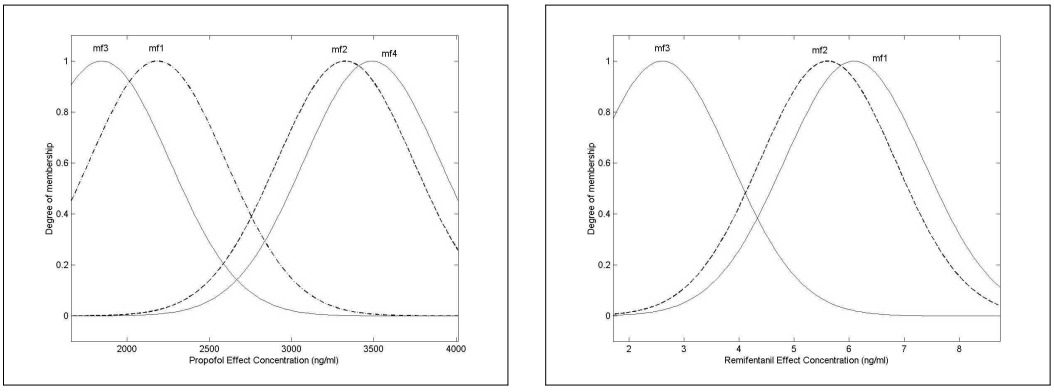

a) b)

Figure D-1: Input membership functions describing the propofol effect concentration (a)) and the remifentanil effect concentration (b)), for the AEP feature D_2 TSK fuzzy model.

Table D-1: Rule-base table for the fuzzy TSK model of the AEP feature D_2. RC_e is the remifentanil effect concentration, PC_e is the propofol effect concentration. f_i is the i output membership function, $i = 1, \ldots, 4$.

PC$_e$	**RC$_e$**		
	mf1	**mf2**	**mf3**
mf1	f_1		
mf2		f_2	
mf3			f_3
mf4		f_4	

The D_2 membership functions (output membership functions) are the following:

$$f_1 = 0.0007PC_e - 0.0190RC_e - 1.3494$$
$$f_2 = -0.0229PC_e - 1.9570RCe + 25.6094$$
$$f_3 = -0.0002PC_e - 0.1049RC_e + 0.6819$$
$$f_4 = -0.0309PC_e + 0.5019RC_e + 162.1829$$

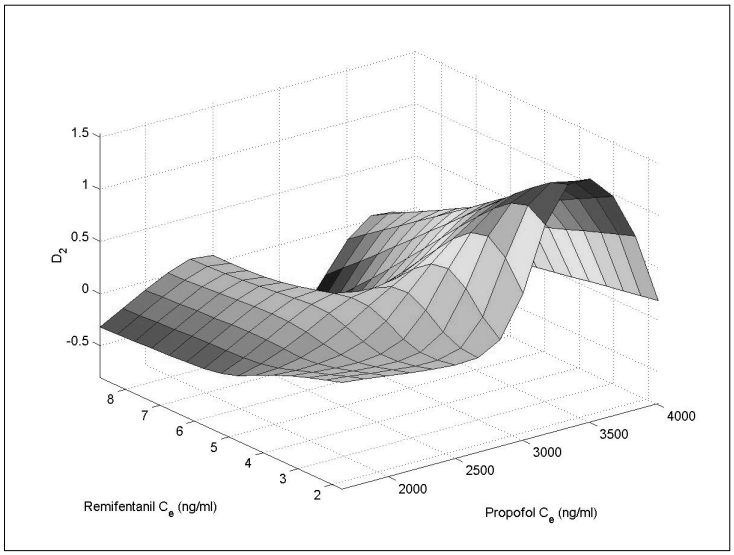

Figure D-2: Output surface of the AEP feature D_2 TSK fuzzy model.

The results of the TSK model on the training and checking data sets are presented in Figure D-3. The training and checking data sets are the same for all the wavelet extracted AEP features, they consist of 2/3 and 1/3 of the whole data, respectively. One out of three samples was selected for the checking data set.

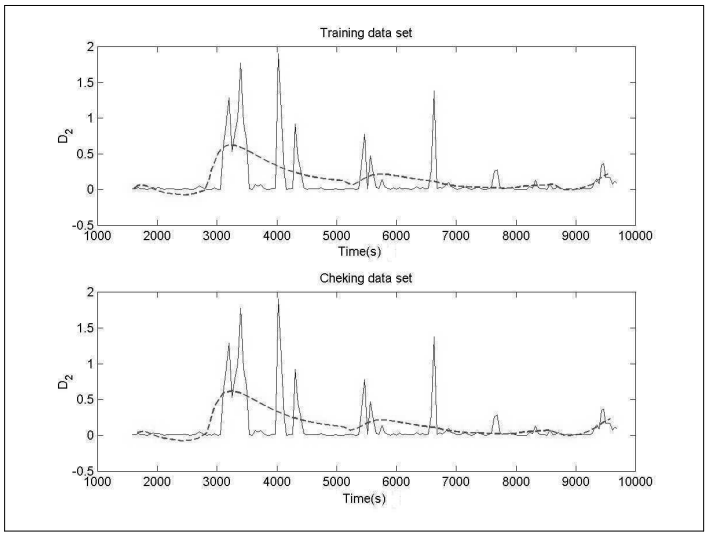

Figure D-3: Results of the AEP feature D_2 TSK fuzzy model on the training and checking data sets (dashed line) versus the AEP feature D_2 from patient Pat1 (solid line), considering the maintenance phase.

D.2 AEP Feature D_{31}

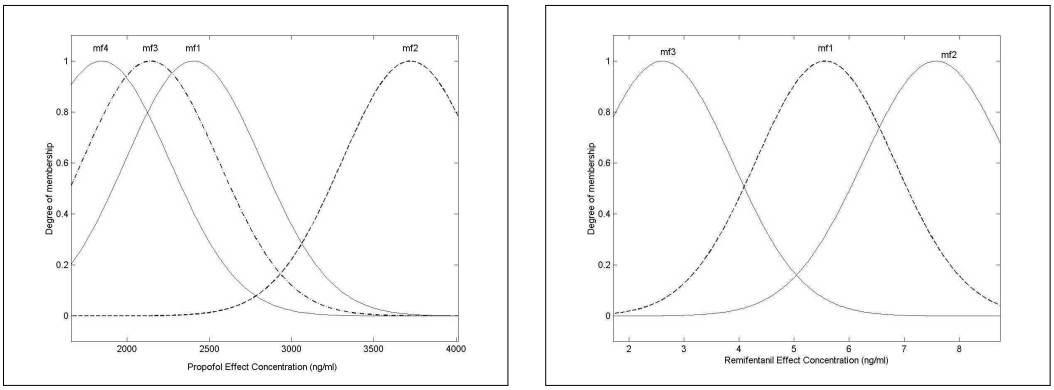

a) b)

Figure D-4: Input membership functions describing the propofol effect concentration (a)) and the remifentanil effect concentration (b)), for the AEP feature D_{31} TSK fuzzy model.

Table D-2: Rule-base table for the fuzzy TSK model of the AEP feature D_{31}. RC_e is the remifentanil effect concentration, PC_e is the propofol effect concentration. f_i is the i output membership function, $i = 1, \ldots, 4$.

PC$_e$	**RC$_e$**		
	mf1	**mf2**	**mf3**
mf1	f_1		
mf2	f_2		
mf3		f_3	
mf4			f_4

The D_{31} membership functions (output membership functions) are the following:

$$f_1 = -0.0032PC_e - 0.6908RC_e + 11.1178$$
$$f_2 = -0.0022PC_e - 0.1321RCe + 9.6112$$
$$f_3 = 0.0157PC_e + 0.1656RC_e - 34.5303$$
$$f_4 = 0.0021PC_e - 1.8165RC_e + 1.0153$$

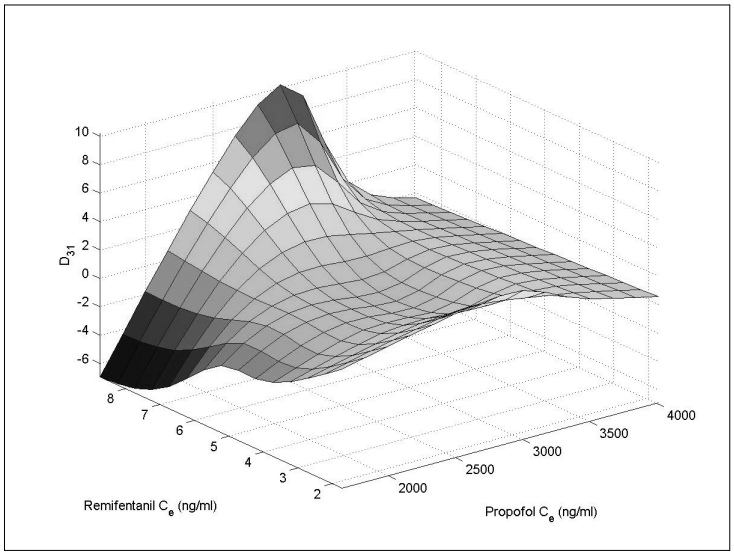

Figure D-5: Output surface of the AEP feature D_{31} TSK fuzzy model.

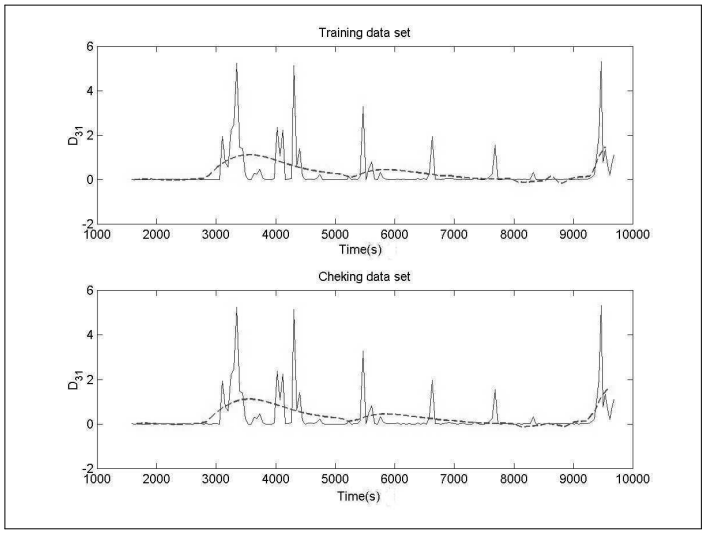

Figure D-6: Results of the AEP feature D_{31} TSK fuzzy model on the training and checking data sets (dashed line) versus the AEP feature D_{31} from patient Pat1 (solid line), considering the maintenance phase.

D.3 AEP Feature D_{32}

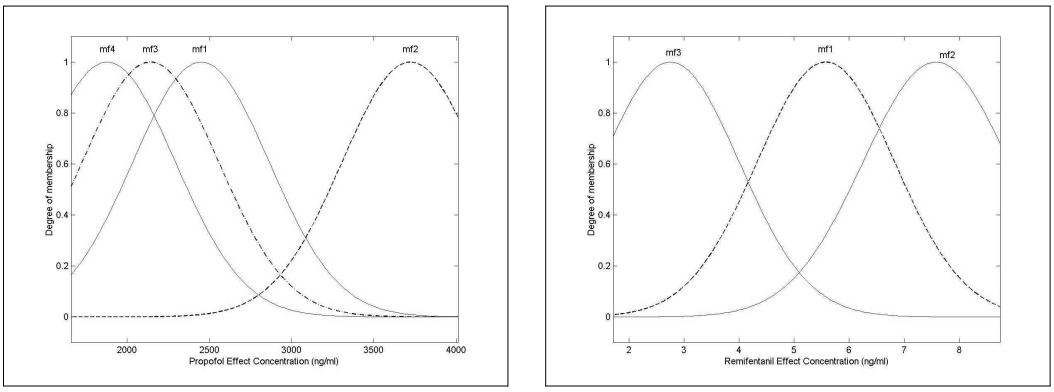

a) b)

Figure D-7: Input membership functions describing the propofol effect concentration (a)) and the remifentanil effect concentration (b)), for the AEP feature D_{32} TSK fuzzy model.

Table D-3: Rule-base table for the fuzzy TSK model of the AEP feature D_{32}. RC_e is the remifentanil effect concentration, PC_e is the propofol effect concentration. f_i is the i output membership function, $i = 1, \ldots, 4$.

PC$_e$	**RC$_e$**		
	mf1	**mf2**	**mf3**
mf1	f_1		
mf2	f_2		
mf3		f_3	
mf4			f_4

The D_{32} membership functions (output membership functions) are the following:

$$f_1 = -0.007PC_e + 1.566RC_e + 8.5694$$
$$f_2 = -0.0043PC_e - 0.3294RCe + 19.2396$$
$$f_3 = 0.0217PC_e + 1.8704RC_e - 61.8629$$
$$f_4 = -0.0008PC_e + 0.0378RC_e + 1.7855$$

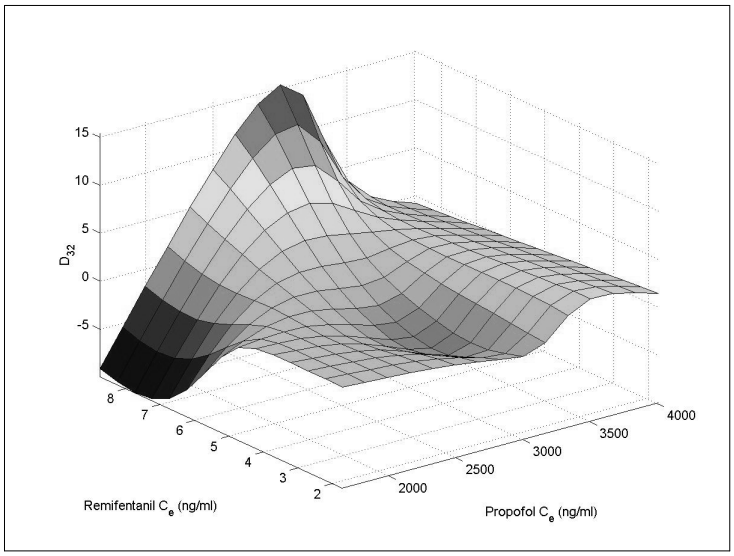

Figure D-8: Output surface of the AEP feature D_{32} TSK fuzzy model.

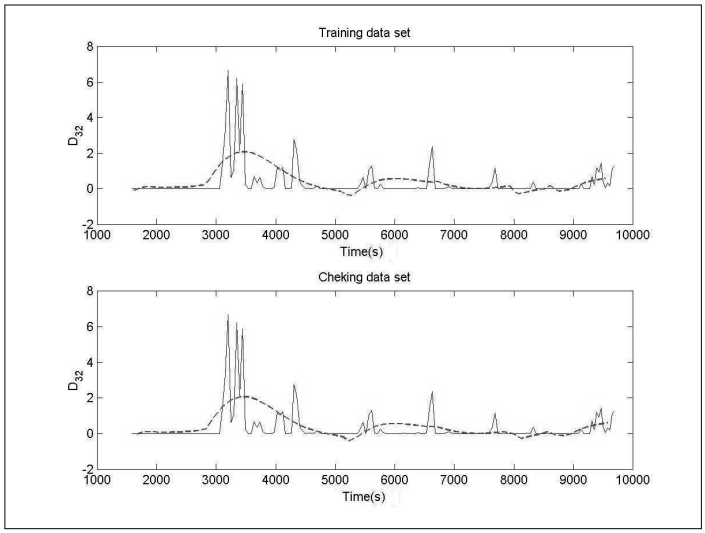

Figure D-9: Results of the AEP feature D_{32} TSK fuzzy model on the training and checking data sets (dashed line) versus the AEP feature D_{32} from patient Pat1 (solid line), considering the maintenance phase.

D.4 AEP Feature D_{33}

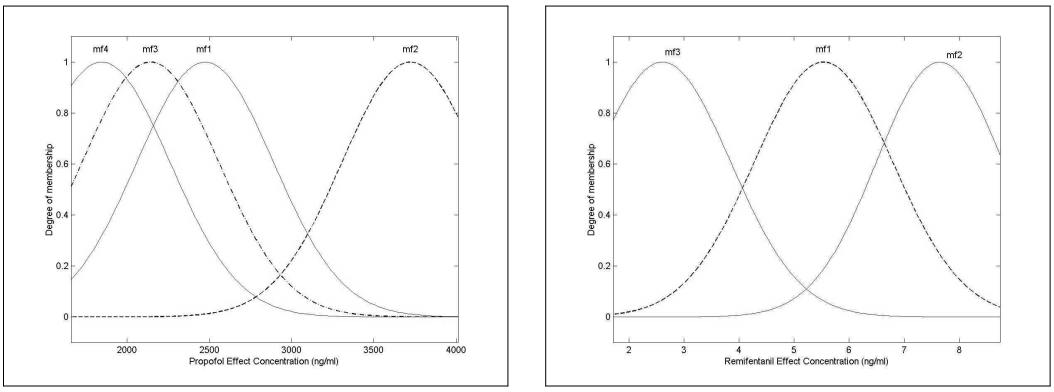

a) b)

Figure D-10: Input membership functions describing the propofol effect concentration (a)) and the remifentanil effect concentration (b)), for the AEP feature D_{33} TSK fuzzy model.

Table D-4: Rule-base table for the fuzzy TSK model of the AEP feature D_{33}. RC_e is the remifentanil effect concentration, PC_e is the propofol effect concentration. f_i is the i output membership function, $i = 1, \ldots, 4$.

PC$_e$	**RC$_e$**		
	mf1	**mf2**	**mf3**
mf1	f_1		
mf2	f_2		
mf3		f_3	
mf4			f_4

The D_{33} membership functions (output membership functions) are the following:

$$f_1 = -0.0024PC_e + 0.4232RC_e + 4.3817$$
$$f_2 = -0.0033PC_e - 0.0888RCe + 13.6081$$
$$f_3 = -0.0007PC_e + 1.0139RC_e - 6.6304$$
$$f_4 = 0.0021PC_e - 1.2998RC_e - 0.1886$$

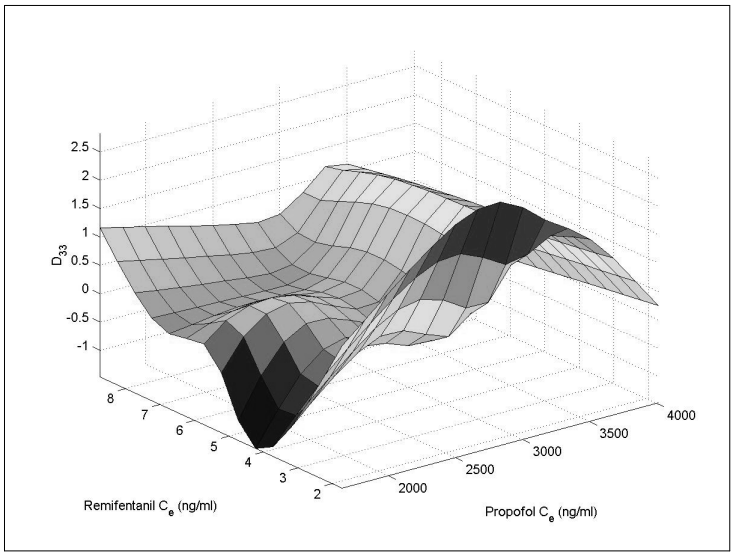

Figure D-11: Output surface of the AEP feature D_{33} TSK fuzzy model.

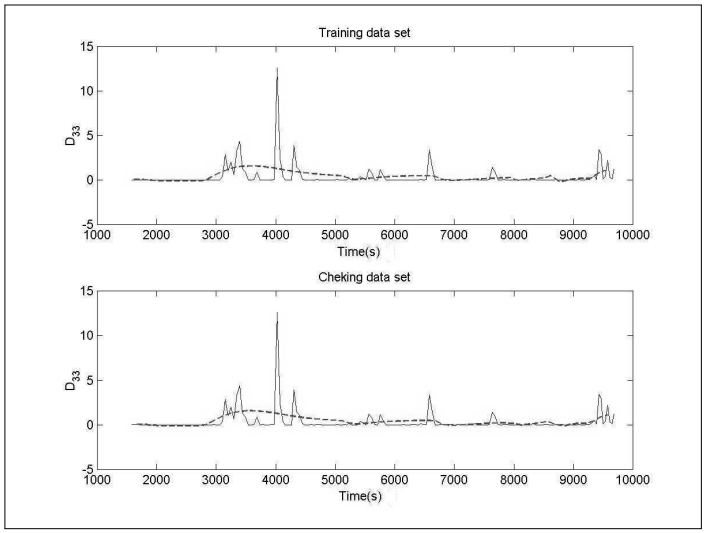

Figure D-12: Results of the AEP feature D_{33} TSK fuzzy model on the training and checking data sets (dashed line) versus the AEP feature D_{33} from patient Pat1 (solid line), considering the maintenance phase.

D.5 AEP Feature D_4

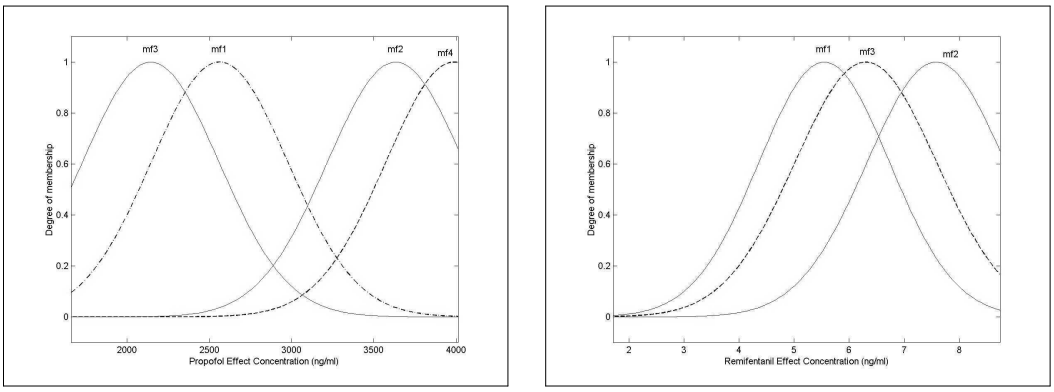

a) b)

Figure D-13: Input membership functions describing the propofol effect concentration (a)) and the remifentanil effect concentration (b)), for the AEP feature D_4 TSK fuzzy model.

Table D-5: Rule-base table for the fuzzy TSK model of the AEP feature D_4. RC_e is the remifentanil effect concentration, PC_e is the propofol effect concentration. f_i is the i output membership function, $i = 1, \ldots, 4$.

PC$_e$	**RC$_e$**		
	mf1	**mf2**	**mf3**
mf1	f_1		
mf2	f_2		
mf3		f_3	
mf4			f_4

The D_4 membership functions (output membership functions) are the following:

$$f_1 = 0.0134PC_e - 2.2962RC_e - 13.6722$$
$$f_2 = 0.2PC_e + 103.4RCe - 1098.8$$
$$f_3 = -0.0416PC_e - 0.128RC_e + 94.7275$$
$$f_4 = 0.3PC_e + 55.1RC_e - 1644.8$$

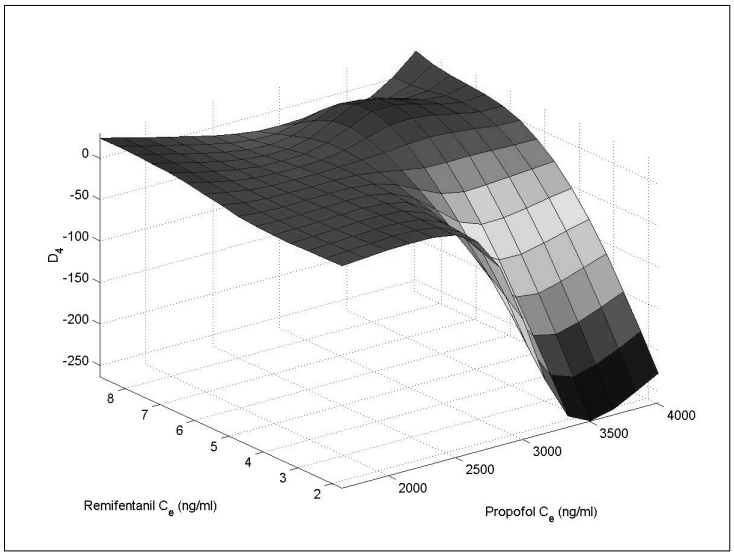

Figure D-14: Output surface of the AEP feature D_4 TSK fuzzy model.

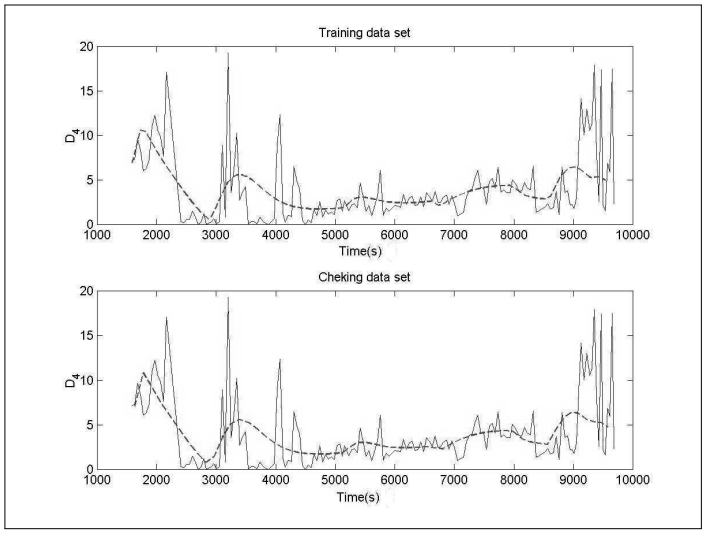

Figure D-15: Results of the AEP feature D_4 TSK fuzzy model on the training and checking data sets (dashed line) versus the AEP feature D_4 from patient Pat1 (solid line), considering the maintenance phase.

D.6 AEP Feature D_{52}

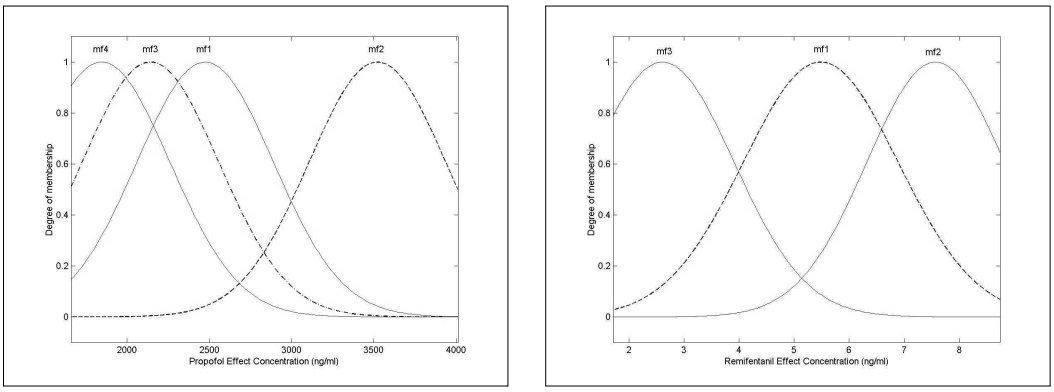

a) b)

Figure D-16: Input membership functions describing the propofol effect concentration (a)) and the remifentanil effect concentration (b)), for the AEP feature D_{52} TSK fuzzy model.

Table D-6: Rule-base table for the fuzzy TSK model of the AEP feature D_{52}. RC_e is the remifentanil effect concentration, PC_e is the propofol effect concentration. f_i is the i output membership function, $i = 1, \ldots, 4$.

PC$_e$	**RC**$_e$		
	mf1	**mf2**	**mf3**
mf1	f_1		
mf2	f_2		
mf3		f_3	
mf4			f_4

The D_{52} membership functions (output membership functions) are the following:

$$f_1 = -0.0006PC_e + 72.2264RC_e - 338.7697$$
$$f_2 = 0.0199PC_e + 9.5601RCe - 123.3977$$
$$f_3 = -0.3571PC_e + 39.6468RC_e + 427.9056$$
$$f_4 = 0.016PC_e + 30.4844RC_e - 73.4977$$

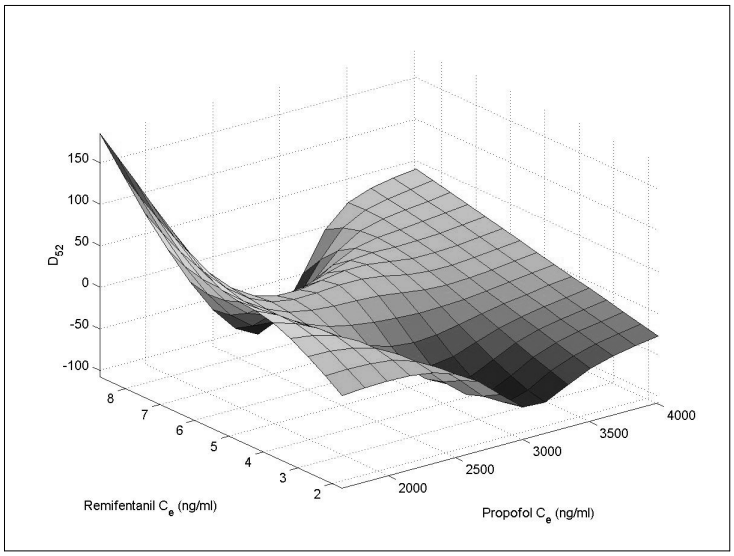

Figure D-17: Output surface of the AEP feature D_{52} TSK fuzzy model.

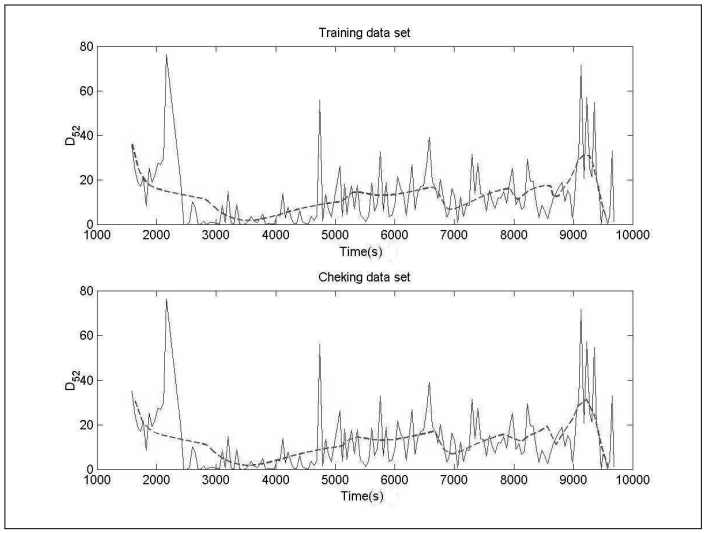

Figure D-18: Results of the AEP feature D_{52} TSK fuzzy model on the training and checking data sets (dashed line) versus the AEP feature D_{52} from patient Pat1 (solid line), considering the maintenance phase.